Herpes Simplex Virus Type-1 Infection and ND10 Characteristics in Cultured Fibroblast and Neuronal-like Cells

by

Wei-Li Hsu

A Thesis Presented for the Degree of Doctor of Philosophy

in

The Faculty of Biomedical and Life Science at University of Glasgow

MRC Virology Unit
Division of Virology
Church Street
Glasgow G11 5JR

SUMMARY

Nuclear domain 10 (ND10) are punctate subnuclear structures that exist in most cell types. It has been suggested that ND10 structures serve as the site for initial viral genome deposition and some viral proteins, such as the ICP0 protein of HSV-1, have been shown to colocalise to, and subsequently induce the degradation of, proteins present in ND10. However the exact function of ND10 during HSV-1 infection is still unknown.

In this study, the potential role of ND10 in HSV-1 infection was investigated by assessing the efficiency of viral IE and E gene expression or viral replication in cultured cells in which the expression of ND10 proteins was increased by IFN treatment or transient transfection methods. Furthermore, this study objective was also approached by using a human neuron precursor cell line (NT2) that naturally lacks one ND10 component, Sp100, and was found to have abnormal ND10 characteristics. The infectivity of HSV-1 in NT2 and differentiated hNT neuronal-like cells was investigated and the function of ICP0 in these cells was studied in more detail.

Treatment with IFN-α increased the number and size of ND10, whereas heat-stress caused dispersal of ND10 proteins, although this did not appear to affect HSV-1 infection. Pre-treatment with IFN-α slightly inhibited HSV-1 gene expression, however it was not clear whether this effect was mediated by the ND10 proteins that are up-regulated by IFN. Examination of cells transiently transfected with plasmids expressing ND10 proteins (either PML, Sp100, SUMO-1 or Ubc9) demonstrated that the expression of viral IE and L genes was not affected by high expression levels of ND10 proteins. However, decreased viral gene expression was observed at an early time of infection in cells co-transfected with three plasmids expressing PML, Sp100, and Ubc9 or with four plasmids expressing PML, Sp100, Ubc9, and SUMO-1. Notably, in cells transfected with multiple plasmids, the exogenous ND10 proteins were sequestered in ND10 to a greater extent than in cells singly transfected. These observations suggested that over-expression of ND10 proteins, properly located in ND10, confers a marginal resistance to HSV-1 infection at an early time of infection, but this effect was less clear at later times of infection. Furthermore, transcription from the ICP6 promoter induced by ICP0 was strongly repressed by two other ND10 associated proteins, HP1 and hDaxx, in a dose-dependent manner in the transient transfection assay.

Study of NT2 cells prior to induction of differentiation revealed atypical ND10 structures. There were fewer PML and hDaxx foci but those present were bigger in size and contained no detectable Sp100. In addition, a track-like distribution of PML was found in many NT2 cells and a high proportion of hDaxx foci were associated with centromeres instead of with ND10. This is distinct from other cell types studied. Immunoblot analysis demonstrated that the expression of PML and levels of SUMO-1 conjugated PML isoforms in NT2 cells were lower than in HFL cells. The normal ND10 pattern was restored in hNT neuronal- like cells obtained from NT2 after treatment with retinoic acid for six weeks. Moreover, both NT2 and hNT cells were poor hosts for HSV-1 and even worse for ICP0-defective viruses. Immunoblot analysis and immunofluorescence assays revealed that in NT2 cells viral gene expression was restricted to IE genes: although expression of ICP0 was higher than in HFL cells, the progression of viral infection (to the E gene stage) was much lower than in HFL cells. Studies of ICP0 function in terms of induction of transcription, reactivation of the viral genome from quiescent infection and degradation of ND10 proteins, found that these functions of ICP0 were compromised in NT2 cells and differentiated hNT cells.

Over-expression of SUMO-1 (but not other ND10 proteins) in NT2 cells inhibited the expression of ICP0 by HSV-1 by 3- to 5-fold at all infection times tested. Three mutant SUMO-1 constructs with a single substitution mutation at residue Gly(96) or Gly(97) or with deletion of four amino acids in the C-terminus were made to determine whether SUMO-1 modification contributes to this effect. Western blot analysis indicated that the C-terminus of SUMO-1 expressed from the Gly(97) substitution mutant was not cleaved by protease, ie the SUMO-1 precursor cannot be processed to the mature form, and immunofluorescence assays showed that this resulted in the redistribution of ND10 proteins such as hDaxx and Sp100 in Hep-2 cells. Although a larger proportion of the mature form of SUMO-1 was produced in cells transfected with the other two mutant constructs, the distribution of ND10 proteins was also affected. Analysis of viral infection revealed that NT2 cells transfected with the three SUMO-1 conjugation mutant constructs had less resistance to HSV-1 infection than wild-type SUMO-1 transfected NT2 cells, implying a role for SUMO-1 modification in HSV-1 infection in NT2 cells.

TABLE of CONTENTS

LIST of FIGURES

Chapter 1 Introduction

Figure **page**

Chapter 3 A study of ND10 proteins and their effects on HSV-1 infection

Chapter 4 Characterisation of human neuronal committed teratocarcinoma NT2 cells and their infection by HSV-1

Chapter 5 Characterisation of SUMO-1 and its conjugation mutants in NT2 and fibroblast cells

LIST of TABLES

Chapter 1 Introduction

Table **page**

Chapter 2 Materials and Methods

Chapter 3 A study of ND10 proteins and their effects on HSV-1 infection

Chapter 4 Characterisation of human neuronal committed teratocarcinoma NT2 cells and their infection by HSV-1

ACKNOWLEDGEMENTS

I would like to acknowledge Professor Duncan McGeoch for providing the opportunity to conduct this study within the Division of Virology.

I express my deepest gratitude to my supervisor Dr. Roger Everett for his helpful advice and inexhaustible patience throughout the project. I am also grateful to him for helpful discussion, language advice during the writing of this thesis and for thoroughly proof reading this manuscript.

My thanks to many members in the laboratory, especially Anne Orr, Jane Parkinson, Patrick Lomonte, and Chris Boutell for their invaluable discussions and technical support during the course of the project.

I wish to thank Dr. Chris Preston for useful advice and providing reagents on the establishment of quiescent infection experiment (in Chapter 4), as well as Dr. Reg Clayton and Dr. David Blackbourn for great assistance on FACS work (in Chapter 5).

I would like to thank Timothy Hart and Jane Parkinson for proof reading this manuscript.

My thanks to staff within the Division who have eased the development of this project, in particular Lesley Taylor, for the automated sequencing service, and wash room and media staff.

Finally, I would like to thank my parents and many good friends for their continual encouragement and support.

The author was a recipient of an Overseas Research Student Award and a University of Glasgow scholarship and unless otherwise stated all the results obtained were through her own efforts.

ABBREVIATIONS

A

A	adenine
Ab	polyclonal antibody
Amp	ampicillin
Amp^r	ampicillin resistance
APL	acute promyelocytic leukemia
APS	ammonium persulfate
ATP	adenosine-5'-triphosphate
ATRA	*all-trans* retinoic acid

B

β-Gal	beta-galactosidase
bp	base pairs
BHK	baby hamster kidney

C

C	carboxy (-terminal end of protein), or cysteine
°C	degrees celsius
CAT	chloramphenicol transferase
cDNA	complementary DNA
CHO	Chinese hamster ovary
Ci	Curie
CIP	calf intestinal alkaline phosphatase
CMV	cytomegalovirus
Co-A	co-enzyme A
CsCl	caesium chloride
CSD	chromo shadow domain

D

dATP	2'-deoxyadenosine-5'triphosphate
DBD	DNA binding domain
dCTP	2'-deoxycytidine-5'-triphosphate
dGTP	2'-deoxyguanosine-5'-triphosphate
DMSO	dimethylsulphoxide
DNA	2'-deoxyribonucleic acid
DNA-PK	DNA-dependent kinase
DNase	deoxyribonuclease
dNTP	2'-deoxyribonucleoside
DRG	dorsal root ganglia
DTT	dithiothreitol

E

E	early (beta)

EBV	Epstein-Barr virus
ECL	enhanced chemiluminescence
E.coli	*Escherichia coli*
EDTA	ethylenediaminotetra-acetic acid
EF1δ	elongation factor 1 δ
EGFR	epidermal growth factor receptor
EHV	equine herpes virus
EtBr	ethidium bromide

F

FCS	foetal calf serum
FITC	fluorescein isothiocyanate

G

g	gram, or glycoprotein
GAP	GTPase-activating protein
GAS	IFN-γ activation site
GMEM	Glasgow modified Eagle's medium
GMP-1	GAP modified protein 1
GST	glutathione-S-transferase

H

h	hour
HAUSP	herpes-associated ubiquitin specific protease
HCMV	human cytomegalovirus
HEL	human embryonic lung
HDAC	histone deacetylase
HDV	hepatitis delta virus
HFL	human foetal lung
HFV	human foamy virus
HHV	human herpesvirus
HMG	high mobility group
HNPP	human nuclear phosphoprotein
HP1	heterochromatin protein 1
hr	hour(s)
HRP	horse radish peroxidase
HSV	herpes simplex virus
HTLV	human T cell leukemia virus

I

IE	immediate early (alpha)
IFA	immunofluorescence assay
IFN(s)	interferon(s)
IPTG	isopropyl-D-thiogalactoside
IR_L	long internal repeat
IR_S	short internal repeat

ISRE	IFN-stimulated response element

K

kb	kilobase pairs
kD	kilo dalton

L

L	Late (gamma), litre
(m/μ)l	(milli/micro)litre
LAT	latency associated transcript
LB	Lauria-Bertani medium
LCMV	lymphocytic choriomeningitis virus

M

(c/μ/n)m	(centi/micro/nano)metre
(m/μ/n)M	(milli/micro/nano)molar
MAb	monoclonal antibody
MDR1	multidrug resistance 1
MHC	major histocompatibility complex
min	minute(s)
MOI	multiplicity of infection
(m/μ/n)mol	(milli/micro/nano)moles
MMTV	mouse mammary tumour virus

N

N	nucleoside, or amino (-terminal end of protein)
ND10	nuclear domain 10
NLS	nuclear localisation sequence
NP40	Nonidet P40

O

OD	optical density
ORF	open reading frame

P

PAGE	polyacrylamide gel electrophoresis
PBS	phosphate buffered saline
PCR	polymerase chain reaction
pfu	plaque forming unit
PIC-1	PML-interacting clone 1
PML	promyelocytic leukaemia protein
PMSF	phenylmethylsulphonyl fluoride
PODs	PML oncogenic domains

R

RAR-α	retinoic acid receptor alpha
Rb	retinoblastoma
RC	replication compartment

REF	rat embryonic fibroblasts, or RNA and export factor binding protein
RGB	resolving gel buffer
RNA	ribonucleic acid
RNase A	ribonuclease A
rpm	revolutions per minute
RT	room temperature

S

SDS	sodium dodecyl sulphate
sec	second(s)
SF-1	steroidogenic factor 1
SGB	stacking gel buffer
SUMO	small ubiquitin-related modifier
SV40	simian virus 40

T

T	thymine, threonine,
TBS	Tris buffered saline
TE	Tris EDTA
TLC	thin-layer chromatography
Tris	tris (hydroxymethyl) aminomethane
TRITC	tetramethylrhodamine isothiocyanate
ts	temperature sensitive
TWEEN-20	polyoxyethylene-sorbitanmonolaurate

U

Ub	ubiquitin
UBL 1	Ubiquitin-like 1
U_L	unique long (region of HSV)
U_S	unique short (region of HSV)
USP	ubiquitin-specific protease
U.V.	ultra violet

V

V	volts
Vmw	apparent molecular weight of viral polypeptide (determined by SDS-PAGE)
VSV	vesicular stomatitis virus
VZV	varicella-zoster virus

W

W	watts

Y

YT	yeast tryptone broth

Amino acid symbols and codons

One letter symbol	Three letter Symbol	Amino acid	Codons
A	Ala	alanine	GCA GCC GCG GCT
C	Cys	cysteine	TCG TCT
D	Asp	aspartic acid	GAC GAT
E	Glu	glutamic acid	GAA GAG
F	Phe	phenylalanine	TTC TTT
G	Gly	glycine	GGA GGC GGG GGT
H	His	histidine	CAC CAT
I	Ile	isoleucine	ATA ATC ATT
K	Lys	lysine	AAA AAG
L	Leu	leucine	TTA TTG CTA CTC CTG CTT
M	Met	methionine	ATG
N	Asn	asparagine	AAC AAT
P	Pro	proline	CCA CCC CCG CCT
Q	Gln	glutamine	CAA CAG
R	Arg	arginine	AGA AGG CGA CGC CGG CGT
S	Ser	serine	AGC AGT TCA TCC TCG TCT
T	Thr	threonine	ACA ACC ACG ACT
V	Val	valine	GTA GTC GTG GTT
W	Trp	tryptophan	TGG
Y	Tyr	tyrosine	TAC TAT
start codon			ATG
stop codons			TAA TAG TGA

Chapter 1 INTRODUCTION

Chapter 1 INTRODUCTION

1A Herpesviruses - overview

Herpesviruses are nuclearly replicating, enveloped double-stranded DNA viruses with an icosahedral capsid. The hosts of these viruses are ubiquitous, including all groups of vertebrates, and the same host can be infected with multiple distinct types of herpesviruses. The family of herpesviruses consists of three subfamilies: alpha (α)-, beta (β)-, and gamma (γ)-herpesvirus, each with unique properties. The alphaherpesvirus subfamily is characterised by a relatively short replication cycle, a broad host and cell range, efficient destruction of infected cells, and an ability to establish latent infection in sensory ganglia. The beta- and gammaherpesviruses differ in genome size and structure but both replicate more slowly and in a much more restricted range of cells. The betaherpesviruses subfamily can be maintained in a latent form in the kidney, secretory glands, and leukocytes. Gammaherpesviruses display specificity for lymphoid and epithelial cells and, at least in culture, have been shown to be associated with transformation of infected cells. To date, eight discrete human herpesviruses have been described, each causing characteristic diseases. Over recent years, human herpesvirus infections have become of increased clinical importance because of advances in organ transplantation techniques and because herpesvirus infections occur with increased frequency in HIV-infected and immunosuppressed individuals. Additionally, interest has increased in the development of human viruses as vectors for gene therapy.

In this section, the classification of human herpesviruses and clinical aspects including symptoms, epidemiology and treatment of diseases caused by human herpesviruses are generally described.

1A.1 General introduction to the Herpesviridae

The Herpersviridae consists of almost 100 members that infect a wide range of hosts including humans, horses, cattle, pigs, and fowl. Herpesviruses that infect humans are responsible for multiple syndromes involving many organ systems. Aside from a similar ultrastructural morphology and some similarities in lytic replication cycles, the only major feature shared by all these agents is the capacity to establish a type of persistent infection, known as latency, in which the viral genome is present but infectious virus is not produced

except during intermittent episodes of reactivation. Thus herpesviruses have been very important medically because they are common and produce diseases in a substantial minority of cases.

1A.2 Herpesviridae classification

According to the universal system of virus taxonomy established by the ICTV (International Committee on Nomenclature of Viruses), the *Herpesviridae* belong to group I as double-stranded DNA viruses. Herpes simplex virus type 1 (HSV-1) was classified as belonging to the family *Herpesviridae*, subfamily *Alphaherpesvirinae*, genus *Simplexvirus*, human herpesvirus type 1.

There are now eight known members of the human herpesvirus family, grouped into three subfamilies based upon details of tissue tropism, pathogenicity, and behaviour under conditions of culture in the laboratory (Table 1.1). More recently, sequences of the genomes of these viruses have been published by (Baer *et al.*, 1984); (Cha *et al.*, 1996); (Chee *et al.*, 1990); (Dargan *et al.*, 1997); (Davison & Scott, 1986); (Dolan *et al.*, 1998); (Gompels *et al.*, 1995); (McGeoch *et al.*, 1985); (Nicholas, 1996); and (Renne *et al.*, 1996).

1A.3 Clinical aspects

1A.3.1 α-herpesviruses: Herpes simplex viruses (subtypes 1 and 2)

Initial episodes of orofacial HSV infection are nearly always caused by HSV-1 but may also be caused by HSV-2 (Lafferty *et al.*, 1987). When symptomatic, infectious virus replicates in susceptible epithelial cells and initiates the formation of an inflamed lesion, usually around the mouth, commonly called a "cold-sore". Recurrent vesicle lesions normally persist for around 2 days, then become pustules or ulcers, followed by the formation of a crust within 3-4 days. Lesions usually heal after 8-10 days (Spruance *et al.*, 1977).

HSV-2 is usually sexually transmitted and is clinically manifested in the genital or adjacent area as primary or recurrent infection. HSV-1 usually causes orofacial disease, but is becoming an increasingly common cause of primary genital infection, as the causative agent of 20-60% of genital infection in the UK (Kinghorn, 1994). Symptoms are caused

Table 1.1 The human herpesviruses

Subfamilies	members (common names)	systematic name	genome size (kb)
α-herpesviruses			
	Herpes simplex virus type 1 (HSV-1)	HHV 1	152
	Herpes simplex virus type 2 (HSV-2)	HHV 2	155
	Varicella zoster virus (VZV)	HHV 3	125
β-herpesviruses			
	Human cytomegalovirus (HCMV)	HHV 5	230
	Human herpesvirus type 6 (HHV-6)	HHV 6	159
	Human herpesvirus type 7 (HHV-7)	HHV 7	145
γ-herpesviruses			
	Epstein-Barr virus (EBV)	HHV 4	172
	Human herpesvirus type 8 (HHV-8)	HHV 8	160-170

by a direct cytopathic effect of the replicating virus destroying tissue, causing ulceration. Such ulceration reduces an important barrier of protection against acquiring HIV infection. Population subgroups at high risk of HIV infection are often already infected with HSV at the time HIV infection was initially diagnosed, thus genital herpesvirus has become a significant cofactor in HIV transmission (reviewed by Brugha *et al.*, 1997).

Herpes simplex viruses also cause conjunctivitis, keratitis, and encephalitis through an aetiology not yet understood (Whitley *et al.*, 1977). Around two-thirds of neonatal infections in the USA are asymptomatic. HSV-1 infection localised to the skin, eye, and mucous membranes is rarely fatal, however without appropriate antiviral treatment, localised infection in the new-born may proceed to disseminated infection and/or meningoencephalitis which is often life threatening (Whitley *et al.*, 1991, Whitley *et al.*, 1988).

1A.3.2 α-herpesviruses: Varicella zoster virus (VZV)

Unlike other herpesvirus infections, VZV regularly produces symptoms in the majority of children who acquire it. Primary infection with VZV generally presents in childhood with a rash, known as chickenpox, which is usually present 14 days after infection. Periodic reactivation from the latent state from neuronal ganglia causes a significant shingles lesion at the relevant dermatome often accompanied by severe pain that can persist for months (Arvin, 1996, Dueland, 1996).

1A.3.3 β-herpesviruses: Human cytomegalovirus (HCMV)

In cytological examination, enlargement and fusion of macrophages, termed cytomegaly, is a characteristic of HCMV infection. Infection with HCMV is ubiquitous among adult populations, although the primary infection is often asymptomatic. Additionally, HCMV infection is an important cause of serious congenital and neonatal disease, which can be fatal to newborns. In the foetus, severe infection of HCMV causes mental retardation and /or hearing loss. If the immune system is immature (as in the foetus), or is compromised by immunosuppressive drugs, HCMV frequently causes gut ulceration or retinitis (reviewed by Alford *et al.*, 1990). Furthermore, HCMV may trigger the immune system of transplant patients to cause rejection of the transplanted organ (Arbustini *et al.*, 1996).

1A.3.4 β-herpesviruses: Human herpesvirus 6 (HHV-6)

Compared to the viruses noted above, less is known about HHV-6 and HHV-7. There are two close variants of HHV-6, HHV-6A and HHV-6B which share greater than 97% of similarity of DNA sequences in some regions, although they are only 75% identical in the immediate early region of the HHV-6 viral genome (Di Luca *et al.*, 1996). HHV-6 is shed as infectious viral particles in the saliva and is ubiquitous in the population; up to 90% of adults in the UK are infected with HHV-6 (Griffiths, 2001). Primary infection occurs in childhood, when it is associated with exanthem subitum, a common childhood illness characterised by a high fever and skin rash (reviewed by Ablashi *et al.*, 1991).

1A.3.5 β-herpesviruses: Human herpesvirus 7 (HHV-7)

As with HHV-6, HHV-7 is shed as infectious viral particles in the saliva and is ubiquitous within the population. HHV-7 has been associated with roseola in infants (Hidaka *et al.*, 1993).

1A.3.6 γ-herpesviruses: Epstein-Barr virus (EBV)

In 1964, Epstein, Achong and Barr discovered that HHV-4 is the pathogenic agent of a unique lymphoma disease (Burkitt's lymphoma), which was first described by Denis Burkitt in African children of Uganda (Epstein *et al.*, 1964). In subsequent studies, HHV-4 was also designated Epstein-Barr virus. Most EBV infections, particularly in childhood, are asymptomatic, and whatever the syndrome induced, primary infection with EBV follows infection and replication of virus in the nasopharynx (reviewed by Crawford, 2001). Following the primary asymptomatic infection in the nasopharynx, EBV ultimately infects B lymphocytes. These become latently infected and enable transmission to other individuals. If this transmission occurs in adolescence or later, the virus causes infectious mononucleosis, a debilitating disease commonly known as glandular fever.

Besides Burkitt's lymphoma, EBV is now suspected to be a pathogenic agent in other non-Hodgkin's lymphomas (e.g. AIDS-associated, post-transplant) and Hodgkin's disease, in nasopharyngeal carcinoma (NPC), and gastric adenocarcinoma, and in leiomyosarcomas associated with immunosuppression (reviewed by Hildesheim & Levine, 1993, McClain *et al.*, 1995). Although these diseases are rare in most populations, their incidence is elevated

in certain groups: NPC is an important source of cancer morbidity in southern China, and Hodgkin's disease is one of the most frequent malignancies affecting young adults (reviewed by Glaser & Jarrett, 1996, Hildesheim & Levine, 1993).

1A.3.7 γ-herpesviruses: Human herpes virus (HHV-8)

HHV-8, also called Kaposi's sarcoma-associated herpesvirus (KSHV), is a relatively recently discovered gamma-herpesvirus identified by molecular cloning techniques that used Kaposi's sarcoma tissues as the starting material (Chang *et al.*, 1994). HHV-8 is relatively widespread, with up to 25% of the adult population having antibodies to HHV-8 lytic proteins and this percentage rises to 90% in HIV-infected men (Lennette *et al.*, 1996). HHV-8 is the etiologic agent of Kaposi's sarcoma of AIDS patients and is associated with primary effusion lymphoma as well as the lymphoproliferative disorder multi-centric Castleman's disease (Corbellino *et al.*, 1996).

1A.4 Epidemiology

HSV primarily infects epithelial tissue through the mucosa and abraded skin. HSV-1 is widespread and usually acquired in childhood. Almost all primary HSV infections occurring before the age of 10 are due to HSV-1, and by the age of 60 years, 60-80% of the US population is HSV-1 seropositive (Nahmias *et al.*, 1990).

HSV-2 infection occurs later in life, and its incidence rates are relatively low; the population of HSV-2 seroprevalence in the USA is 30-50% and is under 5% in the UK (Griffiths, 2001, Kinghorn, 1994).

HSV can be transmitted from infected mothers to neonates, however, the incidence rate is low; 3 per 100000 births according to a report from a UK annual estimate during 1987-1988 (Jeffries, 1991). Transmission of infection from mother to baby usually occurs during vaginal delivery (85% of transmissions) and is dependent on the prevalence of genital viral shedding at the time of delivery (Whitley, 1993). Intrauterine and postnatal transmissions are rare, 5% and 10% respectively (Whitley, 1993).

Either type of HSV may cause conjunctivitis, and keratitis, although HSV-1 is the cause of 78%-98% of cases (Gerdes & Smith, 1983). There are only limited data (1 case

per 200,000 population in USA) on the incidence of HSV encephalitis (Whitley *et al.*, 1977).

1A.5 Treatment

A range of anti-viral agents has become available since the 1980s, however no treatment is currently available to eliminate HSV infection. Acyclovir (9-[(2-hydroxyethoxy) methyl] guanine, Zovirax), a synthetic acyclic purine-nucleoside analogue, was introduced in the early 1980s and has been shown to produce a clinical benefit in primary genital herpes when administered either intravenously or orally (Mindel *et al.*, 1982). Acyclovir reduces the clinical severity of disease episodes, shortens their duration, prevents complications and reduces symptomatic viral shedding, but does not eliminate the infection (Kinghorn, 1993). Even after 20 years of use, resistance to acyclovir is not yet a significant problem in clinical practice because the viruses that escape from control of this drug are profoundly debilitated and acyclovir continues to be the mainstay of treatment (Corey, 1993).

Acyclovir is a particularly effective inhibitor of herpes simplex virus replication *in vitro* and *in vivo* (Elion *et al.*, 1977, Schaeffer *et al.*, 1978). The efficacy and antiviral specificity of the acyclic nucleoside analogues is due in part to their selective phosphorylation in virally infected cells (Biron *et al.*, 1985, Elion *et al.*, 1977). The HSV thymidine kinase enzyme (tk) phosphorylates acyclovir, converting it to a mono-phosphorylated form, which is then phosphorylated further by cellular kinases before it is incorporated into newly synthesised DNA resulting in the arrest of DNA synthesis and leading to subsequent DNA fragmentation (Moolten, 1986, Reardon & Spector, 1989). In addition to acyclovir, precursor drugs, valaciclovir (converted to acyclovir) and famciclovir (converted to penciclovir), have been licensed and have better oral bioavailability than acyclovir and penciclovir respectively (Balfour, 1999).

Therapeutic vaccines may also be useful in the control of genital and neogenital HSV infection, although no vaccine with proven efficacy against a human herpes simplex virus has yet been developed. More recently, three types of prophylactic vaccine are in clinical trial: an adjuvant subunit using viral surface glycoprotein gB and gD antigens, a replication-incompetent viral mutant, and DNA vaccines (Bernstein & Stanberry, 1999,

Corey *et al.*, 1999, Stanberry, 1995). Additionally, genetically attenuated HSV mutants and vectors are in pre-clinical development.

1B HSV-1 biology

The herpes simplex viruses were the first human herpesviruses to be discovered and are also the most intensely investigated (reviewed by Roizman & Sears, 1996). HSV-1 is a common and effective human pathogen capable of establishing both lytic and latent infectious life cycles. HSV-1 is a nuclear replicating virus with a linear double-stranded DNA genome, encoding at least 84 different proteins during lytic (productive) infection. However, in the latent phase of infection, only a limited group of transcripts are expressed. The mechanism of the switches between productive and latent infection is not fully understood, and is the subject of much current research.

In this section, the virion structure, the HSV-1 genome, and general aspects of both lytic and latent infection are briefly described.

1B.1 Virion structure and composition

As with other herpesviruses, the HSV-1 virion is composed of an outer trilaminar lipid envelope containing the viral glycoproteins, an amorphous tegument, an inner icosahedral capsid shell, and a DNA-containing core. The diameters of the complete particle and the capsid are around 180 nm and 100 nm respectively (Morgan *et al.*, 1968).

Located centrally in the virion, the double-stranded DNA genome is condensed into the apparent shape of a torus (Furlong *et al.*, 1972). The folded DNA molecule lies enclosed in an icosahedral capsid assembly of 162 capsomers, of which 150 are hexameric and 12 are pentameric. The hexamers are located on the faces and edges of the capsid and the pentamers are at the vertices (Booy *et al.*, 1991).

The nucleocapsid, formed by capsid plus enclosed DNA, is embedded in the tegument. The tegument contains some twenty distinct structural proteins of various functions that are thought to influence the process of infection (Rixon, 1993). The outer surface of the tegument is enclosed in the viral envelope – a trilaminar lipid membrane of host origin decorated with 12 or more different HSV membrane proteins (Schrag *et al.*, 1989).

1B.2 The HSV-1 genome

The HSV-1 virion contains a double stranded linear genome of 152 kilobase pairs (kb) with a G+C content of 68% (McGeoch *et al.*, 1988). The DNA of HSV-1 consists of two covalently linked segments, designated L (long) and S (short). At the termini of the genome and at the junction of the L and S segments are one or more additional copies of a 400 base pair (bp) unit termed the **a** sequence (Wadsworth *et al.*, 1975). The L and S segments each contain a unique sequence, U_L (unique long) or U_S (unique short), and in turn these are flanked by large inverted repeats termed **b** (bounding U_L) and **c** (bounding U_S). Thus, as shown in Fig. 1.1, U_L is flanked by the sequences **ab** and its inversion **b'a'**, around 9.2 kb each, whereas U_S is flanked by the sequences **a'c** and its inversion **c'a**, 6.6 kb each (McGeoch *et al.*, 1988). Up to now, at least 84 genes have been variously identified, sixty-five mapping in U_L, fourteen in U_S and two copies of five genes in the repeat sequences. These encode proteins that are either structural (contained in the capsid, arrayed in the surrounding tegument or as glycoproteins anchored in the envelope) or nonstructural (often enzymes required for DNA replication and gene expression). The name of each open reading frame refers to genes by their location in the genome, e.g. U_L 1-56, U_S 1-11. Nonetheless, some encoded proteins are assigned multiple names, usually referring to their respective genomic location, function, or molecular weight. For instance, the U_L48 gene encodes a viral transactivator referred to variously as VP16 (Virion Protein 16), αTIF (α gene Trans-Inducing Factor), ICP25 (Infected Cell Protein 25) or Vmw65 (Virus protein of molecular weight 65 kDa).

1B.3 The HSV-1 life cycle

In humans, HSV-1 causes two kinds of infection, lytic and latent. Initially, acute infections by HSV-1 principally involve ectodermally derived tissue such as skin, mucous membranes, and corneal epithelia. The virus attaches and binds to the epithelium cells, enters by fusion with the cell membrane and then starts replication and gene expression. Lytic (productive) infection results in the production of more virions that cause cell death. After the initial infection and many rounds of viral replication at body surfaces, virus particles ascend by retrograde axonal transport in nerve axons to associated somas in sensory ganglia. Viruses in the infected neuron nucleus may replicate to produce progeny, or may enter a non-replicating latent state in which the viral genome is sequestered and no

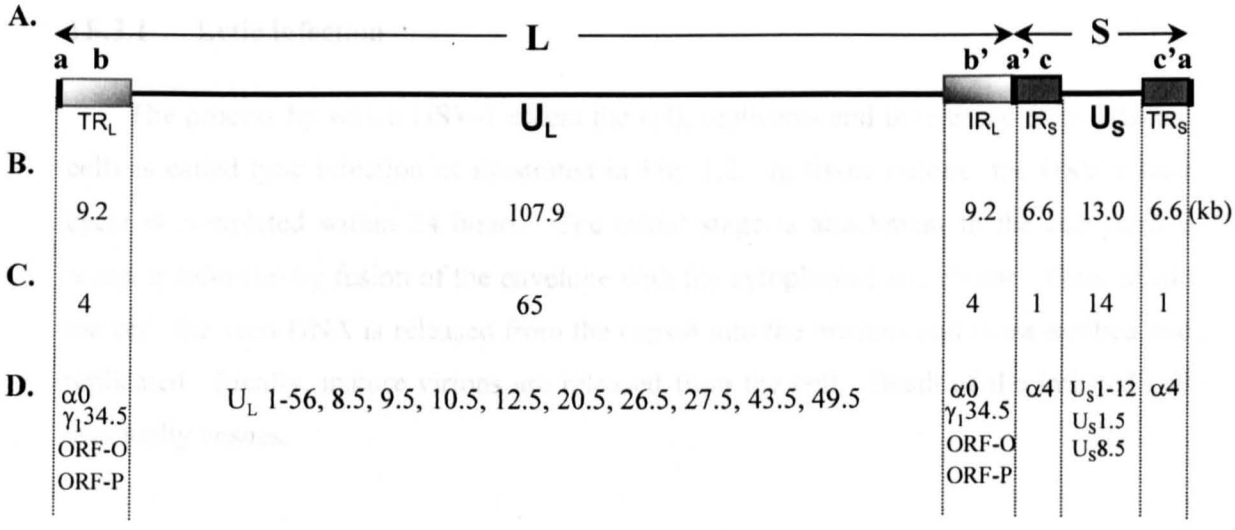

Fig. 1.1 Schematic representation of the HSV-1 genome.

(A) The approximately 152 kb genome is divided into U_L and U_S sequences illustrated as solid lines and major repeat elements (TR_L and IR_L, IR_S and TR_S) as filled boxes. The location of the L and S segments are marked. Terminal **a** sequences and the internal, opposite orientation **a'** sequence are indicated. The filled quadrangles represent terminal sequences **ab** and **c'a** inverted and repeated internally to **b'a'c**. (B-D) Below the genome representation, the sizes (kb) of the major genome regions (B), the numbers of genes (C), and distribution of viral genes (D) proposed for each are listed.

free virus can be detected (Stevens & Cook, 1971). However, the molecular mechanisms by which one of these options is followed have yet to be elucidated.

1B.3.1 Lytic infection

The process by which HSV-1 enters the cell, replicates and is released from infected cells is called lytic infection as illustrated in Fig. 1.2. In tissue culture, the HSV-1 lytic cycle is completed within 24 hours. The initial stage is attachment to the cell surface receptor followed by fusion of the envelope with the cytoplasmic membrane. Once inside the cell, the viral DNA is released from the capsid into the nucleus and is transcribed and replicated. Finally, mature virions are released from the cell. Death of the infected cell eventually ensues.

1B.3.1.1 Adsorption and penetration

Viral surface glycoproteins inserted in the envelope mediate attachment and penetration of HSV-1 into cells. The HSV-1 viral particle firstly attaches to the cell surface through the interaction of virion glycoproteins with cell surface receptors such as heparan sulphate proteoglycan (reviewed by Shukla & Spear, 2001). In alphaherpesviruses, 11 glycoproteins have been described so far; they are glycoproteins B (gB), gC, gD, gE, gG, gH, gI, gJ, gK, gL and gM and a twelfth (gN), the product of the pseudorabies virus (PrV) UL 49.5 gene, is predicted (Jons *et al.*, 1996). Several of these molecules exist as homomeric multimers, such as gC, gB, gD (Claesson-Welsh & Spear, 1986, Handler *et al.*, 1996, Kikuchi *et al.*, 1990), or form heteromeric complexes with other glycoproteins, for example gH:gI; gM:gN (Johnson & Feenstra, 1987, Jons *et al.*, 1998).

In the course of HSV-1 infection, glycoprotein C is required for efficient binding of virions to the cell surface (Herold *et al.*, 1991). Additionally, it has been proposed that gB is the most prominent glycoprotein involved in the interaction with cell surface glycosaminoglycans (GAGs), principally heparan sulfate. A mutant virus in which the heparin sulphate-binding domain of gB is deleted displays reduced penetration kinetics and reduced plaque size, implicating a potential role for gB interactions with GAGs (Laquerre *et al.*, 1998). However, no one virion protein has been found to be solely responsible for attachment to the cell surface; mutant viruses expressing neither gC or gB bind to cells in

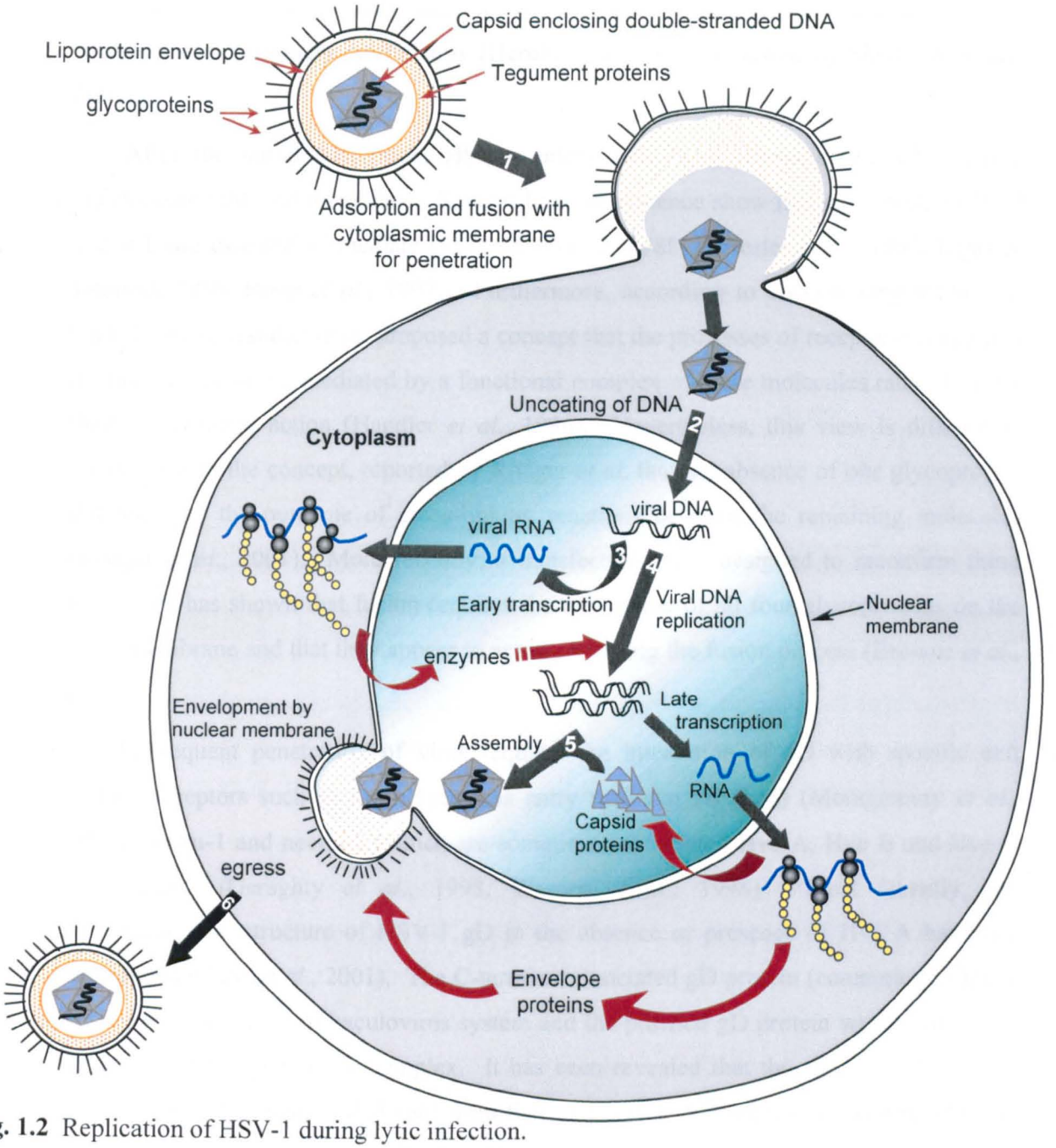

Fig. 1.2 Replication of HSV-1 during lytic infection.

The initial stage of infection is adsorption of HSV-1 virion to the cell surface through the interaction of viral glycoproteins in the viral envelope with host cell receptors in the cytoplasmic membrane (marked as letter 1 in white). The envelope and membrane fuse and the viral nucleocapsid is released into cytoplasm and the viral DNA is then uncoated and imported into the nucleus (labeled as 2). Early transcription and mRNA are synthesised by host enzymes (labeled as 3). The resulting early gene products are used in viral DNA replication (4). Further RNA transcripts are required for synthesis of viral capsid, envelope proteins and glycoproteins. The newly produced capsid subunits are assembled and the viral DNA is packaged into the capsid (as labeled in 5). The latter are enveloped by budding through the nuclear membrane and eventually egress from the infected cell. (Adapted from Ackermann. H-W., Berthiaume, L., and Tremblay, M., Virus life in Diagrams, CRC Press, 1998, 52.)

tissue culture extremely inefficiently (Herold *et al.*, 1994, reviewed by Shukla & Spear, 2001).

After the initial adsorption, HSV-1 enters cells by a fusion between the virion envelope and the cell membrane. Several lines of evidence show that glycoproteins B, D and H:L are essential to mediate fusion (Cai *et al.*, 1988, Forrester *et al.*, 1992, Ligas & Johnson, 1988, Roop *et al.*, 1993). Furthermore, according to cross-linking studies on HSV-1 virion, Handler *et al.* proposed a concept that the processes of receptor-binding and membrane fusion are mediated by a functional complex of these molecules rather than by their independent action (Handler *et al.*, 1996). Nevertheless, this view is difficult to reconcile with the concept, reported by Rodger *et al.* that the absence of one glycoprotein did not alter the outcome of cross-linking reactions between the remaining molecules (Rodger *et al.*, 2001). More recently, a transfection study designed to reconfirm these arguments has shown that fusion requires the expression of all four glycoproteins on the same membrane and that they appear to act in *cis* during the fusion process (Browne *et al.*, 2001).

Subsequent penetration of virus requires the interaction of gD with specific cell surface receptors such as the herpesvirus entry mediator (HVEM) (Montgomery *et al.*, 1996), nectin-1 and nectin-2 (which are sometimes designated Hve A, Hve B and Hve C respectively) (Geraghty *et al.*, 1998, Warner *et al.*, 1998). Most recently, the crystallographic structure of HSV-1 gD in the absence or presence of Hve A has been determined (Carfi *et al.*, 2001). The C-terminal trunctated gD protein (containing residues 1-285) was expressed in baculovirus system and the purified gD protein was prepared for formation of the gD/Hve A complex. It has been revealed that the structure of the free form of the gD protein is different from that of gD/Hve A complex, suggesting that gD may change conformation upon binding Hve A.

Following envelope fusion with the plasma membrane and subsequent penetration, viral capsids are transported to the nuclear membrane in a process mediated by the cell cytoskeleton (Kristensson *et al.*, 1986). The DNA is then released into the nucleus through nuclear pores, followed by genome circularisation to form an episome.

1B.3.1.2 Viral gene expression

During lytic infection, following penetration into the nucleus, viral gene expression occurs in a temporally regulated pattern and genes are classified as alpha (α), beta (β) and gamma (γ) (Clements *et al.*, 1977). The first set of genes (α, immediate-early, or IE genes) is transcribed by cellular RNA polymerase II (Ben-Zeev & Becker, 1977, Costanzo *et al.*, 1977) with the participation of a virion tegument protein VP16, which is released from the tegument after uncoating of the viral capsid. VP16 acts *in trans* together with the cellular octamer DNA-binding protein, Oct-1 and another cellular factor known as HCF also called C1 (Scarr *et al.*, 2000, Wilson *et al.*, 1993). The mode of action of VP16 is quite well understood and is described in more detail in a later section. The expression peak of IE genes is at 2 to 4 hour post infection, although most IE proteins continue to accumulate throughout infection. Functional IE proteins are required for the fully efficient synthesis of all the later classes of virally encoded proteins. The products of at least three IE genes function as transactivators of β or early (E) gene expression, which peaks at 5 to 7 hours and is detectable as early as 2 hours post infection. Many of the products expressed from E genes are enzymes or factors that are required for replication of the viral genome. After the onset of viral DNA replication, the temporal program of viral gene expression continues with the appearance of the γ or late (L) proteins, which generally comprise the structural proteins: tegument proteins, envelope glycoproteins, and proteins necessary for nucleocapsid assembly and genome packaging (Roizman & Sears, 1996). The details of viral gene expression are discussed in more detail in section 1C.

1B.3.1.3 DNA replication

HSV-1 DNA replication begins shortly after the appearance of the E gene products and can be detected as early as two hours post infection and continues up to at least fourteen hours post infection (reviewed by Roizman & Sears, 1996). Replication of viral DNA takes place in large globular replication compartments (Quinlan *et al.*, 1984, Rixon *et al.*, 1983) that initially form adjacent to subnuclear domains called ND10 (further details are described in section 1E, and Ishov & Maul, 1996, Maul *et al.*, 1996).

Seven viral gene products, all located in the U_L segment, have been described to be absolutely necessary for HSV-1 DNA replication (reviewed by Challberg & Kelly, 1989). The functions of these proteins have been defined as a DNA polymerase (UL30) and its

processivity factor (UL42), a single-stranded DNA binding protein (ICP8, also known as UL29), an origin-binding protein (UL9), and components of a helicase-primase complex (UL5, UL8, UL52) (reviewed by Challberg & Kelly, 1989). In transient transfection assays, these molecules are sufficient for amplification of a cotransfected plasmid containing a viral origin of replication (Challberg, 1986, Wu *et al.*, 1988).

As illustrated in Fig. 1.3, parental viral DNA in the nucleus is hypothesized to replicate first via a theta-mode intermediate, then by switching to a rolling circle mechanism that produces long head-to-tail concatameric viral genomes (reviewed by Boehmer & Lehman, 1997, Roizman and Sears, 1996). The HSV-1 genome contains three origins of DNA replication: one copy of ori_L is located between *UL29* and *UL30* genes within the U_L segment, and two identical copies of ori_S map in the 'c' inverted repeat region (IR_S) of the S segment. However neither copy of ori_S is essential for viral growth in cultured cells since deletion of one or both copies of ori_S has no effect on viral DNA replication (Roizman & Sears, 1996). Initially, the UL9 protein (94 kDa), containing helicase activities, binds to its recognition DNA sequence as a homodimer (Lee & Lehman, 1999) through its N-terminal part (Elias *et al.*, 1992). It has been shown that ICP8 interacts with the extreme C terminus of UL9, greatly stimulating its DNA-dependent ATPase and DNA helicase activities (Boehmer *et al.*, 1993). UL9 protein, together with ICP8 (128 kDa) (that binds single-stranded DNA with a 5-fold greater affinity than double-stranded DNA (Lee & Knipe, 1985), can unwind the two strands of the template DNA specifically, permitting entry of the DNA replication machinery (Lee & Lehman, 1997). Subsequently, a 'primosome' (DNA Helicase-Primase complex), which consists of a 1:1:1 association of the *UL5*, *UL8* and *UL52* gene products with a molecular weight of around 270 kDa, associates with the origin to create an initiation bubble in the *theta* (θ) mode of replication (Fig. 1.3). A host DNA polymerase, DNA polymerase α-primase, has been implicated to play a role in the theta phase (Lee *et al.*, 1995). DNA synthesis occurs when this initiation 'bubble' associates with a complex of the DNA polymerase (product of *UL30* gene) and UL42. It has been reported that stimulation of DNA polymerase activity requires UL42, a protein that possesses double-stranded DNA binding activity, since the HSV-1 DNA polymerase lacks DNA binding activity (Gottlieb *et al.*, 1990). DNA synthesis occurs continuously along one strand and discontinuously on the other strand. The growth of the DNA replication fork is maintained by the major DNA-binding protein ICP8. This results in the production of head to tail concatamers that accumulate in the

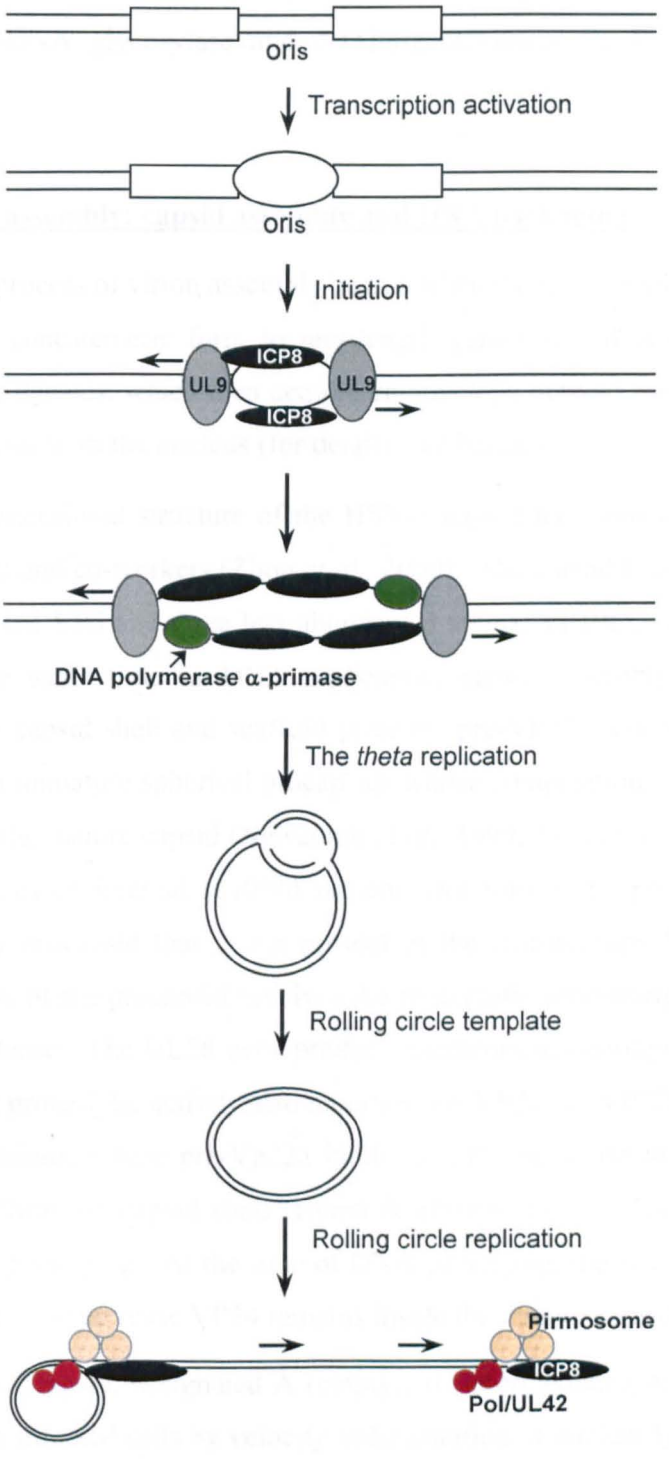

Fig. 1.3 Model for the replication of the HSV-1 genome in which an initial transient phase of *theta* replication is followed by a rolling circle mode, the predominant mode of HSV-1 DNA replication. (modified from Lehman and Boehmer, 1999)

replication compartments (Quinlan *et al.*, 1984). The HSV-1 genome also encodes a set of enzymes involved in nucleic acid metabolism such as thymidine kinase, ribonucleotide reductase, uracil-DNA glycosylase and dUTPase (reviewed by Boehmer & Lehman, 1997).

1B.3.1.4 Virion assembly: capsid assembly and DNA packaging

The overall process of virion assembly begins when the newly replicated viral DNA is cleaved from its concatemeric form to unit-length genomes and is packaged into pre-formed, immature capsids, which then acquire an envelope derived from the inner nuclear membrane upon exit from the nucleus (for details, see below).

The three-dimensional structure of the HSV-1 capsid has been determined at 8.5 Å resolution by Chiu and co-workers (Zhou *et al.*, 2000). The capsid is composed of a major capsid protein called VP5 and three less abundant proteins, VP19C, VP23 and VP26. At approximately the same time as DNA replication, capsid assembly initiates with the association of the capsid shell and scaffold proteins, pre-VP22a (encoded by the *UL26.5* gene), resulting in immature spherical procapsids whose composition is identical to that of the outer shell of the mature capsid (Newcomb *et al.*, 1999, Trus *et al.*, 1996). Procapsids contain an unprocessed internal scaffold protein core formed by pre-VP22a, the major component of the procapsid that is not present in the mature capsid (Newcomb *et al.*, 1996). Maturation of the procapsid involves the proteolytic processing of the scaffold by its associated protease. The UL26 gene product undergoes autoproteolysis to form VP24 and VP21 and the proteolytic activity also modifies pre-VP22a to VP22a by cleaving at the pre-VP22a C terminus, where pre-Vp22a binds to VP5, resulting in the release of the internal scaffold from the capsid shell (Homa & Brown, 1997). The procapsid is then ready for genome packaging. At the time of DNA packaging, the scaffold protein VP22a is expelled and only the protease VP24 remains inside the mature capsid (Gao *et al.*, 1994).

Three types of capsid, designated A (empty), B (intermediate), and C (mature) have been isolated from infected cells by velocity sedimentation of nuclear lysates (reviewed by Homa & Brown, 1997). C capsids containing the viral genome can mature to become infectious virions. B capsids contain the proteolytically processed forms of the internal scaffold (see below). A capsids are believed to be by-products of DNA packaging and are incapable of maturation into infectious virions.

DNA packaging involves the participation of DNA, empty capsids, and additional HSV-1-encoded proteins. Studies on temperature-sensitive mutants have shown that seven gene products; UL6, UL15, UL17, UL25, UL28, UL32, and UL33, are required for the DNA cleavage and packaging processes, however the individual functions of the packaging proteins are unclear.

1B.3.1.5 Nucleocapsid envelopment and virus egress

The processes by which enveloped virions are transported from the perinuclear space through the cytoplasm to the extracellular space are not well understood, primarily because many viral proteins and cellular factors have been described as being involved in membrane fusion. More recently, a comparative ultrastructural study reported that after intranuclear assembly, progeny nucleocapsids exit by budding at the inner leaflet of the nuclear membranes into the perinuclear space, resulting in the acquisition of a primary envelope (Granzow *et al.*, 2001). Additionally, results from immunogold labelling with a TGN (*trans*-Golgi network)-specific antibody showed that the secondary envelopment of released nucleocapsids occurs at the membranes of the *trans*-Golgi area. Finally, egress of virus progeny occurs by exocytosis of virus-containing vesicles. Another model of egress has been illustrated by Skepper *et al.* using immunogold labelling to track the distribution of gD, which was expressed as a fusion protein with an ER (endoplasmic reticulum) retrieval signal (KKXX) in its C-terminus. Most ER-tagged gD was found between the inner and outer nuclear membranes, whereas very little of the protein was present on extracellular virus particles, implying that the primary envelope acquired from nuclear membrane might be lost during egress and that the mature virion must obtain an envelope from a post-ER cytoplasmic compartment (Skepper *et al.*, 2001).

1B3.2 Latent infection

Herpes simplex viruses are best known for their ability to remain latent in humans for the lifetime of the host. During latency, HSV DNA persists in an extrachromosomal state, the most likely physical form of which is a circular episome. Latent infection is characterised by the absence of viral antigens and of infectious virus. Any latent infection can be viewed as having three separable phases: establishment, maintenance, and reactivation.

Virions enter sensory neuron endings and are transported to the cell bodies in sensory ganglia where latent infection is established (Stevens & Cook, 1971). However, the precise mechanism for the establishment phase is unclear since the neurons in which the virus replicates during the first several days after infection obscure the events taking place in the neurons committed to maintaining the virus in a latent state.

During maintenance of the latent infection, viral DNA is maintained as a circular episome, most lytic cycle genes are transcriptionally and functionally quiescent, and only a limited number of viral genes will be expressed, so that the cytopathic results of productive infection do not occur. It is suspected that failure of IE transcription results in an inability to activate the productive cascade. This concept is supported by the observation that latency can be efficiently established following infection of mice with in1814, a HSV-1 mutant that abolishes the interaction of VP16 with Oct-1 and HCF, resulting in reduced IE gene expression (Ecob-Prince *et al.*, 1993, Valyi-Nagy *et al.*, 1992).

Successful reactivation of herpesvirus replication results in the appearance of infectious virus at the site of the initial primary infection. The mechanisms involved in the induction of reactivation remain poorly understood. Reactivation of HSV-1 in humans can be induced by many different non-specific stimuli including abrasion to the skin, fever, exposure to UV irradiation, stress and possibly hormonal irregularities.

1B3.2.1 LATs and their potential role in HSV-1 latency

- **LATs**

During latent infection, HSV-1 gene expression is restricted to a family of RNAs known as the latency-associated transcripts (LATs) (Deatly *et al.*, 1987, Stevens *et al.*, 1987). The LATs are transcribed from a region located within the long repeat (R_L) region, mapping antisense to the IE ICP0 gene (Fig. 1.4A). As shown in Fig. 1.4B, the full-length 8.3-kb LAT transcript (also called the minor LAT) accumulates to low levels in latently-infected neurons, while 2.0- and 1.5-kb introns processed from the full-length transcript (termed major LATs) are more abundant (reviewed by Wagner & Bloom, 1997). The most abundant 2.0-kb LAT is a branched lariat and is neither capped nor polyadenylated (Devi-Rao *et al.*, 1991, Rodahl & Haarr, 1997, Wagner *et al.*, 1988). Further RNA processing to remove 500 bp from within the 2.0-kb LAT sequence results in the production of the 1.5-

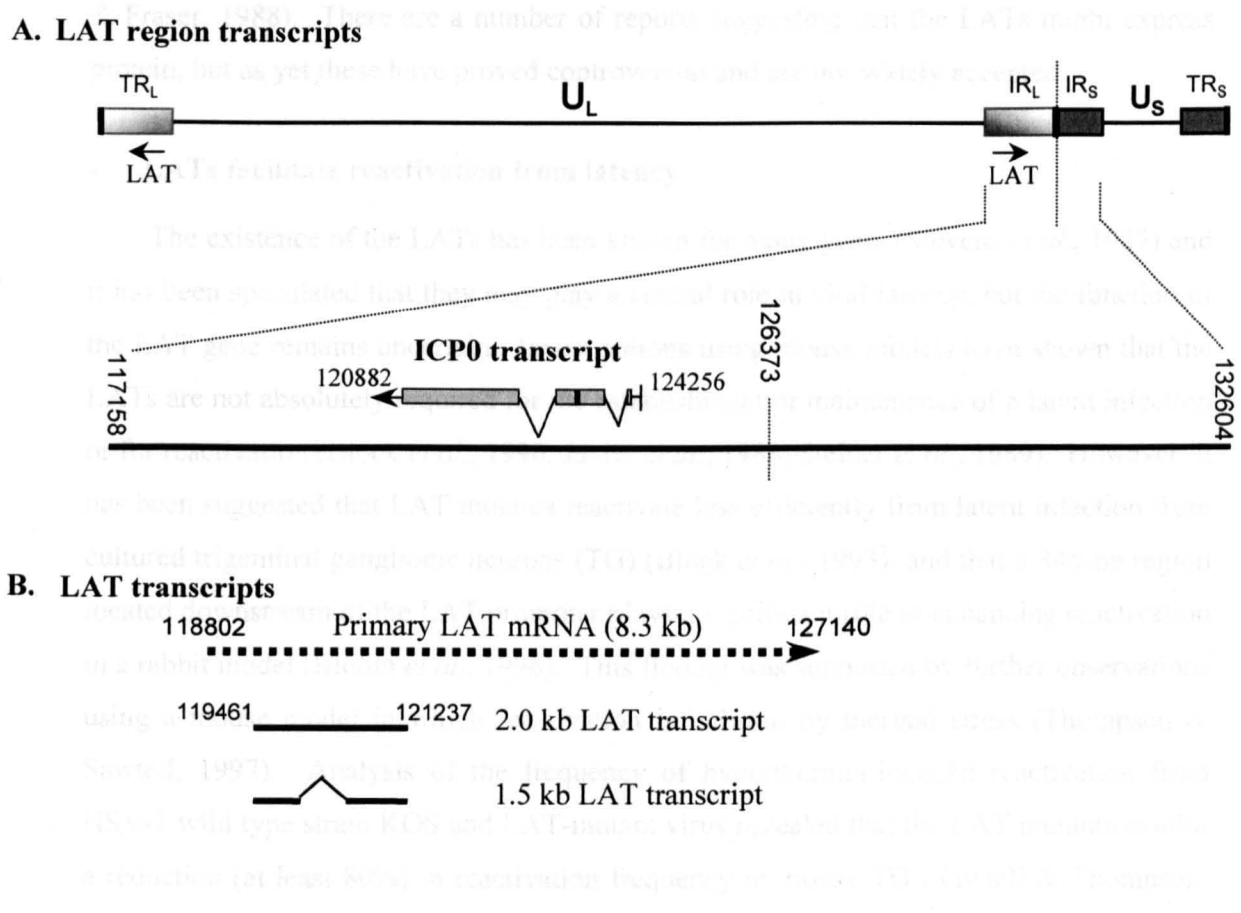

Fig. 1.4 A diagram illustrating the relative positions of sequences within the HSV-1 genome encoding the ICP0 and LAT transcripts.

(A) A schematic diagram of the HSV-1 gemone. The LATs and the α0 gene are encoded by diploid genes that map to the repeat regions (IR_L and TR_L). The horizontal lines drawn underneath represent the IR_L and IR_S regions in which relative positions of LAT and ICP0 transcripts are shown. The coding region of ICP0 is between residue124256-120882, consisting of three exons marked as filled grey boxes and two introns shown as lines. The black box demonstrates the location of the RING finger region in the exon 2.

(B) LAT transcripts. The 8.3-kb primary LAT transcript (minor LAT) is at residues 119461 to 121237. Stable 2- and 1.5-kb RNA species, the intron regions derived from the 8.3-kb primary LAT transcript, accumulate to high levels in latently infected tissue which map toward the 5' end of the 8.3-kb transcript.

kb LAT (Alvira *et al.*, 1999). The 2.0-kb LAT is detected both in productive and latent infection, whereas the 1.5-kb LAT is detectable only in latently infected neurons (Spivack & Fraser, 1988). There are a number of reports suggesting that the LATs might express protein, but as yet these have proved controversial and are not widely accepted.

- **LATs facilitate reactivation from latency**

The existence of the LATs has been known for many years (Stevens *et al.*, 1987) and it has been speculated that they may play a central role in viral latency, but the function of the LAT gene remains uncertain. Investigations using mouse models have shown that the LATs are not absolutely required for the establishment or maintenance of a latent infection or for reactivation (Block *et al.*, 1990, Javier *et al.*, 1988, Steiner *et al.*, 1989). However, it has been suggested that LAT mutants reactivate less efficiently from latent infection from cultured trigeminal ganglionic neurons (TG) (Block *et al.*, 1993), and that a 348-bp region located downstream of the LAT promoter plays a significant role in enhancing reactivation in a rabbit model (Bloom *et al.*, 1996). This finding was supported by further observations using a mouse model in which reactivation is induced by thermal stress (Thompson & Sawtell, 1997). Analysis of the frequency of hyperthermia-induced reactivation from HSV-1 wild type strain KOS and LAT-mutant virus revealed that the LAT mutants exhibit a reduction (at least 80%) in reactivation frequency in mouse TG (Sawtell & Thompson, 1992).

- **LATs increase establishment of latency**

Although several lines of evidence imply that LATs may play a direct role in reactivation from latency, the biological role of LATs in latent infection is still debatable. Most recently, more results support the view that LATs may facilitate the establishment of latent infections and this increase is responsible for efficient reactivation (Thompson & Sawtell, 1997, Thompson & Sawtell, 2001). A new approach, CXA (contextual analysis), was employed to quantify the percentage of neurons that harboured the viral genome in latently infected TG neurons (Sawtell, 1997, Sawtell, 1998, Thompson & Sawtell, 1997). Thomson and Sawtell reported that the number of neurons retaining viral genomes was reduced by approximately 3-fold in ganglia of LAT mutant infected mice compared to that of wild type KOS strain infected mice (Thompson & Sawtell, 1997). Consistently, this finding was also observed using a strain 17+ based LAT mutant (Thompson & Sawtell,

2001). Additionally, increasing the level of establishment of latency by the LAT-null mutants resulted in an increase in the frequency of reactivation, suggesting that LAT is not required for efficient *in vivo* reactivation (Thompson & Sawtell, 1997). However the mechanism by which the LATs facilitate establishment of latency is not yet known, and the controversial views of the role of LATs in reactivation still need to be clarified.

- **LATs promote neuronal survival**

The advantages of CXA are not only that it is possible to determine how expression of LAT is related to genome copy-number in individual neurons, but also that neuronal death after infection can be quantified. Using CXA, it was observed that after 30 days of latent infection more than 50% of TG neurons were lost in mice infected with LAT null mutant virus, while less than 20% of TG neurons were lost following wild type infection. This result suggested that the LAT gene can increase neuronal survival and enhance the establishment of latency in the mouse model (Thompson & Sawtell, 2001). Based on these findings, and together with several recent observations, they hypothesized a new model that when a high copy number of virions enter a neuron, expression of the LAT gene in neurons prevents progression to lytic infection mediated by repression of IE gene expression (Thompson & Sawtell, 2001). In this model, the LAT is viewed as a repressor of IE expression, and this is supported by the observations of Mador *et al.* (1998) using a neuronally derived cell line, constitutively expressing the major 2.0-kb LAT. They reported that replication of HSV-1 was reduced by at least 160-fold at a multiplicity of infection (MOI) of 0.1, and accumulation of mRNA expressing the IE genes ICP0, ICP4 and ICP27 was reduced compared to that in a control transformed cell line (Mador *et al.*, 1998). These findings imply that LAT may repress viral replication by reducing the IE gene mRNA levels and thereby increasing the establishment of HSV-1 latency in neuronal cells

- **LATs prevent apoptosis**

Recently, LATs have been suggested to play a potential role in apoptosis of infected neurones in a rabbit model (Perng *et al.*, 2000). These authors found that in rabbit TG extensive apoptosis occurred when latently infected with a LAT mutant virus, but not with wild type virus. They suggested that the LATs promote neuronal survival after HSV-1 infection by reducing apoptosis. This conclusion, however, is difficult to reconcile with

the observation from other researchers who reported that LATs prevented the destruction of TG in a mouse model, but there was no significant evidence to demonstrate that LAT null viruses induce more extensive apoptosis in infected neurons as measured by the TUNEL assay (Thompson & Sawtell, 2000, Thompson & Sawtell, 2001).

1B.3.2.2 Animal models for the study of HSV latency

The broad host range of HSV-1 has allowed the use of several animal models for the study of viral pathogenesis, neuropathology, neuroinvasiveness, and latency. As described previously, the most appropriate model for latency must allow establishment of a stable latent infection and virus reactivation, which should be similar to that seen in humans. Two animal models, the rabbit and the guinea pig, approximate to this ideal situation, although there are some limitations in both models.

It has been reported that by infection of rabbit eyes, HSV-1 establishes latent infection in TG and infectious virus can be recovered from latently infected TG only when cultivated with feeder cells (Nesburn *et al.*, 1972, Nesburn *et al.*, 1967). Despite the high expense, the rabbit system could mimic human infection in broad detail and may be an appropriate model for the study of reactivation.

The guinea pig model has been promising for the study of vaccine efficiency and other aspects of experimental pathogenesis (Wagner & Bloom, 1997). Vaginal inoculation of female guinea pigs with HSV-1 causes significant primary infection and infectious virus can be recovered from the recurrent vesicular lesion in the vaginal area (Landry & Bull, 1992, Stanberry *et al.*, 1982). However, it has been reported that reactivation can not be reliably induced in this model (Bratcher *et al.*, 1993).

The mouse model has been used extensively due to the relatively lower cost, although this system suffers from the lack of efficient *in vivo* reactivation of virus. To date, at least two murine models have been well established and frequently applied to the study of latency.

- **The footpad/dorsal root ganglion model**

The mouse footpad model was the first *in vivo* latency system to be developed (Stevens & Cook, 1971, Walz *et al.*, 1974). This system is analogous to genital infection of HSV-1

in humans, and is particularly useful for the study of HSV-2 infection. HSV inoculation of a mouse rear footpad results in a local cutaneous infection and following anterograde transfer of virus through the peripheral and central nervous system, which is followed by the establishment of latency in spinal ganglia. The latent infection can be reactivated by explant culture of dissected dorsal root ganglia (DRG) with feeder cells (Stevens & Cook, 1971).

- **Mouse eye/trigeminal ganglion model**

In this model, HSV-1 resides in a latent state in the TG after infection of the cornea via scarification (Sawtell & Thompson, 1992, Walz *et al.*, 1974). As in the footpad model, latent HSV can be recovered by co-cultivation of explanted ganglia. Additionally, Sawtell and Thompson developed a modified method by which the latent HSV genome can be reactivated by hyperthermia treatment followed by preparation of the TG for detection of the viral genome or other expressed markers, often by sensitive quantitative PCR. Without the requirement for further culture of the explanted ganglia, this model is considered closer to an *in vivo* method and offers another way for modelling reactivation in the mouse (Sawtell & Thompson, 1992).

1.B.3.2.3 In vitro models of latency

Animal models have proved invaluable for the study of HSV-1 pathogenesis and latency, however this system is costly, time consuming and ethically restricted. To overcome such difficulties, there have been several reports of promising *in vitro* models applied for latency studies. For instance, using fibroblasts, neuroblastoma, or primary cultures of sensory neurons, latency can be established by limiting virus replication and spread by using antiviral agents or replication-defective viruses (Block *et al.*, 1994, Harris *et al.*, 1989, Wilcox & Johnson, 1987).

- **Primary neuronal culture**

The most well-studied neuronal model system is that of Wilcox and colleagues in which acyclovir (ACV) is used to establish latent infections and nerve growth factor (NGF) is employed to maintain latency (Wilcox & Johnson, 1987, Wilcox *et al.*, 1997). Dorsal root ganglia of a 15-day embryonic or neonatal rat were plated on coverslips and 14

days later ACV was added to the medium. The cultures were infected with HSV-1 after a further 12 hours. After several days, the cultures are free of infectious virus and LATs are detected in a large proportion of cells in an MOI dependent manner (Wilcox *et al.*, 1997). The latent viral genome can be reactivated by withdrawal of ACV, and NGF deprivation by adding 1% of rabbit anti-mouse NGF serum (Wilcox & Johnson, 1987).

More recently, a modified model was developed by Arthur *et al.* (2001). The activity of the LAP (LAT promoter) was stably maintained in up to 83% of primary rat dorsal root neurons infected with defective viruses (gH^-TK^-) with a reporter gene (lacZ) driven by LAP for at least three weeks. In addition, IE promoter (ICP0) activity could be reactivated from over 50% of latently infected neurons by NGF withdrawal or treatment with trichostatin A (TSA), an inhibitor of histone deacetylases (Arthur *et al.*, 2001).

- **Primary TG cell cultures**

Several groups have described a primary TG cell culture model as an alternative model for studying HSV-1 reactivation (Halford *et al.*, 1996, Moriya *et al.*, 1994). In the model of Moriya *et al.* (1994), latently infected mouse TG are dissociated and maintained in a latent state by using BVareU, an inhibitor of HSV replication. These cultures can be induced to reactivate by heat shock, similar to the *in vivo* heat shock system described in section 1B3.2.2 (Sawtell & Thompson, 1992).

More recently, Halford and colleagues established TG cell monolayers from dissociated infected mouse TG in the presence of ACV. After removal of ACV and NGF from the medium, reactivation of latent HSV-1 could be induced in up to 75% of TG cell cultures by heat shock at 43°C for 3 hours (Halford & Schaffer, 2001) or treatment with dexamethasone (Halford *et al.*, 1996). However, the results of Halford *et al.* indicated that TG cell cultures may have spontaneous levels of reactivation during pre-heat stress treatment (Halford *et al.*, 1996).

While this model clearly has promised in the study of a number of molecular and biochemical parameters, the disadvantage of primary TG cell culture is that preparation of dissected ganglia is inconvenient and the samples often contain heterogeneous groups of cells.

- **Fibroblast cell lines**

Another system used cultured cells derived from either human B cells or fibroblast cultures, infected by defective virus. Instead of using an inhibitor of viral replication, Preston *et al.* established latent HSV infection with replication-impaired viral mutants lacking VP16 and/or ICP0 function in cultured human fibroblast (Harris & Preston, 1991, Jamieson *et al.*, 1995, Preston & Nicholl, 1997). It has been shown that the quiescent virus can be reactivated by provision of exogenously-expressed ICP0 (Samaniego *et al.*, 1998, Stow & Stow, 1989), therefore this system has been exploited to investigate the role of ICP0 in the reactivation process (Everett *et al.*, 1998b, Harris & Preston, 1991).

- **Neuronal cell lines**

As studies with fibroblasts or lymphocytes may not be representative of neuronal cell viral latency following natural infection, several groups have developed a model based on PC12 cells to investigate the establishment of latency in a neuronal-like environment *in vitro* (Block *et al.*, 1994, Danaher *et al.*, 1999b). PC12, a rat pheochromocytoma tissue culture line, can be neurally differentiated by exposure to NGF. Differentiated PC12 (Nd-PC12) cells, when cultured on collagen-coated plates in the absence of serum, can be maintained as a non-dividing culture for up to seven weeks (Danaher *et al.*, 1999b). In the presence of NGF, most of Nd-PC12 cells can harbour HSV-1 in a cryptic and non-productive state that is reversible when NGF is removed from the culture (Block *et al.*, 1994). However, *in situ* analysis of long-term infected cultures revealed that LAT was expressed in only a proportion of the cells (Block *et al.*, 1994). More recently, Danaher *et al.* (1999) reported a modified system in which, by transient pre-treatment with ACV prior to infection, non-productive infection was established in all the cells in the culture, and ACV was not need for maintenance of the quiescent infection. After withdrawal of ACV, the quiescent infection state can be reactivated by treatment of forskolin at a high frequency (92-100%) in the culture (Danaher *et al.*, 1999b). Additionally, the reactivation in response to forskolin treatment can be detected in 50-100% of quiescently infected cultures up to 7 weeks post-ACV withdrawal. This group further characterised that in this system, after establishment of a quiescent infection with the transient use of ACV, reactivation could also be induced by heat stress (42°C, 3 hours) (Danaher *et al.*, 1999a). After the heat stress, the IE gene product ICP4 was expressed by 3 h post treatment, whereas other viral gene products (ICP0, ICP27, UL30, and UL18) were detected at 24 h

post induction at high levels (Danaher *et al.*, 1999a). These data imply that ICP4 may play an early role of co-ordinating reactivation from quiescent infection. This model has appealing features for studying gene expression during the establishment, maintenance and reactivation phases of HSV-1 quiescent state in cultures of rodent neuronally-derived cells.

1C Regulation of HSV-1 gene expression

As described in section 1B3.1.2, HSV-1 genes are categorised as immediate early (IE), early (E), and late (L), based on the time of their expression. Since this classification was first described in the early 1980s, the regulation of gene expression has been intensively studied, particularly the mechanisms that regulate this orderly and efficient expression of viral genes. Several lines of investigation have made a clearer picture of the temporal regulation of HSV gene expression, but a complete understanding of the mechanisms that turn on and turn off specific genes at the times required for efficient virus replication is lacking. Many recent studies have shown that some HSV proteins interact with cellular proteins. This indicates that virus-cell interactions play an important part in viral gene regulation by diversion and redirection of key cellular factors.

In this section, regulation of HSV-1 genes by HSV-1 polypeptides, as well as HSV-1 host cell interactions and their effect on viral gene expression, will be discussed.

1C.1 Activation of IE gene expression

IE genes were originally defined as genes whose expression occurs in the absence of *de novo* protein synthesis. The transcription of IE genes during the earliest stage of infection is stimulated by the virion transactivator protein VP16 (reviewed by O'Hare, 1993). As illustrated in Fig. 1.5, IE promoters contain several *cis*-acting elements: a TATA box, Sp1 binding sites, TAATGARAT elements, and in some instances binding sites for ICP4.

Activation of IE genes is initiated by the formation of a tri-partite complex consisting of VP16 and the cellular proteins Oct-1 and HCF (Host Cell Factor). VP16 first binds HCF and subsequently the VP16/HCF complex associates with Oct-1. The complex then binds to the TAATGARAT elements and activates gene transcription. A major factor in this binding is the presence of DNA binding domains within Oct-1 that recognise sequences overlapping the TAATGARAT motif. The C-terminal region of VP16 is responsible for the transactivation function while other regions of the protein are required for DNA binding and protein-protein interactions (reviewed by Flint & Shenk, 1997, Roizman & Sears, 1996). The conserved core region (residues 1-412) has been demonstrated to be required for formation of the tri-partite complex (Liu *et al.*, 1999). Analysis of the crystal structure of the VP16-core region revealed a seat-like structure which has been suggested to form a DNA-binding surface involved in DNA recognition (Liu *et al.*, 1999). It has

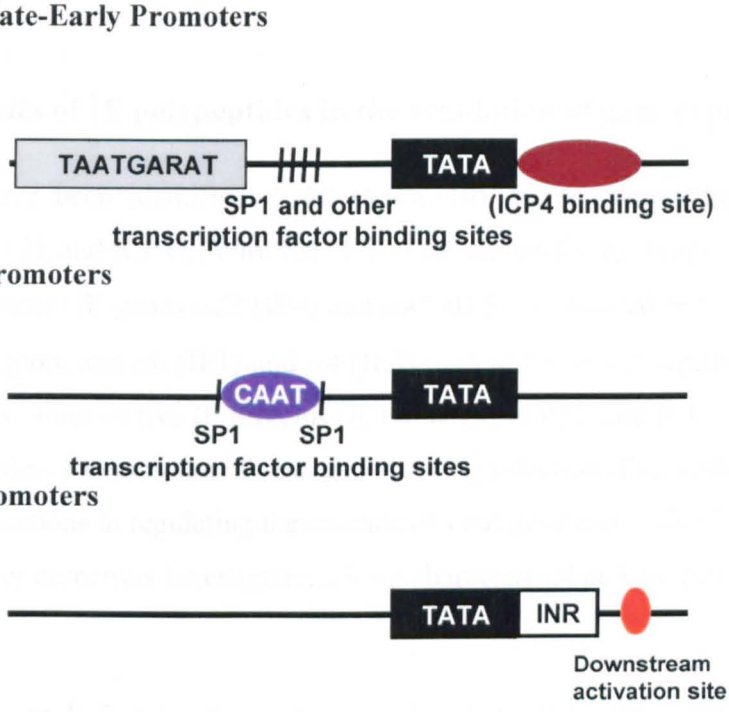

Fig. 1.5 Schematic representation of the cis-acting elements for IE, E, and L HSV-1 promoters.

(A) Expression of IE genes is regulated by various cis-acting elements including the viral IE specific regulating element (TAATGARAT), TATA box, binding sites for SP1 and other transcription factors, and in some cases, binding sites for ICP4.

(B) Early promoters consist of a TATA box, and binding sites for various transcription factors.

(C) Late promoters have a TATA box, an initiator element (Inr) at the start of transcription, and in some promoters, a downstream activation site. (adapted from Weir, 2001)

been reported that during HSV infection, HCF binds to VP16 to promote a stable interaction with Oct-1 (Hughes *et al.*, 1999) and it may also act as a nuclear import factor for VP16 (La Boissiere *et al.*, 1999).

1C.2 The potential roles of IE polypeptides in the regulation of gene expression

Five IE proteins have been identified: ICP0 (Vmw110), ICP4 (Vmw175), ICP22 (Vmw68), ICP27 (Vmw63), and ICP47 (Vmw12). Fig. 1.6A shows the locations of the IE genes in the HSV-1 genome: IE genes α22 (IE4) and α47 (IE5) are located in U_S region, α27 (IE63) lies in U_L region, and α0 (IE1) and α4 (IE3) map in the invert repeat regions with two identical copies. Four of five IE proteins (ICP0, ICP4, ICP22, and ICP27) play a role in controlling the order of expression of viral genes during infection (Fig. 1.6B). How each of these proteins functions in regulating the cascade of viral gene expression is not yet fully understood, however numerous investigations have characterised at least part of their distinctive roles.

ICP0, the α0, IE-1 or R_L2 gene product, is a phosphoprotein with an apparent molecular weight on SDS polyacrylamide gels of 110 kDa. It has been found to be a potent transactivator of expression of all classes of viral genes, as well as of cellular and other heterologous genes. There are no specific promoter sequences required for this activity in transient transfection assays. In some systems, the action of ICP0 is synergistic with ICP4, since in the presence of ICP4, the level of transcription in a transient assay is increased up to 20-fold higher than that with either transactivator alone (Everett, 1984b). Details relating to this function of ICP0 are discussed in section 1D.

ICP4, the α4, IE3 or R_S1 gene product, is another phosphoprotein with an apparent molecular weight of approximately 175 kDa. It is an essential protein for lytic replication of HSV-1, since in its absence infection does not proceed beyond IE gene transcription (Preston, 1979, Watson & Clements, 1980). As ICP4 *ts* mutant viruses overexpress IE products, it was suggested that ICP4 represses IE gene expression, including that of itself (DeLuca & Schaffer, 1985, Preston, 1979).

Several lines of evidence have proposed that this transactivation is mediated through the interaction of ICP4 with DNA and the TBP-containing general transcription factor

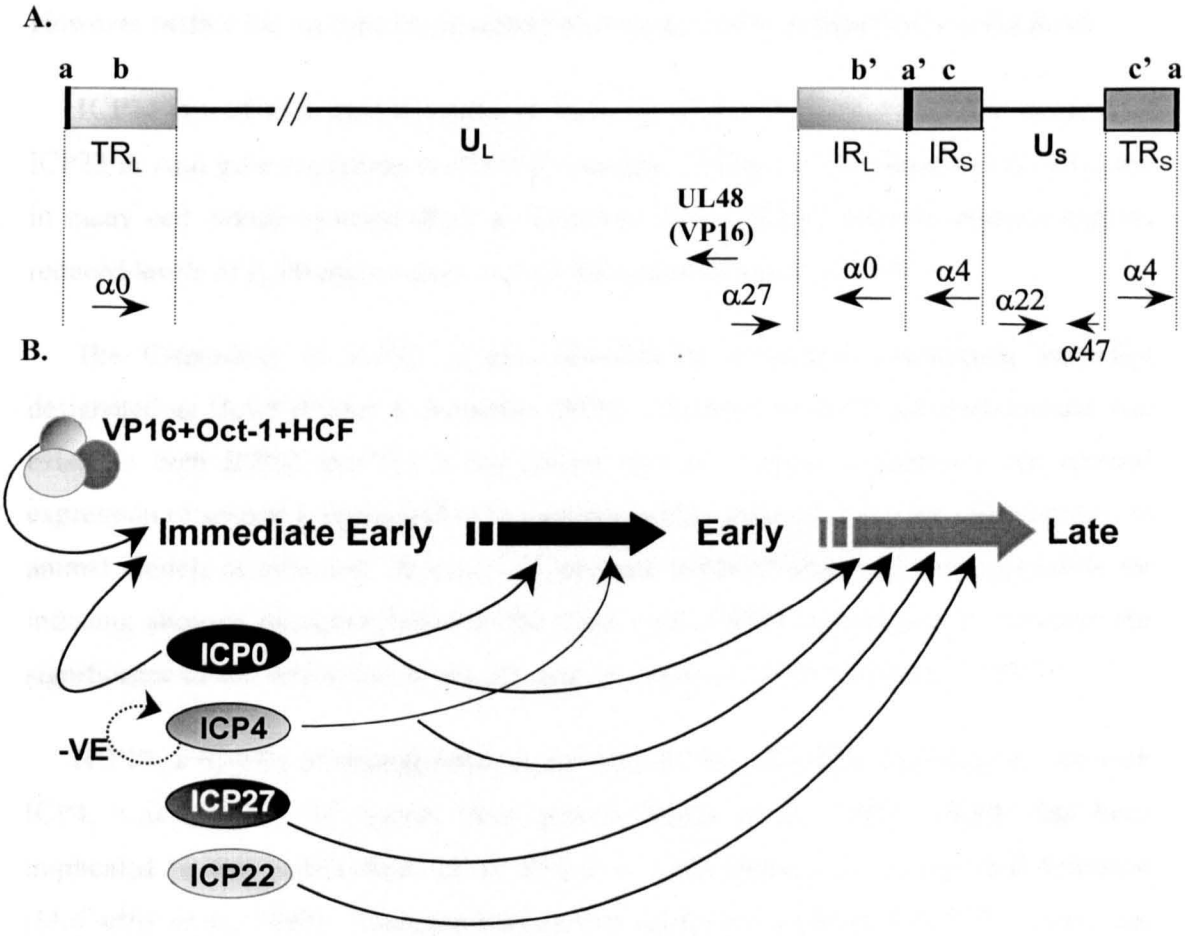

Fig. 1.6 A schematic diagram showing the location of IE genes on the genome of HSV-1 and regulation of gene expression by viral proteins.

(A) The approximate relative positions of HSV-1 IE and VP16 genes on the HSV-1 genome are illustrated. The direction of the arrows represent the direction of translation of each gene product.

(B) The role of four IE proteins in gene regulation is shown. ICP0 can transactivate promoters of the IE, E and L genes. ICP4 is essential for the activation of transcription of E and L promoters but can be a negative regulator for IE promoters. ICP27 is essential for efficient expression of L gene products. ICP22 also contributes to efficient expression of L gene products (modified from Everett, 2000).

TFIID (Gu & DeLuca, 1994). The cellular high mobility group factor 1 (HMG1) might facilitate this interaction by means of its ability to bend DNA (Carrozza & DeLuca, 1998). However neither the mechanism of activation nor repression is completely understood.

ICP22 is a 68 kDa protein expressed from the α22 (IE4, U_S1) gene. The function of ICP22 in viral gene regulation is relatively unclear. While it is non-essential for infection in many cell culture systems (Post & Roizman, 1981), ICP22 deletion mutants express reduced levels of ICP0 and a subset of viral late genes (Sears *et al.*, 1985).

The C-terminus of ICP22 is also encoded by a second overlapping transcript designated as $U_S1.5$ (Carter & Roizman, 1996). Analysis of the C-terminal domain that exists in both ICP22 and $U_S1.5$ has shown that this region is necessary for optimal expression of several L genes and virus mutants lacking these domains are also avirulent in animal models of infection. Recently, it has been reported that ICP22 is responsible for inducing aberrant phosphorylation of the large unit of RNA polymerase II, however the significance of this interaction is not yet clear (Long *et al.*, 1999, Rice *et al.*, 1995).

ICP27, a 63-kDa phosphoprotein, is encoded by the α27 (IE2, U_L54) gene. As with ICP4, it is essential for normal virus growth (Sacks *et al.*, 1985). ICP27 has been implicated in the switch from IE to E and L gene expression during viral infection (McCarthy *et al.*, 1989). Transient transfection assays have shown that ICP27 alone can transactivate the expression of gB (Rice & Knipe, 1988) and act in synergy with both ICP4 and ICP0 to repress expression of IE and E promoters as well as to activate expression from L promoters (Sekulovich *et al.*, 1988).

ICP27 performs multiple-functions that contribute not only to transcription but also to the post-transcriptional regulation of gene expression. It has been shown that ICP27 inhibits host cell pre-mRNA splicing which effectively shuts off host protein synthesis (Hardy & Sandri-Goldin, 1994, Sandri-Goldin & Mendoza, 1992). Most recently, ICP27 has been reported to interact with several cellular proteins, including at least one which inhibits splicing. This suggests a possible mechanism for ICP27-mediated inhibition of splicing (Bryant *et al.*, 2000, Bryant *et al.*, 2001, Wadd *et al.*, 1999). Since only four viral transcripts expressed during HSV-1 infection contain introns, splicing inhibition might to be benefit to viral transcripts over most cellular transcripts.

Furthermore, ICP27 has been reported to mediate the export of intronless viral RNAs, but has no effect on the export of cellular mRNAs (Koffa *et al.*, 2001, Sandri-Goldin, 1998, Soliman *et al.*, 1997). It was initially proposed that ICP27 affects nuclear export of viral RNAs via Crm1-dependent and -independent pathways (Soliman & Silverstein, 2000). However, most recently, investigation of ICP27 by microinjection into *Xenopus laevis* oocytes demonstrated a new model of the role of ICP27 in viral mRNA export (Koffa *et al.*, 2001). ICP27 has been found to bind directly to REF (RNA and export factor binding protein) and RNA and form a complex with REF and TAP. Additionally, an ICP27 mutant defective in REF-binding failed to stimulate viral mRNA export. These observations provide evidence that the function of ICP27 in the export of viral mRNA is via a TAP pathway and interaction with REF.

1C. 3 Activation of E gene expression

It has been established many years ago that functional ICP4 is necessary for the activation of both E and L gene expression (Watson & Clements, 1980). Additionally, the temporal regulation of E gene expression has been described to be mediated not only by ICP4 but is also dependent on *cis*-acting elements in Early promoters. Studies of the activation of E gene expression were extensively done using the thymidine kinase (tk) U_L23 gene. The original work in a *Xenopus oocyte* system illustrated that the *tk* promoter contains similar regulatory elements to those in an eukaryotic promoter. These are a TATA element, two Sp1 binding sites (GC boxes) and a CAAT element (Fig. 1.5B). No additional *cis*-acting element was identified during viral infection (Coen *et al.*, 1986). It was found that the TATA box was necessary for the accurate initiation of transcription and that the presence of upstream elements, the CAAT motif and GC boxes, enhanced transcription. These upstream elements are important for the regulation of *tk* gene transcription. Besides these elements, analysis of gD gene promoter revealed that cap-site region is necessary for E promoter activation; deletion of this region moderately decreased gD gene expression (Everett, 1984a). In absence of Sp1 binding sites and CAAT motif, *tk* was still expressed, but only if ICP4 is present (Imbalzano *et al.*, 1991). These findings strongly suggest that the TATA element and ICP4 may play an essential part in the activation of E gene expression. Furthermore, Cook *et al.* described that the TATA element appears to influence the strength of expression rather than the timing (Cook *et al.*, 1995). In contrast to IE promoters, E promoters do not appear to contain virus-specific *cis*-

acting regulatory elements (Everett, 1984a); how the transcription machinery differentiates between E and L genes to regulate temporal expression is still perplexing.

1C. 4 Activation of L gene expression

Viral DNA replication constitutes a major switch in the program of HSV-1 gene expression. True HSV-1 late genes, also called γ2 genes, require DNA replication for any accumulation of their mRNAs, whilst the expression of leaky-late genes, also referred as γ1 genes, can be detectable in the absence of viral DNA synthesis, however the maximal expression of γ1 genes requires DNA synthesis.

As mentioned previously (section 1C.2) functional ICP27 is required for L gene expression and is involved in multiple ways including transactivation and post-transcriptional regulation. Additionally, ICP4 is necessary for the activation of L gene expression, however the L genes are silent before DNA replication even at the time ICP4 is present. Further studies have proposed that another viral protein, ICP8, might be involved in regulation of L gene expression (Chen & Knipe, 1996, Gao & Knipe, 1991, McNamee *et al.*, 2000). As ICP8 is an essential protein for DNA replication, the reduced levels of L gene expression seen during infections with ICP8 virus mutants might be due to the decreased level of DNA replication resulting from defective ICP8. However, a cell line, stably expressing an ICP8 mutant (d105) protein, inhibited wild type virus DNA replication by 5-fold, and late gene expression by 50 to 100-fold, suggesting a direct role of ICP8 in stimulating late gene expression (Gao & Knipe, 1991, McNamee *et al.*, 2000).

As with IE and E genes, the *cis*-acting element of L promoters consist of a TATA box, but no additional upstream elements from the TATA box have been found (Fig. 1.5C) (Imbalzano & DeLuca, 1992, Johnson & Everett, 1986). Elements located at the start of transcription and further downstream appear to be necessary for maximal expression from these promoters. For instance the presence of a sequence related to the eukaryotic initiator element (Inr) in the gC promoter has been described to increase mRNA expression by a modest amount (Steffy & Weir, 1991, Woerner & Weir, 1998). Moreover, the promoters of some L genes, such as UL38 and gC, appear to contain another regulatory element downstream from the start of transcription called the downstream activation sequence (DAS) (Guzowski *et al.*, 1994, Petroski & Wagner, 1998). Analysis of the promoter region of UL38 has shown that deletion of the DAS, located between position +20 and +33

within the 5' non-translated region, from the UL38 promoter strongly decreased RNA expression to less than 10% of the wild-type level (Guzowski *et al.*, 1994, Petroski & Wagner, 1998). The structural differences between E and L promoters imply a possible mechanism of how the transcription machinery distinguishes E from L genes in the course of infection.

1C.5 The role of vhs in HSV-host cell interactions and viral gene expression

As viral gene expression is reliant on the transcription machinery of host cells, the virus has evolved various mechanisms that alter the cell to divert key cellular constituents from their normal uses and to redirect these components to the viral genome for its own needs. It is clear that some fundamental changes take place within the cell during infection, and one of the best characterised of these is the virion shutoff of host protein synthesis.

During lytic infection, HSV-1 causes the shutoff of host cellular protein synthesis soon after entering cells. The shutoff phenomenon was classified into two stages: early (primary or virion-associated) shutoff, and delayed (secondary) shutoff. The early shutoff is mediated by the virion host shutoff protein (vhs) and does not require *de novo* viral gene expression, whereas the delayed shutoff is induced by the IE protein ICP27 (Read & Frenkel, 1983, Sandri-Goldin & Mendoza, 1992). The role of ICP27 in host shutoff has been described previously (see section 1C.2).

The *UL41* gene product vhs is expressed as two forms, a 58-kDa and a 59.5 kDa highly phosphorylated form (Read *et al.*, 1993). The major 58-kDa vhs protein is a structural component, forms a complex with VP16 that is packaged into the tegument of HSV-1 particles and is then delivered into cytoplasm upon fusion of the viral envelope with the host cell membrane allowing it to exert its effects immediately upon infection (Smibert *et al.*, 1992). Vhs has been described as degrading both cellular and viral mRNAs of all three kinetic classes, resulting in the shutoff of protein synthesis (Kwong & Frenkel, 1987, Oroskar & Read, 1987, Oroskar & Read, 1989). The shutoff of expression of host genes may allow better utilisation of the translational machinery of the infected cells for translation of newly synthesised viral mRNAs. However, why does vhs affect viral RNA? One reasonable explanation of this discrimination of viral mRNA decay is that the presence of vhs likely facilitates rapid transition of viral mRNAs from one

temporal class to the next. Vhs mutants have been found to fail to shut down host cell protein synthesis and exhibit prolonged synthesis of IE and E proteins (Kwong *et al.*, 1988).

Many lines of evidence imply that vhs is either itself an RNase or mediates a ribonuclease activity by interacting with other cellular enzymes. Zelus and coworkers reported that vhs, obtained from partially purified virions or synthesised by *in vitro* translation, possesses an endonuclease activity, strongly implying that vhs protein itself is a ribonuclease (Zelus *et al.*, 1996). Karr and Read (1999) further elucidated the pathway of vhs-induced mRNA degradation by using a RNase protection assay. The kinetic data showed that in infected cells, vhs degrades sequences near the 5' end of the TK mRNA much more efficiently than those at the 3' end (Karr & Read, 1999). In contrast, TK mRNA was more stable and this decay rate difference was not observed in cells infected with a vhs mutant virus (Karr & Read, 1999). It has been speculated that the features of mRNAs i.e. a 5' cap or a 3' poly(A) tail, may play a role in selectively targeting mRNA for degradation, since vhs rapidly destabilises most viral and cellular mRNAs, while it does not affect tRNA and rRNA during viral infection. However Zelus *et al.* (1996) reported that the RNase activity of vhs, observed in *in vitro* reactions using virion extracts, cleaved both capped and uncapped RNAs. Moreover, the results from an *in vitro* assay, by which the susceptibilities of polyadenylated and non-polyadenylated identical mRNA to vhs-induced degradation were compared, demonstrated that both types of mRNA were degraded efficiently in extracts infected with wild type HSV-1 (Karr & Read, 1999). These observations imply that *in vitro* degradation of mRNA requires neither a 5' cap nor a 3' poly(A) tail. More recent work found that vhs produced in a budding yeast system did not lead to global mRNA degradation and the cell extracts of yeast only exhibited a little vhs-dependent endonuclease activity. However, the addition of a rabbit reticulocyte lysate (RRL) to the cell extracts restored its function (Lu *et al.*, 2001). These observations imply that the vhs-dependent RNase activity requires one or more mammalian factors. In addition to the effect on shutoff protein synthesis, vhs has been recently described to play a potential role in a decrease in viral replication as well as viral virulence, and immuno-evasion from a non-specific host defence mechanism (Suzutani *et al.*, 2000).

1D ICP0 (History)

The ICP0 protein, encoded by the α0 genes, was first described as an IE gene product in 1974 by Honess and Roizman (Honess & Roizman, 1974). The α0 genes are located at the repeat sequences that flank the U_L region of the HSV-1 genome (Fig. 1.6A) (Perry *et al.*, 1986, Preston *et al.*, 1978). Little was known of the role of ICP0 in virus infection until the early 1980s, when it was found that ICP0 was a potent transactivator of viral gene expression in transient transfection assays; in synergy with ICP4, the level of transactivation was 12 to 60-fold more effective than that obtained with ICP4 alone (Everett, 1984b). Further studies defined ICP0 as a potent promiscuous transactivator of gene expression of all three classes of HSV-1 viral genes and a number of cellular genes (Gelman & Silverstein, 1985, Mavromara-Nazos *et al.*, 1986, O'Hare & Hayward, 1985). Although it has been found that ICP0 expression is not essential for HSV-1 replication in cell culture, ICP0 null mutant viruses demonstrate reduced expression of IE proteins and impaired viral replication at low multiplicities of infection (Stow & Stow, 1986, Sacks & Schaffer, 1987). Moreover, several lines of evidence have shown that ICP0-defective mutant viruses are unable to induce the reactivation of latent virus in an *in vitro* system, indicating another potential role of ICP0 in HSV-1 infection (reviewed by Preston, 2000).

Most recently, the possible functions of ICP0 in HSV-1 infection have been illustrated through its interaction with cellular proteins and its effects on cell cycle regulation. It has long been noted that in infected cells, ICP0 is located at discrete subnuclear structures that are known as nuclear domain 10 (ND10) (Everett & Maul, 1994, Gelman & Silverstein, 1986, Maul & Everett, 1994). Further studies found that newly synthesised ICP0 initially accumulates at ND10 and then disrupts these structures within a few hours (Everett & Maul, 1994, Maul & Everett, 1994). Later it was found that ICP0 strongly interacts with a 135-kDa cellular protein designated USP7 (previously named HAUSP), a member of the ubiquitin specific protease family (Meredith *et al.*, 1994), and that ICP0 causes the proteasome dependent degradation of two major ND10 proteins, thus bringing about the destruction of ND10 (Everett *et al.*, 1998a). These activities have recently been attributed to the E3 ubiquitin ligase activity conferred by a zinc-binding RING finger domain within the N-terminal segment of the protein (Boutell *et al.*, 2002). Finally, it has been demonstrated that ICP0 affects proteins involved in cell cycle regulation, such as cyclin D3 and CENP-C (Everett *et al.*, 1999a, Kawaguchi *et al.*, 1997b), implying that ICP0 might

play a direct role in the regulation of the cell cycle. This suggestion was further supported by the finding that ICP0 blocked the G1 to S phase progression, and that HSV-1 infection caused dividing cells to become blocked in mitosis in an ICP0-dependent manner (Hobbs & DeLuca, 1999, Lomonte & Everett, 1999).

The interactions described above have been intensively studied and are likely to be crucial to the understanding of both lytic and latent infection. In this section, the details of each aspect: the characteristics of the ICP0 transcript and polypeptide, the potential role of ICP0 in HSV-1 infection, and the interaction of ICP0 with particular cellular proteins will be discussed in turn.

1D.1 The α0 gene and transcript structure

The diploid α0 gene, 3.6 kb in size, was mapped to the long repeat region of the viral genome (Fig. 1.1, 1.6A). In the IR_L region, the transcription of the α0 gene starts at residue 124256 and poly(A) signals 'AATAAA' are located at 120693 and 120734 (McGeoch *et al.*, 1988). As illustrated in Fig. 1.4A, the α0 gene located in IR_L region is partially overlapped in the same orientation by the gene encoding ICP34.5 transcripts and in the opposite orientation in part by the gene expressing LATs.

Among over 80 HSV-1 genes, only four genes contain introns; one of these is the α0 gene that contains two introns separating three coding exons. The three exons (1-3) are located at residues 124,108-124,052 (codons 1-19), 123,286-122,620 (codons 20-241), and 122,483-120,882 (codons 242-775), respectively (McGeoch *et al.*, 1988). After splicing of the pre-mRNA, the transcript encodes a predicted protein product of 775 amino acids. Since it has been described that both introns contain in-frame stop codons, it could be predicted that more than one species of ICP0-related protein product could be generated if alternative or incomplete splicing of the ICP0 pre-mRNA transcripts occurred. For instance, if either the first or the second intron of ICP0 pre-mRNA was not spliced out, premature termination of translation would occur, resulting in a truncated translation product of 72 or 262 residues, respectively. In fact, the predicted 262-residue protein to be expressed after incomplete splicing was detected at low levels in BHK cells infected with wild type virus and mutant virus 110C4 (which lacks the first intron), but not in cells infected with mutants 110C7 or 110C1 which lack the second or both introns, respectively (Everett *et al.*, 1993c). In addition, the amount of this truncated form of ICP0 varied

among cell types, i.e. there were only trace amounts in Vero, HeLa and HFL cells (Everett *et al.*, 1993c). The significance of this alternatively spliced ICP0 protein remains to be determined, especially since more recent experiments have shown it to have ubiquitin E3 ligase activity.

1D.2 ICP0 peptide structure and its functional domains

Although the full-length ICP0 transcript encodes 775 residues with a predicted molecular weight of 78,452 Da, the molecular weight of ICP0 polypeptides as measured by mobility in SDS-PAGE is approximately 110 kDa (Honess & Roizman, 1974). This difference between the predicted and observed molecular weights may be due to post-translational phosphorylation of a serine-rich region between residues 554-591 (Ackermann *et al.*, 1984), or it could be due to structural characteristics imparted by the RING finger (see below).

ICP0 can be detected in both the nucleus and the cytoplasm dependent on the time of the infection. During infection, ICP0 initially accumulates at 2 h post infection (hpi) in punctate structures in the nucleus, known as ND10, but by 8 hpi, ICP0 is present in both the nucleus and the cytoplasm and the punctate nuclear domains are no longer visible (Everett & Maul, 1994). Details of the interaction of ICP0 with ND10 proteins are provided in the later sections.

As described previously, ICP0 has multiple functions, including transcriptional activation in transient transfection assays, activation of gene transcription during the lytic cycle, and reactivation of latent viral genomes. Using mutational analysis combined with functional studies, four main functional domains of ICP0 protein have been revealed as shown in Fig. 1.7A.

Mutational analysis of the functional domains of ICP0 has shown that a cysteine-rich region in the N-terminal region (residues 106-150) is required for ICP0 function (Everett, 1987, Everett, 1988a, Everett, 1989). This particular motif of cysteine and histidine residues (C_3HC_4) is highly conserved in the corresponding proteins of other α-herpesviruses and has been classified as a member the RING finger family (Cheung, 1989, Freemont, 1993). Furthermore, some clusters of acidic and basic residues have been found throughout the ICP0 protein and among these regions a highly basic cluster between

A. The localisation of the functional domains within ICP0

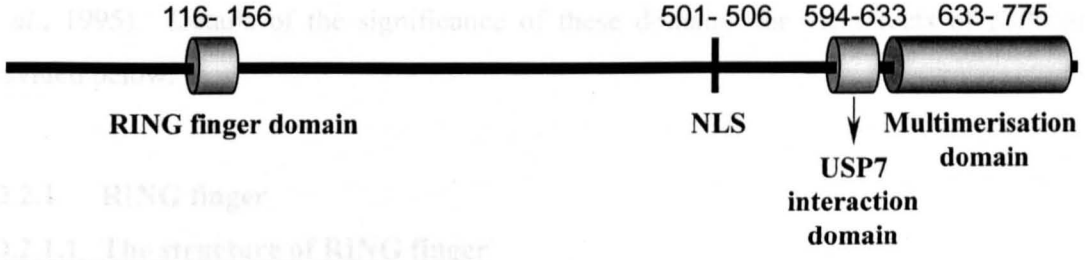

B. Secondary structure of C3HC4 motif

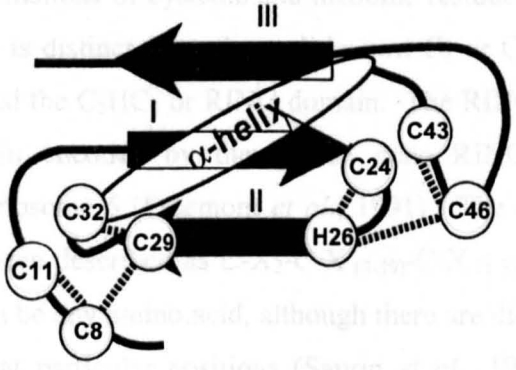

Fig. 1.7 Schematic of the functional domains within ICP0.

(A) Mutational analysis combined with functional studies of ICP0 have revealed the presence of four main functional regions, including the RING finger domain, a nuclear localisation signal (NLS), a USP7 interaction domain and a C-terminal multimerisation domain. The positions of these domains within the primary amino acid sequence of ICP0 is indicated by the numbers shown above.

(B) Arrangement of secondary structure in the RING motif within Eg63 (homologous to ICP0) of EHV-1. NMR revealed that this motif consists of a triple-stranded β-sheet, and two turns of α-helix. Conserved cysteine (C) and histidine (H) residues are mapped onto their approximate position as indicated (modified from Everett *et al.*, 1993b)

residues 501-506 has been implicated in the nuclear localisation of ICP0. Moreover, the C-terminal domain from residues 594-633 has been demonstrated to be required for the interaction of ICP0 with USP7 (Everett *et al.*, 1997, Meredith *et al.*, 1995, Meredith *et al.*, 1994). Finally, it has been reported that ICP0 purified using a baculovirus system exists as a multimer in solution and extensive studies have shown that the region spanning residues 633-775 is required for multimerisation (Ciufo *et al.*, 1994, Everett *et al.*, 1991, Meredith *et al.*, 1995). Details of the significance of these domains for the effects of ICP0 are provided below.

1D.2.1 RING finger

1D.2.1.1 The structure of RING finger

Metal-chelating domains such as zinc finger domains characteristically contain various combinations of cysteine and histidine residues. However, the conserved C_3HC_4 motif of ICP0 is distinct from the well known C_4 or C_2H_4 classes of zinc-fingers and it has been termed the C_3HC_4 or RING domain. The RING finger motif was initially identified in the protein encoded by the human gene RING1 (Really Interesting New Gene 1) on chromosome 6 (Freemont *et al.*, 1991). The consensus sequence of RING finger motifs has been described as $C\text{-}X_2\text{-}C\text{-}X_{(9\text{-}39)}\text{-}C\text{-}X_{(1\text{-}3)}\text{-}H\text{-}X_{(2\text{-}3)}\text{-}C/H\text{-}X_2\text{-}C\text{-}X_{(4\text{-}48)}\text{-}C\text{-}X_2\text{-}C$, where X can be any amino acid, although there are distinct preferences for certain types of amino acid at particular positions (Saurin *et al.*, 1996). In the case of ICP0, this motif lies between the residues 116-156. RING finger domains have been sub-divided into RING-HC and RING-H2 classes, depending on whether a cysteine or histidine occupies the fifth co-ordination site (reviewed by Freemont, 2000). Some other zinc finger-like domains have been found to be present in a subset of RING finger proteins. These are composed of larger motifs such as the RBCC subgroup (now termed TRIM; TRIpartite Motif) containing a RING finger, two B boxes, and a helical coiled-coil motif, and the TRAF subgroup consisting of a RING finger, a large number of putative zinc fingers (cysteine-/histine-rich regions), and a TRAF (tumour necrosis factor receptor-associated factor) domain. Many proteins containing the RBCC motif are proto-oncoproteins e.g. PML, while the most proteins in the TRAF family are involved in signal transduction pathways (reviewed by Jensen *et al.*, 2001).

As the C_3HC_4 motif has been predicted as a metal chelating domain, the structure of the RING finger was characterised by Everett *et al.* (1993). RING finger region peptides of ICP0 and two other homologous proteins in VZV (gene 61) and EHV-1 (gene 63) were overexpressed, purified, and analysed for their zinc content by atomic absorption spectroscopy and their concentration was determined by amino acid analysis (Everett *et al.*, 1993b). The most reliable results were obtained with the EHV-1 gene 63 protein RING domain (the other proteins tended to aggregate in solution) which was found to contain between 1.4 (± 0.4) and 3.7 (± 1.4) atoms of zinc per molecule (Everett *et al.*, 1993b). While some proteins containing RING finger domains have been implicated in the recognition of nucleic acids, no significant DNA or RNA binding of either full length or RING domain ICP0 was found in gel retardation assays (Everett *et al.*, 1993b).

Since the RING domain of ICP0, purified from a bacterial expression system, appeared aggregated or incompletely folded, only the secondary structure of this domain of the soluble equivalent protein of EHV-1 was studied (Barlow *et al.*, 1994, Everett *et al.*, 1993b). NMR (nuclear magnetic resonance) analysis of the secondary structure of the RING domain of the EHV-1 gene 63 protein (Eg63), overexpressed and purified using an *E. coli* system, revealed that starting from the N-terminus, this motif consists of an irregular loop, two strands of β-sheet, two turns of α-helix, a second irregular loop, and the third strain of the β-sheet (Fig. 1.7B) (Barlow *et al.*, 1994, Everett *et al.*, 1993b). Furthermore, two zinc atoms are co-ordinated at either end of the helix, which extends basic and polar side chains into solvent. The spacing between His 1 and Cys 4 leads to an observed inter-zinc distance of approximately 14 Å, which is highly conserved among members of the RING finger family (Fig. 1.7B).

1D.2.1.2 The RING finger family

Over two hundred proteins have been discovered containing a RING finger. The members in this family are derived from a wide range of eucaryotes including vertebrates, plants, and a number of DNA viruses, insects, and yeast (reviewed by Freemont, 1993). Many of these proteins have been implicated in regulatory events including transcription, DNA repair, inhibition of apoptosis, or site specific recombination, however up until recently no known function has been assigned to the RING finger motif (reviewed by Freemont, 1993, Freemont, 2000).

Since first proposed in 1998 by Bachmair, further studies have demonstrated that a large number of RING finger proteins are implicated in mediating E2-dependent ubiquitination (reviewed by Freemont, 2000). These investigations have shown that RING finger proteins can specifically interact with an E2 ubiquitin conjugating enzyme, thereby mediating ubiquitination, implying that the RING finger domain can act as an E3 ubiquitin ligase. Details of the process of ubiquitination and how the RING finger of ICP0 is involved in ubiquitination are discussed in a later section (1D.4.4).

1D.2.1.3 The role of the RING finger domain in the function of ICP0 in HSV-1 infection.

Results from a series of experiments have demonstrated that the RING finger domain is crucial for ICP0 function in HSV-1 infection, in terms of viral growth, establishment of latency and reactivation of the latent viral genome (Everett, 1989, Harris *et al.*, 1989, Wilcox *et al.*, 1997).

Single-step growth experiments have demonstrated that compared to wild type virus, the ICP0 RING finger mutant virus (FXE) reduced the yield of virus progeny by 1000-fold, indicating that the RING finger region of ICP0 is important for viral growth at least in cell culture (Everett, 1989). In the *in vitro* latency systems, it was found that the FXE mutant failed to reactivate a HSV-2 latent genome, indicating that the RING finger region is required for reactivation (Harris *et al.*, 1989). A recent report from Wilcox *et al.* (1997) showed that in the *in vitro* neuronal model (DRG culture), establishment of latency by virus FXE was decreased by at least 10-fold as measured by cell expression of LATs and the amount of viral DNA in neuronal culture during latency. Additionally, after establishment of latent infection, induction of reactivation by NGF deprivation in neuronal culture infected with FXE was much less than that with wild type virus (Wilcox *et al.*, 1997). These results indicate that a RING finger is required for the function of ICP0 in latent infection.

1D.2.1.4 Role of RING finger domain for the function of ICP0 in transcriptional regulation.

As described previously, ICP0 can stimulate gene expression either by itself or synergistically with ICP4. Studies of a number of ICP0 deletion mutants in transient

transfection assays showed that the RING finger domain was essential for the activation of HSV-1 genes by ICP0 (Cai & Schaffer, 1989, Everett, 1987, Everett, 1988a). Further analysis of single amino acid substitutions in a potential RING finger helix region (at residues: lysine 144, tryptophan 146, glutamine 148 and asparagine 151) was carried out to investigate the effect of this region on ICP0 function in detail. The results demonstrated that substitution of residues 144, 148, 151 affected ICP0 activation of gene expression, and that lysine 144 had the most substantial effect, which is similar to that of the RING finger deletion mutant, FXE. These observations imply that the helix region of the RING finger is responsible for the transcriptional activation function of ICP0 (Everett *et al.*, 1995).

1D.2.1.5 The RING finger domain of ICP0 is essential for disruption of ND10 and induced degradation of other cellular proteins.

At early stages of HSV-1 infection, ICP0 localises to ND10 structures and the disruption of these structures occurs a few hours post infection (Maul *et al.*, 1993). ICP0 has been shown to be absolutely required for this effect (Maul & Everett, 1994). The observation that punctate PML staining was retained in cells infected with the RING finger mutant virus FXE demonstrated that the RING finger domain is necessary for the disruption of ND10 proteins but not for the location of ICP0 to ND10 (Maul & Everett, 1994).

ICP0 also triggers the degradation of a number of cellular proteins such as PML, Sp100, CENP-C, and CENP-A (Everett, 1999, Everett *et al.*, 1999a, Everett *et al.*, 1998a, Lomonte *et al.*, 2001, Parkinson *et al.*, 1999). Subsequent investigations revealed that the RING finger domain of ICP0 is absolutely essential for the induction of protein degradation. The interactions of ICP0 with cellular proteins as well as the involvement of the RING finger in the effects are described in more detail in section 1D.4.

1D.2.2 Nuclear localisation sequence (NLS)

A highly basic region of ICP0 from residues 501-506 has a similar sequence to the SV 40 large T antigen nuclear localisation motif (Everett, 1988a). In a transfection assay, immunofluorescent staining of ICP0 deletion mutant p110D8 construct in which residues 475-548 were deleted, revealed a cytoplasmic expression pattern of ICP0, implicating a nuclear localisation sequence (NLS) located in this region (Everett, 1988a). In the viral

context, ICP0 expressed from D8 virus did not penetrate the nucleus at low multiplicities of infection. However at a higher multiplicity of infection, ICP0 staining was found in the nucleus at later stages, indicating that defective nuclear targeting can be overcome when D8 proteins are highly expressed (Maul & Everett, 1994). In addition, insertion of a oligopeptide (VRPRKRR) at residue 500 of an ICP0 mutant in which residues 500-506 were deleted resulted in the restoration of ICP0 nuclear localisation phenotype, suggests that the highly basic region at residues 500-506 might promote nuclear targeting (Mullen *et al.*, 1994). However a previous finding described a cytoplasmic pattern of ICP0 when expressed from p110D16, a large C-terminal deletion mutant construct that retains the 501-506 region (Everett, 1988a). These observations imply that this basic motif alone is not sufficient for nuclear localisation and that residues on its C-terminal side are also required.

This region has also been implicated in the regulation of gene expression and the efficiency of viral infection. Deletion of the NLS motif demonstrated a lower transactivation ability of ICP0 in the presence of ICP4 (Everett, 1988a). Furthermore, the D8 mutant virus caused a moderate reduction of viral protein synthesis resulting in a lesser yield of viral progeny in single-step infection as well as inefficient plaque formation in tissue culture (Everett, 1989).

1D.2.3 The USP7 interaction domain

Glycerol gradient centrifugation showed that ICP0 extracted from infected cells sedimented in a high molecular weight complex that contained a cellular protein of approximately 135 kDa. This was later identified as a novel ubiquitin specific protease named USP7. Further results obtained from GST pull-down experiments revealed that the C-terminus of ICP0 (residues 594-775) bound strongly and specifically to USP7 in all cell types tested (Meredith *et al.*, 1994). An extensive characterisation of this domain narrowed down a region between residues 594-633 that was required for the interaction of ICP0 with USP7 (Meredith *et al.*, 1995).

Characterisation of ICP0 mutant viruses demonstrated that deletion virus D12, lacking the sequences involved in USP7 binding, had greatly reduced viral growth (Meredith *et al.*, 1995). This domain has also been implicated as being important for the stimulation of gene expression, as the ICP0 expressed from the p110D12 construct (deletion of residues

594-633) showed significantly reduced ability to activate gene expression in transfection assays (Everett, 1988a).

1D.2.3 Multimerisation domain

Everett *et al.* initially described that ICP0 exists as a dimer or as a higher order oligomer in solution according to the sedimentation rate of purified ICP0 on glycerol gradients compared to that of known standards (Everett *et al.*, 1991). Observations by subsequent studies using *in vitro* translated polypeptides and GST-fusion proteins indicated that a region between residues 617-712 is required for fully efficient multimerisation and that the 60 residues on either side of this region were also involved (Ciufo *et al.*, 1994). This result was confirmed by the finding that a protein containing the C-terminal residues 633-755 expressed in an *E. coli.* system was purified as a dimer or a trimer, implying that the multimerisation domain of ICP0 lies between 633 and 775 (Meredith *et al.*, 1995).

Additional studies revealed another functional domain within the region between residues 633 and 755. Maul *et al.* (1994) reported that in immunofluorescence assays the expression pattern of ICP0 in cells infected with mutant virus D13, which lacks C-terminal residues 633-680, revealed a nuclear diffuse phenotype instead of the normal punctate staining pattern indicating that this region is essential for the binding of ICP0 to ND10.

The C-terminal multimerisation domain has been reported as being important for the transactivation ability of ICP0. A reduction in the level of transcription was found in cells transfected with the construct lacking this region (Everett, 1988a). However, the level of requirement of the multimerisation domain varied for different promoters and cell types. In addition, a number of mutant viruses, including D13, D14, D15, in which the C-terminus region at residues 633-680, 680-720, 723-767 were deleted, respectively, showed a lower growth efficiency than wild type (Everett, 1989). Taken together, the C-terminal of ICP0 is important for viral gene expression and viral growth.

1D.3 Role of ICP0 in HSV-1 infection

The principle functions of ICP0 have been assessed both in transient transfection systems and during HSV-1 infection. These studies have focused on the effect of ICP0 on

viral growth, gene expression, reactivation and interaction with cellular proteins as discussed below.

1D.3.1 ICP0 is not essential for viral growth at high virus inputs

Studies using mutant virus, dl1403, containing a 2-kb deletion within both copies of the α0 gene, found that the mutant virus was able to grow in BHK cells, but that the yield of virus was 20- to 100-fold lower than that of wild type HSV-1 (Stow & Stow, 1986). The efficiency of plaque formation by dl1403 varied between the different cell types tested; Vero and human foetal lung cells (HFL) were much less efficient in supporting the growth of dl1403 than BHK cells. Surprisingly, the protein profiles generated by dl1403 in time course experiments at a high MOI (5 pfu/cell) were qualitatively similar to that of wild type HSV-1. In addition, replication and encapsidation of viral DNA in cells infected with dl1403 were not significantly different from that in cells infected with wild type virus.

Consistent observations were reported by Schaffer's group using two different ICP0 mutant viruses, the dlx0.7 virus, containing a deletion of 0.7-kb in both α0 genes, and the dlx3.1 virus, containing a 3.1-kb deletion removing the majority of the transcriptional regulatory signal and coding sequences (Sacks & Schaffer, 1987). Although both mutants grew in cell culture, the yields were 10- to 100-fold lower than those of wild type HSV-1 irrespective of the cell types used. These findings imply that although ICP0 is not absolutely essential for productive infection in the majority of cell lines, this protein plays a significant role in viral growth, as demonstrated by the impaired ability of the mutant to replicate.

The role of ICP0 in HSV-1 infection was studied in more detail by Everett (1987) using strategies involving a series of mutant viruses with defined lesions in ICP0, different cell types and various amounts of virus inputs. These assays illustrated that the reduction in plaque-forming efficiency by ICP0 mutants is dependent on cell type, the position of the mutation as well as multiplicity of initial virus input (Everett, 1989). At a high multiplicity of infection, all mutant viruses gave similar levels of gene expression to wild type virus, whereas less viral gene expression was observed in cells infected with mutant viruses at a lower multiplicity, especially in HFL cells. These results strongly suggest that the presence of ICP0 confers a strong selective advantage for the earliest stage of low multiplicity infections in certain types of cells.

Consistent with the requirement of ICP0 for viral infection at low multiplicities, Cai *et al.* illustrated that in Vero cells transfected with infectious viral DNA of an ICP0-null mutant, virus production was delayed for 2 days and the level of *de novo* synthesis of the virus was reduced (Cai & Schaffer, 1989). Additionally, at a very low multiplicity of infection (0.004 pfu per cell), they found that 90% or more of the ICP0 coding sequence was required for efficient replication of HSV-1.

Although ICP0 confers a significant growth advantage on the virus, especially at low MOIs, further experiments using the osteosarcoma line U2OS found that the function of ICP0 is dispensable, even for low MOIs (Yao & Schaffer, 1995). In contrast to the equal plating efficiencies of wild type viruses on Vero and U2OS cells, the plating efficiencies of the ICP0-null mutant virus 7134 was increased by 100-fold in U2OS cells compared to Vero cells. Transient transfection of U2OS cells with reporter gene constructs containing IE, E, and L gene promoters followed by chloramphenicol acetyltransferase (CAT) assay revealed enhanced basal levels of expression from IE and E, but not the L promoters tested, in this cell line. These observations strongly support the argument that the requirement of ICP0 in HSV-1 infection varies between cell types and also implies that there may be a cellular activity in U2OS cells that substitutes for the function of ICP0 at low MOIs. Alternatively, U2OS cells may lack a factor that in the absence of ICP0 is able to repress viral gene expression.

1D.3.2 ICP0 activates the transcription of viral genes

The function of ICP0 in HSV-1 infection was first shown as that of a potent transactivator of gene expression in transient transfection assays (Everett, 1984b). The experiments were designed to investigate the role of IE gene products in terms of transactivation of viral E promoters. In HeLa cells, ICP4 stimulated expression from the E gD promoter, but this effect could be increased by a further 20-fold in the presence of ICP0 (Everett, 1984b). Later investigations from other groups showed that ICP0 can independently stimulate expression from the HSV-1 thymidine kinase promoter (Gelman & Silverstein, 1985, O'Hare & Hayward, 1985). A number of further studies revealed that ICP0 is able to transactivate promoters from all three classes of HSV-1 genes (Chen *et al.*, 1991, Everett, 1984b, O'Hare & Hayward, 1985, Quinlan & Knipe, 1985).

The transactivation function of ICP0 appeared not to be limited to HSV-1 promoters but rather has a non-specific nature. A variety of heterologous viral promoters including the SV40 early promoter, HSV-2 38K promoter, and the HIV long terminal repeat have been reported to respond to ICP0 (Everett, 1988b, Mosca *et al.*, 1987, O'Hare & Hayward, 1985). In addition, it has been shown that ICP0 can induce transcription of some cellular genes, for example the rabbit β-globin promoter and the human ε-globin promoter (Everett, 1985). Observations from transient expression assays led to the conclusion that ICP0 alone is a potent and promiscuous activator of both viral and cellular gene expression and can act in synergy with ICP4.

Recently, the level at which ICP0 activates viral gene expression was defined by comparing the activation levels of promoters representing the major kinetic classes of viral genes (such as *tk*, ICP8, gC) in both transient expression assays and during HSV-1 infection (Jordan & Schaffer, 1997). The levels of transcription and translation were determined by quantitative RNase protection and CAT assays respectively. The experiments utilised transfection in the presence or absence of ICP0, and cells infected with wild type (KOS strain) or ICP0 null mutant, n212 viruses. In both transfection and infection experiments at all multiplicities tested, the levels of mRNA and protein were significantly lower in the absence of ICP0. Changes in the levels of CAT activity were approximately proportional to change in the levels of CAT mRNA in cells infected with wild type or n212. Taken together, these findings indicate that ICP0 activates gene expression by increasing the amount of mRNA and it has no significant effect on the efficiency of translation in both transient transfection assays and during infection.

It has been reported that mutants of ICP0 that are defective in transactivation function are also defective in promoting viral growth, indicating that the ability to activate gene expression reflects the requirement for ICP0 in viral growth (Everett, 1989, Sacks & Schaffer, 1987)

1D.3.3 ICP0 is essential for reactivation of HSV-1 from quiescent infection

The potential involvement of ICP0 in the establishment or reactivation of HSV-1 from latency was indicated initially by Russell *et al.* (1987) in an *in vitro* system. In this model three HSV-1 mutant viruses including two ICP4 mutants (*ts*K and *in*1411) and the ICP0 deletion mutant dl1403 were able to establish a latent infection in HFL cells as efficiently

as wild type HSV-1 and HSV-2 at 42°C, a temperature preventing the onset of lytic infection. These observations imply that the presence of ICP0 is not an absolute requirement for establishment or maintenance of latent infection *in vitro*. Cultured cells quiescently infected with HSV-2 could be induced to reactivate the resident virus if superinfected with wild type HSV-1, but not if the ICP0 deletion mutant dl1403 was used. This indicates that ICP0 is specifically required for the reactivation of quiescent genomes (Russell *et al.*, 1987). As illustrated in Fig. 1.4, the 3' part of the LAT region is complementary to the 3' end of the ICP0 gene. Since the region deleted from dl1403 includes large portions of both the ICP0 and LAT genes, phenotype of dl1403 could be a consequence of the loss of LAT function. Therefore, HSV-1 mutants with more precise deletions in ICP0 were employed to investigate this issue in more detail (Harris *et al.*, 1989). The establishment and reactivation of HSV-2 latent infection was set up in the same way as by Russell *et al.* (1987). The results demonstrated that adenovirus recombinants expressing ICP0 were able to reactivate HSV-2 latent genomes, implicating a direct role of ICP0 in reactivation from latency. In addition, superinfection with the ICP0 deletion mutant virus D14 (deletion of residues 680-720) caused reactivation of quiescent virus, but deletion of the ICP0 RING finger domain in mutant FXE eliminated the ability of the superinfecting virus to reactivate the quiescent HSV-2. These results indicate that sequences in the 3' end of the LAT region are not necessary to induce reactivation in this system, but that the RING finger domain of ICP0 is essential for this process.

The role of ICP0 in latency has also been extensively investigated in the mouse model. Lieb *et al.* (1989) initially approached this study using a mouse ocular model. Three ICP0 deletion mutants, dl1403, dlx0.7 and dlx3.1 (described in section 1D3.1) were tested for their ability to establish latency in mouse ganglia. It was found that all three mutant viruses were able to replicate in ganglia, although with a reduced efficiency. The dlx0.7 and dlx3.1 mutant viruses failed to reactivate from the explanted trigeminal ganglia of infected mice, implying that ICP0 might play an important role in establishment and/or reactivation from latency (Leib *et al.*, 1989). However, Clements and Stow (1989) demonstrated a contrary finding that ICP0 is dispensable for the establishment and maintenance of latency, and for reactivation from latently infected mouse ganglia. The assays by footpad route and intracranial inoculations revealed that dl1403 exhibited a much lower virulence than the wild type 17+ strain. After footpad inoculation, the mutant virus established latency in

sensory ganglia and by 20 days post-explantation, reactivation occurred from an average of 3.4 explanted ganglia/mouse (Clements & Stow, 1989). However, reactivation of dl1403 was delayed compared to the wild type virus.

For these different findings in the reactivation phenotypes of ICP0 mutants derived from the wild type strains KOS (dlx0.7 and dlx3.1) and 17+ (dl1403), the authors suggested that the differences might be due to strain-specific variations or reflect residual activities of the undeleted portion of ICP0 and LAT genes. However, it is more likely that the apparent discrepancies reflect differences in the latency models used and other criteria such as the exact multiplicities of infection and the methods of explant co-cultivation used. Later work from Schaffer's group has proposed strong evidence supporting a role for ICP0 in the establishment and reactivation of latency (Cai *et al.*, 1993). A series of ICP0 mutations which express ICP0 with C-terminal truncations, all of which express nearly wild type 2.0-kb LAT, were constructed and characterised for their ability to establish and reactivate from latency in a mouse ocular model. All of the mutants entered and reactivated from latent infection less efficiently than wild type virus, and reactivation frequencies correlated well with the levels of transactivating activity induced by the individual ICP0 mutant polypeptides. In addition, the defective reactivation of an ICP0-LAT-double mutant virus, 7134, from latency could be restored by insertion of one copy of $\alpha 0$ gene into the 7134 viral genome. These findings indicated a role for ICP0 distinct from the role of LAT in the establishment and reactivation of latency.

More recently, Halford and Schaffer demonstrated that a reduction in the size of the inoculum (from 2×10^6 to 2×10^5 pfu per eye) of ICP0 null mutants coupled with transient immunosuppression of mice, enabled ICP0 null mutants to reach wild type levels of viral load in the TG of latently infected mice (this model was described in section 1B.3.2.3) (Halford & Schaffer, 2000). Based on this procedure, the role of ICP0 in reactivation was determined by comparison of the reactivation efficiencies of two ICP0 null mutants, n212 and 7134 with that of wild type in four different assay systems in which the TG were either treated with or without ACG followed by various reactivation methods such as heat stress or superinfection with ICP4$^-$ (ICP0$^+$) mutant virus (Halford & Schaffer, 2001). The results showed that superinfection with the ICP4$^-$ virus, expressing ICP0, resulted in the 100% reactivation of TG cultures latently infected with KOS, n212, or 7134. Moreover, with reactivation by means of heat shock, two ICP0 mutants reactivated inefficiently from

latently infected TG cells, strongly implying that ICP0 is required for inducing efficient reactivation of the HSV-1 genome from latency.

1D.4 The effects of ICP0 on cells and cellular proteins.

ICP0 has been proposed to interact with a number of cellular factors representative of a variety of cellular pathways, including components of cellular transcriptional (Kawaguchi *et al.*, 2001, Lees-Miller *et al.*, 1996), translational (Kawaguchi *et al.*, 1997a), protein degradation (Boutell *et al.*, 2002, Everett *et al.*, 1999a, Everett *et al.*, 1998a, Everett & Maul, 1994), and cell cycle control pathways (Hobbs & DeLuca, 1999, Kawaguchi *et al.*, 1997b, Lomonte & Everett, 1999). It has been assumed that the potential interactions of ICP0 with cellular factors might contribute to its functions in HSV-1 infection via effects on host cell metabolism and pathways. The details of these interactions are described below.

1D.4.1 ICP0 induces the destruction of ND10

Gelman and Silverstein (1985) first observed the localisation of ICP0 in punctate foci in the nucleus of infected cells, but it was not until later that Maul and co-workers (1993) defined that early in HSV-1 infection ICP0 colocalised with the punctate subnuclear structures known as ND10 (nuclear domain 10). Details of ND10 constituents, their effects on cellular processes and their fate in response to viral infection are discussed in section 1E and reviewed by Negorev & Maul (2001)and Sternsdorf *et al.* (1997).

It was found that the colocalisation of ICP0 with ND10 was transient, since at later times of infection ND10 structures were disrupted and the constituent proteins dispersed in infected cells (Everett & Maul, 1994, Maul *et al.*, 1993). ICP0 was reported to be sufficient for this effect, as ND10 structures were retained in cells infected with dl1403, the ICP0 deletion mutant, but not in those infected with wild type virus at a later time of infection, 6 hpi (Maul & Everett, 1994). Western blot analysis of infected cell extracts revealed that several high-molecular-weight isoforms of PML, one of the most well known ND10 constituents, were lost or reduced in quantity, implying that loss of the bands might correlate with the disruption of ND10 during HSV-1 infection (Everett *et al.*, 1998a). A variety of evidence strongly suggests that the high molecular weight PML isoforms comprise covalent conjugates with another ND10 constituent, the small ubiquitin-like

protein SUMO-1 (Duprez *et al.*, 1999, Muller & Dejean, 1999, Sternsdorf *et al.*, 1999). The loss of PML and its isoforms did not occur in cells infected with ICP0 mutant viruses, particularly the RING finger deletion mutant FXE, and the effect could be inhibited in wild type virus infections by the addition of proteasome inhibitors (MG132 and lactacystin) during infection (Everett *et al.*, 1998a). These observations indicate that the degradation of PML isoforms requires fully functional ICP0 and is also dependent on an active proteasome-dependent proteolysis pathway.

1D.4.2 ICP0 interacts with ubiquitin-specific protease USP7

As described in section 1D.2.3, ICP0 immunoprecipitates with USP7 via an interaction with sequences in the C-terminal region of ICP0 between residues 594-775 (Meredith *et al.*, 1995, Meredith *et al.*, 1994).

Analysis of expressed sequence tag libraries from a variety of tissues demonstrated that USP7 is expressed in a wide variety of cell types and tissues, such as human brain, liver and placenta. The function of USP7 is unclear, however one function of USP enzymes is to cleave ubiquitin adducts from substrate proteins, thereby protecting the substrates from proteasome degradation and recycling free ubiquitin. Alternatively, USP enzymes cleave ubiquitin precursor molecules, again producing free ubiquitin for use in proteasome-dependent degradation. Results from indirect immunofluorescence assays, using an anti-USP7 rabbit serum (r206), showed that USP7 is predominantly a nuclear protein with a microspeckled nuclear staining pattern (Everett *et al.*, 1997). Double-staining with antibodies for USP7 and PML revealed that accumulations of USP7 were associated with a proportion of ND10.

Definition of the minimal region of ICP0 required for the interaction with USP7 demonstrated that ICP0 residues 594 to 646 are sufficient for binding to USP7 and residues 618-631 are essential for this interaction *in vitro* (Everett *et al.*, 1999c). Interestingly, in the region between residues 618 and 638, 7 charged residues are precisely conserved in the equivalent protein of HSV-2. Binding studies of a number of single and double amino acid substitutions in this region revealed that lysine 620 and lysine 624 of ICP0 were critical for USP7 binding.

Transfection studies using mutants of ICP0 that are unable to bind to USP7 demonstrated that all exhibited reduced activation of gene expression. For instance,

activation of gene expression in transfected cells expressing the M1 (K620R, K624R) and M4 (K620R) mutants was reduced to the same level as that observed with a RING finger deletion mutant. These observations strongly suggest that the ability to bind to USP7 contributes to the activation of gene expression induced by ICP0 in transient transfection assays. In addition, in single-step growth curve experiments, the yields of virus progeny from cells infected with mutant viruses derived from constructs M 1 and M4 were reduced by approximately 10-fold at 16 and 24 hours post infection. Taken together, specific single or double point mutations in ICP0 can reduce USP7 binding to background levels and also cause significant growth defects, indicating that the ability of ICP0 to bind to USP7 is important for its biological functions (Everett *et al.*, 1999c, Meredith *et al.*, 1995).

1D.4.3 ICP0 interferes with the cell cycle progression

It has been reported that the impairment of plating efficiency and synthesis of viral proteins characteristic of the ICP0 null mutant virus 7134 can be overcome by plating the virus on a synchronised Vero cell monolayer 8 h after release from growth arrest. This corresponds to a stage in the cell cycle between G_0/G_1 and S phase (Cai & Schaffer, 1991). Further studies demonstrated that CAT expression driven by the ICP0 promoter (but not by the E and L promoters tested) was enhanced 10- and 3-fold in Vero and NB41A3 (mouse neuroblastoma) cells transfected at 6 and 2 h post release from growth arrest, respectively (Ralph *et al.*, 1994). These observations suggest that a cellular function may be expressed during the transition of growth-arrested cells from G_0 into the G_1 phase of the cell cycle that can functionally substitute for the transactivating activity of ICP0.

Another line of studies showed that ICP0 may interact directly with the cell cycle regulatory machinery since it has been found to bind to and stablise cyclin D3 (Kawaguchi *et al.*, 1997b). This interaction was abolished by replacement of the aspartic acid at position 199 with alanine (mutant D199A) (Kawaguchi *et al.*, 1997b). A subsequent study used two recombinant viruses, R7801 (expressing wild type ICP0 and also cyclin D3) and R7916 (expressing the D199A substituted ICP0 and cyclin D3) to investigate the potential effect of this interaction and the role of cyclin D3 in the biology of ICP0 (Van Sant *et al.*, 2001). The results demonstrated that early in infection with R7801, ICP0 colocalised with cyclin D3 in the vicinity of ND10 structures, whereas the D199A substituted ICP0 remained in ND10, and did not colocalise with cyclin D3. Furthermore, in cells infected

with recombinant virus expressing cyclin D3, ICP0 was translocated to the cytoplasm from the nucleus more efficiently than wild type virus infections. These results indicated that the interaction of ICP0 with cyclin D3 might be responsible for the stabilisation and activation of G1-phase cyclins by activating cdk4 (cyclin-dependent kinase 4), localising cyclin D3 to the vicinity of ND10 structures, and the acceleration of the translocation of ICP0 from the nucleus to cytoplasm. Although the net effect of this interaction is unclear, it was shown that failure to bind cyclin D3 correlated with reduced replication in quiescent HEL (human embryonic lung) cells implying that interaction of ICP0 with certain D-type cyclins contributes to viral replication (Van Sant *et al.*, 1999).

More recently, a number of studies demonstrated that ICP0 possesses the ability to inhibit the progression of the cell cycle (Hobbs & DeLuca, 1999, Lomonte & Everett, 1999). Hobbs and DeLuca (1999) reported that infection with the mutant virus *d*106, in which IE gene expression is restricted to that of ICP0, caused cell cycle arrest at both the G1/S and G2/M transitions, whereas mutant virus *d*109, which does not express any viral proteins, failed to induce this phenotype. These data indicate that functional ICP0 is able to induce cell cycle arrest. Consistent with the above findings, Lomonte and Everett (1999) demonstrated that transfected cells expressing an EGFP-ICP0 fusion protein became stalled at the G1/S phase boundary. Infection of synchronised cells in the S phase or G2 with wild type HSV-1 resulted in a block of the infected cells at an unusual stage of mitosis named pseudo-prometaphase (Everett *et al.*, 1999a). The dysregulation of the cell cycle in mitosis was shown to be caused by the ICP0 induced proteasome-dependent degradation of CENP-C (Everett *et al.*, 1999a), a centromeric protein component of the inner kinetochore plate which is essential for cell division (Earnshaw & Rothfield, 1985). Most recently, ICP0-induced degradation of another centromere protein, CENP-A, has been shown to contribute to mitotic arrest of HSV-1 infected cells (Lomonte *et al.*, 2001). The 17-kDa CENP-A protein is a histone H3-like protein associated with the nucleasome structure in the inner plate of the kinetochore (Sullivan *et al.*, 1994). As with CENP-C, the CENP-A protein was degraded by ICP0 via a proteasome-dependent pathway in infected cells (Lomonte *et al.*, 2001). Taken together, all the observations described above imply that HSV-1 is able to influence and is influenced by cellular factors involved in the G_1/S or mitotic phases of the cell cycle.

1D.4.4 ICP0 has ubiquitin E3 ligase activity *in vitro*

As previously described in this section (section 1D.4), ICP0 has been reported to bind strongly to USP7 and has also been implicated in triggering degradation of a number of cellular proteins via a proteasome-dependent pathway. In addition, several studies have described that a variety of RING finger proteins are involved in the ubiquitin-proteasome pathway by acting as ubiquitin E3 ligases (reviewed by Freemont, 2000). Recently, two laboratories have published evidence that ICP0 possesses E3 ubiquitin ligase activity in a variety of *in vitro* assays (Boutell *et al.*, 2002, Van Sant *et al.*, 2001). The ubiquitin-conjugation pathway involves three enzymes, E1, E2 and E3. Protein ubiquitination initialises with the formation of a thiol-ester linkage between the C-terminus of ubiquitin (Ub) and the active site cysteine of E1 (Ub activating enzyme) and then its transfer to a similar thiol-ester linkage on an Ub conjugation enzyme (Ubc or E2). Cells express only one E1 enzyme, but there are several different E2 enzymes that are related by their possession of a conserved active site domain. E3 Ub ligase proteins have been defined by their ability to stimulate the activity of E2 enzymes and in some cases to confer substrate-specific ubiquitination activity. E3 Ub ligases facilitate the formation of isopeptide bonds between the C-terminal glycine of Ub and the side chain amide group on lysine residues either on the target protein, or on the last Ub of a protein-bound poly-Ub chain.

Boutell *et al.* demonstrated that in *in vitro* reactions containing free ubiquitin, E1 and E2 (UbcH5a or UbcH6) enzymes, addition of purified proteins including His-ICP0 (expressing full length ICP0), GST262 (a GST fusion protein incorporating ICP0 residues 1-262) or GST241 (containing ICP0 residues 1-241) strongly induced the accumulation of poly-ubiquitin chains (Boutell *et al.*, 2002). ICP0 mutant derivatives of these constructs containing a variety of mutations in the region of the RING domain failed to stimulate E2 enzyme activity. These observations indicate that ICP0 acts as an E3 Ub ligase and that the RING finger region is absolutely required for this activity. Moreover, immunofluorescence staining of transfected cells revealed that ICP0 sequestered a proportion of co-expressed UbcH5 and UbcH6 in the ICP0 foci in both the nucleus and in the cytoplasm of many cells. However no substantial interaction between ICP0 and the E2 enzymes was found in GST-pull down assays. On the other hand, the conclusion of Van Sant *et al.* (2001) that ICP0 has *in vitro* E3 Ub ligase activity was based on the observation that the activity of E2 enzyme cdc34 was stimulated by a GST-ICP0 fusion protein containing C-terminal residues 543-768. This region does not include the RING finger

domain of ICP0, therefore they suggested that ICP0 uses an alternative region for its E3 ligase activity. These results conflict with the observations of Boutell *et al.* (2002).

1D4.5 Interaction with proteins involved in the regulation of transcription and translation.

ICP0 has been implicated in the regulation of transcription and translation through interactions with or affect on cellular factors involved in gene expression. Parkinson *et al.* (1999) demonstrated that in the course of HSV-1 infection, expression of ICP0 alone was sufficient for degradation of the catalytic subunit of DNA-dependent protein kinase (DNA-PK). DNA-PK is a multi-functional nuclear enzyme that plays a part in double-stranded DNA break repair, V(D)J recombination, and possibly in the regulation of transcription by RNA polymerases I and II (Lees-Miller *et al.*, 1996). As in the previously described examples of PML and Sp100, the RING finger domain of ICP0 was found to be required for the induction of degradation of DNA-PK via a proteasome-dependent pathway (Parkinson *et al.*, 1999). Recently, two other proteins, BMAL1 and elongation factor 1δ (EF-1δ) that are involved in transcription and translation regulation respectively, have been identified to interact with ICP0 in the yeast two-hybrid system (Kawaguchi *et al.*, 1997a, Kawaguchi *et al.*, 2001). These studies suggested that the C-terminal region of ICP0 interacts with EF-1δ (Kawaguchi *et al.*, 1997a). EF-1δ is expressed as a cytoplasmic protein and is a subunit of EF-1, a complex of factor that mediates the elongation of polypeptide chains during translation (reviewed by Merrick, 1992). Although ICP0 is initially expressed as a nuclear protein and many actions of ICP0 occur in the nucleus, however as described previously, at later stages of infection ICP0 is translocated into the cytoplasm. These findings indicate that the translocation of ICP0 into the cytoplasm might enable ICP0 to interact with EF-1δ. The effects of this interaction are not fully understood, although some results demonstrated that a HSV-1 viral protein (UL13) mediated hyperphosphorylation of EF-1δ (Kawaguchi *et al.*, 1998), an effect that has been associated with efficient translation (Wasserman *et al.*, 1982).

Most recently, Kawaguchi and coworkers (2001) reported that ICP0 also interacts with the transcription factor BMAL1 in the yeast two-hybrid system. BMAL has been described as a basic helix-loop-helix-PAS transcription factor (Hogenesch *et al.*, 1997). Subsequent studies using GST-pull down assays revealed that residues encoded in exon II

of ICP0 were able to interact with full length BMAL1, and that BMAL1 residues between 95 and 450 containing the bHLH and PAS domains appeared to be important for this interaction. Furthermore, co-expression of ICP0 and BMAL1 increased reporter (luciferase) gene activity in transient transfection assays by approximately 5-fold compared to ICP0 and BMAL1 alone, indicating that ICP0 might form a transcriptionally active complex with BMAL1 in mammalian cells. Finally, since during viral infection the BMAL1 is more stable in cells infected with wild type HSV-1 than in those infected with ICP0 null mutant viruses, these workers suggested that ICP0 may mediate stabilisation of this protein.

1E. ND10 structures and their interactions with viral proteins

The nucleus in eukaryotic cells contains several discrete domains or sub-structures, such as the relatively well characterised nucleolus, Cajal (or coiled) bodies and ND10, and several less well understood foci characterised by discrete accumulations of various particular cellular proteins. These domains appear to be involved in distinct cellular processes including DNA replication, transcription, pre-mRNA processing, and ribosome assembly (reviewed by Spector, 2001). The structures that later became known as ND10, PML nuclear bodies or PODs were initially described as punctate nuclear foci by Bernstein *et al.* (1984) using sera from patients with primary biliary cirrhosis for immuno-fluorescence analysis (Bernstein *et al.*, 1984). ND10 appeared similar to small dense structures, termed nuclear bodies, which had been recognised by electron microscopy. The interest in ND10 increased dramatically when one of the principal protein components was identified as PML, a protein that is disrupted by chromosomal translocations that cause promyelocytic leukaemia (reviewed by Piazza *et al.*, 2001).

The designation of ND10 is derived from their appearance as nuclear dots or domains and the initial finding of approximately 10 nuclear dots per cell in several human cell lines by immunofluorescence analysis (Ascoli & Maul, 1991). However the number of ND10 varies, ranging from 5 to 30 per nucleus, considerably dependent on cell type and other factors (reviewed by Sternsdorf *et al.*, 1997, Negorev & Maul, 2001).

To date, at least six proteins, including Sp100, PML, SUMO-1, hDaxx, BLM and NDP55 have been found to be present in ND10 constantly (reviewed by Negorev & Maul, 2001). Apart from these six constituents, a number of proteins have been reported to transiently associate with ND10 (Table 1.2). Details of ND10 constituents are discussed in greater depth in separate sections below.

With the list of proteins associated with ND10 growing fast, ND10 have been implicated in regulation of gene expression (Vallian *et al.*, 1998), cell transformation (Le *et al.*, 1998), growth control (Mu *et al.*, 1994), and cellular stress response (Maul *et al.*, 1995). To date, the role of ND10 is poorly understood. However, ND10 structures have been demonstrated as preferential sites for deposition of incoming viral genomes and for the development of replication compartments (Ishov & Maul, 1996). Furthermore, several viral oncoproteins and transactivators have been found to affect the stability of ND10

Table 1.2 Proteins present at ND10

Proteins present at ND10 at endogenous levels of expression	
PML	essential in ND10 formation; in SUMO-modified form recruits Daxx; interacts with CBP, pRb, p53; considered a co-repressor
Sp100	interacts with HP1; ND10 are limited in their capacity to recruit Sp100.
Daxx	recruited by SUMO- modified PML; binds to an increasing number of proteins.
BLM	low relative amount of BLM is stationed in ND10.
SUMO	modifies PML and Sp100 covalently changing their capacity to bind other proteins.
NDP55	uncharacterised protein(s); potentially a protein modification recognised by Mab 138; increase after heat shock.
Proteins conditionally present in or at ND10	
TRF1/2 NBS1 P95/nibrin Mre11 RAD51 RAD52 Repl. factor A WRN	present in a subset of ND10 containing telomere repeats in cells depending on an alternative telomere maintenance mechanism. These proteins colocalised with PML in telomerase-negative immortalised cells during the late S/G_2-phase of the cell cycle.
SENP-1	removes SUMO from PML.
HP1	interacts with Sp100 but is present in ND10 in variable amounts depending on the cell cycle phase.
Sp100C	present in some ND10.
HMG2	interacts with Sp100B.
CBP	interacts with PML, found in some cell type but not others.
pRb	phosphorylated form found by some groups and not by others; possibly cell cycle related colocalisation.
USP7	at or beside some ND10; probably cell cycle dependent.
PA28	proteosomal activator; increased recruitment to ND10 by IFN-γ exposure..
proteosome	only after application of proteosome inhibitors or after IFN-γ as immunoproteosomes.
RFP	interacts with PML and associates with a subset of ND10.
GAPDH	interaction with PML is RNA dependent.
eIF-4	interacts with PML.
PLZF	no interaction with PML but side by side localisation in nucleus.
HSF2	heat shock transcription factor 2 after overexpression in lower number of cells, mostly cytoplasmic.
Tax	recruited into ND10 when PML is overexpressed.
P53	in specific cells, after overexpression or proteosome inhibition or beside ND10 with T-ag down regulation.
ISG-20	after overexpression of a fragment
Mutant ataxin	PML but not the other ND10 proteins are located in ataxin-1 aggregates after polyglutamine tract extension.
PKM	Mx interaction kinase after transient expression.
Int6	
PAX3	in some cells possibly by binding to overexpressed Daxx.
Sp1	interacts with PML.
FIST/HIPK3	after overexpression interacts with Daxx.
hGCNP	besides ND10 upon transient overexpression.
Sp140	after overexpression with some ND10.
BRAC1	breast cancer protein 1 beside ND10 upon transient overexpression.

Adapted from Negorev & Maul, 2001

structures and composition (reviewed by Everett, 2001). These observations indicate that ND10 proteins might potentially affect viral infection. Relevant aspects of ND10 biology are discussed in later sections.

1E.1 Discovery of ND10

Visualisation of nuclear structures by electron microscopy has discovered a variety of nuclear bodies. The atypical sphere subnuclear structure described by Bernstein (1984) was later known as ND10 through the studies of Ascoli and Maul (1991). Their experiments, set out to screen over 1,700 human autoimmune sera in immunofluorescence assays, revealed a novel nuclear domain with an average of 10 dots per nucleus, hence the name ND10. Double-staining immunofluorescence experiments demonstrated that ND10 structures were stably attached to a nuclear matrix component but separate from chromosomes, kinetochores and centromeres (Ascoli & Maul, 1991).

1E.2 Proteins present at ND10

The anti-ND10 autoimmune antibodies, used in a series of biochemical fractionation experiments followed by western blot analysis, first discovered a 55kDa protein (NDP55) as a component of ND10 (Ascoli & Maul, 1991). However this protein has not yet been further characterised. Using the sera of patients with primary biliary cirrhosis, Sp100 was identified earlier than NDP55 (Szostecki *et al.*, 1990), but its ND10 localisation was not confirmed until double-staining was performed with sera against NDP55 and Sp100 (Stuurman *et al.*, 1992). A third constituent was demonstrated to localise to ND10 in immunofluorescence assays using the monoclonal antibody 5E10 that was later found to recognise PML (Stuurman *et al.*, 1992). SUMO-1 was found to interact with PML in the yeast two-hybrid system (Boddy *et al.*, 1996). Subsequent studies demonstrated that SUMO-1 covalently modifies both PML and Sp100 and co-localises with these proteins in ND10 (Muller *et al.*, 1998a, Sternsdorf *et al.*, 1997). Another ND10 component, hDaxx, was initially shown to have a nuclear localisation similar to that of ND10 and was further identified as a PML-interaction protein through yeast two-hybrid screening (Ishov *et al.*, 1999, Li *et al.*, 2000). Similarly, BLM had a ND10-like nuclear distribution in most cells (Neff *et al.*, 1999) and was later defined as a component of ND10 (Yankiwski *et al.*, 2000).

Four relatively well characterised ND10 proteins including PML, Sp100, SUMO-1, and hDaxx are discussed individually below.

1E.2.1 PML

1E.2.1.1 PML and APL

PML (ProMyelocytic Leukaemia) was initially discovered as the part of a fusion protein with retinoic acid receptor α resulting from a t(15;17) reciprocal chromosome translocation in most patients with the hematopoietic malignancy acute promyelocytic leukaemia (APL) (de The *et al.*, 1991). This chromosome translocation fuses the retinoic acid receptor α (RAR-α) gene to the N-terminal part of PML (Goddard *et al.*, 1991), and in consequence ND10 domains are disrupted and form large numbers of small scattered speckles (described as a microspeckled pattern), distributed both in the cytoplasm and the nucleus (Daniel *et al.*, 1993). The PML-RARα fusion protein is sufficient for transformation of cells and induction of leukaemias (Altabef *et al.*, 1996). Retinoic acid and As_2O_3 treatments, which have been effectively applied in clinics, results in destruction of the PML-RARα fusion protein and restoration of normal ND10 distribution (reviewed by Zhang *et al.*, 2001).

1E.2.1.2 The structure of PML transcripts and polypeptides

Sequence analysis has revealed that the PML gene consists of nine exons, and at least seven PML isoforms are produced as a consequence of alternative splicing of the 3' exons (reviewed by Jensen *et al.*, 2001). However, little is known about the functions of the PML splice variants at present. The promoter region of PML harbours IFN-stimulated response elements (ISREs) and IFN-γ activation sites (GAS) mapped at 100-500 bp upstream of the start codon (Stadler *et al.*, 1995). Furthermore, it has been shown that transcription of PML is up-regulated by IFNs and that the PML-ISRE element alone is sufficient to mediate type I and type II IFN-enhanced gene expression.

The structure of PML protein contains several domains, listed in the direction from the N- to the C- terminus: a zinc-binding RING finger domain (residues 45-105); two B-boxes (B1 and B2 at residues 124-166 and 184-23, respectively); and a predicted alpha-helical Coiled-Coil domain (residues 229-323). This arrangement of domains is present in

a number of other proteins and has been designated the RBCC motif, or more recently termed the TRIM (Tripartite Motif) motif (reviewed by Jensen *et al.*, 2001). In addition, three lysine residues have been found to be SUMO-1 modification sites (at residues 65, 160, and 490) that are present in all PML isoforms, and a bipartite NLS signal (overlapping the SUMO-1 modification site at residue 490) is located in exon 6. The gene structures and position of these domains are illustrated in Fig. 1.8. Extensive structural and functional analyses of PML have showed that several cellular and viral proteins interact specifically with certain PML isoforms, implying that the different domains of PML mediate its distinct functions (reviewed by Jensen *et al.*, 2001).

Immunofluorescence analyses demonstrated that mutations in the conserved zinc-binding residues of the PML RING finger disrupted formation of ND10 *in vivo* (Borden *et al.*, 1996, Kastner *et al.*, 1992). In addition, it was found that the RING finger of PML was important both for its localisation to ND10 and its PML-PML oligomerisation (Boddy *et al.*, 1997). Furthermore, the domains of PML necessary for the ND10 formation have been shown to correlate with its transformation suppressing effects (Fagioli *et al.*, 1998, Mu *et al.*, 1994), apoptosis (Zhong *et al.*, 2000) and anti-viral activities (reviewed by Regad & Chelbi-Alix, 2001).

The two B-boxes, adjacent to the RING domain, contain conserved zinc binding residues in a cysteine-rich region that have been reported to be important for ND10 formation, but not in PML-PML oligomerisation (Borden *et al.*, 1996). Together with the RING finger, the B-boxes have been shown to mediate the growth suppressor function of PML (Fagioli *et al.*, 1998). Moreover, PML has been shown to colocalise with the retinoblastoma protein (pRb) and this interaction was abolished when PML with deletions in the B-boxes region was used in co-immunoprecipitation experiments, indicating that B-boxes play an indispensable role in this interaction (Alcalay *et al.*, 1998).

The coiled-coil regions of PML are thought to be important for PML multimerisation (Peng *et al.*, 2000). Deletion analysis of PML revealed that the coiled-coil domain was required for the transcriptional repression by PML (Vallian *et al.*, 1997). However an intact RBCC/TRIM motif of PML is essential for optimal function of PML in ND10 formation, PML growth suppressor, apoptotic and antiviral activities (reviewed by Jensen *et al.*, 2001).

Fig. 1.8 The functional domains of PML.

The N-terminal region of PML contains the RBCC motif: RING finger domain (residues 45-105), two B-boxes (residues 124-166, 184-230) and Coiled-Coil domain (residues 229-323). A nuclear localisation signal has been mapped near the C-terminus of PML as indicated. SUMO-1 modified sites at amino acid positions 65, 160, and 490 are indicated.

1E.2.1.3 PML and its potential functions

The exact function of PML has yet to be characterised, however it has been implicated in growth suppression (Mu *et al.*, 1994) and transformation suppression, transcription repression (Vallian *et al.*, 1997), apoptosis (Pearson & Pelicci, 2001) and inhibition of viral infections (reviewed by Regad & Chelbi-Alix, 2001).

- **A growth suppressor**

This potential function of PML was initially described by Mu *et al.* (1994). In transient transfection experiments, expression of PML in APL-derived NB4 cells significantly reduced the number of colonies growing on soft agar (Mu *et al.*, 1994). Additionally, PML was also found to suppress oncogenic transformation of rat embryonic fibroblasts (REF) and NIH3T3 cells by co-expression of oncogenes including Ha-*ras* and mutant p53 or Ha-*Ras* (RasV12) and *c-myc*. These observations implicate PML in growth suppression.

The role of PML in tumorigenesis was further conclusively demonstrated by Wang *et al.* using a PML knockout mouse model. PML -/- mice, pre-treated with the tumour initiators DMBA followed by TPA, developed more papillomas suggesting that PML may function as a tumour suppressor (Wang *et al.*, 1998).

- **A transcriptional repressor**

Chang and coworkers first discovered that transient expression of PML repressed transcription from specific promoters including those of the human multi-drug resistance (MDR1) and epidermal growth factor receptor (EGFR) genes (Mu *et al.*, 1994). Further studies from the same group proposed that the negative regulation of EGFR transcription by PML might result from the interaction of PML with Sp1 that leads to disruption of Sp1 DNA binding activity and subsequently affect the activation of the EGFR promoter by Sp1 (Vallian *et al.*, 1998). PML has also been reported to interact with the non-phosphorylated fraction of the pRb protein in ND10, and it displayed an inhibitory effect on pRb-regulated transcriptional activation of glucocorticoid receptor-responsive promoters (Alcalay *et al.*, 1998). Functional analysis revealed that the coiled-coil (dimerisation) domain was essential for this interaction. Additionally, recent studies by Wu *et al.* (2001) demonstrated that the transcription function of PML is associated with histone deacetylase (HDAC). The

PML isoform, containing 633 residues, directly interact with all three isoforms of HDAC genes in GST pull down assays and the basal transcription of PML was shown to be repressed by a HDAC specific inhibitor, implying that HDAC activities may contribute (Wu *et al.*, 2001b).

- **Induction of apoptosis**

Quignon *et al.* (1998) reported that overexpression of PML in SV40 large T-transformed REF (rat embryonic fibroblast) cells resulted in a 40-fold reduction of colony formation and induced morphological changes that were associated with a moderately positive TUNEL assay, suggestive of induction of apoptosis. This apparent PML-induced cell death led to the appearance of cytoplasmic shrinkage features, rather than the typical DNA cleavage type of apoptosis. This apoptosis was not blocked by caspase inhibitors suggesting that PML triggers caspase-independent apoptosis (Quignon *et al.*, 1998). At the same time, studies on PML-/- knockout mice from Pandolfi's group also implicated PML in an apoptotic pathway, but they concluded that PML was a mediator of caspase-dependent cell death, since it was required for activation of caspase 1 and caspase 3 upon treatment with several exogenous apoptosis-inducing stimuli (Wang *et al.*, 1998). The fact that such different experimental models were used, one depending on overexpression of PML *in vitro*, the other one investigating the removal PML activity *in vivo*, and both methods using distinct stimuli that might trigger different pro-apoptosis pathways, provides an explanation for the paradoxical findings. More recently, Pandolfi's group provided further evidence for the involvement of ND10 proteins in apoptosis (Zhong *et al.*, 2000). These results demonstrated that the overexpression of hDaxx, a ND10 constituent, which has been shown to function as a pro-apoptotic protein enhancing Fas-mediated apoptosis, induced cell death in PML+/+ cells, but not in PML-/- cells (Chang *et al.*, 1998). PML is also required for the ND10 localisation of Daxx because of a direct interaction between Daxx and SUMO-1 modified PML, indicating that the interaction of PML and Daxx might contribute to a novel nuclear pathway for apoptosis.

- **A potential role of PML in anti-viral infection**

Several groups have demonstrated that PML might mediate an anti-viral response as part of the host-cell defence system. Chelbi-Alix *et al.* (1998) initially showed that over-expression of PML diminished infections by vesicular stomatitis virus (VSV) and

influenza A virus. Most recently, PML has also been found to induce resistance to lymphocytic choriomeningitis virus (LCMV), human foamy virus (HFV) and the herpesvirus HCMV in cell cultures (reviewed by Regad & Chelbi-Alix, 2001). Considering that expression of PML, like some other ND10 proteins, is induced by IFNs, these results imply that PML may contribute to the antiviral state induced by the interferon pathway. The details of the function of PML in viral infection are included in section 1E.5.

1E.2.1.4 Proteins that interact with PML

A growing number of other proteins have been reported to interact with PML, such as SUMO-1 (Boddy *et al.*, 1996), Ret RING finger protein (Rfp) (Cao *et al.*, 1998), p53 (Fogal *et al.*, 2000), pRb (Alcalay *et al.*, 1998), BLM (Ishov *et al.*, 1999), and Daxx (Li *et al.*, 2000). As previously referred to in this section, interaction with PML appeared to be important to the function and recruitment of p53, pRb and Daxx, into ND10 structures implicating PML in the maintenance of ND10. Interestingly, recent studies have shown that PML (Boddy *et al.*, 1996; Muller *et al.*, 1998a) and p53 (Gostissa *et al.*, 1999) are covalently modified by SUMO-1. Additionally, SUMO-1 conjugation of PML has been demonstrated to be essential for the recruitment of Daxx into ND10 and for efficient inhibition of Daxx-mediated transcriptional repression (Li *et al.*, 2000), and to play an important part in transactivation of p53 (Gostissa *et al.*, 1999). This implies that the modification of PML by SUMO-1 plays an essential part in its function. Information on SUMO-1 and SUMO-1 modification is discussed in greater detail in a later section.

1E.2.2 Sp100

1E.2.2.1 Introduction

Sp100 was the first ND10 constituent to be characterised biochemically (Ascoli & Maul, 1991, Szostecki *et al.*, 1990). Among the currently known ND10 constituents, Sp100 and PML are the best characterised at present. Although very different in primary structure, Sp100 and PML share many properties: IFN-induced gene expression, alternative splicing and SUMO-1 modification.

The Sp100 promoter region consists of ISRE and GAS elements that mediate transcriptional induction in response to IFNs (Grotzinger *et al.*, 1996). Sp100 is an acidic,

phosphorylated protein with a calculated molecular weight of 54 kDa, but it shows an aberrant electrophoretic mobility in SDS-PAGE corresponding to approximately 100 kDa (Szostecki *et al.*, 1990). In addition, a number of transcripts, alternatively spliced at their C-termini and encoding several Sp100 isoforms have been identified (reviewed by Sternsdorf *et al.*, 1997) (see below). As with PML, Sp100 is post-translationally modified by SUMO-1. It has been shown that Sp100, together with its SUMO-1-modification isoforms, was degraded in cells infected with HSV-1 (Chelbi-Alix & de The, 1999, Parkinson & Everett, 2000). Little is known about the functions of Sp100, however it has been found to interact with a cellular protein, HP1, suggesting a connection between Sp100 and the chromatin compartment (see below).

1E.2.2.2 The structures of Sp100 and its splicing variants

Analysis of a number of the λgt11 cDNA expression library clones revealed that the primary Sp100 transcript was alternatively spliced (Szostecki *et al.*, 1990). Immunoblot analysis with extracts from HeLa S3 cells treated with IFNs revealed additional proteins, immunoreacted with antibodies for Sp100 (Grotzinger *et al.*, 1996). Additionally, comparison of the expression pattern with that of proteins synthesised *in vitro* provides strong evidence that alternative splicing or post-translational modification occurs during expression of Sp100. Several groups have revealed a number of alternatively spliced Sp100 variants containing homologies to high mobility group 1 (HMG1) and a human nuclear phosphoprotein-box (HNPP) motif as a C-terminal domain (Guldner *et al.*, 1999, Lehming *et.al.*, 1998, Seeler *et al.*, 1998). To date, at least four Sp100 splicing variants have been identified including SpAlt-C, SpAlt-212 (Sp100-B), SpAlt-HMG (Sp100-HMG) and Sp100C (Seeler *et al.*, 2001, reviewed by Sternsdorf *et al.*, 1997). An illustration of the structure of Sp100 and its splicing variants is shown in Fig. 1.9.

- **Sp100 A (480 a.a.)**

This isoform, usually referred to as simply Sp100, is the protein commonly studied and used for ND10 analysis. In its N-terminal region, Sp100 harbours significant sequence homology to the peptide-binding groove of MHC class 1, termed the MHC-like motif, followed by a domain that is conserved in its murine homologue, designated Homogeneously Staining Region (HSR) (Sternsdorf *et al.*, 1997). The C-terminus of

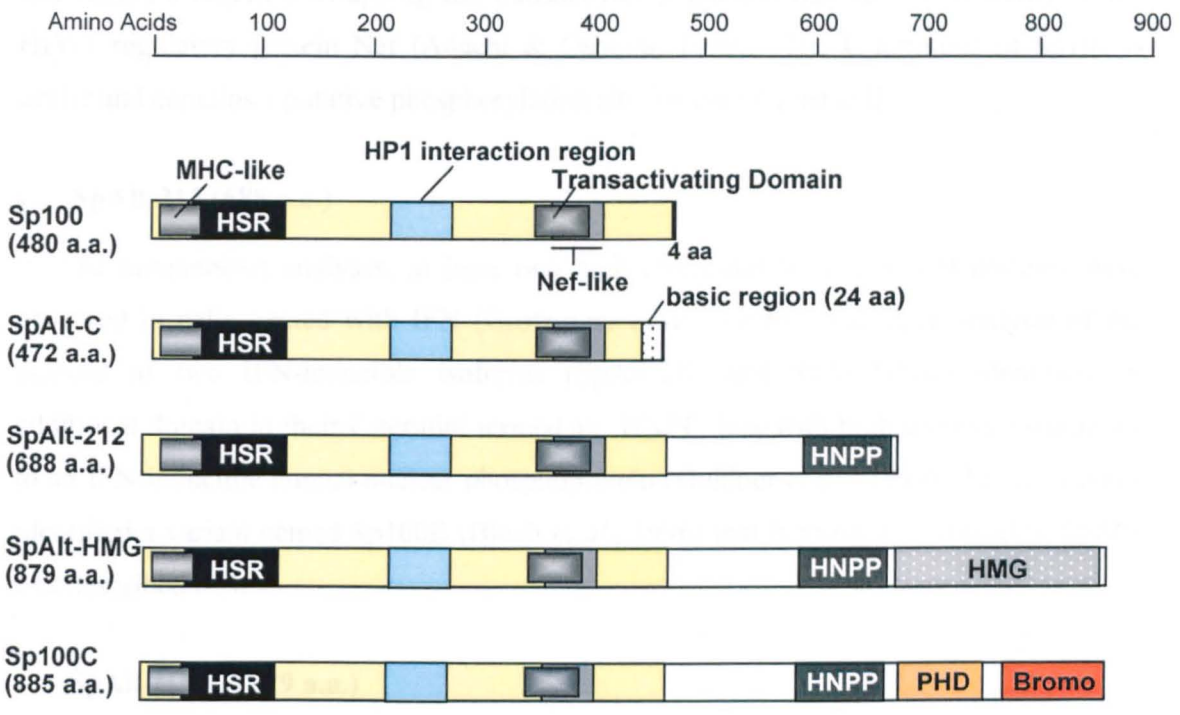

Fig. 1.9 Schematic representation of the Sp100 and Sp100 alternative splicing variants and their corresponding motifs.

Sp100 contains an MHC-like motif followed by a HSR domain near the N-terminus and a transactivating domain, which is overlapped by a Nef-like region near the C-terminus. Sp100 and all the splicing variants share most of the N-terminal 476 amino acids (the yellow region indicated), except **SpAlt-C** in which a basic region (24 a.a.) replaces the acid region (32 a.a.) at the C-terminus of Sp100. Sp100 and all the all the splicing variants contain a HP1 interaction region (residues 287-334) and one SUMO-1 modification site (K297).

SpAlt-212 contains the entire Sp100 sequence except for the last 4 amino acids, as indicated. An extra HNPP region is located in the C-terminal end.

SpAlt-HMG is identical to SpAlt-212 up to amino acid 684 and has a HMG domain in the N-terminus.

Sp100C contains 700 N-terminal residues of the SpAlt-HMG and two additional regions, PHD and Bromodomain in its C-terminus. The details for each domain are discussed in text in section 1E2.2.

Sp100 contains a transactivating domain involved in the transactivation ability of Sp100 in transfection assays when Sp100 was tethered to DNA (Lehming *et al.*, 1998), and a Nef-like motif, a region overlapping the transactivating domain that shows similarity to the HIV-1 regulatory protein Nef (Adachi & Oshima, 1999). The C-terminus of Sp100 is acidic and contains a putative phosphorylation site for casein kinase II.

- **SpAlt-212 (688 a.a.)**

In immunoblot analyses, at least two high molecular weight Sp100 proteins were observed in cells treated with IFN (Grotzinger *et al.*, 1996). Sequence analysis of the cDNAs of two IFN-inducible isoforms (SpAlt-212 and SpAlt-HMG) identified an additional domain in their C-termini termed an 'HNPP' box with high sequence similarity to an IFN-inducible human nuclear phosphoprotein (Guldner *et al.*, 1999). Earlier studies identified a variant named Sp100B (Bloch *et al.*, 1996) that is virtually identical to SpAlt-212 described here.

- **SpAlt-HMG (879 a.a.)**

The SpAlt-HMG variant, with the highest molecular mass, contains a domain (the HMG box) that represents an almost complete and highly conserved copy of the HMG-1 protein, after the HNPP box (Guldner *et al.*, 1999). Various proteins, including many transcription factors and coactivator proteins, belong to the HMG-superfamily and are involved in processes as diverse as rRNA transcription and sex determination in mammals (Affara *et al.*, 1993, Yang-Yen & Rothblum, 1988). Therefore, it is conceivable that Sp100 variants also have regulatory functions.

- **SpAlt-C (472 a.a.)**

In contrast to the other two variants, the SpAlt-C variant has no additional domains. The C-terminus contains a basic region (24 amino acids) of several lysine residues that replace the acid region (32 amino acids) at the C-terminus of Sp100A, resulting in loss of the consensus casein kinase II phosphorylation site.

1E.2.2.3 Functional domains of Sp100

Sternsdorf *et al.* (1999) used a series of truncated version of Sp100 and specific point mutation constructs to characterise domains necessary for dimerisation, nuclear localisation, ND10 targeting and SUMO-1 conjugation. The initial work suggested that the C-terminal region (residues 334-480) might contain a NLS. Sequence analysis of this region revealed a putative NLS sequence (PSRKRRF) mapping to residues 444-450, and Sp100 expressed from a substitution mutation (K447E) construct was found mainly in the cytoplasm indicating that Lys447 is required for nuclear localisation. In addition, immunofluorescence analysis of Sp100 transfected cells co-stained with PML demonstrated that Sp100 residues 33-149 are the minimal region for targeting Sp100 to ND10. Consistently, Negorev *et al.* (2001) also reported that the region between residues 29 and 152 was the shortest Sp100 polypeptide to be deposited at ND10. Results from immunoprecipitation experiments concluded that Sp100 can form homodimers and subsequent analysis of Sp100 homomeric interactions using the mammalian two-hybrid assay defined the region between residues 33-149 (that responsible for ND10 targeting) is also essential for Sp100 homodimerisation (Sternsdorf *et al.*, 1999). Since SUMO-1 only modifies lysine residues of a target protein, analysis of three constructs in which lysine residues K297, K298 and K300 were changed to arginine, showed that K297 is the SUMO-1 modification site (Negorev *et al.*, 2001, Sternsdorf *et al.*, 1999).

1E.2.2.4 Proteins that interact with Sp100

Recently, it has been shown that Sp100 binds to members of the heterochromatin binding protein (HP1) family both *in vitro* and *in vivo* (Lehming *et al.*, 1998, Seeler *et al.*, 1998). HP1, a member of the family of non-histone chromosomal proteins, bears a chromo shadow domain (CSD) that is required for the form of gene repression termed position effect variegation (Eissenberg *et al.*, 1990). Lehming *et al.* (1998) demonstrated that in a yeast two-hybrid system using the Sp100B variant as bait, two proteins (human HP1α, HP1γ) interact with Sp100B. By means of yeast two-hybrid screening and GST-pull down assays, findings consistent with these were obtained by Seeler *et al.* (1998). Further analyses revealed that HP1 residues 113-191 are sufficient for Sp100 binding and Sp100 residues between 287-334 are required for interaction with full length HP1 (Seeler *et al.*, 1998). Moreover, immunofluorescence assays demonstrated that Sp100 colocalised with HP1 in ND10 structures and the enhancement of Sp100 expression by transient

transfection promoted HP1 accumulation in ND10. Finally, it has been shown that both Sp100 and HP1 act as transcriptional repressors when tethered to DNA in transient transfection assays.

As HP1 has been implicated in the proper functioning of centromeres during mitosis (Kellum *et al.*, 1995), these findings raise the interesting possibility that the ND10 may be involved with the control and maintenance of chromatin or heterochromatin architecture.

1E.2.3 SUMO-1

1E.2.3.1 Discovery of SUMO-1 and its related proteins

A novel 101-residue protein designated PIC-1 (PML-interacting clone 1, now commonly called SUMO-1) was discovered to have a strong and specific interaction with PML, using yeast two-hybrid screening from a human B-cell cDNA library (Boddy *et al.*, 1996). This protein is 18% identical to ubiquitin, a highly conserved 76-residue protein, and as with ubiquitin, SUMO-1 has been shown to be covalently conjugated to a number of proteins, therefore it has been named as SUMO-1 (for Small Ubiquitin-related Modifier 1) (Mahajan *et al.*, 1997, Saitoh *et al.*, 1997). Intriguingly, cDNAs identical to that encoding vertebrate SUMO-1 were discovered almost simultaneously by several research groups and given other names, including Sentrin (Okura *et al.*, 1996), UBL1 (ubiquitin-like protein 1) (Shen *et al.*, 1996), and GMP-1 (GAP modifying protein-1) (Matunis *et al.*, 1996).

Recently, two cDNAs encoding proteins related to SUMO-1 have been identified in humans and mice, designated SUMO-2/SMT3A (Lapenta *et al.*, 1997) and SUMO-3/SMT3B (Chen *et al.*, 1998) respectively. Sequence analyses have shown that SUMO-1 displays a relatively high identity to SUMO-2 (48%) and SUMO-3 (46%). However amino acid sequence identity between SUMO-2 and –3 is 95%, suggesting that SUMO-2 and SUMO-3 should group into a subfamily distinct from SUMO-1. Saitoh and Hinchey have revealed that SUMO-2 and -3 are more abundant than SUMO-1 in COS-7 cells using semiquantitative immunoblot assays. In addition, over 70% of SUMO-2 and -3 was found as a free or non-conjugated forms *in vivo*, whereas SUMO-1 existed mainly (over 90%) in the conjugated form (Saitoh & Hinchey, 2000).

1E.2.3.2 The pathway of SUMO-1 conjugation

Like ubiquitin, SUMO-1 is believed to form an isopeptide bond between the carboxy terminal glycine of SUMO-1 and the ε-amino group of a lysine residue of a target protein (Kamitani *et al.*, 1997, Mahajan *et al.*, 1998). The pathway of SUMO-1 conjugation (Fig. 1.10) is mechanically analogous to ubiquitination, but SUMO-1 modification requires a set of specific enzymes that are distinct from those involved in ubiquitination (reviewed by Seeler & Dejean, 2001). As illustrated in Fig. 1.10, the C-terminus of pre-SUMO-1 needs to be proteolytically processed to the mature form of the SUMO-1 molecule prior to its conjugation. SUMO-1 is subsequently activated in an ATP-dependent reaction by the formation of a thioester bond with the SUMO-activating enzyme (E1), followed by the transfer of the SUMO-1 molecule to the SUMO-1 conjugating enzyme (E2). In ubiquitination, sometimes, a further enzyme, the E3 ligase, may be needed to transfer ubiquitin from the E2 to substrate. Whether SUMO-1 conjugation requires an E3 ligase is still uncertain, although a number of proteins have recently been identified that may have SUMO-1 E3-like properties (reviewed by Hochstrasser, 2001, Jackson, 2001). In contrast to ubiquitination, SUMO-1 conjugation does not appear to form SUMO-SUMO chains. Finally, SUMO-1 conjugation is a reversible process by which the attached SUMO-1 can be cleaved from target proteins by SUMO isopeptidases, which are thought to be the same type of enzyme for that is used for SUMO-1 maturation.

- **Maturation**

SUMO-1 is expressed as a precursor protein with 4 extra amino acids (His-Ser-Thr-Val) following the C-terminal Gly-Gly residues of the mature SUMO-1 molecule (Kamitani *et al.*, 1997). As with ubiquitination, the cleavage of these extra residues to expose the C-terminal glycine residue is essential for SUMO-1 ligation to target proteins (reviewed by Hochstrasser, 1996). To date, at least four SUMO-1 specific hydrolases have been identified. Li and Hochstrasser (1999) first identified the 72-kDa Ulp1, which can specifically cleave Smt-3 (the yeast homologue of SUMO-1) and SUMO-1 from their conjugates, but not ubiquitin (Li & Hochstrasser, 1999). In addition, a 30-kDa SUMO-1 C-terminal hydrolase has been isolated from bovine brain extracts (Suzuki *et al.*, 1999). This enzyme cleaved the SUMO-1 precursor and also SUMO-1 conjugated RanGAP1, but not ubiquitin. Furthermore, two SUMO-1 specific hydrolases, the 126-kDa SUSP1 (Kim *et al.*, 2000) and the 73-kDa SENP1 (Gong *et al.*, 2000), were obtained through the basic

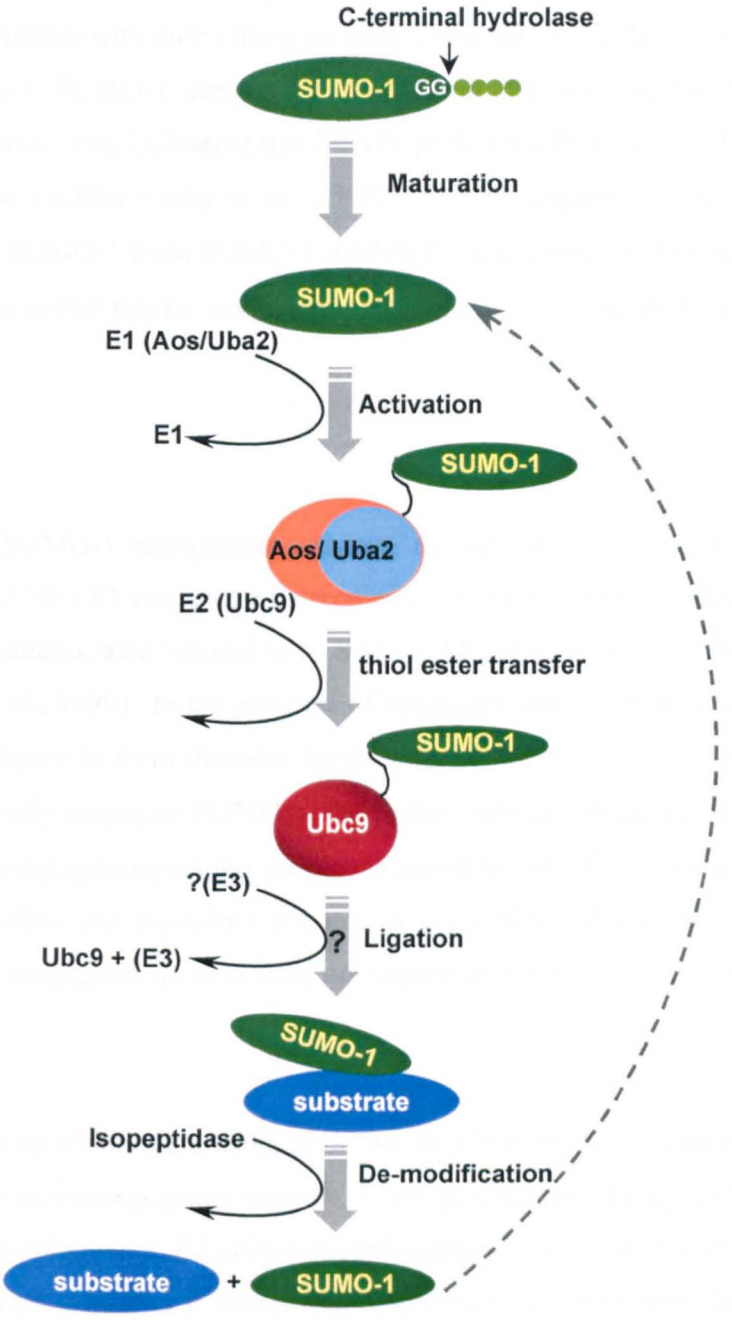

Fig. 1.10 The SUMO-1 pathway. SUMO-1 is synthesised as a precursor molecule that is processed C-terminally by a hydrolase to expose a C-terminal Gly residue. The mature SUMO-1 subsequently forms thioester intermediates with E1 enzyme (Aos1/Uba2), E2 (Ubc9) and possibly an E3 enzyme before being coupled to the substrates. The SUMO-1 modification pathway is a reversible process. The conjugated SUMO-1 can be cleaved from substrates by isopeptidases.

local alignment search tool program (BLAST) on the basis of homology to Ulp1, from a human cDNA or EST library. Interestingly, these two enzymes have different intracellular localisations that correlate with their effects on preferential targets. SENP1 has been shown to specifically cleave SUMO-1 conjugates of PML in the nucleus, but not SUMO-RanGAP1 in the nuclear rim, indicating that SENP1 preferentially removes SUMO-1 from its conjugates in the nucleus (Gong *et al.*, 2000). SUSP1, expressed in the cytoplasm, efficiently released SUMO-1 from SUMO-1 modified β-galactosidase, but was unable to process other ubiquitin-like protein conjugates, such as Smt-3 conjugated β-galactosidase (Kim *et al.*, 2000).

- **Activation**

In the human SUMO-1 conjugation pathway, the activation of mature SUMO-1 is carried out by the SUMO E1 enzyme, a heterodimer consisting of the 38-kDa Aos-1 and the 72-kDa Uba-2 proteins, also referred to as SAE1/SAE2 (Desterro *et al.*, 1999, Gong *et al.*, 1999, Okuma *et al.*, 1999). In the presence of the E2 enzyme (hUbc9), the Aos1/Uba2 complex has been shown to form thioester bonds with SUMO-1, -2, and -3 (Gong *et al.*, 1999), and to efficiently conjugate SUMO to the protein substrate IκBα *in vitro* (Desterro *et al.*, 1999). These conjugation proteins are also required for SUMO-1 conjugation of p53 (Rodriguez *et al.*, 1999) and RanGAP1 (Okuma *et al.*, 1999). These observations also imply that SUMO-1 conjugation *in vitro* does not require an E3 protein ligase activity.

- **Conjugation**

In the yeast two-hybrid system, using SUMO-1 as a bait to screen a human placenta cDNA library, a ubiquitin-conjugating enzyme, Ubc9 was identified (Gong *et al.*, 1997). Although Ubc9 is homologous to E2 ubiquitin conjugating enzymes, it is unable to form a thioester with ubiquitin. Instead it forms a thioester with SUMO-1 with high affinity, demonstrating that Ubc9 is a SUMO-1 specific E2 enzyme. In addition, thioester linkage between SUMO-1 and Ubc9 required the C-terminal Gly-Gly residues of SUMO-1. Furthermore, it has been shown that a conserved Cys residue (Cys93) of Ubc9 is required to form a thioester bond with SUMO-1 prior to conjugation with the target protein (reviewed by Seeler & Dejean, 2001).

IE.2.3.2 SUMO-1 targets

SUMO-1 was initially found to be covalently conjugated to the 90-kDa form of the Ran GTPase-activating protein, RanGAP1, a protein required for nuclear transport (Mahajan *et al.*, 1997). SUMO-1 modification of RanGAP1 was thought to facilitate the association of cytosolic RanGAP with Ran binding protein 2 (RanBP2) at the nuclear pore complexes to form the functional nuclear import machinery (Mahajan *et al.*, 1997, Mahajan *et al.*, 1998, Matunis *et al.*, 1998, Saitoh *et al.*, 1998). Recently, SUMO-1 has also been found to conjugate with a growing list of cellular proteins (Table 1.3) that are important cellular regulators, including ND10 proteins, transcription factors (p53, c-Jun, TIF-1α, etc.), and chromatin-associated proteins as well as some viral proteins (see below). However, how SUMO-1 modification influences the function of its target proteins is not well understood.

IE.2.3.3 SUMO-1 and ND10

Sternsdorf *et al.* (1997) initially proposed that a fraction of nuclear PML is covalently modified by SUMO-1. In addition, Muller *et al.* (1998) have shown that SUMO-1 is covalently attached to a subset of PML isoforms in a reversible and phosphorylation-dependent manner in non-APL cells. Unmodified PML is found in the soluble fraction of the nucleus, whereas SUMO-1-modified PML is compartmentalized in ND10, indicating that SUMO-1 modification of proteins plays a general role in the regulation of their subcellular localization (Muller *et al.*, 1998a). Three lysine residues in PML (Lys65 in the RING finger domain, Lys160 in the B1 box, Lys490 in the NLS) have been found to be modification sites for SUMO-1 (Kamitani *et al.*, 1998).

The second ND10 protein modified by SUMO-1 is Sp100. Mutagenesis of Sp100 revealed a single lysine residue (Lys297) that serves as the SUMO-1 acceptor site (Sternsdorf *et al.*, 1999). In contrast to PML, mutation of Lys297 completely abolished SUMO-1 modification of Sp100, but did not affect the localisation of Sp100 to ND10. Furthermore, Sp100(K447E), a nuclear localisation mutant construct that encodes cytoplasmic unmodified Sp100, when expressed with a functional NLS, was efficiently modified by SUMO-1, suggesting that modification of Sp100 by SUMO-1 is strongly correlated to nuclear localisation. More recently, studies from Seeler *et al.* demonstrated

Table 1.3 SUMO substrates and the potential functions of SUMO modification

Proteins	***Suggested function or observed effect***
ND10 proteins:	
PML and PML-RARα	ND10 integrity, potentiation of arsenic-induced degradation
Sp100	Stabilisation of Sp100-HP1 interaction *in vitro*
Cytoplasmic proteins:	
RanGAP1	Targeting to RanBP2 at nuclear pore complex
IκBα	Antagonise ubiquitylation
GLUT1, GLUT4	Unknown; weak SUMOylation but differentially regulated by Ubc9
Yeast septins:	
Cdc3p **Cdc11p** **Sep7p**	Regulation of septin ring dynamics during budding yeast cytokinesis
Viral proteins:	
CMV-IE1	Unknown
CMV-IE2	Reduction in transactivation
BPV-E1	Nuclear translocation/localisation
EBV-BZLF1	ND10 disruption, subnuclear targeting
Transcription factors and chromatin-associated proteins:	
p53	Modest increase in transactivation and apoptotic response; no effect on p53 stability
p73α	Potentiation of proteasomal degradation; relocalisation to detergent-insoluble fraction
c-Jun	Modest reduction of transcriptional activation
HSF2	Increases DNA binding
Dorsal (*Drosophila*)	Enhancement of nuclear translocation and transcriptional activation
Tkt69 (*Drosophila*)	Unknown
Androgen Receptor	Slight enhancement of transcriptional activation
TEL	Subnuclear targeting to TEL bodies
TOP1	Unknown
TOP2	Unknown
TIF1α	Unknown
Other:	
Mdm2	Antagonise ubiquitylation
HIPK2 (kinase)	Subnuclear localisation to speckles
CaMKII (*Drosophila*)	Unknown

Adapted from Seeler & Dejean, 2001

that SUMO-1 conjugated Sp100 enhanced the interaction of Sp100 with HP1, suggesting that SUMO-1 modification might directly mediate this interaction (Seeler *et al.*, 2001).

As mentioned in section 1E.2.1.4, SUMO-1 modification of PML appears to be important for certain proteins (e.g. Daxx and p53) to be targeted to ND10 and subsequently modulating their transcriptional activity. However, it is unknown how SUMO-1 regulates transcriptional processes mechanistically.

IE.2.3.4 SUMO-1 modification and viral infection

During infection, the IE proteins of many certain viruses localise to and then trigger disruption of ND10 which correlates with the disruption of ND10 components (PML and Sp100) as well as their SUMO-1 modified isoforms (see section 1D.4.1, reviewed by Maul, 1998, Everett, 2001, Seeler & Dejean, 2001). Intriguingly, some viral IE proteins including IE1 and IE2 (HCMV), BZFL1 (EBV), and E1 (bovine papillomavirus and human papillomavirus) are themselves conjugated by SUMO-1. Recently, studies from Hayward and coworkers have discovered more direct evidence for the interaction of IE proteins with SUMO-1 during HCMV infection. Xu *et al.* (2001) reported that SUMO-1 modification of IE1 can be enhanced either by overexpression of PML or SUMO-1. In addition, they have identified that Lys(450) in IE1 is the SUMO-1 conjugation site, but the IE1 mutant (K450R) in which Lys (450) was changed to arginine still efficiently localised to ND10, indicating that SUMO-1 modification is not required for targeting of IE1 to ND10 (Xu *et al.*, 2001). Furthermore, SUMO-1 conjugated IE1 is not required for efficient IE inhibition of PML-mediated transcriptional repression whereas IE1 mutants, defective in displacing PML from ND10, failed to inhibit the repression function of PML. IE2 of HCMV has been shown to physically interact with, and to be modified by, SUMO-1 (Ahn *et al.*, 2001). Further work demonstrated that an increase in SUMO-1 modification enhanced IE2-mediated transcription. These observations highlight the potential significance of SUMO-1 modification and ND10 in viral gene expression.

1E.2.4 Daxx

1E.2.4.1 Identification of hDaxx as a ND10 protein

Human Daxx (hDaxx) was initially isolated using a yeast-one hybrid screen to detect transcription factors regulating a steroidogenic factor 1 (SF-1)-like DNA element

(Kiriakidou *et al.*, 1997). It was later found to be an ND10 component, since it appeared to colocalise with PML at ND10 (Everett *et al.*, 1999b, Ishov *et al.*, 1999). Further work showed that hDaxx physically interacted with PML, but not Sp100, in yeast two-hybrid assays suggesting that the spatial colocalisation of PML and hDaxx in ND10 reflects an interaction between these two proteins (Ishov *et al.*, 1999).

1E.2.4.2 The potential function of Daxx

- **A potent transcription repressor**

The hDaxx protein has been demonstrated to potently repress transcription from the HCMV promoter (27-fold decrease) and its C-terminal domain (residues 625-740) has been found to be both necessary and sufficient for transcriptional repression (Torii *et al.*, 1999). This finding was later supported by Li *et al.* (2000). In addition, studies using a number of mutants with various deletions in the C- or N-termini of hDaxx revealed that multiple regions of hDaxx are involved in transcriptional repression in a cell-type-dependent manner. Several lines of evidence have shown that hDaxx interacts with certain proteins (e.g. Pax3, PML, histone deacetylases) and that the interaction subsequently influences Daxx-mediated transcriptional repression (Hollenbach *et al.*, 1999, Ishov *et al.*, 1999, Li *et al.*, 2000). For instance, through interaction with Pax3, Daxx repressed the transcriptional activity of Pax3 by up to 80% (Hollenbach *et al.*, 1999). The potential effect of the interaction between Daxx and PML has been intensively studied, as described in previous sections (1E2.1.4, 1E2.3.4) as well as in Ishov *et al.* (1999) and Li *et al.* (2000). In transient transfection assays, co-expression with wild type PML significantly reversed Daxx-mediated transcriptional repression (4-fold increase), while a PMLΔSUMO mutant lacking all three SUMO-1 modification sites was less effective in reversing the repressor function of Daxx. These observations indicate that SUMO-1 modified PML is required not only for localisation of Daxx to ND10 but also for Daxx-mediated transcriptional repression.

- **A role in apoptosis**

Murine Daxx (mDaxx) was identified as a novel Fas-binding protein that showed a strong interaction with the Fas death domain in yeast two-hybrid screens (Yang *et al.*, 1997). Overexpression of mDaxx alone greatly enhanced the activation of the Jun N-

terminal kinase (JNK) to a level similar to that of Fas and was able to enhance Fas-induced apoptosis, indicating that mDaxx acts as an activator of the JNK pathway. Consistently, hDaxx was shown to mediate enhancement of Fas-induced apoptosis, but this effect was through activation of the caspase pathway instead of with JNK (Torii *et al.*, 1999). It was shown that hDaxx did not appear to interact with Fas, but showed a strong interaction with PML in yeast two-hybrid assays and colocalised with PML in ND10 structures (Ishov *et al.*, 1999, Torii *et al.*, 1999). Intriguingly, the truncated mutant lacking the residues (625-740) required for transcriptional repression also failed to localise to ND10, implying that hDaxx possibly enhances Fas- induced apoptosis and regulates transcription of genes by a mechanism that requires it to be able to localise to ND10 structures (Torii *et al.*, 1999). A consistent result was shown in PML knockout mice (PML-/-) (Zhong *et al.*, 2000). In PML+/+ splenocytes (particularly in B-cells), mitogen Con A enhanced the expression of Daxx and localisation of Daxx to ND10, which is correlated with B cell apoptosis. However, the absence of PML (in PML -/- splenocytes) resulted in a dispersed nuclear pattern of Daxx and in impaired apoptosis of splenocytes upon Con A treatment. Similarly, activation of apoptosis only occurred in PML+/+ primary keratinocytes transfected with Daxx, but not in PML-/- cells whether or not they were transfected with Daxx. These findings indicate that interaction of PML with Daxx might be involved in a novel nuclear pathway for apoptosis (Zhong *et al.*, 2000).

1E.2.4.3 The interaction with centromere proteins

In addition to Fas, PML, and Pax3, Pluta *et al.* (1998) reported that hDaxx physically interacted with CENP-C, an intrinsic protein of the human centromere, and further determined that the C-terminal 104 amino acids of hDaxx and the N-terminal 315 amino acids of CENP-C were required for this interaction (Pluta *et al.*, 1998). Moreover, immunostaining of HeLa cells with hACA (human autoimmune serum recognising CENP-A, -B, -C) antibodies revealed that many hDaxx foci were colocalised with centromeres in interphase nuclei. The association of hDaxx with chromatin structures has also been reported by other research groups. Ishov *et al.* (1999) demonstrated that in the absence of PML (in PML-/- mouse embryo fibroblast cells), hDaxx redistributed from ND10 to foci associated with condensed heterochromatin. Li *et al.* (2000) reported that in NT2 cells, expressing low levels of PML and with fewer ND10 foci, a subset of hDaxx is found to accumulate at condensed chromatin and to be preferentially associated with centromeres

(more details are shown in the Results and Discussion, Chapter 4, of this thesis). These findings suggest that with low PML expression or in the absence of SUMO-1 modified PML, condensed chromatin provides an alternative site for hDaxx accumulation.

1E.3 Factors involved in the integrity of ND10 structures

ND10 are highly dynamic structures that can be modified by a number of factors, including the cell cycle, cellular stress (heat shock, heavy metals, chemicals), and interferon treatment. These factors result in changes in size, number and cellular distribution of the ND10 structures, or sometimes cause complete loss of the punctate staining pattern. In addition, the integrity of ND10 structures, in terms of assembly and disassembly, is affected by several other factors including viral infection, progression of cell cycle and interaction with other cellular proteins.

1E.3.1 Effect of cellular stress: heat shock

Time course experiments using various temperatures revealed that in Hep-2 cells a short, mild heat shock treatment (42°C, 10 min) was sufficient for induction of ND10 redistribution. Treatment with such a heat shock led to dispersion of ND10 into hundreds of tiny dots, forming a microspeckled pattern (Maul *et al.*, 1995). Whilst subsequent incubation at 37°C restored normal ND10 structures. The number of PML foci were increased significantly after 10-min heat treatment followed by a 10-min recovery at 37°C and the "microspeckled" pattern caused by 1 h heat treatment was restored to normal completely after 8 h recovery at 37°C. The effect of heat shock on Sp100 was similar to that on PML, but microdots were smaller and less intensely stained after a 1 h heat shock. In contrast, the staining of NPD55 was enhanced after heat treatment for 1 hour, suggesting that the effect of heat shock is not universal for all components of ND10 proteins and might differ between cell types.

A similar effect was observed in cells treated with $CdSO_4$ (Cd^{++} ions) (Maul *et al.*, 1995). A significant redistribution, similar to the pattern of 20-min heat shock, was observed after a 60-min treatment of $CdSO_4$.

IE.3.2 Effect of interferon (IFN) treatment

Immunofluorescence assays revealed that the staining of ND10 was increased, their number increased and their size was more homogeneous upon treatment with IFN-β and IFN-γ (1000U/ml) for 18 hours (Maul *et al.*, 1995). However, subtle differences in the staining of ND10 proteins in the nucleoplasm were observed. After IFN treatment, the nucleoplasmic staining of PML was increased, whereas there was no change in that of Sp100. In contrast to PML and Sp100, the staining of NDP55 was diminished throughout the nucleus as compared to untreated cells. Additionally, no significant difference of the effects of treatment with IFN-β or IFN-γ was found.

Analysis of promoter regions of ND10-associated proteins indicated that a number of them contain the IFN-stimulated responses element and/or IFN-γ activation sites (Grotzinger *et al.*, 1996, Stadler *et al.*, 1995). To date, at least six ND10-associated proteins, PML, Sp100, Sp140, Sp110, ISG20 and PA28, have been found to be up-regulated by IFN treatment (reviewed by Regad & Chelbi-Alix, 2001).

IE.3.3 Effect of chemicals: As_2O_3, and *all-trans* retinoic acid

As described in section 1E.2.1.1, the "microspeckled" distribution of ND10 has also been found in APL affected cells which were characterised as resulting from the specific chromosomal translocation resulting in the expression of the PML-RARα oncoprotein (de The *et al.*, 1991, Goddard *et al.*, 1991). This leukemia is caused by a differentiation block of myeloid precursors at the promyelocyte stage and is sensitive to therapy using *all-trans* retinoic acid (ATRA) and As_2O_3 (reviewed by Zhang *et al.*, 2001).

After treatment with 1 μM ATRA, the PML-RARα fusion protein in APL-derived NB4 cells was selectively degraded through the proteasome pathway, resulting in the release of wild-type PML and leading to differentiation of the transformed cells within 24 h (Dyck *et al.*, 1994, Muller *et al.*, 1998b). Muller *et al.* reported that As_2O_3 treatment induced the degradation of PML-RARα and restoration of ND10 in NB4 cells more efficiently than ATRA: after 2 h As_2O_3 (1 μM) treatment, the amount of PML-RARα fusion protein was decreased dramatically, and it was under the detectable level after 6 h treatment (Muller *et al.*, 1998b). Over the past several years, As_2O_3 has been an effective treatment for primary and relapsed APL patients. Although the exact mechanism of action of As_2O_3 on APL is not fully understood, it was proposed that a low dose of As_2O_3 (0.1-0.5

μM/kg/day) induces slow degradation of the oncoprotein resulting in normal differentiation and high-dose treatment (1-2 μM/kg/day) induces apoptosis (Zhang *et al.*, 2001).

1E.3.4 PML and its SUMO-1 modified isoforms

Ishov *et al.* (1999) noted that in PML -/- MPEF (mouse primary embryonic fibroblast) cells, the distribution of many ND10-associated proteins (Sp100, Daxx, ISG20, BLM, and CBP) was seen as a nuclear diffuse pattern that was re-located into ND10 when wild type PML was later transfected into the cells, suggesting that PML is essential for the assembly of ND10.

As mentioned, ND10 structures can be restored from the microsparkled pattern following treatment with As_2O_3 in APL derived NB4 cells (Muller *et al.*, 1998b). In about 30% of As_2O_3 treated NB4 cells, the size of PML dots greatly enlarges after a 4 h treatment, which correlates with an increase in SUMO-1 modified PML isoforms (Muller *et al.*, 1998b). These observations imply that post-translational modification by SUMO-1 might be involved in ND10 dynamics.

1E.3.5 Cell cycle

Koken *et al.* (1995) proposed that the average number and size of ND10 change during progression through the cell cycle. When cell growth was arrested at G_0 phase, the lowest number of ND10 was observed (Koken *et al.*, 1995). As the cell progressed through G_1 phase, the number of ND10 increases gradually and the highest number of ND10 is in S phase. ND10 are disrupted and the components are redistributed during mitosis and then are quickly re-formed in G_1 phase (Ascoli & Maul, 1991). In M phase, PML is though to be the most persistent ND10 protein, and can be found between chromosomes at metaphase and anaphase, forming large aggregations at the periphery of the mitotic cell in telophase (reviewed by Maul *et al.*, 2000). More recently it has been found that the disruption of ND10 that occurs during mitosis can be attributed to the complete loss of SUMO-1 modification from both PML and Sp100. In addition, a mitosis-specific hyperphosphorylated form of PML appears (Everett *et al.*, 1999b). Previous work had suggested that phosphorylation of PML might induce the loss of SUMO-1 modification (Muller *et al.*, 1998a).

1E.3.6 Effects of viral infections on ND10

Viral infection has been considered a factor affecting the integrity of ND10 structures since Maul and co-workers demonstrated disruption of ND10 in the course of herpesvirus infection (Maul *et al.*, 1993). In the past few years, the interaction with viruses and ND10 has been extensively studied, in particular the effects of DNA viruses: herpesviruses, adenoviruses, papilloma viruses and some RNA viruses: hepatitis delta viruses, retroviruses, and influenza viruses. A recent report from the Wilcox's group demonstrated that IFN co-ordinately inhibits the disruption of ND10 and viral IE gene expression during HSV-1 infection. The results showed that pre-treatment of cells with IFNs induced a specific and almost complete inhibition of expression from the IE-3 promoter, concomitant with enlargement and stabilisation of the ND10 structures in HSV-1 infected cells (Taylor *et al.*, 2000).

1E.3.6.1 Herpesviruses

Infection by several herpesviruses including HSV-1, HCMV, and EBV results in the disruption of ND10 (Maul *et al.*, 1993). Further investigations have demonstrated that IE gene products of these viruses are required for this effect. For example, as described previously (section1D.2.2, 1D.4.2), studies using a number of HSV-1 mutants revealed that ICP0 alone is sufficient for such disruption and its RING finger region is required for this effect.

As with HSV-1, HCMV (Town strain) infection has been reported to disrupt ND10 structures (Kelly *et al.*, 1995). Subsequent studies from the Hayward's group showed that at early times of infection (2 hpi), two IE products; IE1 (IE72) and IE2 (IE86), colocalised with PML in ND10. Observations from infection and transfection assays revealed that the IE2 protein localised within or adjacent to ND10 continuously, whereas IE1 transiently colocalised to and subsequently induced the redistribution of ND10 proteins into a nuclear diffuse pattern (Ahn & Hayward, 1997). These results were supported by the observations by Ishov *et al.* (1997). In addition, a potential zinc finger region of the IE1 protein has been shown to be essential for ND10 disruption and this process appears to be required for efficient viral gene expression and replication (Ishov *et al.*, 1997).

For γ-herpesviruses, EBV encoded nuclear antigen 5 (EBNA-5) has been demonstrated to associate with ND10 in EBV-infected B cells and cells of EBV-transformed lymphoblast cell lines (LCL), although EBNA-5 does not cause the redistribution of ND10 structures (Szekely *et al.*, 1996). In addition, heat treatment has been reported to cause dissociation of EBNA-5 from ND10 structures (Szekely *et al.*, 1996). Most recently, BZLF1 (Zta), one of the earliest viral proteins expressed, was reported to disrupt PML in transient transfection experiments, but only when BZLF1 was highly expressed (Adamson & Kenney, 2001). Infection by another γ-herpesvirus, HHV-8, has also been shown to involve interactions with ND10 (Katano *et al.*, 2001, Wu *et al.*, 2001a). Wu *et al.* (2001) demonstrated that the HHV8 K8 protein, shares significant homology to the BZLF1 protein of EBV and colocalised to but did not disrupt ND10 in both transient transfection and during viral infection experiments. The results of Katano *et al.* (2001) confirmed this observation and also defined the functional domain for K8 protein ND10 localisation to be its leucine zipper motif. In addition, it was observed that PML was highly expressed in HHV-8 and also in EBV-infected cells when compared to non-infected B cell lines. Intriguingly, transient expression of the K8 protein with the leucine zipper domain facilitated the recruitment of p53 to ND10. Taken with the finding that K8 represses the transcriptional activity of p53, this implies that colocalisation of K8 to ND10 might be associated with its interaction with cellular factors.

1E.3.6.2 Adenoviruses

Ishov and Maul (1996) reported that the peripheries of ND10 were the preferential sites for the early stages of transcription and replication of SV40, adenovirus 5 (Ad5) and HSV-1. However, as with HSV-1, infection of Ad5 has been demonstrated to disrupt ND10 before replication. Cells infected with adenovirus mutants with a deletion in the E4orf3 region retained intact ND10, indicating that E4orf3 is sufficient to disrupt ND10 structures (Carvalho *et al.*, 1995, Ishov & Maul, 1996). Moreover, a special track-like redistribution of ND10 proteins was observed at 8 h after infection (Ishov & Maul, 1996). Immunostaining for ND10 associated proteins such as PML, Sp100, NDP55 and NDP52 revealed that all proteins tested redistributed to the tracks before DNA replication began. After replication progression, only PML still remained in the tracks throughout the replication cycle, but other ND10 proteins segregated from the tracks to replication domains (detected by staining for the major viral DNA binding protein). The mechanism

of disruption of ND10 by E4orf3 remains unknown, but it has been observed that infection with adenovirus leads to progressive apparent phosphorylation of PML and loss of its SUMO-1 modified isoforms in an E4orf3-dependent manner (Leppard & Everett, 1999).

1E.3.6.3 Hepatitis delta viruses

The hepatitis delta virus (HDV) genome consists of a single coding region encoding the hepatitis delta antigen (HDAg) in two isoforms: large (L-HDAg) and small (S-HDAg) (Kuo *et al.*, 1989). S-HDAg is required for HDV replication whereas L-HDAg inhibits viral replication. Bell *et al.* (2000) described that L-HDAg was located in hollow sphere-like aggregates in the nucleus of Hep-2 cells transfected with HDV vectors at 4 days post-transfection. Double-staining with antibodies for L-HDAg and ND10 proteins (SUMO-1, PML, Sp100 and NDP55) revealed that approximately 55% of L-HDAg aggregates were often located adjacent to ND10. Furthermore, at later times, the distribution of ND10 constituents diverged visibly, with PML in the rims of the spheres, and others (Sp100, hDaxx and NDP55) in the centers of the spheres (Bell *et al.*, 2000). The observation that relocalisation of ND10 proteins into L-HDAg spheres differs to the phenotypes previously observed using other DNA viruses raises new possibilities for the regulation of both viral replication and ND10 function.

1E.3.6.4 Retroviruses

Infection with two retroviruses, human T cell leukemia virus (HTLV) and murine mammary tumour virus (MMTV), have been demonstrated to be associated with ND10 dynamics or proteins (Desbois *et al.*, 1996, Marchetti *et al.*, 1995). During MMTV infection, integration of the viral genome into the Int-6 gene locus (one of the proteins transiently associated with ND10) resulted in disruption of the gene and generation of a truncated form of the Int-6 protein (Marchetti *et al.*, 1995). HTLV interacts with ND10 by a different mechanism to MMTV, but it targets the same ND10 protein, Int-6. It has been found that the Tax protein of HTLV, which plays an important part in provoking transformation of infected cells, directly bound to Int-6 and diverted this protein into the cytoplasm from the nucleus (Desbois *et al.*, 1996).

1E.3.6.5 Arenavirus

It has been shown that during infection by the arenavirus lymphocytic choriomeningitis virus (LCMV), the viral Z protein interacted with PML resulting in the redistribution of PML into the cytoplasm (Borden *et al.*, 1998). Studies using a number of PML mutant constructs discovered that the Z protein, which consists of a RING finger domain, bound to the N-terminal region of PML. More recently, Djavani *et al.* reported that stable expression of PML in fibroblasts diminished LCMV virus replication, resulting from a decrease in transcription and translation levels of viral genes (Djavani *et al.*, 2001). Details of this aspect are described in section 1E.5 and reviewed by Regad & Chelbi-Alix (2001).

1E. 4 Various ND10 patterns in certain cell types

Little is known about ND10 in cells from species other than humans since most ND10 studies have been conducted using antibodies recognising only human forms of the ND10 proteins. However, it has been found that the presence or distribution of ND10 proteins can vary in a cell type-specific manner. A set of immunofluorescence and immuno-precipitation experiments using monoclonal antibodies 1150 and 138, which recognise Sp100 and NDP55 respectively, were employed to investigate the distribution of ND10 in various cell types including normal and neoplastic human tissues (Cho *et al.*, 1998). The results showed that ND10 size was increased in some sex-hormone dependent neoplastic cell types including breast ducal epithelium, endometrium, myometrial cells and testicular Leydig cells, compared with other cell types tested. Besides this, tumour cells with estrogen receptors have been found to have large ND10. Moreover, the number and size of ND10 were strongly increased in malignant tumours compared to benign tumours. These observations indicate that the distribution patterns of ND10 are closely associated with external factors such as hormonal stimulation and oncogenesis.

A number of studies revealed that some peripheral lymphoid tissues such as the germinal centre of spleen, lymph nodes and Peyer's patches lacked ND10 (Daniel *et al.*, 1993, Flenghi *et al.*, 1995, Gambacorta *et al.*, 1996, Lam *et al.*, 1995). In certain cells, loss of some but not all ND10 proteins was observed. For instances, no Sp100 was detected in Sertoli cells, whereas PML was expressed at a high level, and NDP55 was missing from hepatocytes whereas PML and Sp100 were detectable (reviewed by Negorev & Maul,

2001). Another example is that NT2 cells, an embryocarcinoma cell line, have no detectable expression of Sp100 and although other ND10 components are present, the expression pattern was different from other fibroblast cell lines tested (Hsu & Everett, 2001, Ishov *et al.*, 1999, Negorev *et al.*, 2001). As regards this last aspect, more details will be presented in this thesis.

1E. 5 Potential roles of ND10 on viral infections

As described in section 1E.3.2, the promoters of two major ND10 components, Sp100 and PML, contains both ISRE and GAS elements (Grotzinger *et al.*, 1996); (Stadler *et al.*, 1995), which mediate primary transcriptional induction in response to IFN-α/β and IFN-γ, respectively (Darnell *et al.*, 1994). It has been noted that Sp100 and PML expression, both at the RNA and protein level, were strongly enhanced by IFNs (Chelbi-Alix *et al.*, 1995, Grotzinger *et al.*, 1996, Stadler *et al.*, 1995). Together with the findings that viral infection causes ND10 disruption or reorganisation, this strongly implies that ND10 might play a role in host antiviral defence.

Chelbi-Alix *et al.* first demonstrated that the viral yields of VSV and influenza A viruses in CHO (Chinese hamster ovary) cells stably expressing PML, were decreased by up to 125- and 100-fold respectively, compared to control CHO cells (Chelbi-Alix *et al.*, 1998). Subsequent studies revealed that the function of PML in inhibition of viral replication was through interference with viral mRNA and protein syntheses and in an MOI dependent manner. However, resistance to viral infection is not a global effect shown by all ND10 proteins, since stable expression of Sp100 in CHO cells appeared to have no effect on the multiplication of VSV and influenza virus.

Recent work by Ahn and Hayward (2000) showed that disruption of ND10 correlates with efficient viral gene expression and replication in HCMV infection. Their previous reports initially demonstrate the association of HCMV infection with ND10 structures. At the early stages of HCMV infection, the major IE proteins IE1 and IE2 initially targeted to ND10. Within 3 hours, both IE1 and PML are redistributed into a nuclear diffuse pattern (Ahn & Hayward, 1997) whereas IE2 was stably remained adjacent to ND10 but later associated with viral DNA replication compartments (Ahn *et al.*, 1999). Later studies found that disruption of ND10 by HCMV was significantly delayed in U373-PML cells that express high levels of PML(560) (isoform VI) compared to the control U373 cell line

(Ahn & Hayward, 2000). Additionally, at 48 h after HCMV (Towne) infection, the formation of replication compartments (RC) in U373-PML cells was 5-fold lower than that in U373 cells. Notably, the delay of RC formation in cells expressing high levels of PML that had been infected with IE1 deletion mutants was 10-fold lower than in the control cells. Furthermore, western blot analysis revealed that in U373-PML cells, expression of E (Pol) and L (pp28) genes was repressed by 5- and 22-fold respectively, compared to that in U373 cells. These findings imply that at very early times after infection, disruption of ND10 resulting from interaction of IE1 with PML might play an important part for the progression of HCMV infection.

Recently, PML has been reported to mediate the interferon-induced antiviral state against two RNA viruses (Djavani *et al.*, 2001, Regad *et al.*, 2001). Djavani *et al* (2001) described that 48 hpi with LCMV at which time the highest virus yield is found, 4- to 5-fold decreases in PML +/+ MEF cells expressing PML compared to PML-/- cells. In addition, the decrease of viral replication in PML expressing cells was exacerbated by IFN-γ pre-treatment, up-regulating PML expression, suggesting that PML contributes to the antiviral effect of IFN. Consistent with this, Regad *et al.* (2001) proposed that infection with HFV (a retrovirus) was diminished in U373 MG cells stably expressing PML, but not that expressing Mx1 or MxA proteins. Further investigations found that IFN treatment inhibits HFV infection only in wild type cells but not in PML-/- cells. These two individual studies provide evidence that PML might play an important part in mediating an IFN-induced antiviral state.

As described in this section, during HSV-1 infection ICP0 induces disruption of ND10. However the effect of redistribution of ND10 proteins on the progress of HSV-1 infection is poorly understood. Studies investigating the effect of over-expression of ND10 proteins on HSV-1 infection have been carried out and are included in Chapter 3 of this thesis.

The aims of this study

As illustrated in the Introduction, several lines of evidence led me to investigate the role of ND10 in viral infection. Firstly, the expression of several ND10 proteins is up-regulated by IFNs. Secondly, in the course of viral infection some DNA viruses preferentially deposit their parental genomes close to ND10 structures. Thirdly, many viral IE gene products colocalise with ND10 proteins at early times of infection and subsequently trigger the degradation of these proteins resulting in the disruption of ND10 structures. Finally, it has been demonstrated that the formation of HSV-1 replication compartments is correlated with the disruption of ND10 structures. The IFN-inducible character, the spatial relationships, and the effect of viral proteins on ND10 during infection indicate that these events might not be a simple accident, but imply a role for ND10 in an antiviral effect.

The aim of this study is to investigate the potential role of ND10 proteins in HSV-1 infection in different cultured fibroblast cells. To address this question, I initially compared the infectivity of HSV-1 under various conditions such as stress or transient transfections by which the integrity of ND10 was disrupted or the expression of ND10 proteins was induced, respectively (Chapter 3 and Chapter 5). Secondly, I characterised a human neuronal committed cell line (NT2) that contains abnormal ND10 expression pattern and further investigated its susceptibility to HSV-1 infection (Chapter 4). Finally, a series of mutant constructs of SUMO-1, which had a potential antiviral effect (based on the observations of the earlier work in this thesis), were made to study the effect of this ND10 component on viral infection in the NT2 cell line (Chapter 5).

Chapter 2 MATERIALS AND METHODS

Chapter 2 MATERIALS and METHODS

2.1 Materials

2.1.1 Plasmids

- The following plasmids were provided by the acknowledged investigators:
- pPML (F) (also known as pPML-ER(F)/pTL2) (Kastner *et al.*, 1992) expresses PML isoform IV (633aa) with a C-terminal tag derived from the estrogen receptor. It was a gift from Pierre Chambon.
- pcDNA3/PML-RH (Kamitani *et al.*, 1998) expresses PML coding sequences (isoform undefined by originators) as a fusion protein with a polyhistidine tag at the C-terminus under the control of the HCMV promoter. It was generated by inserting a 2.03-kb full-length PML cDNA into pcDNA3/RH-C between the *Hind* III and *Kpn* I sites. It was kindly proved by Tetsu Kamitani (University of Texas).
- pcDNA3/UbcH9 was a gift from Dr. Joanna Desterro. The cDNA of UbcH9 was cloned with a C-terminal SV5 tag into pcDNA3 using its *Bam*H I and *Xho* I sites (Desterro *et al.*, 1997).
- pcDNA3-HP1 was kindly provided by Dr. Alexander Ishov. The HP1 was expressed as a fusion protein with N-terminal FLAG tag (unpublished).
- pEGFP-NLS-hDaxx was a gift from Dr. Alexander Ishov. The hDaxx protein was expressed as a fusion protein with N-terminal EGFP and the nuclear localisation signal from SV40 large T-antigen (Ishov *et al.*, 1999).
- pCIQEUb52 (Everett *et al.*, 1997) expresses the polyhistidine tagged Ub52 ubiquitin precursor gene under the control of the HCMV promoter.
- pCImycSp100 expresses Sp100 (isoform A) with an N-terminal myc tag driven by the HCMV promoter.
- pCIPIC-1 (Everett *et al.*, 1998) was used to express SUMO-1 and contains the SUMO-1 coding region with an N-terminal c-myc epitope tag sequence inserted downstream of the HCMV promoter in vector pCIneo.

- pSS80 contains the CAT gene under the control of the ICP6 promoter (Everett *et al.*, 1995).

- pCI-rtag-cICP0: This plasmid expresses ICP0 from its cDNA with an N-terminal tag derived from HSV-1 UL30 protein that is recognised by rabbit serum r113. It is the cDNA version of a related plasmid described by Parkinson and Everett, 2001.

- p175 contains the ICP4-coding region under the control of the SV40 early promoter (Everett, 1988).

- pTK1 contains the HSV-1 *Bam*HI P fragment including the HSV-1 TK gene (Wilkie *et al.*, 1979).

2.1.2 Bacteria (*E. coli* strains):

Escherichia coli (*E. coli*) strain DH5α (F'/*end*A1 *hsd*R17 (r_k^-mk+) *sup*E44 *thi*1 *rec*A1 *gyr*A (Nal^r) *rel*A1 Δ(*lac*ZYA-*arg*F) U169 (ϕ80*dlac*Δ(*lac*Z) M15) was used for propagation and maintenance of plasmid DNA.

2.1.3 Bacterial culture media

DH5α bacteria were grown in Lauria-Bertani medium (LB) (10g NaCl, 10g Bactopeptone, 5g yeast extract in 1L water, pH7.5). Agar plates were made with 1.5% (w/v) agar in LB. Where necessary, media and agar plates were supplemented with antibiotics: 100 μg/ml ampicillin for bacteria harbouring plasmids containing the ampicillin resistance gene and 30 μg/ml kanamycin for EGFP plasmids.

2.1.4 Cells and tissue culture media

All cell culture media were obtained from Life Technologies (Gibco BRL).

- **Hep2 cells** (obtained from the cytology department of the Institute of Virology), an epithelial cell line, were grown in Dulbecco's modified Eagle's medium (DMEM) supplemented with 10% foetal calf serum (FCS), 100 units/ml penicillin and 100 μg/ml streptomycin.

- **Baby hamster kidney-21 C13 (BHK-21 C13) fibroblast cells** were derived from baby hamster kidney and were cultured in Glasgow-modified Eagle's medium (GMEM) supplemented with 10% (v/v) tryptose phosphate broth, 10% newborn calf serum and 100 units/ml penicillin and 100 μg/ml streptomycin.
- **Vero cells,** derived from African green monkey kidney, were grown in DMEM supplemented with 10% FCS, 100 units/ml penicillin and 100 μg/ml streptomycin.
- **Human foetal lung (HFL)** diploid fibroblast cells (Imperial Laboratories) and osteosarcoma U2OS cells were propagated in DMEM supplemented with 5% FCS, 5% NBCS, 1% non-essential amino acids, 100 units/ml penicillin and 100 μg/ml streptomycin.
- **The Ntera 2/D1 (NT2) cell line** was obtained from Stratagene and was grown in DMEM with nutrient mixture F12, supplemented with 4 mM glutamine, 10% FCS, 100 units/ml penicillin and 100 μg/ml streptomycin.

2.1.5 Viruses

- HSV-1 **strain 17+**, the wild type virus (Brown *et al.*, 1973), was the parental strain used for the construction of all mutant derivatives.
- **Virus FXE** has an in-frame deletion of ICP0 residues 106-150, which removes the zinc binding RING finger domain of the protein (Everett, 1989).
- **Viruses vEG-110wt** and vEG-FXE express derivatives of wild type and FXE mutant ICP0 with EGFP linked to their N-terminal ends (Lomonte & Everett, 1999).
- ***dl*1403** is a ICP0 null mutant virus, from which the majority of ICP0 coding region (from residue 106 onwards) has been deleted (Stow & Stow, 1986).
- **Virus M1** contains double amino acid substitutions (R623L, K624I) in the USP7 binding region of ICP0, such that the mutant M1 ICP0 protein does not bind to USP7 (Everett *et al.*, 1999c).
- **Virus *tsK*** has a single amino acid substitution that inactivates the ICP4 transactivator protein at 38.5°C. As a result, there is a failure to activate early and late gene expression and high level expression of the other IE proteins at the nonpermissive temperature of 38.5°C (Preston, 1979).

- **Virus in1330** carries an HCMV lac Z gene cassette inserted into UL43, the ICP4 *tsK* mutation, and a deletion in the ICP0 coding region inducing a frameshift in codon 105 (Homer *et al.*, 1999).

2.1.6 Antisera and monoclonal antibodies (Table 2.1)

2.1.7 Oligonucleotides

Oligonucleotides used in PCR and generation of the c-myc tag were supplied by MWG. They were used without further purification.

2.1.8 Enzymes

Restriction enzymes were purchased from Roche Biochemicals and New England BioLabs. T4 DNA ligase and *E. coli* DNA polymerase I Klenow fragment were purchased from Life Technologies. Lysozyme and RNase A were purchased from Sigma. T4 polynucleotide kinase, calf intestinal phosphatase, proteinase K, and Taq DNA polymerase were obtained from Roche Biochemicals.

2.1.9 Sequencing

All sequences in this thesis were kindly carried out by Mrs. L. Taylor at the Institute of Virology and performed on an ABI Prism 377 DNA sequencer.

2.1.10 Phosphor-imaging

The results of CAT assays were analysed on a BioRad MolecularImager FX machine using a Biorad Pentium computer with QuantityOne Phospho and Multi-imager software (4.0.3). Instruction was generously provided by Mr. Colin Loney.

Table 2.1 Antibodies used

Primary antibodies			*Dilution used*		*Reference*	*Source*
Antibody	**Antibody against**	**Type**	**IFA**	**W. blot**		
11060	ICP0	mouse	1:10,000	1:10,000	(Everett *et al.*, 1993b)	R. D. Everett, MRC Virology Unit, Glasgow
10176	ICP4	mouse	1:5,000	1:5,000	(Everett *et al.*, 1993a)	R. D. Everett, MRC Virology Unit, Glasgow
r190	ICP0	rabbit	1:200	ND	(Everett *et al.*, 1998)	R. D. Everett, MRC Virology Unit, Glasgow
r76	UL39	rabbit	ND	1:10,000	(Conner *et al.*, 1995)	H. Marsden, MRC Virology Unit, Glasgow
r515	UL29	rabbit	1:200	ND	(Marsden *et al.*, 1996)	H. Marsden, MRC Virology Unit, Glasgow
Z1F11	UL42	mouse	ND	1:5,000	(Schenk *et al.*, 1988)	H. Marsden, MRC Virology Unit, Glasgow
r127141/2	β-galactosidase	rabbit	1:1,000	ND	NP	H. Marsden, MRC Virology Unit, Glasgow
SpGH	Sp100	rabbit	1:1,000	ND	(Sternsdorf *et al.*, 1995)	T. Sternsdorf, University of Hamburg
5E10	PML	mouse	1:20	ND	(Stuurman *et al.*, 1992)	Roel van Driel, University of Amsterdam
r8	PML	rabbit	1:1,000	ND	(Boddy *et al.*, 1996)	P. Freemont, Imperial Cancer Research Fund
r554	CENP-C	rabbit	1:300	ND	(Saitoh *et al.*, 1992)	W. Earnshaw, University of Edinburgh
r1866	hDaxx	rabbit	1:2,000	ND	(Pluta *et al.*, 1998)	A. Pluta, University of Maryland
ACA-GS	centromeres	human	1:20,000	ND	(Earnshaw, 1988)	W. Earnshaw, University of Edinburgh
9E10	c-myc	mouse	1:1,000	ND		Santa Cruz Biotechnology
A14	c-myc	rabbit	1:1,000	ND		Santa Cruz Biotechnology
F3	F tag	mouse	1:1,000	ND	(Ali *et al.*, 1993)	Chambon, (IGBMC), College de France, France
MRGS-His	MRGS-His	mouse	1:1,000	ND		Qiagen
pp65	pp65 (HCMV)	mouse	1:1,000	ND		Capricorn Products Inc.
SV5	SV5-P-K	mouse	1:500	ND	(Dunn *et al.*, 1999)	R. E. Randall, University of St. Andrews

Secondary antibody	*IFA*	*W. blot*	*Source*
Anti Mouse FITC Conjugate	1:100	ND	Sigma
Anti Rabbit FITC Conjugate	1:100	ND	Sigma
Anti Mouse Cy3 Conjugate	1:5,000	ND	Amersham
Anti Rabbit Cy3 Conjugate	1:5,000	ND	Amersham
Anti Rabbit Cy5 Conjugate	1:200	ND	Amersham
Anti Human TRITC Conjugate	1:100	ND	Sigma
Anti Mouse HRP Conjugate	ND	1:1,000	Sigma
Anti Rabbit HRP Conjugate	ND	1:5,000	Sigma

Abbreviations: ND, not done; NP, not published; IFA, immunofluorescence assay; W. Blot, western blot.

2.1.11 Common solutions

Recipes of general solutions have been listed below and the details of all other solutions have been included either in the text or at the end of the relevant section.

DNA gel solutions:

Blue juice (10x Loading buffer)	1x TBE, 1% SDS, 50% glycerol, bromophenol blue
20x TBE	2.5 M Tris, 0.8 M boric acid, 54 mM EDTA (pH 8.0)
50x TAE	0.2 M Tris, 50 mM EDTA, pH to 7.6 with acetic acid
1xTE	10 mM Tris-HCl, 1 mM EDTA (pH 8)
STET	8% sucrose, 5% Triton-X100, 50 mM EDTA, 50 mM Tris-HCl (pH 8)

Cell culture solutions:

PBS(A)	170 mM NaCl, 3.4 mM KCl, 10 mM Na_2HPO_4, 1.8 mM KH_2PO_4, pH 7.2
Versene	0.6 mM EDTA in PBS(A), 0.02% phenol red
Trypsin	0.25% (w/v) trypsin in Tris-saline containing phenol red, adjusted to pH 7.5 with $NaHCO_3$
Water	Sterile deionised water obtained from a "Milli-Ro 60 plus" deioniser (Millipore, USA) and sterilised by autoclaving.

Solutions for immunofluorescence:

Fix solution	2% (w/v) sucrose, 5% (v/v) formaldehyde (37.5%) in PBS (A)
Permeabilisation solution	10% (w/v) sucrose, 0.5% NP40 in PBS (A)

Southern blot assay:

Cell lysis buffer (total DNA extraction)	0.6% SDS, 10 mM EDTA, 10 mM Tris-HCl (pH 7.4), 0.5 mg/ml Proteinase K
20x SSC	0.3 M Na_3Citrate, 3 M NaCl
denaturing solution	0.5 M NaOH, 1.5 M NaCl
Neutralising solution	0.5 M Tris-HCl (pH 7.2), 1.5 M NaCl, 1 mM EDTA
Prehybridisation buffer	5x SSC, 0.5% SDS, 0.1% (w/v) Ficol (type 400), 0.1% (w/v) polyvinylpyrrolidone, 0.1% (w/v) bovine serum albumin, salmon sperm DNA (20 μg/ml)
Wash solution	2x SSC, 0.1% SDS

Solutions for SDS-polyacrylamide gel electrophoresis:

3x boiling mixture (protein loading buffer)	6% SDS, 30% glycerol, 30% SGB, 0.3% bromophenol blue, 2 M β-mercaptoethanol
SGB (stacking gel buffer)	0.5 M Tris-HCl, 0.4% SDS, pH 6.7
RGB(resolving gel buffer)	1.5 M Tris-HCl, 0.4% SDS, pH 8.9
Running buffer	0.05 M Tris, 0.05 M glycine, 0.1% SDS
Towbin (blotting buffer)	25 mM Tris base, 192 mM glycine, 20% (v/v) methanol
Stripping buffer	100 mM β-mercaptoethanol, 2% SDS, 62.5 mM Tris-HCl, pH 6.7
PBS-T	PBS(A), 0.2% TWEEN-20

CAT assays:

TNE buffer	50 mM Tris-HCl, 1 mM EDTA, 0.15 M NaCl, adjusted to pH 7.2
TLC running buffer	95% Chloroform, 5% Methanol

2.1.12 Chemicals and reagents

All chemicals and reagents were purchased from BDH Chemicals UK or Sigma Chemical Company, unless otherwise stated below or in the relevant sections:

compound	Supplier
30% acrylamide (37.5:1)	National Diagnostics
agar	Difco
ampicillin	Beecham Research Laboratories Ltd
APS (ammonium persulphate)	Bio-Rad
bactotryptone	Difco
boric acid	Prolabo
butanol	Prolabo
chloroform	Prolabo
Citifluor	Citifluor Ltd
coomassie brilliant blue	Bio-Rad
caesium chloride	Melford Laboratories Ltd
dNTPs	Pharmacia
DMSO (dimethyl sulphoxide)	Koch-Light Laboratory Ltd
dried skimmed milk	Marvel
Ethanol (ultra pure)	Prolabo

glacial acetic acid	Prolabo
Glycerol	Prolabo
hydrochloric acid	Prolabo
isopropanol	Prolabo
Methanol	Prolabo
Nitro-cellulose membranes	Hybond
Rainbow markers™	Amersham Life Science
TEMED (N,N,N′,N′-tetramethylethylenediamine)	Bio-Rad
TLC plates (polygram SIL G)	Machery-Nagel
yeast extract	Difco

2.1.13 Radiochemicals

Compound	Specific activity (concentration)	Supplier
[α^{32}P] dCTP	3000 Ci/mmol (10 mCi/ml)	Amersham
[C^{14}] chloramphenicol	58.5 mCi/mmol (0.1 mCi/ml)	Amersham

2.1.14 Autoclaving and glassware sterilisation

Equipment and solutions were sterilised by autoclaving at 15 psi for 20 min by the staff in the wash room, Institute of Virology, Glasgow. Glassware was sterilised by baking in an oven at 180°C for at least 12 h. Heat labile solutions were sterilised by filtration through a Whatman syringe filter (0.2 μm pore size) into a sterile tube.

2.2 METHODS

2.2.1 Nucleic acid manipulation

2.2.1A Restriction enzyme digestion of DNA

Restriction enzyme digestion of DNA was carried out according to the manufacturer's instructions for the relevant enzyme. Usually, 0.5 μg DNA was digested for diagnostic analysis and 5-20 μg for isolation of specific restriction fragments.

2.2.1B Phenol/Chloroform extraction and alcohol precipitation

When the enzyme buffers were incompatible for double enzyme digestions or further enzyme reactions, the DNA was purified by a method involving several stages. The first stage was the heat inactivation of enzymes for 10 min at 65°C. A Leder phenol (phenol: chloroform: isoamyl alcohol = 25:24:1) extraction was performed on the sample. An equal volume of TE-saturated Leder phenol was added to the sample and mixed by inversion, followed by centrifugation at 13,000 rpm for 5 min at room temperature (RT). The upper aqueous phase containing the DNA was transferred to a fresh tube and precipitated using an ethanol precipitation method. This involved the addition of 2.5 volumes of absolute ethanol and $1/10^{th}$ the sample volume of 3 M NaOAC (pH 5.2) to the sample, which was then left at -20°C for 30 min. The DNA was pelleted by centrifugation at 13,000 rpm for 10 min at RT and the DNA pellets were washed with 70% ethanol and resuspended in water before use or storage at -20°C.

2.2.1C Production of blunted ends on DNA fragments

Fragments generated by enzymes, which produce 5' overhangs sometimes required modification (i.e. "blunt ending") to enable ligation. DNA was blunt-ended by incubation of the digestion mixture with dNTPs (at 50 μM per dNTP) and 2 units of DNA polymerase I large Klenow fragment for 30 min at 37°C.

2.2.1D Dephosphorylation of 5' ends of DNA (Phosphate removal from 5' ends)

The removal of phosphate residues at the 5' ends of vector fragments with complementary ends produced by digestion with a single restriction enzyme was performed to prevent re-circularisation of the vector fragment upon ligation. This was achieved with the incubation of the digestion mixture with 1 unit of calf intestinal alkaline phosphatase (CIP) in the appropriate buffer for 20 – 30 min at 37 °C.

2.2.1E Electrophoretic separation and purification of DNA fragments

DNA fragments produced by restriction enzyme digestion or PCR were resolved by agarose gel electrophoresis. Horizontal slab gels approximately 0.5 cm thick were utilised and samples were loaded following addition of the relevant amount of agarose gel loading buffer. Appropriate size markers were always run on the gels. Agarose gels of between 0.7% and 1.5%, depending on the size of the fragments to be analysed, were made up in 1x TAE and run at 12 V/cm in 1x TAE buffer. Following electrophoresis, the gels were stained in 1 μg/ml EtBr (ethidium bromide) solution followed by rinsing the gel three times with water. DNA was visualised under U.V. light (normally short wave, but long wave was used for preparative gels). Photography was carried out using The Imager (Appligene).

2.2.1F Preparation of annealed oligonucleotide DNA fragments by polyacrylamide gel electrophoresis (PAGE)

The oligonucleotide pellet supplied by MWG was resuspended in water at a concentration of 100 pmol/μl. The oligonucleotide DNA fragments (0.5μg) were mixed with 0.1M NaCl in a total volume of 50 μl and denatured at 90°C. The heat- denatured DNA fragments were then annealed at room temperature and purified using PAGE when it was cooled to 30°C. 8% vertical non-denaturing polyacrylamide (acrylamide: N,N'-methylene-bisacrylamide 19:1) gels containing 1x TBE were used to resolve DNA fragments of between 50-200 bp. Polymerisation was initiated by adding 0.01 volumes 10% APS and 0.001 volumes TEMED. Samples were mixed with a gel loading buffer containing glycerol, bromophenol blue and xylene cyanol ("blue juice") were loaded on the gels in a kit manufactured in-house and run in 1x TBE running buffer at up to 16 V/cm.

DNA fragments were visualised using the EtBr staining method described in Section (2.2.1E)

2.2.2 Isolation of DNA fragments from agarose gels

Agarose blocks containing appropriate DNA fragments were excised from gels under long-wave U.V. using a U.V. Products Inc. transilluminator and the DNA recovered using a commercial kit, GENECLEANII (BIO101) Inc., La Jolla, CA. The kit contains a silica matrix, which binds DNA in the presence of high concentrations of sodium iodide (Vogelstein & Gillespie, 1979).

The gel slice was weighed to estimate its volume and cut into small pieces to facilitate gel dissolution in 3 volumes of NaI solution. This sample was incubated at 55°C for 5 min, or until the gel slices were dissolved. The silica matrix was then added (5 µl for up to 5 µg DNA) and the mixture vortexed and left on ice for 5-10 min. Following a 10 sec full-speed (13,000 rpm) centrifugation, the silica matrix pellet was washed twice in 700 µl 'NEW' wash. The DNA was eluted into water by mixing the washed pellet with 20 µl water and incubating the sample at 55°C for 5 min. The matrix was pelleted and the supernatant containing the DNA transferred to a fresh tube and stored at -20°C.

2.2.3 Ligation of DNA fragments

Before ligation, extraction of linearised DNA from a previous enzyme reaction was done by using the Leder phenol method followed by alcohol precipitation described in section (2.2.1B).

Ligation of appropriately ended insert and vector DNA fragments was done by incubation of a 3:1 respective ratio of insert/vector DNA in a reaction volume of 20 µl with 1x ligation buffer and 1 unit of T4 DNA ligase at RT overnight.

2.2.4 Transformation of *E. coli*

2.2.4A Preparation of frozen transformation-competent bacterial cells

Frozen transformation-competent *E. coli* DH5α cells were prepared using the calcium chloride method. A fresh single colony from a LB plate was inoculated into 5 ml of LB broth and grown at 37°C overnight. The next day, 1 ml of the overnight bacteria culture was added to 100 ml fresh LB broth and cultured at 37°C to an optical density (OD) 550 of 0.3 - 0.5. Cells were chilled on ice for 15 min, pelleted by centrifugation at 3000 rpm for 10 min at 4°C in a Sorvall GS3 rotor, drained, and resuspended by pipetting up and down in 10 ml of 0.1 M $MgCl_2$. The cells were then washed in 10 ml of 0.1 M $CaCl_2$ in the same way and incubated on ice for 45 min. The cells were re-pelleted, drained, resuspended in 5 ml of the competent cell storage buffer (20% Glycerol, 50 mM $CaCl_2$, 0.1 M Na salt MOPS) and then the competent cells used immediately for plasmid transformation or flash frozen in 100 µl aliquots using a dry-ice/ethanol bath and stored at –70°C.

2.2.4B Transformation of competent cells

Frozen competent cells were thawed slowly on ice. A half volume (10 µl) of ligation mixture (for plasmid DNA subcloning) or 10 ng of intact plasmid (for DNA amplification) was added to 100 µl of competent cells, gently mixed, and incubated on ice for 30 min. The cells were heat shocked at 42°C for 90 sec, chilled on ice for 1 min, and 400 µl of LB broth without any antibiotics added, before incubation at 37°C for 1.5 h with agitation. 100 µl of the culture was plated onto pre-dried nutrient agar plates, supplemented with appropriate antibiotics, for example 100 ug/ml ampicillin for selection for ampicillin resistant colonies. Plates were incubated inverted at 37°C overnight.

2.2.5 Preparation of plasmid DNA

2.2.5A Small scale crude plasmid preparation

The boiling method was used to produce plasmid DNA for diagnostic purposes. A single fresh colony was inoculated into 3 ml LB broth with appropriate antibiotics (for example 50 µg/ml ampicillin) and cultured in a 37°C incubator with shaking for 5 h. The bacterial culture (1.5 ml) was pelleted using a bench top centrifuge (Micro Centaur, SANYO) at full speed for 2 min, the supernatant was discarded and the pellet was

resuspended in 200 µl of STET buffer. A 5 µl aliquot of a lysozyme solution (10 mg/ml) was added to the bacterial suspension, which was then transferred to a boiling water bath for 50 sec, followed by full-speed centrifugation for 10 min. The supernatant was transferred into a new eppendorf tube and precipitated with 0.9 volumes of iso-propanol and centrifuged for another 10 min. The plasmid pellet (containing RNA) was dissolved in 20 µl of either 1x TE buffer or water and 4 µl of the DNA was analysed by restriction enzyme digestion.

2.2.5B Large scale plasmid preparation

E.coli containing the desired plasmids were streaked from an older culture onto a LB agar plate containing the appropriate antibiotics and incubated at 37°C overnight. Plasmid DNA was prepared from bacteria according to the 'maxi-boiling' method (Holmes & Quigley, 1981) and the supercoiled DNA was purified on a caesium chloride gradient. A single colony was picked from a fresh plate and used to inoculate 350 ml LB broth containing antibiotics as appropriate, which was incubated in a shaking incubator at 37°C overnight. Bacterial cultures were centrifuged at 5,000 rpm for 10 min at RT in a Sorvall GS3 rotor, then the pellets were resuspended in 20 ml STET and 2.5 ml of a freshly prepared 10 mg/ml lysozyme solution was added to the bacteria culture for 1 minute. The mixture was brought to the boil over a bunsen flame and placed in a boiling water bath for 45 sec, before pelleting the cell debris by centrifugation in a Sorvall SS34 rotor at 18,000 rpm for 50 min at RT. Nucleic acids were precipitated from the supernatant by the addition of 0.9 volumes of isopropanol, and pelleted by centrifugation in a Beckman GPR centrifuge at 3,000 rpm for 5 min at RT. The pellet was resuspended in 5.5 ml 1x TE (to give a volume of around 6.3 ml), then 7 g caesium chloride and 0.2 ml 10 mg/ml EtBr were added. The samples were incubated on ice for 20 min prior to centrifugation at 3,000 rpm for 10 min at 4°C. The supernatant was transferred to a Dupont 03945 crimp-seal centrifuge tube using a syringe and centrifuged at 45,000 rpm for 16-18 hr, at 15°C in a Sorvall TV865 vertical rotor. The lower fluorescing DNA band containing supercoiled plasmid DNA was removed using a syringe, taking care to avoid contamination with bacterial chromosomal DNA from the upper band. The EtBr was removed from the plasmid solution by 2-3 extractions with butanol saturated with 1x TE, and the caesium chloride was removed by dialysing against 1x TE at RT for 2 hr. Following this, the

solution was treated with 100 μg/ml RNase A at 65°C for 1 hr, and 100 μg/ml proteinase K plus 0.1% SDS at 37°C for another 1 hr. The plasmid DNA was cleaned by phenol followed by chloroform extraction, and concentrated by ethanol precipitation at –20°C overnight. The DNA was pelleted by centrifugation at 3,000 rpm for 15min at 4°C, resuspended in 400μl 1X TE transferred in a new eppendorf tube and ethanol precipitated again. The final pellet was washed in 70% ethanol and resuspended in an appropriate volume of 1xTE before storage at 4°C. The plasmid DNA concentration was determined by measuring the absorbance at 260 nm on a Beckman DU-62 spectrophotometer, assuming 1OD A_{260} = 50 μg/ml.

2.2.6 Amplification of DNA by polymerase chain reaction (PCR)

2.2.6A Oligonucleotide primers

The oligonucleotide primers were supplied by MWG, and prepared for use by dissolving in distilled H_2O.

2.2.6B PCR

PCR was used to generate wild type and mutant forms of the SUMO-1 cDNA. PCR reactions were performed in sterile 0.5 ml Eppendorf tubes using a thermocycler (Techne) and *Taq* DNA polymerase (Roche).

Two units of Taq DNA polymerase were added to 1 ng of *Sal* I – *Not* I fragment from plasmid DNA (pCIPIC1) in 100 μl of 1x *Taq* PCR buffer (supplied with the enzyme), containing 0.2 mM dNTPs and 2.5 mg/ml oligonucleotide primers and the reaction was overlaid with a drop of molecular biology grade mineral oil (Sigma). DNA was denatured at 95°C for 5 min and amplified by 25 cycles of denaturation at 95°C for 1 min, annealing for 3 min at the lowest calculated annealing temperature for the primers used, where:

Annealing temperature = n (G+C) x 3 + n(A+T) x 2 °C

and elongation at 72°C for 3 min, and then finally elongated for 5 min at 72°C. The Amplified DNA was clarified by Leder phenol extraction and alcohol precipitation followed by appropriate restriction enzyme digestion to produce the appropriate ends for cloning.

2.2.7 Southern blot analysis of DNA

2.2.7A Preparation of labeled probes by random priming

50 ng of plasmid DNA was denatured at 95°C for 10 min, cooled on ice, and radioactively labeled with 50 μCi of [α^{32}P]dCTP (Amersham) using a Megaprime DNA labelled kit (Amersham), according to the manufacturer's protocol. The reaction was stopped with 0.2 M EDTA (pH 8) and unincorporated nucleotides removed by column chromatography (section 2.2.7.B).

2.2.7B Column chromatography purification of radiolabelled probes

"Nick" columns (Pharmacia) containing a size exclusion resin were washed three times with 2 ml 1x TE, 0.1% SDS before use. The Megaprime (Amersham) reaction mix was applied to the column with 100 μl 1x TE, 0.1% SDS and 1 ml 1x TE, 0.1% SDS were further added to wash the radiolabelled mix through the column. Fractions (5 drops) were collected and monitored using the Geiger counter. The initial peak (within the first 10 fractions) contained the probe while the unincorporated radioactivity was eluted later.

2.2.7C Southern blot hybridisation (Southern, 1975)

i. Southern transfer

DNA fragments were resolved by agarose gel electrophoresis (Section 2.2.1.E). The gel was washed in water and submerged in 200 ml denaturing solution on a shaker for 60 min to denature the double stranded DNA. After a brief rinsing of the gel in deionised water, the gel was incubated in 200 ml neutralising solution on a shaker for 30 min and in fresh neutralising buffer for another 60 min. The gel was rinsed in 2X SSC for 2 min and the DNA was transferred to a Hybond-nitrocellulose membrane, which had been pre-soaked in water and 2X SSC for 5 min, by capillary action for 12-15 h overnight at RT. Subsequent hybridisations and washes were performed with rotation in an oven (Hybaid).

ii. Hybridisation with probes

The membrane was soaked for 2 min in 6X SSC and incubated at 65°C for 3 h in 5 ml of prehybridisation buffer. ^{32}P-labeled probes were denatured by boiling for 5 min, rapidly

chilled on ice, added to the prehybridisation buffer, and hybridised to the membrane at 65°C overnight. The nitrocellulose was washed twice in 2X SSC, 0.1% SDS at RT for 10 min, followed by washing three times in 2X SSC, 0.1% SDS at 65°C for 30 min, dried, wrapped in cling-film, and exposed to X-ray film or a phosphor-imager screen.

2.2.8 Tissue culture

2.2.8A Maintenance and subculture of cell stocks

Mammalian cells were passaged in sterile disposable 75cm^2 plastic flasks in appropriate media (Section 2.1.4) and grown at 37°C in a humidified incubator containing 5% CO_2. Confluent layers were trypsinised by washing the monolayer once with 10 ml of versene and once with versene/trypsin (4:1, supplied by Institute of Virology Media services) respectively. Rounded cells were resuspended in 10 ml of fresh medium. For continual passage, BHK cells were split 1:10 every 4 days, HFL 1:3 every 4 days, Vero cells and Hep-2 cells 1:6 every 4 days. For the NT2 cell line, a seeding density of 4 x 10^4 cells per 25 cm^2 flask area was used to avoid spontaneous differentiation.

2.2.8B Differentiation of NT2 cells

NT2 cells were harvested from flasks as described above by trypsinising and resuspending in 10 ml of medium. 1 x 10^6 NT2 cells were seeded into 25cm^2 flasks with 5 ml of medium containing 10 μM all-trans-retinoic acid (ATRA). The culture medium was changed 3 times per week for 6 weeks. The 6-week differentiated hNT cells were transferred to a 75 cm^2 flask in media without ATRA and cultured for an additional 2 days. The loosely adherent hNT cells were recovered in the culture medium by striking the flask sharply, resulting in a population of cells with more than 30% having a significant neuronal morphology.

2.2.8C Frozen stocks of NT2 and hNT cells

Confluent cell monolayers of NT2 or hNT cells were harvested from 175 cm^2 flasks by trypsinising and resuspending as described above in 15 ml of media followed by centrifuged at 1000 rpm at 4°C for 5 min. Cell pellets were resuspended in NT2 cell storage buffer (95% Foetal calf serum, 5% DMSO) at a density of 2 x 10^6 cells/ml.

Aliquots of 1 ml were added to 1.5 ml cryo-vials, kept at 4°C overnight followed by an overnight period at –70°C, then transferred to a liquid nitrogen freezer for long term storage.

2.2.9 Protein expression and analysis (transient expression in mammalian cells)

2.2.9A Electroporation

Hep2 cells from a 175cm^2 flask were trypsinized as described previously, then washed with serum- and antibiotic-free DMEM twice. After the final wash, cells were resuspended in an appropriate volume, such that the concentration of cells was 5 x 10^6 cells/ml. For each electroporation, 4 x 10^6 cells and 20 μg of DNA were used. DNA was put in a 4 mm cuvette and incubated with the cells on ice for 10 min. After pipetting gently to resuspend settled cells, the cells were electroporated at 400 V (Hybaid cell shock electroporator), and incubated on ice again for 10 min. Electroporated cells were added to 10 ml complete medium to give a final cell density of 4 x 10^5 cells/ml and cells distributed into Linbro wells as required. For immunofluorescence, a density of 2 x 10^5 cells per Linbro well was required.

2.2.9B Lipofection

The Lipofectamine PLUS kit (Life techonologies) was employed for all the lipofection experiments. According to the manufacturer's protocol, cells were seeded in a Linbro well with a coverslip at a density of 1 x 10^5 cells per well one day prior to transfection to reach 60-80% confluent next day. For each well, 100 ng of DNA and 2 μl of PLUS reagent were mixed in 100 μl of plain DMEM (without serum and antibiotics) and the mixture incubated at RT for 15 min. Pre-mixed lipofectamine solution (1 ul of Lipofectamine with 100 μl of plain DMEM for each well) was added to the DNA-PLUS reagent solution and kept at RT for another 15 min. In the meantime, cell monolayers were washed with plain DMEM twice (the conditioned medium was kept for further use), and 200 μl of DMEM was added after this wash. The 250μl sample of DNA-PLUS-Lipofectamine mixture was poured over the cell monolayer and incubated at 37°C for 3 h followed by the addition of an equal volume of complete medium with 20% of FCS for a

further 2 hr. At this time, the transfection mixture was removed and the conditioned medium retained from the original growth of the cells was added, and the cells were left in the 37°C incubator overnight.

2.2.10 Resolution of proteins by SDS-polyacrylamide gel electrophoresis

Proteins were resolved by electrophoresis through SDS polyacrylamide minigels (Laemmli, 1970) using the Bio-Rad miniprotein II apparatus. The resolving gel mixes were prepared first and poured into glass plate sandwiches in the BioRad gel former apparatus, overlaid with butanol and left to set. Once the gel had set, the butanol was washed away with water. The set gel was then overlaid with stacking gel mixture and a comb inserted. Details of how the resolving and stacking gel mixes were prepared are given in Table 2.2. Protein samples were mixed with the relevant gel loading buffer and placed in a boiling water bath for 2 min prior to loading. Gels were run in tank buffer at 200 V until the tracking dye reached the bottom.

Table 2.2 Solutions used to make SDS-polyacrylamide gels

Solution	7.5%	10%	12.5%	Stacking gel
30% acrylamide	2.5 ml	3.33 ml	2.5 ml	0.4 ml
RGB	2.5 ml	2.5 ml	2.5 ml	NA
SGB	NA	NA	NA	0.6 ml
Water	5 ml	4.17 ml	3.33 ml	1.4 ml

Note: Amounts of 30% acrylamide *(2.5% cross linker)* and water were adjusted accordingly for preparation of 7.5%, 10% or 12.5% resolving gel mixes. To each resolving gel mix 80 µl 10% APS and 8 µl of TEMED were added and 20 µl 10% APS and 3 µl TEMED were added to stacking gel mixes, in order to catalyse setting of the gels.

2.2.11 Western blot analysis of proteins

2.2.11A Electroblotting to a nitrocellulose filter

Proteins resolved on SDS-PAGE minigels were transferred to a nitrocellulose filter by the method in (Towbin *et al.*, 1979) in a BioRad mini transblot cell. A blotting sandwich was set up such that the gel was in contact with a sheet of nitrocellulose (Schleicher and Schuell Inc.) and both were sandwiched between Whatman 3mm paper of the appropriate size. This was in turn sandwiched between sponges provided by BioRad and blotting carried out in Towbin buffer at 250 mA for 3 hr.

2.2.11B Immunodetection of proteins

Following transfer the nitrocellulose membranes were removed from the tank and immersed in 5% Marvel (made in PBS-T) overnight at 4°C to prevent non-specific binding of antibodies, or for at least an hour at RT. The blots were washed once for 5 min at RT in PBS-T, and then incubated with a primary antibody (made up to the appropriate dilution in 20 ml of 5% Marvel in PBS-T for each blot) and left shaking for 2-4 hr at RT. Following this the blots were washed 6 times, for 5 min each time, in PBS-T at RT and then incubated with the relevant secondary antibody for 60 min at RT followed by 6 final 5 min washes as previously. The secondary antibodies were all diluted in 20 ml of 2% Marvel in PBS-T: anti-mouse IgG whole molecule peroxidase conjugates were used at a 1/1,000 dilution and goat anti-rabbit IgG whole molecule peroxidase was used at a 1/50,000 dilution.

2.2.11C Protein detection by enhanced chemiluminescence (ECL)

Bound antibodies were detected using the NEN enhanced chemiluminescence (ECL) system. The two reagents provided in the kit were mixed in equal volumes and a total of 1.5 ml poured on to the filter, which was then agitated for 1 min. The filters were wrapped in cling film and exposed to Kodak X-OMAT S film for variable lengths of time.

2.2.11D Stripping and re-probing membranes

The complete removal of primary and secondary antibodies from membranes was sometimes required in order to re-probe a membrane. This involved submerging the

membrane, after immunodetection, in stripping buffer (100 mM β-mercapto-ethanol, 2% SDS, 62.5 mM Tris-HCl, pH 6.7) and incubating it at 55°C for 60 min with occasional agitation. The membrane was then washed twice with PBS-T for 10 min at RT. The membrane was then re-probed using one of the blocking protocols, followed by the detection of proteins by ECL as described above.

2.2.12 Immunoflurorescence assay

Samples for analysis by immunoflurorescence assay using a confocal microscope were prepared on 13 mm glass coverslips in 24-well plates. Cells were washed twice with PBS(A), and incubated with 0.5 ml fix solution (section 2.1.11) for 10 min at RT. Fixed cells were washed with PBS(A) twice and kept in 0.5 ml of permeabilisation solution for 10 min at RT. Cells were washed twice with PBS(A)-1% FCS, and incubated with 20 µl of appropriate diluted first antibody (Table 2.1) for 1 h at RT. Unbound antibody was removed by six washes with PBS(A)-1% FCS over a 15 min period. 20 µl of secondary antibody was added, and after 1 h at RT in the dark, the cells were washed as before. The labelled samples on coverslips were mounted on microscope glass slides with a drop of Citiflour anti-fade reagent, sealed with nail varnish, and stored at 4°C in the dark, or viewed immediately.

2.2.13 Confocal microscopy

Confocal analysis was performed using a Zeiss LSM 510 Laser Scanning Microscope system, with three lasers giving excitation lines at 488 nm (for fluorescein isothiocyanate and EGFP), 543 nm (for Cy3) and 633 nm (for Cy5), and using a 63x oil immersion objective lens, NA 1.4. Data collection was performed under conditions of no detectable channel overlap. Images were exported as .tif files for presentation using Photoshop or Powerpoint.

2.2.14 CAT assays

The CAT enzyme assay system is an adaptation of that described by Gorman *et al.* (1982) and Cullen (1987)(Gorman *et al.*, 1982; Cullen, 1987). Cells were scraped into 400 µl TEN buffer (section 2.1.11) and pelleted by centrifugation at 13,000 rpm for 30 sec in a

bench top centrifuge. The pellet was resuspended in 30 µl 0.25 M Tris-HCl, pH 7.5 and cells lysed by freeze-thawing three times on dry ice and in a 37°C water bath. Cell debris was pelleted by centrifugation at 13,000 rpm for 10 min and the cell extract was incubated with 1 µl 50 mM acetyl Co-A, 1 µl ^{14}C-radiolabelled chloramphenicol and 13 µl 0.25 M Tris, pH 7.5 at 37°C for 1 hr. 200 µl of ethyl acetate was added to terminate the reaction, mixed by vortexing for 10 sec and centrifugation for 5 min to separate the aqueous and organic phases. The upper organic phase was lyophilised and then resuspended in 25 µl ethyl acetate before being applied to a TLC plate (Polygram SIL G; Machery-Nagel) which was placed in a tank containing 95 ml chloroform and 5 methanol in a fume hood. When the chloroform/methanol mix had reached the top of the TLC plate, the plate was removed, air-dried and subjected to autoradiography for 16 h.

2.2.15 Fluorescence-Activated Cell sorting (FACS)

2.2.15A Preparation of cells for FACS

Cells were grown in a 35 mm petri-dish. Infected and transfected cells were harvested at specific times. Cell monolayers were washed once with versene followed by trpsin/versene once and incubated in 0.5 ml of trypsin/versene for 5 min or until the monolayers became loose and the cell were no longer in large clumps. The dissociated cells were transferred to a 15 ml Falcon tube, washed in PBS (complete) twice, and centrifuged at 1,000 rpm at 4°C for 2 min. The mono-dispersed cells were then transferred to an eppendorf tube for further immuno-staining.

2.2.15B Immuno-staining

The medium was aspirated from the pellet, and the cells from each Petri-dish were thoroughly resuspended in 0.5 ml fix solution (section 2.1.11) and incubated for 10 minutes. Fixed cells were washed with PBS(A)-1% FCS once and incubated in 0.5 ml of permeabilisation solution (section 2.1.11) for another 10 minutes and the washing repeated. Cells were resuspended in 200 µl and labeled with primary antibody for 60 minutes at RT and were then washed once and resuspended in PBS(A)-1% FCS as previously described. The fluorescent labeling of cells was achieved by addition of 1 µl of anti-IgG-PE (Sigma) resulting in a 1:100 dilution of the secondary antibody. The cells were incubated in

secondary antibody for 50 min at RT and were washed once and resuspended in a final volume of 0.5 ml.

2.2.15C FACS

Fluorescence quantitation and analysis was achieved by passing the cells through a Becton Dickson FACScan using CellQuest software.

2.2.16 Production of TK$^-$ /EGFP mutant virus

2.2.16A Recombination of TK deleted EGFP plasmid with HSV-1 DNA in mammalian cells

The pTK-/EGPF plasmid, in which the TK open reading frame had been replaced by that of EGFP, was co-transfected with 1 μg of HSV-1 DNA into BHK cells using the lipofection method (see section 2.2.9B). Three days after transfection, when CPE was observed, the transfected cells were harvested by scraping into the medium and sonicated for 15 sec three times using a soni-bath (Kerry).

2.2.16B Selection and plaque purification of HSV-1 virus recombinants

Petri dishes (35 mm^2) of 80% confluent BHK cells were infected with 0.5 ml of the initial viral supernatant from the above transfection at dilutions of 10^{-1} to 10^{-3}, and overlaid with 3 ml of 0.5% agar overlay containing 0.1 ug/ml of ACG to select for propagation of viruses with the TK negative phenotype conferred by insertion of the EGFP open reading frame. The plates were incubated for 2-3 days at 37°C for plaques to develop. Viral plaques with EGFP fluorescence, visualised by phase contrast and fluorescence microscopy, were picked using a plastic pipette tip, added to 1 ml of BHK medium and sonicated for 20 sec twice. One tenth of the stock of positive plaques were further amplified in BHK cells in 24-well plates for one day and the infected cells and medium were harvested and purified as above, by infecting cells with 10^{-3} to 10^{-5} dilutions of the amplified virus stocks. Plaque purification was repeated three times until a pure recombinant viral DNA pattern was obtained from Southern blotting assay (section 2.2.7).

2.2.16C Preparation of working stocks of virus

Three 175cm^2 flasks of 70% confluent of BHK cells were infected with virus at a multiplicity of 0.01 pfu/cell, and incubated at 37°C until compete CPE occurred. Cells were dislodged into the medium by sharply hitting the edges of the flask and recovered by centrifugation at 3000 rpm for 10 min. The supernatants containing CRV (cell released virus) and the pellets containing CAV (cell associated virus) were processed separately.

- ***CRV:***

The supernatant was transferred into SORVAL GS3 tubes and centrifuged at 12000 rpm for 2 h at 4°C. The viral pellet was resuspended in BHK medium, sonicated for 30 sec three times on ice, aliquoted to cryo-vials, and stored at –70°C.

- ***CAV:***

The cell pellet was resuspended in BHK medium, sonicated for 30 sec three times on ice, and re-pelleted at 3000 rpm for 10 min to remove cell debris. The supernatant was transferred into a new tube and stored at –70°C.D.

2.2.16D Titration of virus

Ten-fold serial dilutions were prepared from virus stocks and 100 µl of dilutions from 10^{-4} to 10^{-9} were used to infect BHK cells in 6-well plates in duplicate. After absorption of the virus for 1-2 hr at 37°C, the cells were overlaid with 500 µl of Eagle's medium (140 ml of Eagle's A, 20 ml of Eagle's B, 5% of human serum). After the required incubation at 37°C, plaques were visible and the cells were stained with 0.5 ml of Giemsa reagent prior to quantitation.

RESULTS AND DISCUSSIONS

Chapter 3 A study of ND10 proteins and their effects on HSV-1 infection

Chapter 3 A study of ND10 proteins and their effects on HSV-1 infection

Nuclear domain 10 (ND10) are subnuclear structures, containing a number of proteins including PML, Sp100 NDP52 and Daxx. Several other proteins have been found in at least a proportion of ND10 in a variety of studies. Among these proteins, PML and Sp100 are the most well studied (reviewed by Negorev & Maul, 2001). It has been reported that ND10 domains are dynamic structures that are highly sensitive to environmental stimuli such as stress, heat shock, interferons (IFNs), and metal ions, as well as viral infections (reviewed by Maul, 1998). The number and size of ND10 foci and the distribution of ND10 associated proteins can be dramatically altered by these stress factors.

It has been reported that the promoter regions of both Sp100 and PML contain *cis*-acting interferon response elements and the expression of these two ND10 associated proteins has been shown to be enhanced by IFNs (an integral part of the innate immune response against viral infection) on the mRNA and protein levels (Chelbi-Alix *et al.*, 1995, Grotzinger *et al.*, 1996, Guldner *et al.*, 1999, reviewed by Regad & Chelbi-Alix,). As described in the Introduction, the regions of ICP0 that are required for ND10 localisation and disruption closely correlate with those required for its ability to stimulate viral infection. These findings indicate that ND10 may play a crucial role in virus-host interactions.

The aim of the experiments described in this chapter was to study the distribution of ND10 associated proteins under environmental stress, including heat shock and IFN treatment in different cell lines and to investigate whether the alteration or up-regulation of expression of ND10 associated proteins affects HSV-1 infection.

3.1 Heat shock

3.1.1 The effect of heat shock on ND10

Hep-2 and HFL cell lines were used to characterise the heat shock effect at a temperature of 42°C for 15, 30, and 60 min followed by immunofluorescent double-staining for Sp100 and PML. In Hep-2 cells, after a 15-min heat shock, some of the Sp100

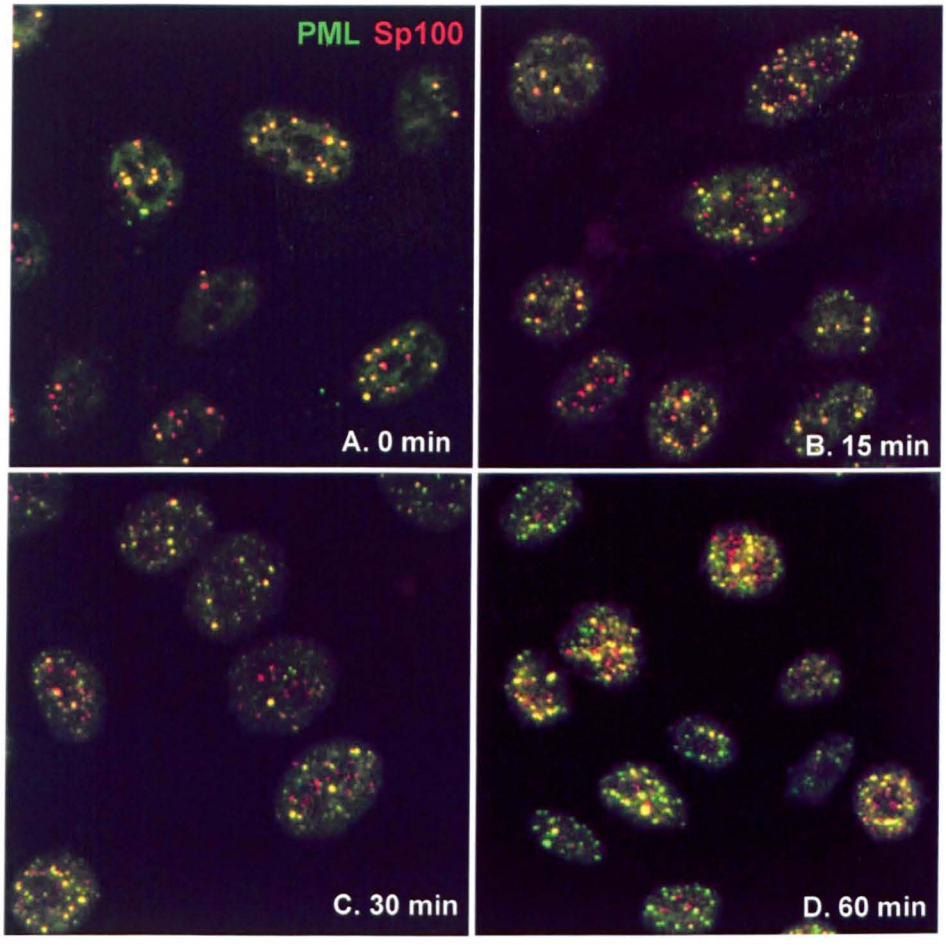

Fig. 3.1 The effect of heat shock on ND10 proteins in Hep-2 cells.

Hep-2 cells were incubated at 42°C (heat shock) for 15, 30, and 60 min. The cells were then fixed and stained for PML (5E10) and Sp100 (SpGH). The labeled proteins are indicated in the uppermost row, and are the same in each panel. The merged view of PML and Sp100 indicates the localisation of these two proteins. PML and Sp100 were largely separated after a 60 min heat shock, as indicated by the increase in the number of dots that were either red or green, rather than yellow.

dispersed into microdots throughout the nucleus (Fig. 3.1B). By 60 min, distribution of PML and Sp100 was chaotic in most Hep-2 cells, and only few cells still retained intact ND10 domains (Fig. 3.1D).

In HFL cells, the effect of heat shock on ND10 was slower compared with Hep-2 cells, but with a similar effect (Fig. 3.2). An obvious response was observed after a 30-min heat shock, and the staining and number of Sp100 and PML foci were decreased in HFL cells after a heat shock of 60 min. In addition, the heat shock response of Sp100 was more rapid than that of PML, since with a 15-min heat shock treatment, most Sp100 foci were dispersed into tiny microdots, but many PML foci were still located in apparently normal ND10. This effect was more obvious after a 30-min heat shock (Fig. 3.3).

3.1.2 The effects of prior heat shock on HSV-1 infection

During the course of HSV-1 infection, expression of ICP0 leads to disruption of ND10. Since the ability of ICP0 to bring about this disruption correlates with its stimulation of viral infection, it was thought possible that prior disruption of ND10 by heat shock might increase the efficiency of HSV-1 infection in the absence of functional ICP0. To explore whether the alteration of ND10 by heat shock affected the efficiency and progress of viral infection, HFL cells were infected by the ICP0 mutant virus FXE, diluted in 37°C pre-warmed medium, at an MOI of 1 after a 60-min heat shock. The initiation and progression of HSV-1 infection were monitored by staining the cells for ICP0 (an IE gene) and UL29 (an Early gene) respectively, at 2 and 6 h post-absorption (hpa) at 37°C. The images were collected with a LSM 510 confocal microscope, using a 20x objective lens, to quantify the viral infection after heat shock in HFL cells.

At an early time of infection (2 hpa), 56% of heat shocked HFL cells were infected and expressed ICP0 and 5% of cells had progressed to Early gene expression (Table 3.1). At 6 hpa, 65% of cells were infected and up to 24% of cells expressed UL29. However, there were no significant differences between these results and those of cells that had been incubated at 37°C prior to infection (Table 3.1). Therefore prior disruption of ND10 by heat shock had no significant effect on the expression of selected IE and Early gene products in the absence of functional ICP0.

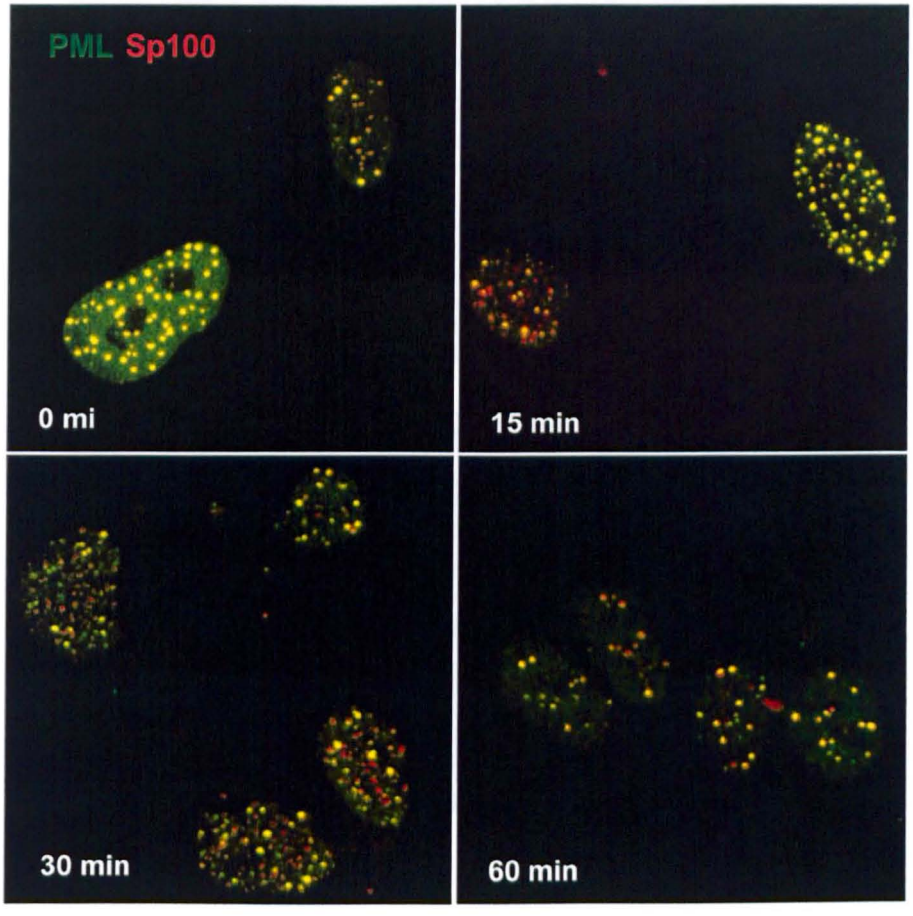

Fig. 3.2 The effect of heat shock on ND10 proteins in HFL cells.

HFL cells were incubated at 42°C (heat shock) for 15, 30, and 60 min. The cells were then fixed and stained for PML (5E10) and Sp100 (SpGH). The labeled proteins are indicated in the uppermost row, and are the same in each panel. The merged view of PML and Sp100 indicates the localisation of these two proteins. PML and Sp100 were partially separated when cells were incubated at 42°C. However the effect of heat shock was less marked in HFL cells compared with Hep-2 cells (not very clear at 60 min-better at 30 min).

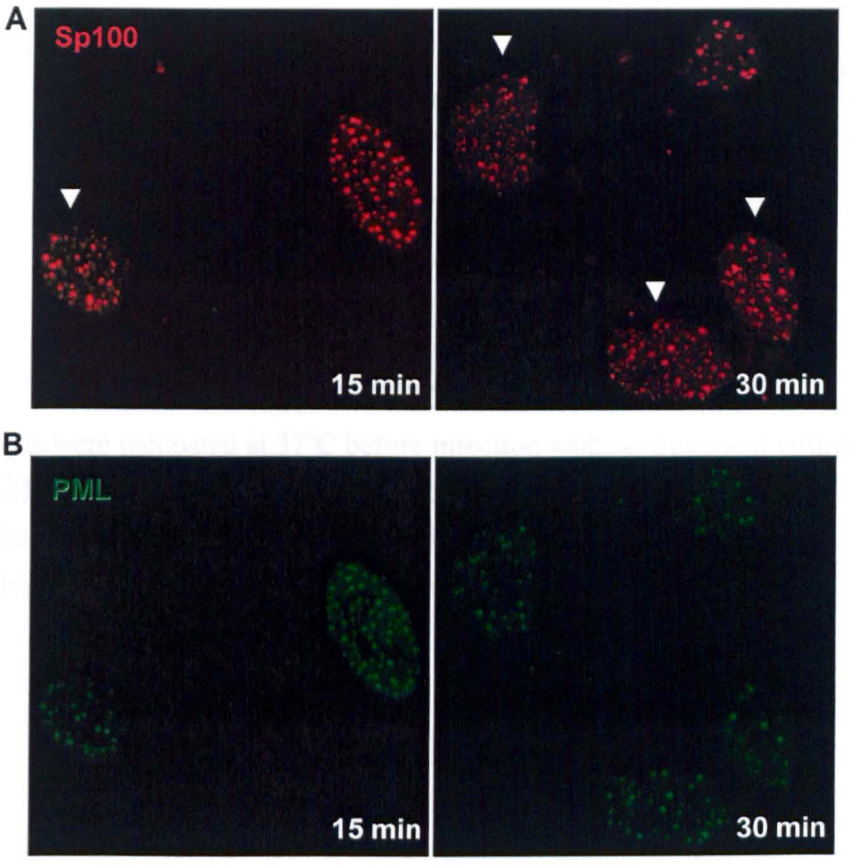

Fig. 3.3 The effect of heat shock on ND10 proteins in HFL cells.

HFL cells were incubated at 42°C (heat shock) for 15 and 30 min as labeled in the lower right-hand corner in each image . The cells were then fixed and stained for Sp100 (SpGH, panel A) and PML (5E10, panel B). In HFL cells, dispersion of Sp100 was faster than PML. The white arrow-heads indicate that most Sp100 foci were dispersed into microdots, whereas most PML foci were still intact and located in ND10.

Table 3.1 The effect of heat shock on HSV-1 infection

	37°C[a]		42°C[b]	
	% ICP0[c]	%UL29[d]	% ICP0	% UL29
2hpa	54	5	56	5
6hpa	62	22	65	24

[a] Cells were incubated at 37°C before infection without treatment with heat shock.

[b] Cells were incubated at 42°C for 1 hour prior to infection.

[c] The proportion of HFL cells expressing ICP0.

[d] The proportion of HFL cells expressing UL29.

3.2 IFN-α

3.2.1 The effect of IFN-α on ND10

The expression patterns of ND10 associated proteins were determined using a rabbit serum (SpGH) specific for Sp100 after IFN-α (1000U/ml) treatment for 24 h. After treatment of IFN-α, the number of ND10 foci was increased and their sizes were enlarged and more homogeneous than in untreated Hep-2 cells (Fig. 3.4).

3.2.2 The effect of IFN-α on HSV-1 infection

As previous results had shown that the expression of ND10 proteins was up-regulated by IFN-α, I then asked whether this increase in ND10 protein expression affects HSV-1 infection. Hep-2 cells were pre-treated with IFN-α for 24 hours then infected by 17+ at an MOI of 5 for various times. The efficiency of infection in IFN-α treated cells was detected by immunostaining at 2, 8, and 12 hour postinfection, followed by confocal microscopy and compared to that in untreated cells. As illustrated in Table 3.2, pre-treatment of IFN-α moderately inhibited initiation of HSV-1 infection, since generally, expression of ICP0 was reduced around 2 to 3 fold at all infection times tested, compared to those in IFN-α untreated cells. Similarly, progression of infection was slightly affected by IFN-α.

3.2.3 The effect of IFN-α on HSV-1 infection at various MOI

Another experiment was designed to examine further whether the effect of IFN-α was dependent on virus input. HFL cells, pre-treated with or without IFN-α, were infected with 17+ at MOI 5, 2, and 0.5 for 2 hours and then processed for the detection of infection efficiency. The fold reduction of infection in IFN-α treated cells is shown in Table 3.3. As described previously, infection of HSV-1 was affected by IFN-α, however the replication of HSV-1 was even worse when less virus was added (Table 3.3). This implies that IFN-α has slightly greater effect on cells infected with HSV-1 at lower MOIs.

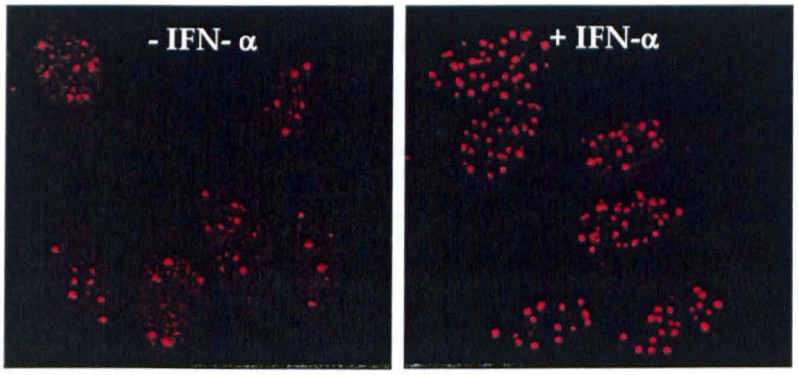

Fig. 3.4 The effect of IFN-α on Sp100 structures.

Hep-2 cells treated with 1000U/ml IFN-α. The expression of Sp100 was up-regulated and more Sp100 foci were observed in IFN treated cells (right-hand panel) compared to that in untreated cells (left-hand panel).

Table 3.2 The effect of IFN on HSV-1 infection

	- IFN-α[a]	- IFN-α	+ IFN-α[b]	+ IFN-α
	% ICP0[c]	%UL29[d]	% ICP0	% UL29
2 hpa	42	1	18	0
8 hpa	56	14	19	3
12 hpa	59	11	24	5

[a] Cells were infected with HSV-1at an MOI of 5 without pre-treatment of IFN-α.
[b] Cells were treated with IFN-α for 24 hours prior to infection.
[c] The proportion of Hep-2 cells expressing ICP0.
[d] The proportion of Hep-2 cells expressing UL29.

Table 3.3 The effect of IFN on HSV-1 infection at various MOI

	+ IFN-α[a]	- IFN-α[b]	Fold reduction
	% ICP0[c]	% ICP0	
MOI 5	60	90	1.5
MOI 2	30	60	2.0
MOI 0.5	15	35	2.3

[a] Cells were infected with HSV-1 without pre-treatment of IFN-α.
[b] Cells were treated with IFN-α for 24 hours prior to infection.
[c] The proportion of HFL cells expressing ICP0.

3.2.4 Association of ND10 proteins with centromeres

It has been shown that in the presence of the proteasome inhibitor MG132 cells have a greater number of ND10. In a proportion of these cells the ND10 can be found in association with CENP-C, a centromere component protein, particularly on progression of the cell cycle into G2 phase (Everett *et al.*, 1999a). To explore whether the up-regulation of ND10 proteins by IFN-α has the same effect as MG132 on the localisation of Sp100 and CENP-C, IFN-pretreated Hep-2 cells were examined by double-staining with antibodies Sp26 (a rat serum for Sp100) and r554 (a rabbit serum for CENP-C), followed by microscopy. Three fields of cells were selected randomly from each coverslip for statistical analysis. The total number of ND10 foci was counted in a separate laser channel for Sp100 (red colour), then the colocalisation of Sp100 with CENP-C was determined in the Sp100-CENP-C merged channel.

After treatment with IFN-α, it was observed that although the number of Sp100 foci was increased, the proportion of Sp100 foci associated with CENP-C in individual cells was not increased in IFN-α treated cells (data not shown). Therefore the increase in this association seen in MG132 treated cells is in some way specific to proteasome inhibition, and not simply due to the increase in ND10 number.

3.3 The effect of over-expression of ND10 proteins by transient transfection on HSV-1 infection

3.3.1 Electroporation

3.3.1A The strategy of this study

To examine the potential effects of ND10 associated proteins on viral replication, transient transfection was employed to highly express ND10 associated proteins in mammalian cells (Fig. 3.5). As illustrated in Fig. 3.5, plasmids encoding epitope tagged ND10 associated proteins, in particular PML, Sp100, and two proteins involved in post-translational modification of ND10 proteins, SUMO-1 and Ubc9, were introduced by electroporation into Hep-2 cells, followed by infection with virus vEG110wt in which

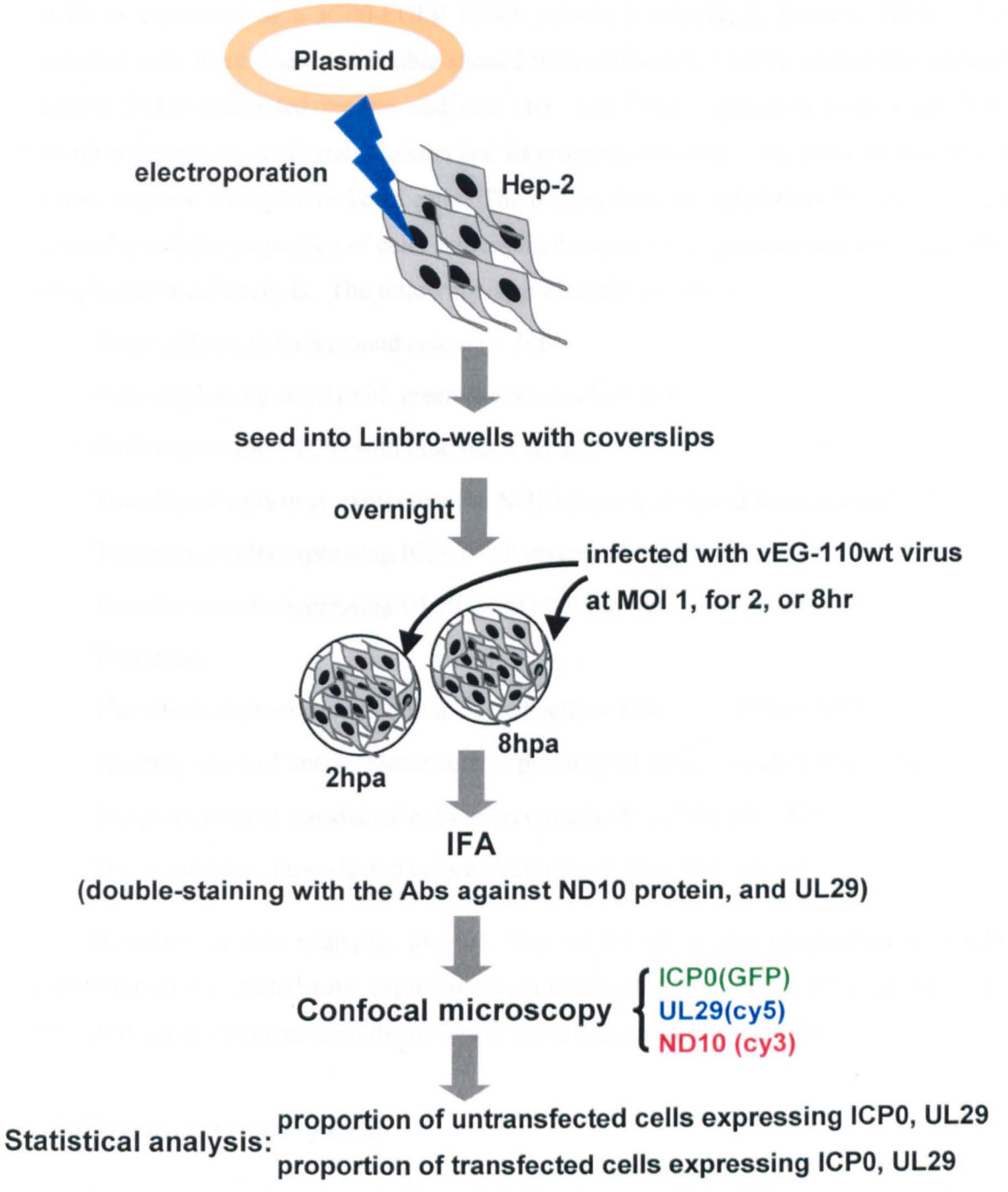

Fig. 3.5 Analysis of the effect of ND10 on HSV-1 infection in Hep-2 cells.

The ND10 associated proteins were highly expressed in Hep-2 cells via electroporation. The electroporated cells were seeded on 13mm coverslips in Linbro-wells and were infected by vEG-110wt virus for 2 or 8 hr followed by immuno-staining for UL29 and ND10 proteins. The proportion of cells expressing two viral proteins, ICP0 and UL29 were determined to indicate viral immediate-early and early gene expression.

ICP0 is expressed as a ICP0-EGFP fusion protein (Lomonte & Everett, 1999). The infected cells were fixed and double-stained with antibodies directly against the relevant tagged ND10-associated protein and also the viral DNA replication protein UL29 to monitor the initiation of viral infection and its progression to the Early phase in transfected cells compared with untransfected cells. The images were collected from 10 fields of each coverslip and the proportion of cells expressing these two viral proteins was determined by simple statistical analysis. The following is an example calculation:

Total cells (with background colour) = 566

Cells expressing ICP0 (with green fluorescence) = 108

Cells expressing UL29 (with blue fluorescence) = 16

Transfected cells over-expressing the ND10 protein (with red fluorescence) = 133

Transfected cells expressing ICP0 (with green and red fluorescence) = 37

Transfected cells expressing UL29 (with blue and red fluorescence) = 3

Therefore:

The infection proportion in untransfected cells is 16% (108-37/566-133);

The proportion of untransfected cells expressing UL29 is 3% (16-3/566-133);

The proportion of transfected cells expressing ICP0 is 28% (37/133);

The proportion of transfected cells expressing UL29 is 2.3% (3/133).

Therefore in this example, the initiation of infection and progression to UL29 expression in transfected cells expressing high levels of an exogenous ND10 protein, are not significantly different from the results in untransfected cells (Fig. 3.6).

3.3.1B Over-expression of PML

To test a possible antiviral effect of PML, plasmid pPML-RH was transfected into Hep-2 cells followed by infection of vEG-110wt virus at an MOI of 1 for 2 and 8 hr. Through statistical analysis of the immunofluorescent images collected from confocal microscopy, a representative result is shown in Fig. 3.7A. Due to the relatively slow progression of infection by HSV-1 in Hep-2 cells, with only a few cells expressing ICP0 and even fewer expressing UL29, Fig. 3.7 only includes the data from the late time point of infection (8 hpa). Expression of ICP0 was assessed to determine whether the initiation of

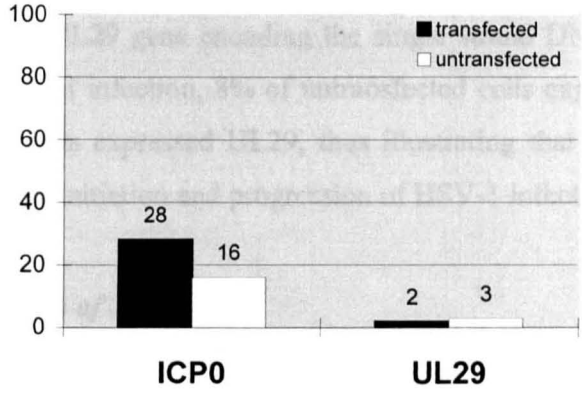

Fig. 3.6 A histogram of the effect of overexpression of ND10 proteins on HSV-1 infection.

The results obtained from microscopy were analysed and converted into a histogram. The proportion of transfected cells expressing ICP0 is slightly higher than that of untransfected cells. The expression of UL29 in transfected cells was similar to that in untransfected cells.

HSV-1 infection is reduced in cells over-expressing PML. At 8 hpa, around 40% of untransfected cells were detected expressing ICP0 and about 45% of transfected cells expressed ICP0. Progression to the productive middle stage of infection was defined by the expression of the UL29 gene encoding the single strand DNA binding protein ICP8. At the late time point of infection, 8% of untransfected cells expressed UL29 and around 10% of transfected cells expressed UL29, thus illustrating that high level expression of PML did not affect the initiation and progression of HSV-1 infection.

3.3.1C Over-expression of Sp100

Sp100, another ND10 associated protein, is also induced by IFNs. Although over-expression of PML did not confer antiviral resistance (Fig. 3.7A), there is still the possibility that ND10 are involved in an antiviral mechanism via Sp100, instead of PML. To generate a plasmid expressing tagged Sp100 protein, two fragments containing the full-length Sp100 ORF were subcloned from plasmid pCMVSp100 (digested with *Nco* I-*Xho* I and *Xho* I-*Hinc* III) into pp65-ICP0 plasmid (Parkinson & Everett, 2000). Since the pp65-ICP0 plasmid contains a HCMV pp65 epitope tag up stream of its ICP0 coding region, insertion of the Sp100 fragments between the *Nco* I and *Hinc* III sites of pp65-ICP0 replaced the ICP0 ORF but the pp65 tag was retained at the 5' end of Sp100. The strategy described in section 3.3.1B was used to address the effect of Sp100 on HSV-1 infection. The proportion of transfected cells expressing epitope tagged pp65-Sp100 and expressing ICP0 after infection (46%) was slightly lower than in untransfected cells (65%) and the proportion of Sp100 over-expressing cells progressing to the early gene stage was two-fold lower than in untransfected cells (Fig. 3.7B).

3.3.1D Over-expression of SUMO-1 or Ubc9

It has been found that the ND10 associated proteins PML and Sp100 are modified by covalent linkage with the ubiquitin-like protein, SUMO-1 and this modification may promote the assembly of these structures (Muller *et al.*, 1998a, reviewed in Sternsdorf *et al.*, 1997). In addition, during the course of HSV-1 infection, PML and Sp100 together with their SUMO-1 modified isoforms are degraded by the proteosome in response to ICP0 expression (Everett *et al.*, 1998a, Parkinson & Everett, 2000). These findings imply that the SUMO-1 modification pathway may play an important role in antiviral resistance. To

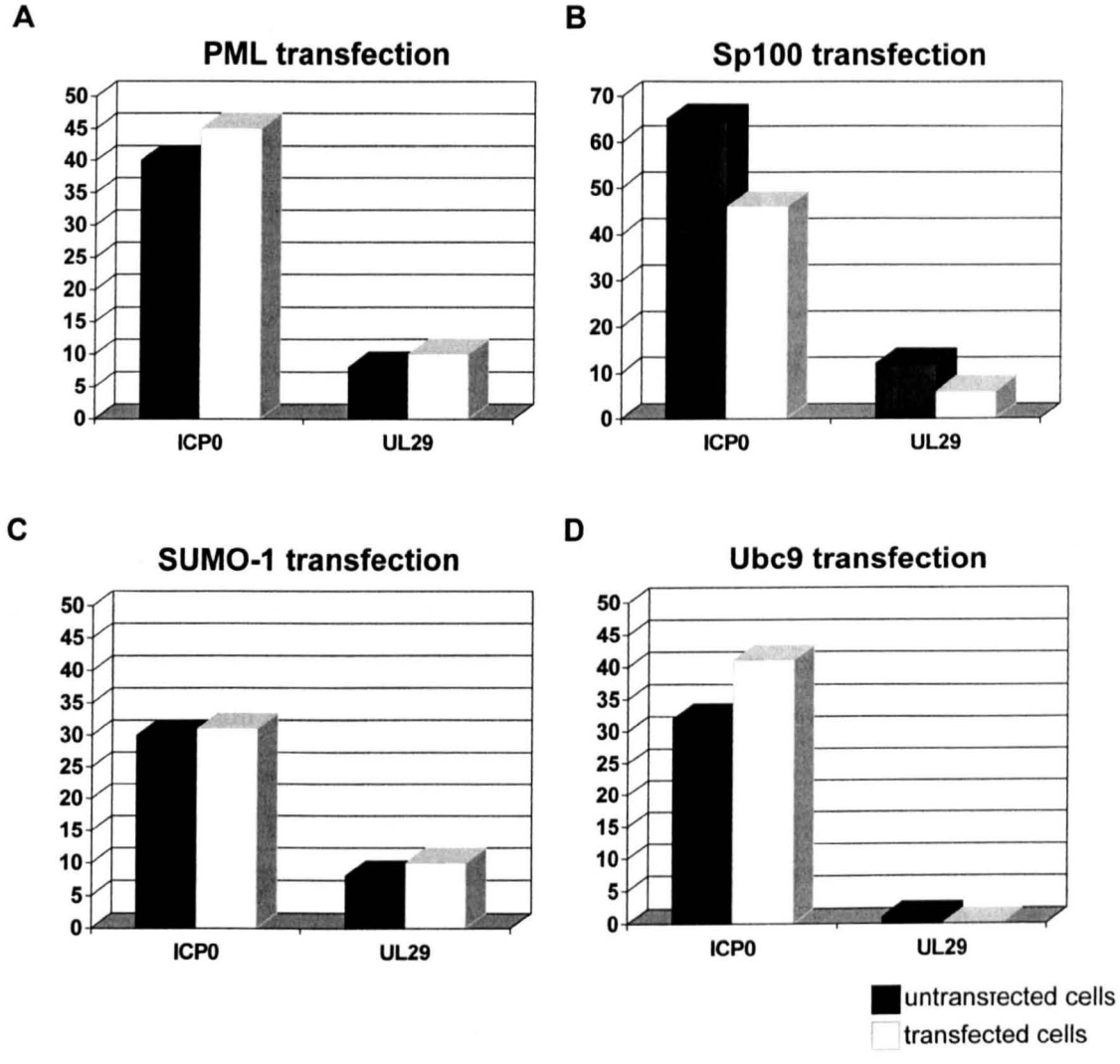

Fig. 3.7 The effect of ND10 proteins on viral infection in Hep-2 cells.

The transfected Hep-2 cells, infected by EG110 for 8 hr, were examined by confocal microscopy followed by statistical analysis. The proportion of cells expressing ICP0 and UL 29 in untransfected cells are shown as ■ , and the proportion of transfected cells expressing ICP0 and UL29 are shown as □ . These results were obtained from a single experiment, but were reproduced on at least two individual experiments.

address this question, SUMO-1 and its E2 conjugating enzyme Ubc9 were overexpressed in Hep-2 cells and infected transfected cells were analysed by the same method as described in section 3.3.1A. The proportion of pCIPIC-1 transfected and untransfected cells expressing ICP0 were 30% and 31% respectively (Fig. 3.7C). The proportion of transfected cells expressing UL29 was up to 10%, which is not a significant difference from that of untransfected cells (8%). In the case of pUBC9 plasmid transfection, similarly to SUMO-1, Hep-2 cells highly expressing Ubc9 had a slightly higher percentage of infection, however, in these experiments the progression of viral infection to UL29 expression was too low to be detected.

3.3.2 Lipofection

Transient transfection via electroporation offered an efficient and representative way to study the effect of ND10 proteins in Hep-2 cells. However, since viral gene expression and the progression of HSV-1 infection were relatively slower in Hep-2 cells, the population of cells expressing UL29 was too small to give a reliable statistical analysis, even at input virus of 1pfu (plaque forming unit) per cell. BHK cell line is an efficient host cell for HSV-1, but they were found unsuitable for the electroporation method. Therefore a lipofection method was employed with BHK cells to explore in more detail the effects of exogenous ND10 protein expression on the progress of HSV-1 infection. As with the electroporation method, a plasmid expressing PML, Sp100, SUMO-1, or Ubc9 was transfected into BHK cells seeded in a 35 mm petri-dish with 4 coverslips. Transfected cells were infected by 17+ at an MOI of 0.5 for 2 and 6 hr, followed by immunofluorescence staining to detect the expression of viral immediate-early and Early proteins in transfected cells compared with untransfected cells (Fig. 3.8).

3.3.2A Single-plasmid transfections

- ***3.3.2A.1 Results from IFA***

Among those plasmids used for expressing ND10 proteins, the average transfection efficiency via lipofection of BHK cells was up to 40% (Fig. 3.9A). Due to the efficient infection progression of 17+ infection in BHK cells, the infected transfected cells were

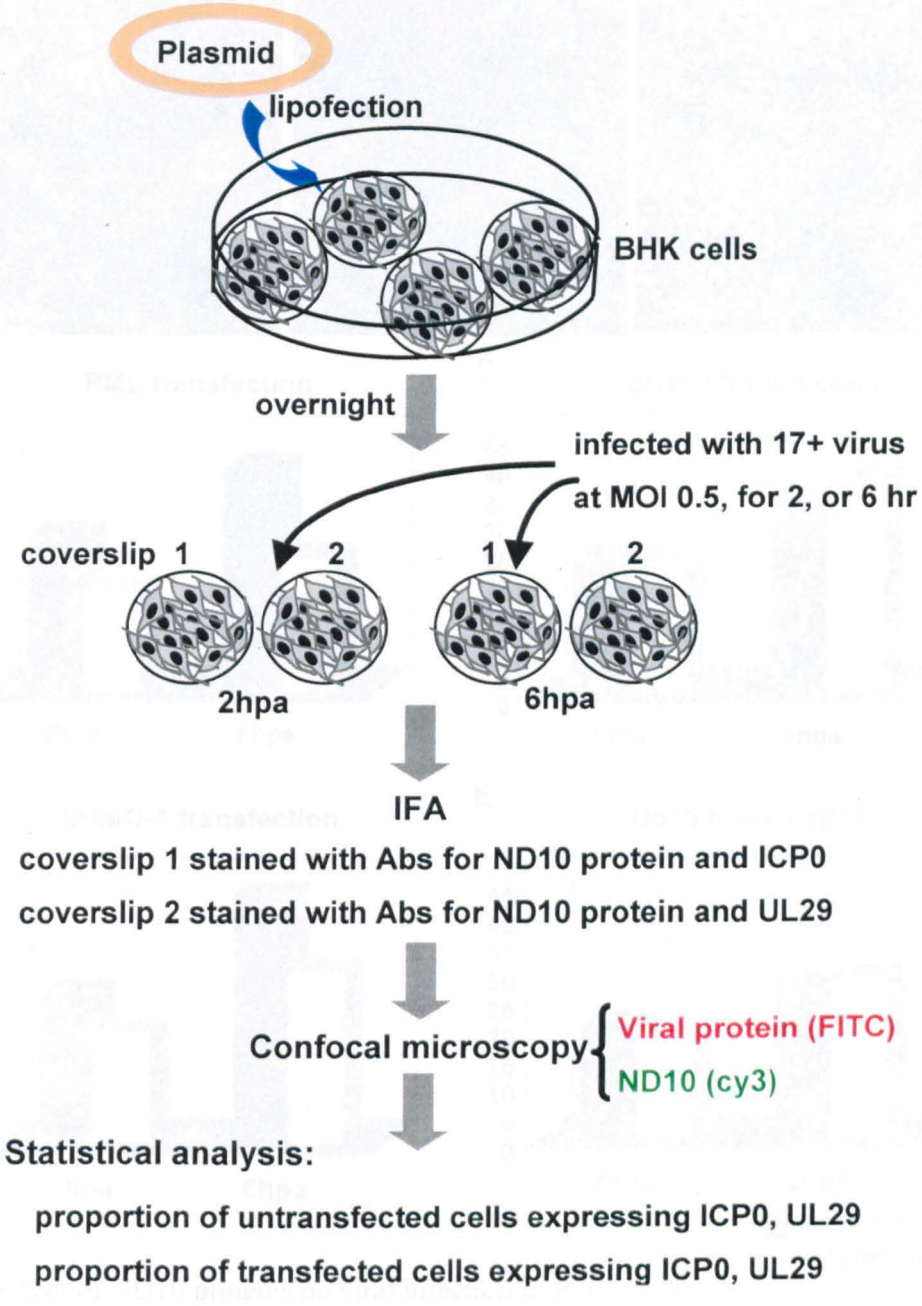

Fig. 3.8 Analysis of the effect of ND10 on HSV-1 infection in BHK cells.

The ND10 associated proteins were highly expressed in BHK cells via lipofection. BHK cells were seeded on 13mm coverslips in 35mm Petri-dish and were transfected with ND10 plasmids and then infected by 17+ wild type virus for 2 or 6 hr followed by immuno-staining for ICP0, UL29 and ND10 proteins. The images collected from confocal microscopy were statistically analysed to compare viral gene expression and progression of infection in transfected cells with untransfected cells.

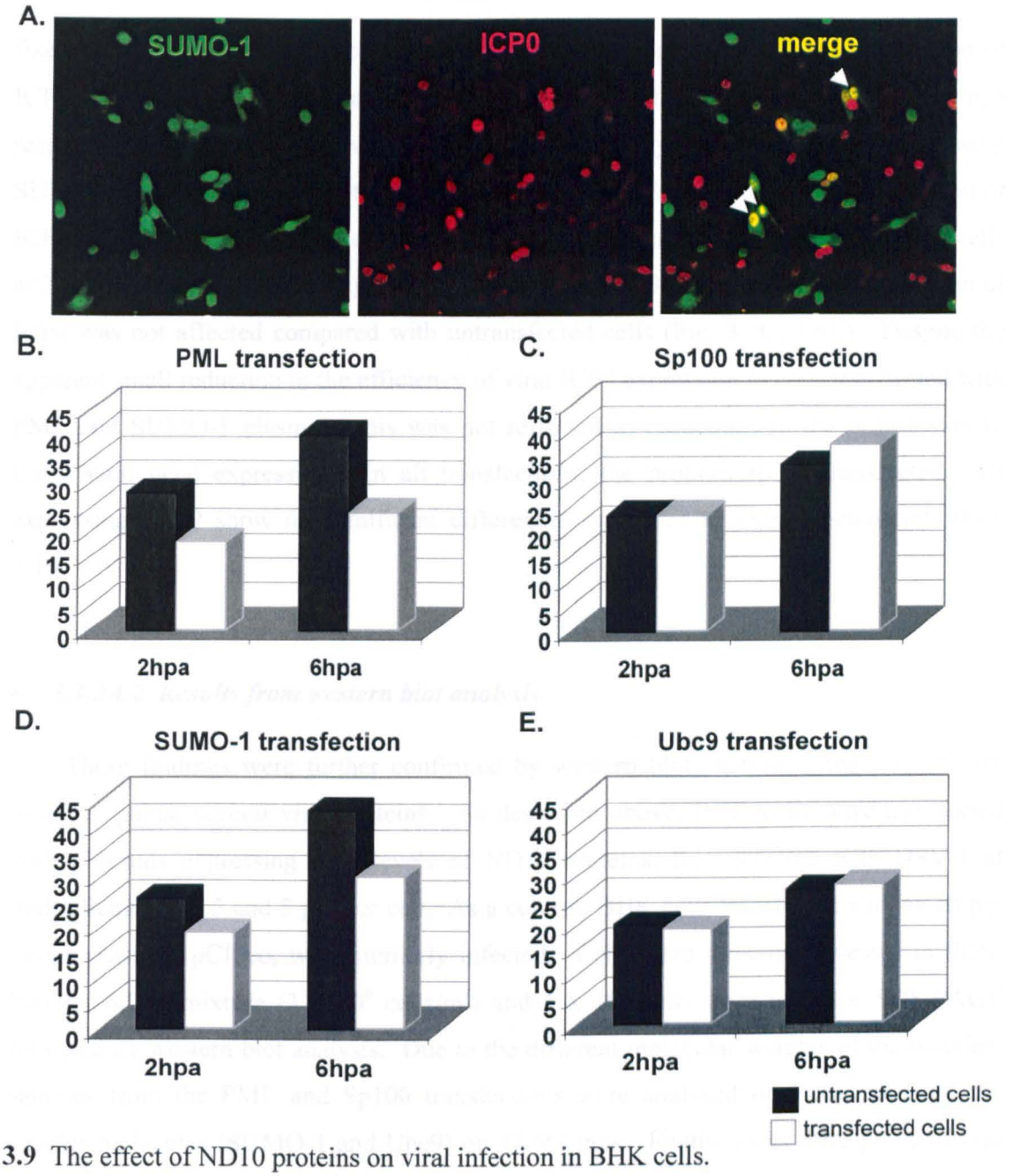

Fig. 3.9 The effect of ND10 proteins on viral infection in BHK cells.

A. Immuno-staining of infected and transfected BHK cells with SUMO-1 (5E10) and ICP0 (r190). In the merge (right) panel, the white arrows show that the SUMO-1 transfected cells were infected by HSV-1.

B.- D. The transfected BHK cells, infected by 17+ for 2 and 6 hr, were examined by confocal microscopy followed by statistical analysis. The proportion of untransfected cells expressing ICP0 are shown as ■, and the proportion of ND10 protein transfected cells expressing ICP0 are shown as □. Counts of over 1000 cells were made to determine the proportion of cells expressing ICP0. Each experiment was repeated 3 times. The results shown for each length of infection are those from a single experiment, but are representative of all three repetitions.

fixed at 2 and 6 hpa. In transfected cells expressing exogenous PML, the expression of ICP0 was decreased to 36% and 40% of that of untransfected cells at 2 hpa and 6 hpa respectively (Fig. 3.9B). As with PML transfection, many of the cells highly expressing SUMO-1 conferred slight resistance to HSV-1 infection (Fig. 3.9A), and the expression of ICP0 in SUMO-1 transfected cells was 27% and 30% lower than that in untransfected cells at 2 and 6 hpa, respectively (Fig. 3.9D). In Sp100 or Ubc9 transfected cells, expression of ICP0 was not affected compared with untransfected cells (Fig. 3.9C, 3.9E). Despite the apparent small reduction in the efficiency of viral ICP0 expression in cells transfected with PML and SUMO-1 plasmids, this was not reflected in reductions in the progression to Early viral gene expression. In all transfections, the proportions of transfected cells expressing UL29 show no significant differences compared to untransfected cells (Fig. 3.10).

- ***3.3.2A.2 Results from western blot analysis***

These findings were further confirmed by western blot analysis using an antibody mixture against several viral proteins. As described above, BHK cells were transfected with plasmids expressing high levels of ND10 proteins, then infected with HSV-1 at multiplicities of 0.5 and 5 pfu per cell. As a control, BHK cells transfected with an empty vector plasmid, pCIneo, were similarly infected. Cells were directly harvested in SDS-PAGE boiling mixture (3 x 10^6 cells/ml) and 1 x 10^5 cells were used for SDS-PAGE followed by western blot analysis. Due to the different molecular weights of the proteins, samples from the PML and Sp100 transfections were analysed on 7.5% gels and the smaller molecules (SUMO-1 and Ubc9) on 12.5% gels. Firstly, blots were probed using antibodies against the ND10 proteins to determine the expression level, then the previously bound antibodies were stripped from the membranes and another antibody mixture against viral proteins including immediate-early and early gene products was added. PML, Sp100, and their SUMO-1 modified isoforms were highly expressed in transfected BHK cells, but as expected no tagged ND10 proteins was detected in the pCIneo transfected cell extract (Fig. 3.11A). However, compared with control cells, neither PML nor Sp100 transfected cells had reduced levels of viral protein expression (Fig. 3.11B). Similar to the PML and Sp100 transfections, overexpression of SUMO-1 and Ubc9 also showed no effect on viral gene expression (Fig. 3.12). It should be remembered that a limitation of this experiment

A.

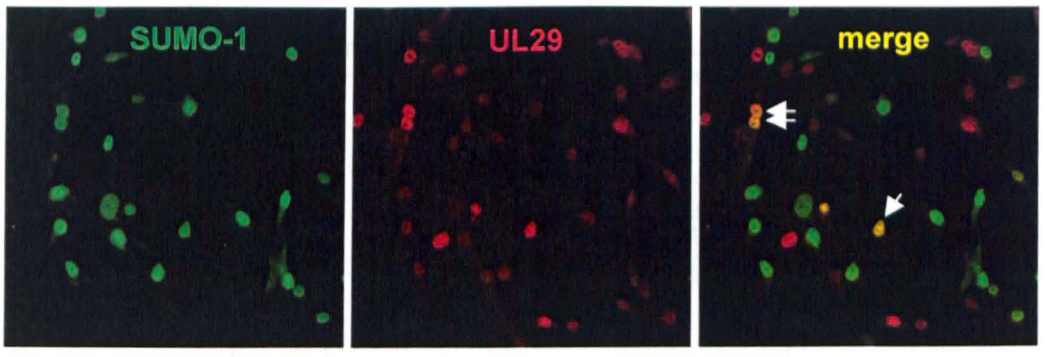

B.

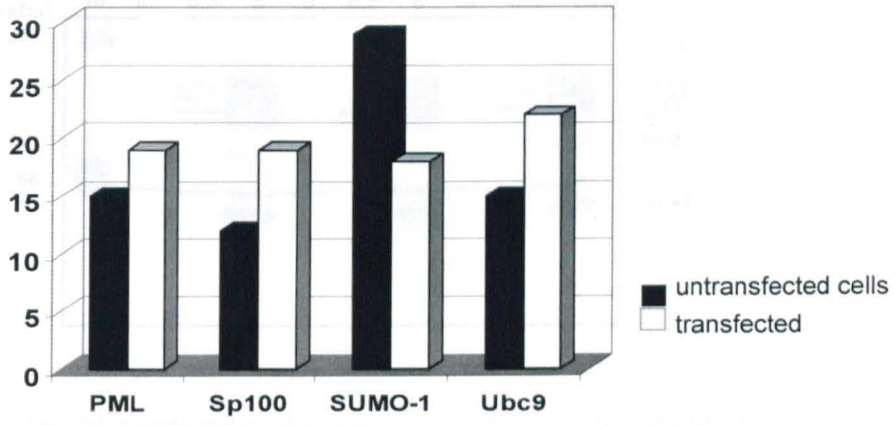

Fig. 3.10 The effect of ND10 proteins on viral infection in BHK cells.

A. Immuno-staining of infected and transfected BHK cells with SUMO-1 (5E10) and UL29 (r515). In the merge (right) panel, the white arrows show that the SUMO-1 transfected cells were infected with HSV-1 and viral infection had successfully progressed to the early gene stage.

B. The transfected BHK cells, infected by 17+ for 8 hr, were examined by confocal microscopy followed by statistical analysis. The proportion of untransfected cells expressing UL29 are shown as ■ , and the proportion of transfected cells expressing UL29 are shown as □ . Counts of over 1000 cells were made to determine the proportion of cells expressing ICP0. Each experiment was repeated 3 times. The results shown are from in a single experiment, but are representative of all three repetitions.

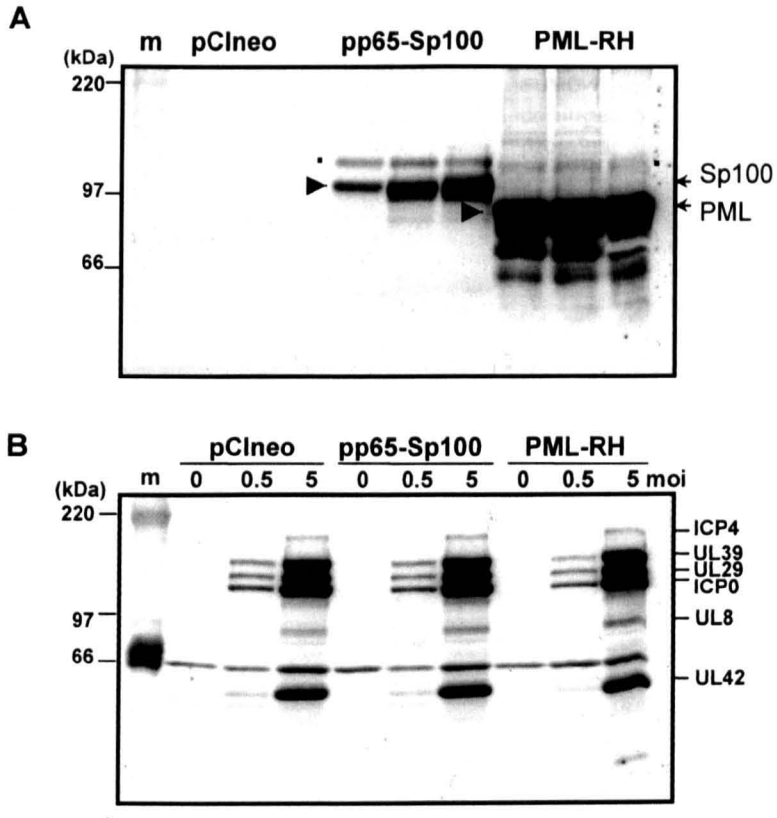

Fig. 3.11 Western blot analysis of the viral gene expression in transfected cells.

Western blot analysis of the extracts of cells transfected with either PML-RH, pp65-Sp100 plasmid, or the empty vector, pCIneo (as labelled on top of the panels), followed by infection with 17+ at MOI 0 (as mock infection), 0.5, and 5 for 6 hr.

A. Blotted with pp65 Ab for tagged-Sp100 and monoclonal Ab MRGS-His for tagged-PML. The arrow-heads indicate the overexpressed ND10 proteins and the black dots show SUMO-1 modified ND10 proteins.

B. The membrane from panel A was reused for blotting with a mixture of antibodies recognising viral IE proteins, ICP0 and ICP4, and also the E genes UL8, UL39, UL29, and UL42 as indicated on the left-hand side.

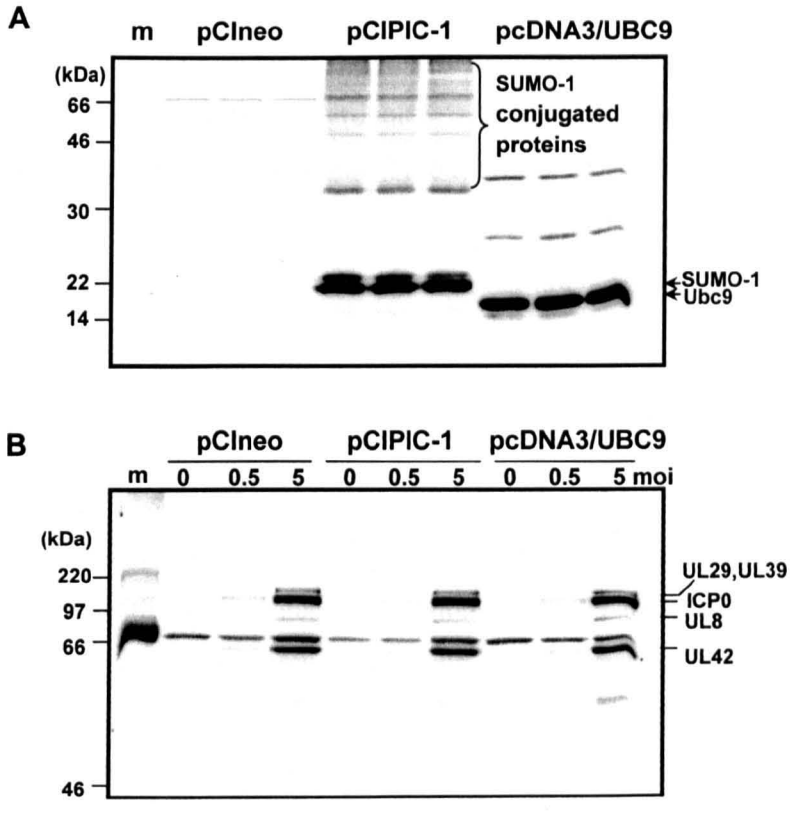

Fig. 3.12 Western blot analysis of the viral gene expression in transfected cells.

Western blot analysis of the extracts of cells transfected with either pCIPIC-1, pUbc9 plasmid, or the empty vector, pCIneo (as labelled on top of blots), and followed by infection with 17+ at MOI 0 (as mock), 0.5, and 5 for 6 hr.

A. Blotted with 9E10 Ab for c-myc tagged-SUMO-1 and monoclonal antibody PK5 for SV5 tagged-Ubc9.

B. The membrane from panel A was reused for blotting with a mixture of antibodies recognising viral IE proteins, ICP0 and ICP4, and also the E genes UL8, UL39, UL29, and UL42 as indicated on the left-hand side.

is that the potential maximum reduction in viral gene expression is limited by the transfection efficiency. For example, if the transfection efficiency was 50%, even if viral protein expression was reduced to background levels, the reduction in total viral protein expression in the culture as a whole would be only 50%. Despite this limitation, these experiments illustrate that the plasmids are expressing high levels of full-length ND10 proteins.

- ***3.3.2A.3 Detection of progeny viral yield from transfected cells***

Since all antibodies used in immunofluorescent staining and western blot analysis are for detecting the immediate-early and early gene products, there is a possibility that ND10 proteins may interfere with viral late gene expression or virion packaging. To analyse this, the yields of progeny virus from transfected cells, which were infected with 17+ at a multiplicity of 0.1 for 24 h, were titrated on BHK cells. The titers from two individual experiments showed that overexpression of PML, Sp100, SUMO-1, and Ubc9 had no protective effect against HSV-1 infection at an MOI of 0.1 (Fig. 3.13). The same limitation of transfection efficiency as described in the previous section applies to this experiment.

3.3.2B Co-transfection of plasmids expressing PML, Sp100, and Ubc9

The expression level of ND10 proteins was drastically augmented by transient transfection, however most of those exogenous proteins were observed to be improperly located in the nucleoplasmic fraction, rather than sequestered in ND10 domains. SUMO-1 modification has been implicated in the recruitment of proteins to ND10 domains (Li *et al.*, 2000, Muller *et al.*, 1998a). To investigate this observation, firstly, co-transfection of plasmids expressing various combinations of ND10 proteins, such as PML-Sp100, PML-SUMO-1, and PML-Ubc9, was used to determine the distribution of overexpressed ND10 proteins when expressed in combination with another ND10 protein. The size and number of ND10 foci were increased in many transfected cells expressing two ND10 associated proteins compared with single transfected cells, and most of the exogenous proteins localised to ND10 domains (Fig. 3.14). To test whether this more appropriate localisation of highly expressed exogenous ND10 proteins could affect viral infection, cells co-transfected with three plasmids expressing PML, Sp100 and Ubc9, were infected by 17+ at

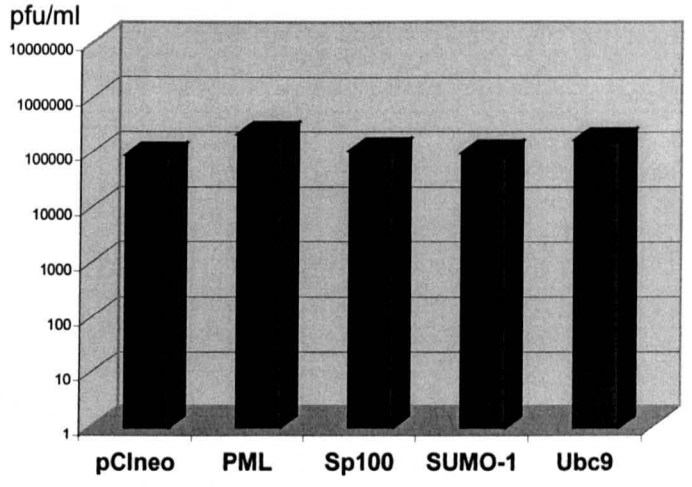

Fig. 3.13 The titres of progeny viruses from transfected cells.

BHK cells were transfected either plasmids expressing PML, Sp100, SUMO-1 or Ubc9 and then were infected by HSV-1 on next day. The progeny viruses were titrated on BHK at 24 hpa. The titers of progeny viruses were similar among cells transfected with different plasmids.

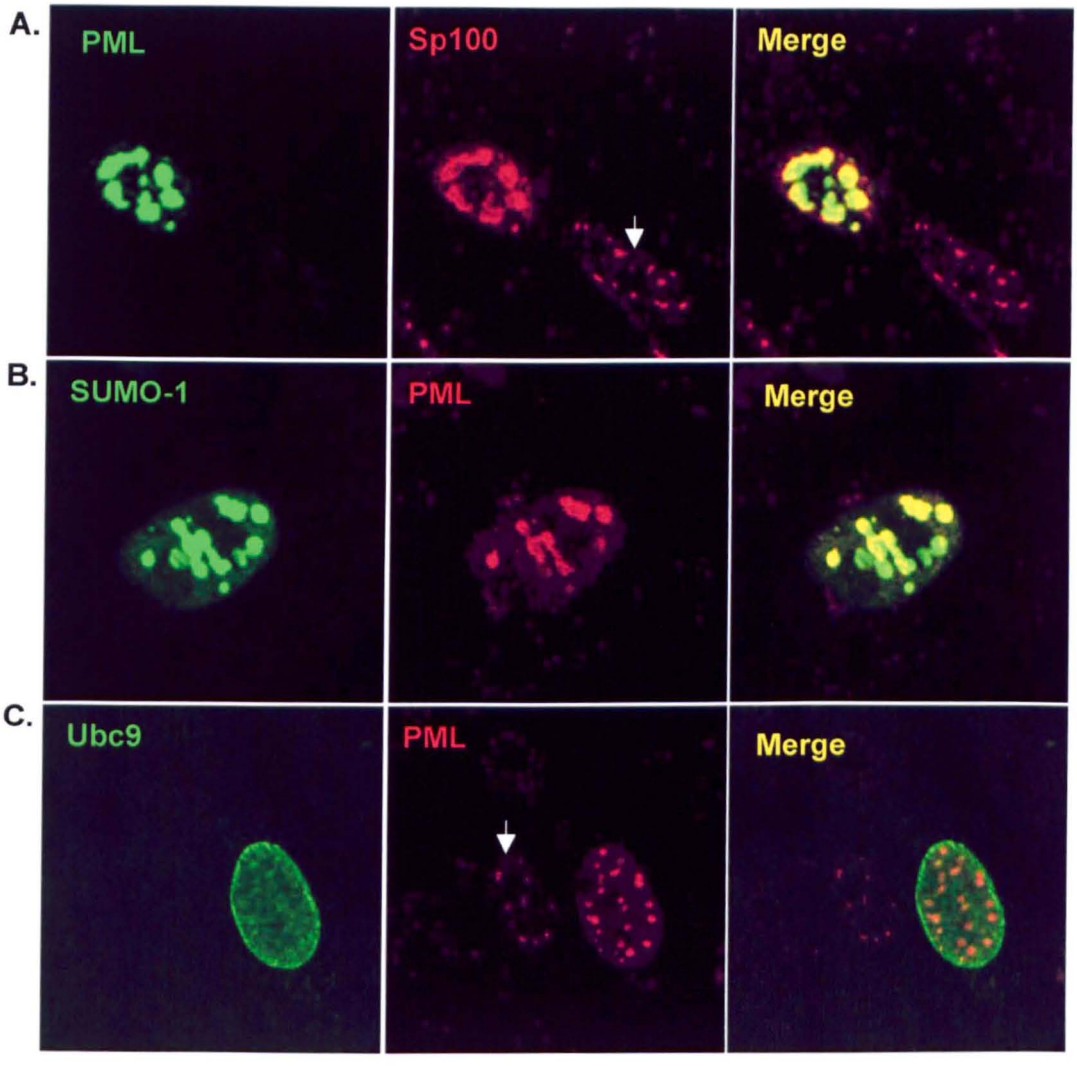

Fig. 3.14 Co-expression of ND10 proteins in Hep-2 cells.

Hep-2 cells were co-transfected with PML/Sp100, PML/SUMO-1, or PML/Ubc9 plasmids, fixed and immuno-stained 24 hour after transfection. The images from each transfection are shown in panel A, B, and C respectively. The different components probed for are indicated with their respective colours in the upper left corners. The size of ND10 domains was increased in cells co-expressing ND10 proteins compared with single transfected cells indicating in white arrows.

an MOI of 0.5. At early times of infection, the proportion of transfected cells expressing ICP0 was found to be two-fold less than in untransfected cells (the histogram in Fig. 3.15). As shown in Fig. 3.15, most of the transfected cells, with green fluorescence, were not infected. However when viral infection progressed to middle stages, there was no resistance to infection of the transfected cells (Fig. 3.15).

3.3.2C Co-transfection of plasmids expressing PML, Sp100, Ubc9, and SUMO-1

As an extension of the above experiment, the plasmid expressing SUMO-1 was also introduced into BHK cells in a quadruple plasmid transfection. After infection of the transfected cell population with 17+, at 2 hpa the proportion of transfected cells infected by virus and expressing ICP0 was found to be around 30% lower than that of untransfected cells (Fig. 3.16). Similar to the effect of three-plasmid transfection, at later infection, the proportion of transfected cells expressing ICP0 and UL29 was not significantly different from that of untransfected cells (Fig. 3.16).

3.4 The effects of ND10 associated proteins on transactivation function of ICP0

3.4.1 HP1

It has been reported that Sp100 interacts *in vitro* and *in vivo* with members of the HP1 (heterochromatin protein 1) family of non-histone chromosomal proteins and that HP1 can significantly repress transcription when fused to a heterologous DBD (DNA binding domain) in transiently transfected mammalian cells (Lehming *et al.*, 1998, Seeler *et al.*, 1998). Since the region of HP1 required for interaction with Sp100 is also essential for its repression activity (Lehming *et al.*, 1998), it is an interesting question whether the HP1 protein could regulate ICP0 function in terms of transactivation of early genes. A CAT assay was used to address this question. The reporter cassette used for these experiments was pSS80, which contains the promoter of the ICP6 gene that has been shown previously to be efficiently activated by ICP0 in transfected cells. The amount of pSS80 used in the transfection was first optimised to give a detectable but low level of background expression. Next, to assess whether HP1 represses the transactivation activity of ICP0, the amount of ICP0 expression plasmid (pCI-rtag-cICP0), which can induce a relative high

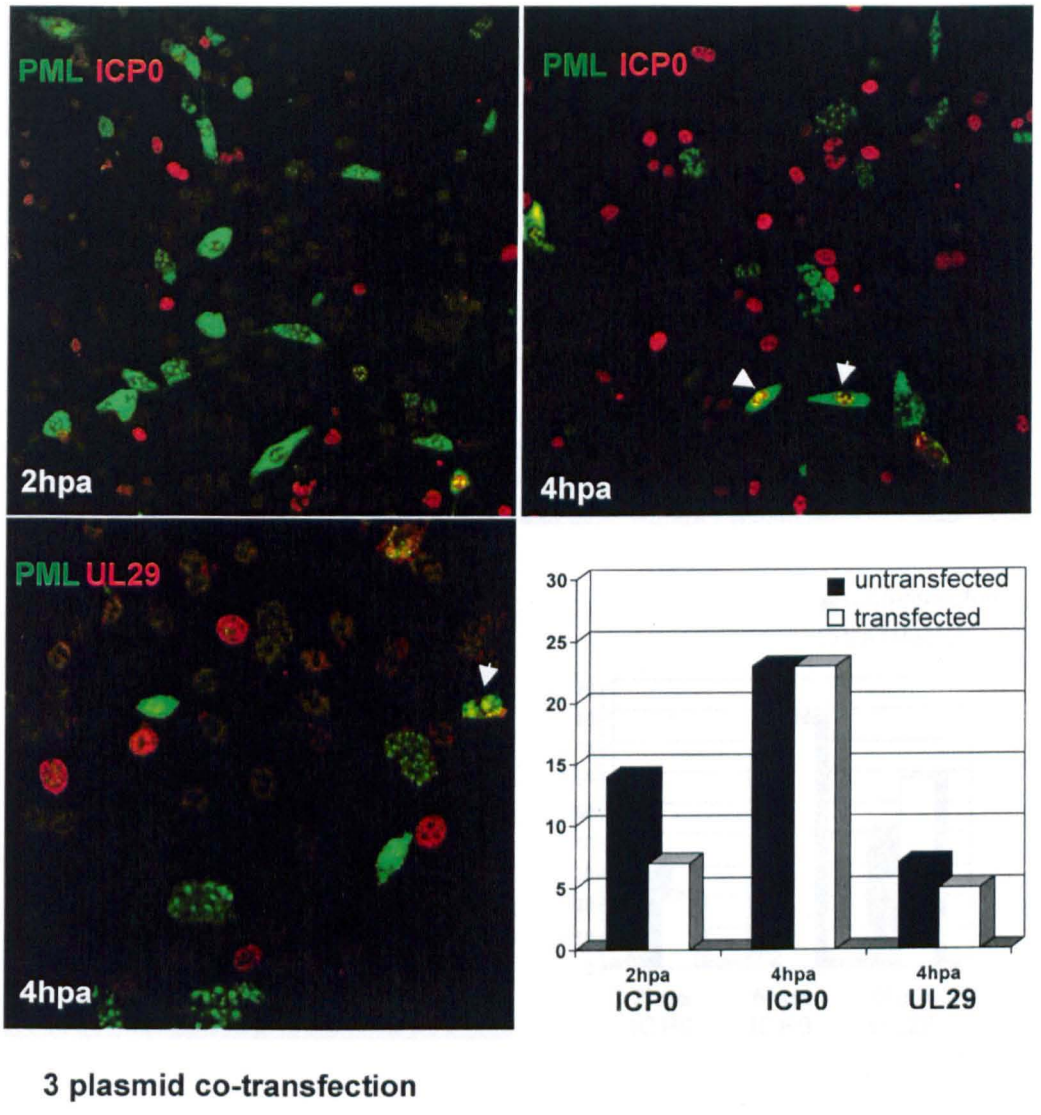

Fig. 3.15 Co-expression of ND10 proteins in BHK cells.

BHK cells were co-transfected with plasmids expressing PML, Sp100, and Ubc9 followed by infection with HSV-1 the next day. The transfected, infected BHK cells were then fixed and immuno-stained 2 and 4 hr after infection and examined by confocal microscopy followed by statistical analysis. Three plasmids were transfected, but only PML was assayed to identify the cells that were transfected. The proportion of cells expressing either ICP0 or UL29 in untransfected cells are shown as ■ , and the proportion of ND10 protein transfected cells expressing UL29 are shown as □.

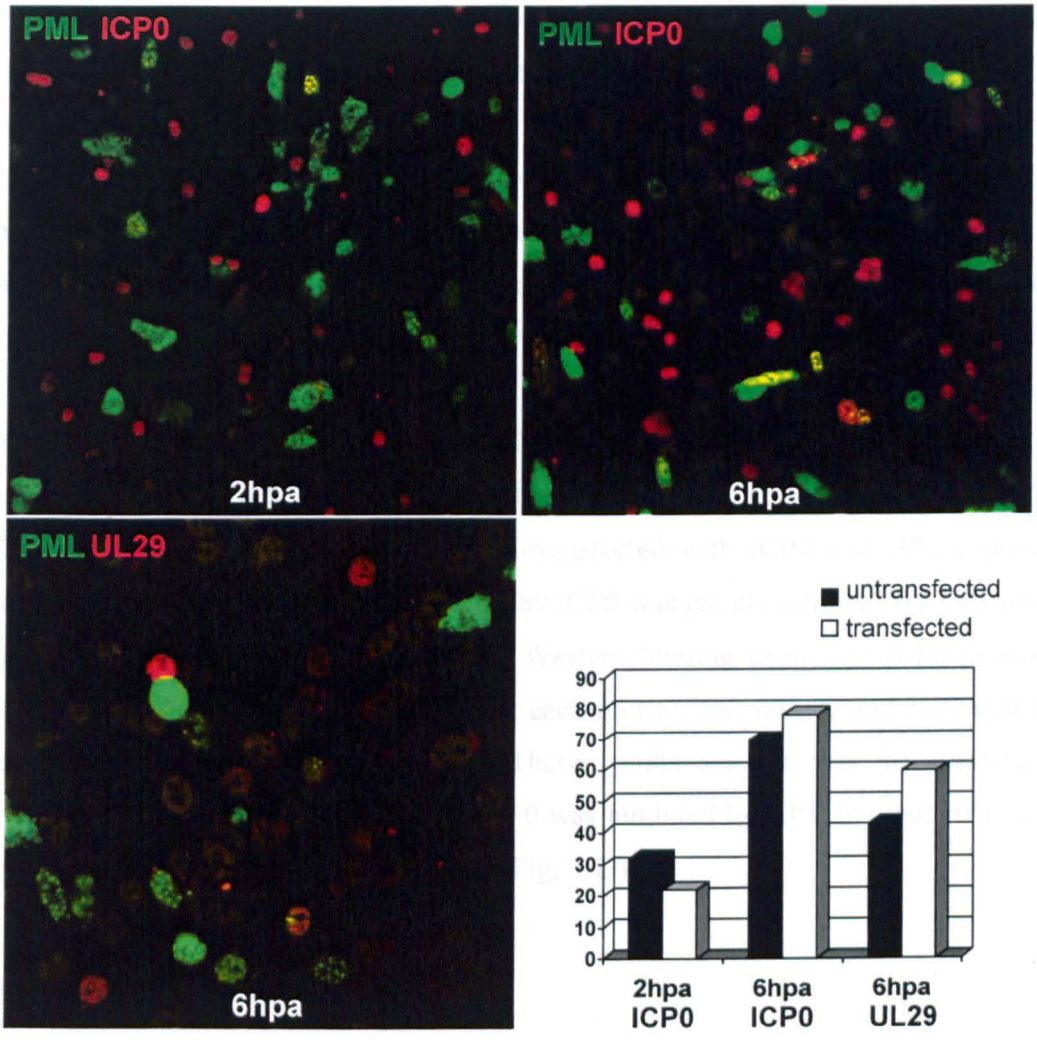

Fig. 3.16 Co-expression of ND10 proteins in BHK cells.

The BHK cells were co-transfected with plasmids expressing PML, Sp100, SUMO-1, and Ubc9 followed by infection with HSV-1 the next day. The transfected, infected BHK cells were then fixed and immuno-stained 2 and 4 hpa and examined by confocal microscopy followed by statistical analysis. Four plasmids were transfected but only PML was assayed to identify the cells that were transfected. The proportion of cells expressing either ICP0 or UL29 in untransfected cells are shown as ■ , and the proportion of ND10 protein transfected cells expressing UL29 are shown as □.

CAT activity (up to 70%), was determined by cotransfection of the CAT reporter plasmid with a series of dilutions of the plasmid expressing ICP0. To investigate the function of HP1, Vero cells (seeded in Linbro-well) were transfected with various amounts of HP1 expression plasmid (pcDNA3-HP1) together with 3ng of pCI-rtag-cICP0 expressing ICP0 and 10ng of pSS80. The total amount of DNA was equalised using plasmid pUC9. Each transfection was done in duplicate, one for the CAT assay and the another for western blot to monitor the expression of the proteins from the transfected plasmids. Transfected cells were harvested on the next day, and one fifth of the crude cell extract was processed for a CAT assay, followed by thin layer chromatography (TLC). When cells were transfected with ICP0 alone, without HP1 plasmid, the ICP6 promoter was highly activated by ICP0, resulting in a high CAT activity (up to 90% conversion of substrate to product) (Fig. 3.17A). Significantly, when cells were co-transfected with ICP0 and HP1 expression plasmids, the activation of the CAT reporter by ICP0 was greatly inhibited by HP1 protein in a dose-dependent manner (Fig. 3.17A). Western blotting using anti-ICP0 antibodies revealed that ICP0 was expressed equally in each transfection sample and increased HP1 levels did not affect ICP0 expression. These results suggest that the transcription activation of the early gene promoter via ICP0 was inhibited by HP1, but that HP1 has no significant effect on the expression of ICP0 (Fig. 3.17B).

3.4.2 hDaxx

In addition to HP1, the Fas-binding protein hDaxx was recently identified as a PML-interacting protein in a yeast two-hybrid screen (Li *et al.*, 2000). The study also reported that hDaxx colocalised with PML in ND10 and had transcriptional repressor activity. Based on the same localisation of hDaxx with the viral protein ICP0 and being a transcriptional repressor, it is possible that hDaxx might regulate viral gene transcription. Following the system already described for HP1 study, the activation of the ICP6 promoter via ICP0 was drastically inhibited by GFP-hDaxx fusion proteins in a dose-dependent manner. Notably, the transcription of CAT was decreased by 70% when cells were transfected with 10ng of pEGFP-NLS-hDaxx plasmid and was completely repressed when cells were transfected with 500ng of the hDaxx expression plasmids (Fig. 3.18A). Furthermore, western blotting using antibodies against ICP0 and GFP proteins demonstrated that expression of ICP0, driven by HCMV promoter, was also repressed by

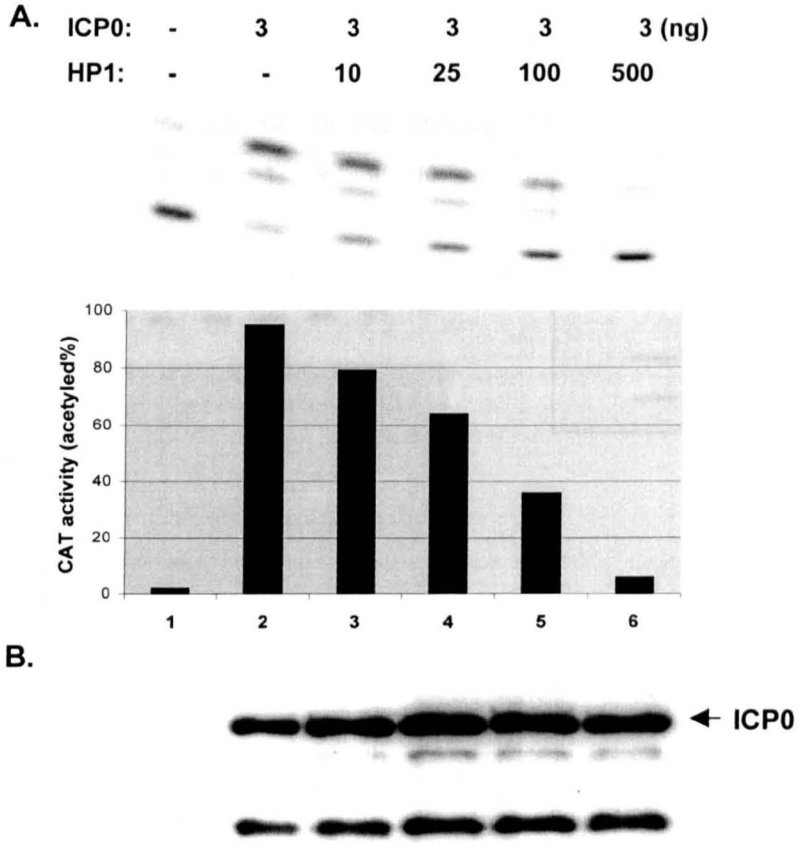

Fig. 3.17 Effect of HP1 on transactivation of an ICP6 expression cassette by ICP0 in Vero cells.

Cells were co-transfected with reporter plasmid pSS80 (ICP6 promoter linked to the CAT gene), ICP0 expression plasmid pCI-rtag-cICP0 and the indicated amounts of plasmid expressing HP1 followed by CAT assay (see Materials and Methods section).

A. The TLC result of CAT assay (upper panel) was analysed by using the Phosphorimager analysis system and the data were analysed to calculate the percentage conversion of substrate to product (middle panel). The decrease of CAT activity was more significant when more HP1 protein was expressed.

B. The western blot analysis of total cell proteins in samples transfected in parallel with the same amounts of plasmid and probed for ICP0 are shown below. Repressor HP1 did not affect the expression of ICP0, since ICP0 was equally expressed among samples. The results of this single experiment were reproduced on several independent occasions.

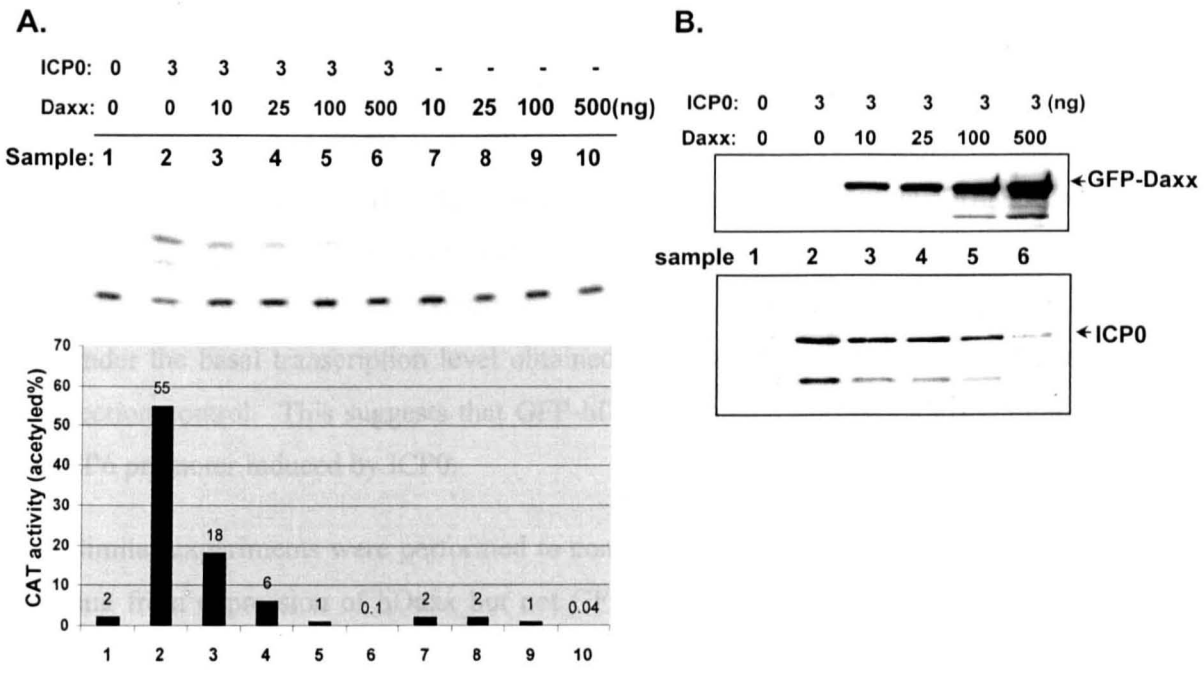

Fig. 3.18 Effect of GFP-hDaxx on transactivation of an ICP6 expression cassette by ICP0 in Vero cells.

Cells were co-transfected with reporter plasmid pSS80 (ICP6 promoter linked to the CAT gene), ICP0 expression plasmid pCI-rtag-cICP0 and the indicated amounts of pEGFP-nls-hDaxx plasmid followed by CAT assay (see Materials and Methods section).

A. The TLC result of CAT assay (upper panel) was analysed by using the Phosphorimager analysis system and the data were analysed to calculate the percentage conversion of substrate to product (lower panel). The decrease of CAT activity was more significant when more hDaxx protein was expressed.

B. The western blot analysis of total cell proteins in samples transfected in parallel with the same amounts of plasmid and probed for GFP-hDaxx and ICP0 are shown below. Expression of ICP0 was repressed by hDaxx. The results of this single experiment were reproduced on several independent occasions.

GFP-hDaxx in a dose-dependent manner (Fig. 3.18B). This raises the question as to whether the inhibition of CAT activity seen in the sample expressing a high level of GFP-hDaxx is simply due to the reduction in ICP0 expression or whether GFP-Daxx causes a global effect on both HCMV and ICP6 promoters? The CAT activity in sample 3, expressing a high level of GFP-Daxx, was one third of that in sample 2 (hDaxx mock transfection), whereas ICP0 was equivalently expressed in those two samples (Fig. 3.18). In addition, although ICP0 was expressed at a lower level in sample 6, the CAT activity was under the basal transcription level obtained from sample 1, which is an ICP0 mock transfection control. This suggests that GFP-hDaxx strongly represses transcription from the ICP6 promoter induced by ICP0.

Similar experiments were performed to confirm that the inhibition of transcription is resulting from expression of hDaxx but not GFP. To generate a plasmid expressing the entire hDaxx protein without GFP, firstly, two fragments (*Bam*H I-*Hin*d III and *Hin*d III-*Xba* I) containing full-length of hDaxx ORF, were subcloned from the pEGFP-NLS-hDaxx plasmid into pCDNA3.1+ vector digested with *Bam*H I-*Xba* I. Following the same strategies, a consistent result was obtained. As shown in Fig. 3.19, without hDaxx transfection, ICP0 strongly induced ICP6 promoter activity, resulting in nearly 100% conversion of substrate to product, while the CAT activity was repressed by more than 50% when cells were cotransfected with 10ng of plasmid pcDNA 3.1/hDaxx. Notably, the CAT activity was lower than the basal level when 500ng of hDaxx expression plasmid was introduced into cells, indicating that hDaxx possessed a strong transcription repression activity.

3.4.3 SUMO-1

Results from 3.3.2A.1 demonstrated that transfected cells over-expressing SUMO-1 had a lower infectivity compared with untransfected cells. Furthermore, recently, Li *et al.* (2000) reported that in transient transfection assays, the transcriptional repression mediated by hDaxx was reversed by co-expression of wild type PML, while a PML mutant lacking SUMO-1 modification sites was less effective. To examine whether SUMO-1 itself affects the transactivation function of ICP0 or whether SUMO-1 is involved in the function of hDaxx in transcriptional repression, a multiple plasmid transfection was performed. As illustrated in Fig. 3.20, compared with the CAT activity of samples transfected with hDaxx

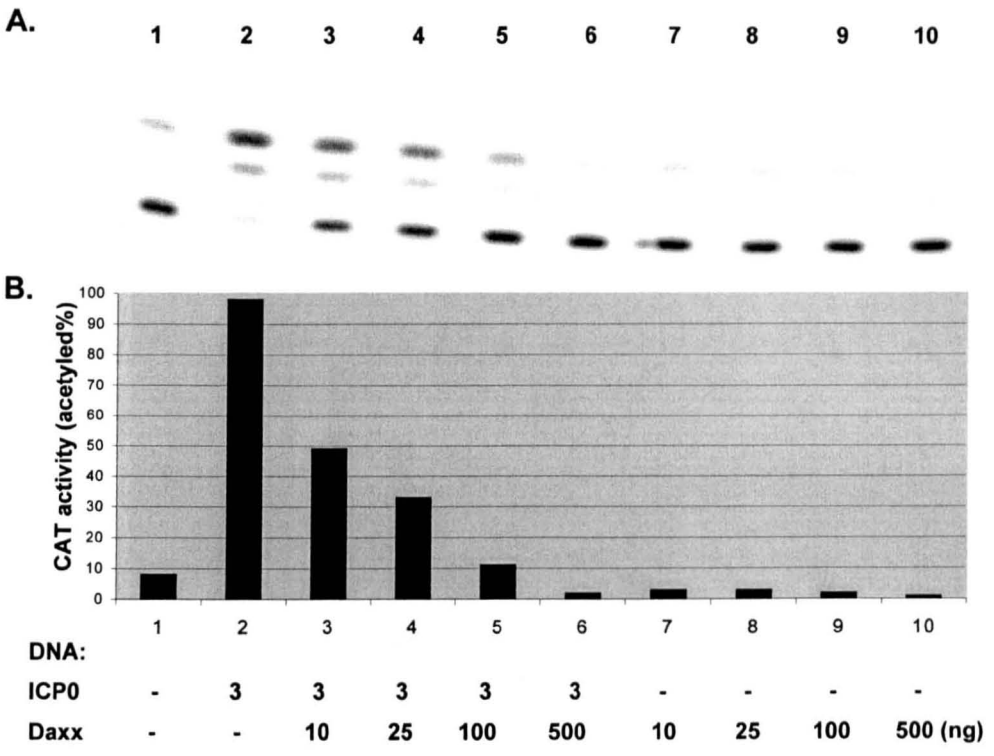

Fig. 3.19 Effect of hDaxx on transactivation of an ICP6 expression cassette by ICP0 in Vero cells.

Cells were co-transfected with reporter plasmid pSS80 (ICP6 promoter linked to the CAT gene), ICP0 expression plasmid pCI-rtag-cICP0 and the indicated amounts of pcDNA3-hDaxx plasmid followed by CAT assay.

The TLC result of CAT assay (panel A) was analysed by using the Phosphorimager analysis system and the data were analysed to calculate the percentage conversion of substrate to product (panel B). The decrease of CAT activity was more significant when more hDaxx protein was expressed.

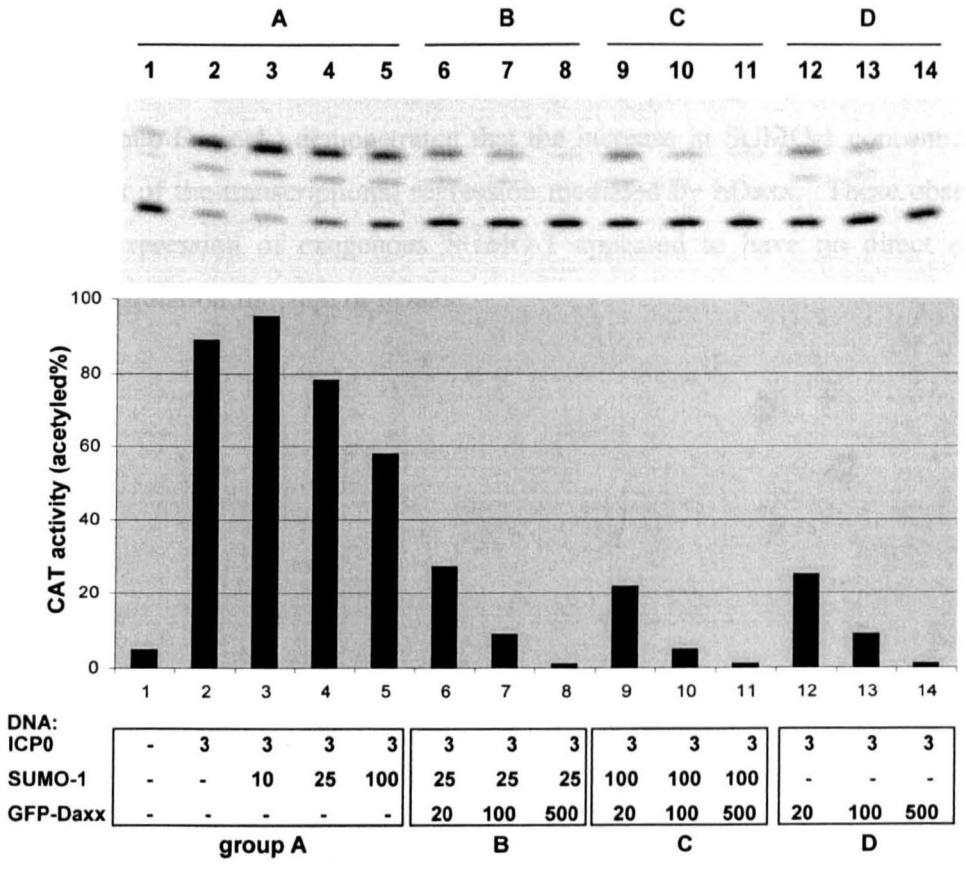

Fig. 3.20 Effect of SUMO-1 on repression function of hDaxx on transactivation of an ICP6 expression cassette by ICP0 in Vero cells.

Cells were co-transfected with reporter plasmid pSS80, the indicated amounts of ICP0 expression plasmid pCI-rtag-cICP0, pEGFP-nls-Daxx and SUMO-1 plasmids followed by CAT assay (see Materials and Methods section).

The TLC result of the CAT assay (upper panel) was analysed by using the Phosphorimager analysis system and the data were analysed to calculate the percentage conversion of substrate to product (lower panel). Addition of SUMO-1 had a slight effect on the activation of the ICP6 promoter (group A). However the CAT activities in group D had no significant differences from the CAT activities in groups B and C which were transfected with various amounts of the SUMO-1expression plasmid.

(group D), expression of SUMO-1 triggered a very moderate repression of transcription even at high amounts of SUMO-1 transfection (sample in group A). In addition, results from cells cotransfected with various amounts of SUMO-1 (group B: 25 ng, group C, 100ng, and group D mock) demonstrated that the increase in SUMO-1 concentration did not alter levels of the transcriptional repression mediated by hDaxx. These observations suggest that expression of exogenous SUMO-1 appeared to have no direct effect on transcription regulation function of hDaxx.

3.5 Discussion

The antiviral cytokine interferon increases the expression of ND10 proteins PML and Sp100, leading to an increase in the size and number of ND10 foci (Grotzinger *et al.*, 1996). Since many DNA viruses express proteins that cause redistribution of ND10 proteins such as PML and Sp100, it is possible that ND10 associated proteins may play a part in an antiviral mechanism in host cells. If so, the increase in expression level of ND10 proteins or their SUMO-1 modified forms may promote resistance to viral infection.

Transient transfection using electroporation and lipofection with a 40-50% transfection efficiency greatly increased the expression of ND10 associated proteins (Fig. 3.9- 3.12). However progression of viral infection was not affected by the raised ND10 protein levels. It was observed that in singly transfected cells, only a very low proportion of PML and Sp100 was covalently modified by SUMO-1, and most overexpressed PML was in the unmodified form (Fig. 3.11A), and located throughout the nucleoplasm (data not shown). This implies that transiently overexpressed proteins may not produce their proper biological activity. In addition, since SUMO-1 has been found to be a factor promoting the recruitment of PML into ND10 structures (Muller *et al.*, 1998), this finding suggests a possibility that the amount of endogenous SUMO-1 may be not sufficient to modify all the overexpressed ND10 proteins. To improve the SUMO-1 modification level, plasmids expressing SUMO-1 and Ubc9 were cotransfected into BHK cells. The results from 3-plasmid and 4-plasmid cotransfections showed that at an early time of infection, the initiation of HSV-1 infection in transfected cells were decreased by two-fold compared to untransfected cells, but no significant effect on the progression of viral infection at 6 hpa was observed (Fig. 3.15, 3.16). Taken together, this study indicates that transfected cells expressing high levels of ND10 proteins conferred a marginal resistance to infection by HSV-1 at an early time of infection, 2 hpa, but did not appear to compromise the overall efficiency of HSV-1 infection in Hep-2 and BHK cells.

It has been reported that some DNA viruses, such as HSV-1 and HCMV, disperse ND10 structures at early times of infection by the action of their immediate early gene products, ICP0 and IE72 respectively (Everett & Maul, 1994, Korioth *et al.*, 1996). It is not clear whether dispersion of ND10 is advantageous to the viral infection, but in the case of ICP0 and IE72, loss of these proteins reduces productive infectivity at low multiplicities

of infection. These findings imply that if ND10 is a crucial factor for the establishment of productive virus infection, then this structure must be the premier target for viral proteins (for example ICP0) early in infection. However, HFL cells pre-treated with heat shock lose the integrity of the ND10 structure, but this did not affect or increase the susceptibility for HSV-1 infection (Table 3.1). This suggests that while the interaction between ND10 and ICP0 may play a role in the initiation of viral infection, it can not be a simple case of disruption of the cellular structure of itself. It is clear from the results of many other studies that the mechanism by which ICP0 disrupts ND10 is an essential factor in its ability to stimulate viral infection and increase gene expression.

The limitation of the transfection study is that an ideal cell line to study the function of ICP0, in terms of viral-host cell interactions, is HFL (human foetal lung) cells in which the virus has a high requirement for ICP0. However, HFL cells are poorly transfectable and therefore not amenable for this type of analysis. Apart from this, infection with lower input virus (< 0.1 MOI) or at early times of infection (<2 hpa), the fluorescence of ICP0 and UL29 were too faint to be detected. Due to the dynamic property of ND10 structure and the function of ICP0 in an MOI-dependent manner, a suitable cell line, virus inputs, and infection times are important factors that should be considered in the study of ICP0-ND10 proteins interaction by these methods. A further limitation of these methods is that the scoring of both transfected and infected cells was simply by presence or absence of signal above background, and not by the intensity of signal. This means that if relatively reduced levels of viral proteins occurred in cells expressing high levels of exogenous ND10 proteins, such inhibition would not be detected by this analysis. Indeed, the method could only detect high levels of inhibition as any more moderate effects would be less likely to reduce the number of virally infected cells scored as positive.

Although results from transient transfection in this chapter shown that overexpression of ND10 proteins does not significantly compromise HSV-1 infection, two ND10 associated proteins, hDaxx and HP1 strongly repressed the activation of transcription induced by ICP0 as detected by CAT assay. SUMO-1 modification of PML has been shown to efficiently inhibit the hDaxx-mediated repression (Li *et al.*, 2000). However exogenous expression of SUMO-1 did not increase the repression activity of hDaxx in CAT assay (Fig. 3.20). These observations implicate a possible role of ND10 constituents involved in the function of viral proteins.

RESULTS AND DISCUSSIONS

Chapter 4 Characterisation of human neuronal committed teratocarcinoma NT2 cells and their infection by HSV-1

Chapter 4 Characterisation of human neuronal committed teratocarcinoma NT2 cells and their infection by HSV-1

After primary infection, HSV-1 remains in a latent state in nervous tissue for the lifespan of the host. This latent infection may be reactivated by various stimuli, including stress. As described in some detail in the Introduction, the mechanism controlling reactivation from latency is not fully understood, since no single animal or cultured cell model has been established to mimic the situation in the natural human host exactly. Many *in vitro* studies have used rat or mouse cultured explanted foetal neurons or neuronal-like cell lines, since there are difficulties in using primary human neurons. Rodent cells do not readily lend themselves to examination of their ND10 structures since most antibodies available recognise only human forms of the major constituent proteins. Therefore we sought to use a human neuronal cell line to study the interaction of viral proteins with cellular factors during lytic or latent infection in cultured cells with at least some resemblance to human neurons.

The NT2 cell line, derived from a human teratocarcimona, represents a committed neuronal precursor stage of differentiation (Pleasure & Lee, 1993, Pleasure *et al.*, 1992). NT2 cells can be induced by retinoic acid to differentiate *in vitro* into a mixture of postmitotic cells that resemble central nervous system (CNS) neurons since they express many well-defined neuronal markers and elaborate axonal and dendritic processes (hNT neurons) (Pleasure *et al.*, 1992). Furthermore, NT2 cells can be transfected, allowing for the study of genes of interest in a neuronal precursor environment.

The aims of this study were to investigate the characteristics of ND10 and HSV-1 gene expression and replication in both NT2 and the differentiated hNT cells. I also aimed to assess the role of ICP0 in the interaction with ND10 proteins and in viral infection in these cell lines.

4.1 The expression status of ND10 proteins in NT2 cells

The expression pattern of ND10 proteins in NT2 cells, prior to retinoic acid induced differentiation, was determined and compared with fibroblast HFL cells by staining these cells with antibodies recognising constituents of ND10, such as PML (r8), Sp100 (SpGH), and hDaxx (r1866) as well as a centromere protein, CENP-C (r554). On average, there were less than 10 foci of PML in each NT2 cell (Fig. 4.1A) and in many NT2 cells, the distribution of PML was commonly seen to be as short rods or strings of small PML foci throughout the nucleoplasm (see the inset in Fig. 4.1A). Surprisingly, expression of Sp100 in NT2 cells was not detectable by immunofluorescence (Fig. 4.1B). The staining of hDaxx was present throughout the nucleus of NT2 cells with a high background of diffuse material, within which many large and small clumps of hDaxx were observed (Fig. 4.1C).

In HFL cells, as with many other cultured human cell lines, the major ND10 components Sp100, PML, and hDaxx were observed in distinct foci with an average number of around 20 to 30 per nucleus (right-hand panel in Fig. 4.1). In NT2 cells, as compared with HFL cells, there were fewer PML and hDaxx foci of various sizes and Sp100 was absent in NT2 cells. In contrast to the unusual staining profile of ND10 proteins, staining of CENP-C was quite similar in both NT2 and HFL cells (Fig. 4.1D).

Double staining for PML and hDaxx revealed that the majority of hDaxx foci were perfectly colocalised with PML in the nucleus of HFL cells, whilst in NT2 cells, many hDaxx foci were separate from PML (Fig. 4.2A). As reported, hDaxx accumulates at both ND10 and centromeres, although the association of hDaxx with these two structures varies between cells, and represents a dynamic distribution dependent on cell status (Everett *et al.*, 1999b). To explore the association of hDaxx in NT2 cells, double labeling with antibodies for hDaxx (r1866) and centromeres (human serum GS) showed that hDaxx proteins were preferentially associated with centromere structures (Fig. 4.2B). In HFL cells, however, only a small proportion of hDaxx was localised in the vicinity of centromeres (Fig. 4.2B).

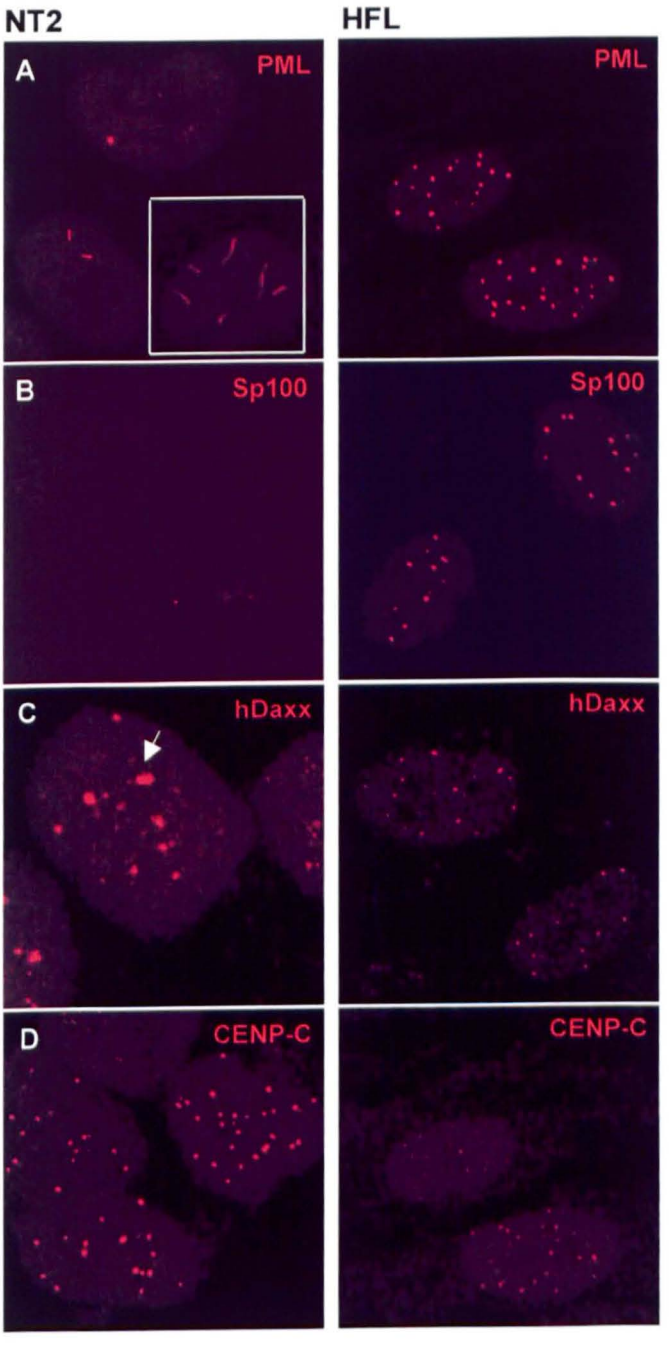

Fig. 4.1 Comparison of the appearance of ND10 between NT2 and HFL cells.

NT2 (left-hand panel) and HFL (right-hand panel) cells were stained for ND10 and centromere proteins as labeled in the right-top in each image. The expression status of ND10 proteins in NT2 cells was distinct from that in HFL cells. There was no detectable Sp100, and fewer PML and hDaxx foci in NT2 cells.

Fig. 4.2 Distinct expression pattern of ND10 and centromere proteins in HFL, NT2, and hNT cells.

Confocal micrographs of the three cell lines are presented, as indicated by white lettering. (A) The labeled proteins are indicated in the top row and are the same in each vertical row of panels. PML was stained with mouse MAb 5E10 (green), and the cells were also stained with SpGH (left-hand panels), rabbit serum r1866 (center panels), or rabbit serum r554 (right-hand panels) for Sp100, hDaxx, and CENP-C, respectively. There is no Sp100 expression and less PML expression in NT2 cells, and PML does not colocalise efficiently with hDaxx. In HFL and hNT cells, PML extensively colocalises (yellow) with Sp100 and hDaxx but not with CENP-C.

(B) localisation of hDaxx (green) and centromere proteins (red). Cells were double labeled with r1866 and human serum ACA-GS which contains antibodies against several centromere proteins. In NT2 cells, a significant proportion of centromeres are associated with local accumulations of hDaxx, but this occurs more rarely in HFL and hNT cells.

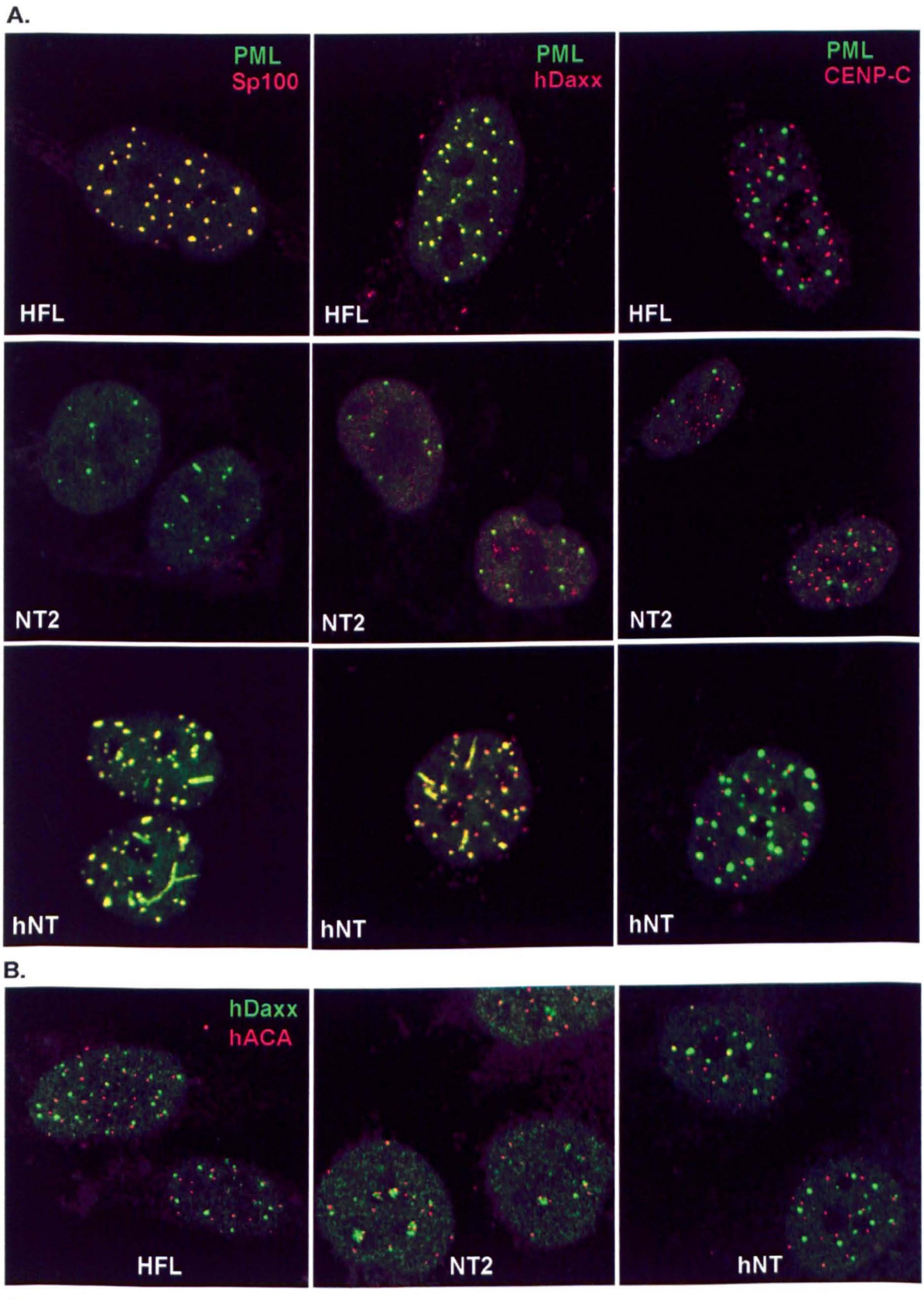
A.
PML
Sp100
HFL
PML
hDaxx
HFL
PML
CENP-C
HFL
NT2
NT2
NT2
hNT
hNT
hNT
B.
hDaxx
hACA
HFL
NT2
hNT

Fig. 4.2

4.2 Differentiation of precursor NT2 cells to hNT neurons

The methodology used for the differentiation of NT2 cells to hNT neurons was described in the Materials and Methods chapter (section 2.2.8B). A time course experiment was employed to monitor the development of ND10 structures throughout the 6-week differentiation process. NT2 cells from the same flask were split and seeded into 35-mm Petri dishes with 4 coverslips in each plate and then cultured in medium containing 10μM retinoic acid at 37°C. The cells were stained for ND10 proteins including PML, Sp100, hDaxx, as well as a centromere protein, CENP-C, after a period of differentiation of 1 day, 1 week, 3 weeks, 5 weeks, and 6 weeks. During retinoic acid induction, the localisation patterns of ND10 changed gradually and displayed characteristics more similar to those of differentiated fibroblast HFL cells (Fig. 4.3). Intriguingly, after a 3-week treatment of retinoic acid, the expression level of Sp100 was increased dramatically, with the novel Sp100 foci colocalising with PML (Fig. 4.3).

A 6-week induction of NT2 cells with retinoic acid followed by incomplete purification (as described in section 2.2.8B), resulted in a population of cells with more than 30% having a significant neuronal phenotype. The morphology of hNT cells observed by phase contrast microscopy showed that the average size of differentiated hNT neurons was larger than that of NT2, with typical multiple lengthy cell processes (Fig. 4.4). Staining of hNT neurons for PML and Sp100 presented a similar expression profile of ND10 to that of HFL cells, except that the fluorescence intensity of both proteins was comparatively bright in the hNT cells. More than 20 foci of ND10 were seen on average per cell, and these foci showed perfect co-localisation of Sp100 with PML (Fig. 4.2A). In addition, the string-like accumulations of PML were observed in some hNT neurons (Fig. 4.2A). The clumps of hDaxx accumulation observed in NT2 cells were no longer present in the differentiated hNT neurons and in contrast to NT2 cells, hDaxx was strongly associated with PML and much less associated with centromeres (Fig. 4.2B). Therefore a significant alteration in ND10 composition and ND10 protein localization has occurred during the differentiation process.

The expression level of ND10 proteins in the three cell lines was also quantified by western blot analysis. An equal number of cells from HFL, NT2 and hNT neurons were simply lysed in a boiling mixture, and the proteins were separated by SDS-PAGE and

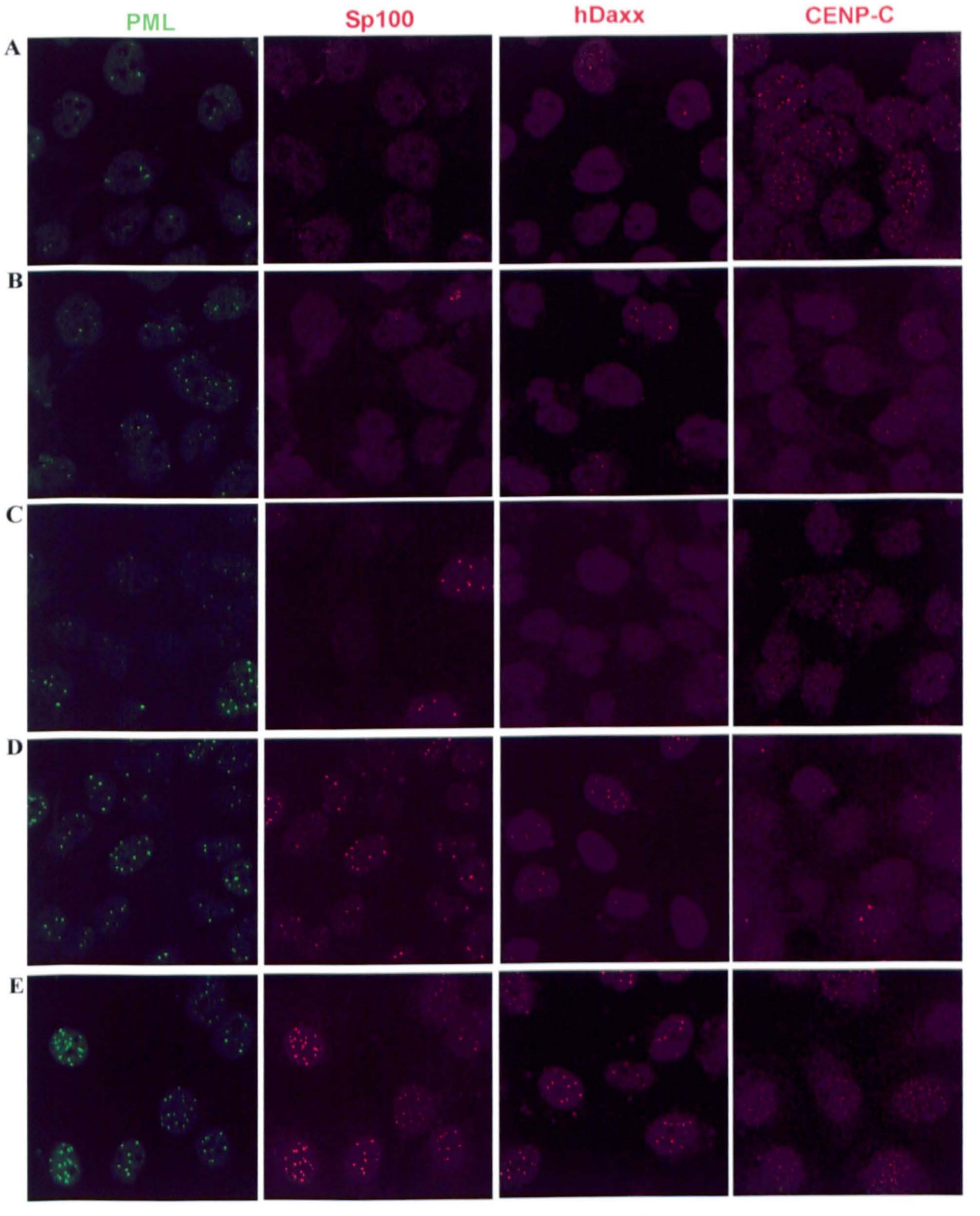

Fig. 4.3 The ND10 expression pattern in NT2 cells during differentiation. Differentiation of NT2 cells was induced by treatment of retinoic acid for 1 day (panel A), 1 week (panel B), 3 weeks (panel C), 5 weeks (panel D), and 6 weeks (panel E). The expression of ND10 was revealed by immuno-staining for PML (5E10), Sp100 (SpGH), hDaxx (r1866), and a centromere protein (r554).

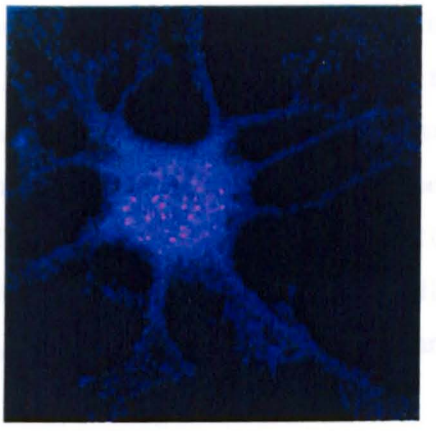

Fig. 4.4 A differentiated hNT neuron.

NT2 cells differentiated to hNT neurons by induction of retinoic acid for 6 weeks. The typical multiple length cell processes were observed in differentiated hNT neurons (shown in blue fluorescence).

Note: the red fluorescence in the nucleus was labelled for centromere protein, CENP-C.

detected by antibodies against PML, Sp100 as well as an antibody for actin as an internal control. In hNT neurons, long-term induction of retinoic acid resulted in an extreme increase in the unmodified and SUMO-1 modified forms of both PML and Sp100. Moreover, the expression of both ND10 proteins in hNT neurons was even higher than that in HFL cells (Fig. 4.5). SUMO-1 modified PML was hardly detectable in NT2 cells (Fig. 4.5). Therefore the differences in ND10 morphology and composition between HFL, NT2 and hNT cells can be correlated in changes in the biochemical characteristics of the major ND10 proteins. The abnormal appearance of ND10 in NT2 cells appears to be caused by lack of Sp100 expression, low levels of PML expression, poor SUMO-1 modification of PML and, probably in consequence, lesser amounts of associated hDaxx.

4.3 The susceptibility of NT2 and hNT cells to HSV-1 infection

4.3.1 The temporal progression of HSV-1 infection in NT2 cells

At least three DNA viruses, including HSV-1, have a tendency to deposit their parental genomes adjacent to ND10, from where viral replication begins (Ishov & Maul, 1996). It has been reported that rodent neuroblastoma cell lines were poorly infected by HSV-1 due to the inefficient transcription of IE genes (Kemp *et al.*, 1990), however the ability of HSV-1 to infect human neuroblastoma cell lines has not been rigorously studied. Together with the results described in sections 4.1 and 4.2 which illustrate that NT2 cells contain unusual ND10 with fewer PML foci and no detectable Sp100, it was interesting to explore whether HSV-1 replicates successfully in NT2 cells. To this end, the efficiency of HSV-1 replication in NT2 cells was compared with that in HFL cells. Both cell lines were infected by HSV-1 at an MOI of 1 pfu per cell for 12, 24, 36, and 48 hours and the yields of the progeny viruses were determined in BHK cells. At early times of infection, the yields of HSV-1 from NT2 cells were around 10-fold lower than in HFL cells, but after 36 hpa, viral yields were just slightly reduced in NT2 cells (Fig. 4.6).

4.3.2 Infection of HSV-1 in NT2 cells and hNT cells

To study the susceptibility of both NT2 and hNT cell lines to HSV-1 infection in more detail, cells were infected with various multiplicities ranging from 50 to 0.01 pfu per cell. Results from the time course of HSV-1 infection in NT2 cells (Fig. 4.6) show that the

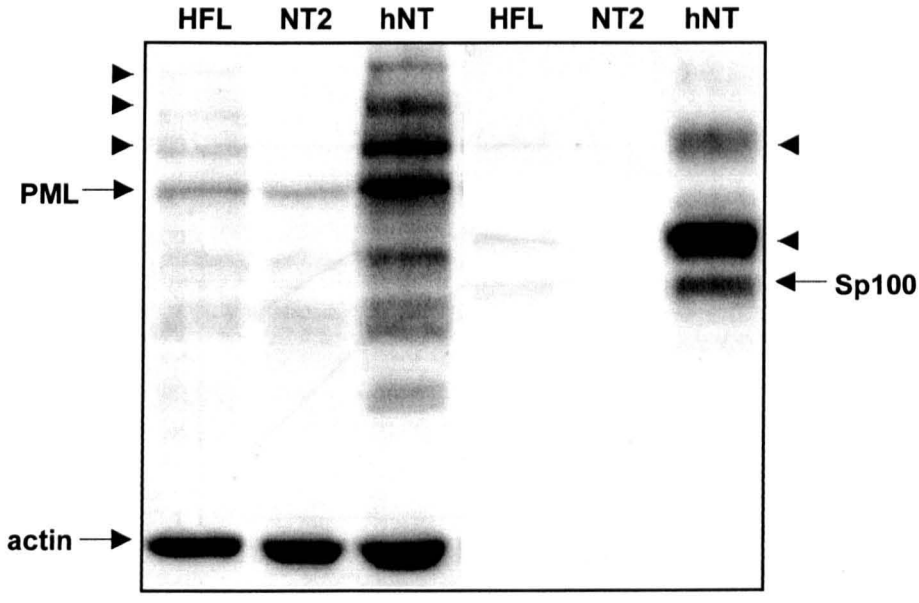

Fig. 4.5 Western blot analysis of the expression patterns of Sp100 and PML in HFL, NT2, and hNT cells.

The left-hand three tracks show PML species detected by 5E10, with actin detected simultaneously as the internal control. The right-hand three lanes show the same filter after stripping and re-probing for Sp100 with SpGH. The arrows mark the presumed unmodified forms of PML or Sp100, and the arrowheads indicate the high molecular mass isoforms of PML and Sp100. NT2 cells do not express Sp100, whereas in hNT cells, long-term induction of retinoic acid results in a drastic increase of both unmodified and modified forms of Sp100 and PML. The extent of SUMO-1 modification of PML is reduced in NT2 cells.

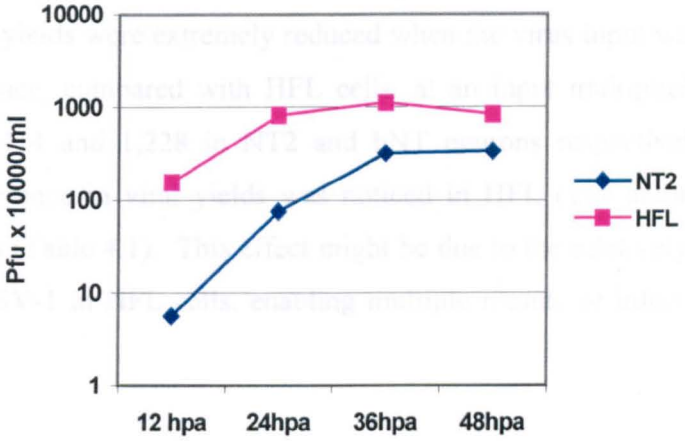

Fig. 4.6 Growth curves of HSV-1 strain 17+ in HFL and NT2 cells.

Cells were infected with the virus at 1 pfu per cell and both cells and medium were harvested at the indicated times after infection and progeny virus titers were determined on BHK cells. The data are the average of two independent experiments.

exponential stage of viral replication was between 12 to 36 hpa, and therefore progeny viruses were harvested and titrated in BHK cells at 36 hours postinfection. In general, the yields of progeny viruses from NT2 cells were lower than from HFL cells, and this reduction was slightly more pronounced in hNT neurons (Table 4.1). While the yields of progeny virus in NT2 and hNT cells were only modestly reduced after high multiplicity infection, virus yields were extremely reduced when the virus input was less than 1 pfu per cell. For instance, compared with HFL cells, at an input multiplicity of 0.01, the fold reduction was 414 and 1,228 in NT2 and hNT neurons respectively (Table 4.1). No significant difference in viral yields was noticed in HFL cells among the various virus inputs at 36 hpa (Table 4.1). This effect might be due to the relatively efficient replication of wild type HSV-1 in HFL cells, enabling multiple rounds of infection at this length of incubation.

4.4 Viral gene expression in NT2 and hNT cells

4.4.1 Results from western blot analysis

To explore the efficiency of viral gene expression in NT2 and hNT2 cells, the cells were infected by HSV-1 at various MOIs and were harvested at 1, 2, 3, 4 hours post infection. Total cell extracts were probed for IE proteins ICP0 and ICP4 as well as for products of typical E genes such as UL29, UL39 and UL42. At high multiplicity of infection (5 pfu per cell), viral gene expression was extremely inefficient in hNT neurons; even at 4 hours after infection only ICP0 was observed (Fig. 4.7A). In NT2 cells, expression of the two IE genes was slightly greater than in HFL cells, whereas all the early genes were less well expressed in NT2 cells (Fig. 4.7A). This phenomenon was more significant when virus input was reduced to 1 pfu per cell (Fig. 4.7B). By 2 hpa in NT2 cells, expression of ICP0 was detected at a higher level than in HFL cells, but the two early genes UL39 and UL29 were observed only after 4 hours of infection. In contrast to infections in NT2 cells, the early genes UL39 and UL29 were highly expressed in HFL cells after infection for 3 hours and expression of UL29 was even higher than ICP0 at 4 hpa (Fig. 4.7B). These effects of reduced viral gene expression in NT2 cells compared to HFL cells were more obvious at a multiplicity of 0.2 (Fig. 4.7C). In NT2 cells, the only viral gene expression detected was that of ICP0, even after 4 hours of infection (Fig. 4.7C). The relatively high levels of ICP0 expression in NT2 cells in these experiments suggest

Table 4.1 Replication of HSV-1 strain 17+ in HFL, NT2, and hNT cells[a]

	Titer (pfu/ml) at 36 hr in cell type			Fold reduction	
Input MOI[b]	HFL	NT2	hNT	NT2	hNT
50	9.4×10^7	7.4×10^7	1.2×10^7	1.3	7.8
10	6.3×10^7	2.7×10^7	1.0×10^7	2.4	6.3
1	6.2×10^7	1.9×10^7	5.6×10^6	3.0	11
0.1	7.8×10^7	1.1×10^6	6.8×10^5	70	114
0.01	7.3×10^7	1.8×10^5	5.9×10^4	414	1,228

[a] The three cell types were infected with HSV-1 strain 17+ at the indicated multiplicities, and then the cells and medium were harvested after 36 hr and sonicated. The virus progeny was titrated on BHK cells. The fold reduction of virus titers in NT2 and hNT cells compared to hNT cells is shown. Note that the yields of virus in HFL cells do not decrease with multiplicity because rapid viral replication ensures all the cells become infected during the time course of the experiment.

[b] MOI, multiplicity of infection.

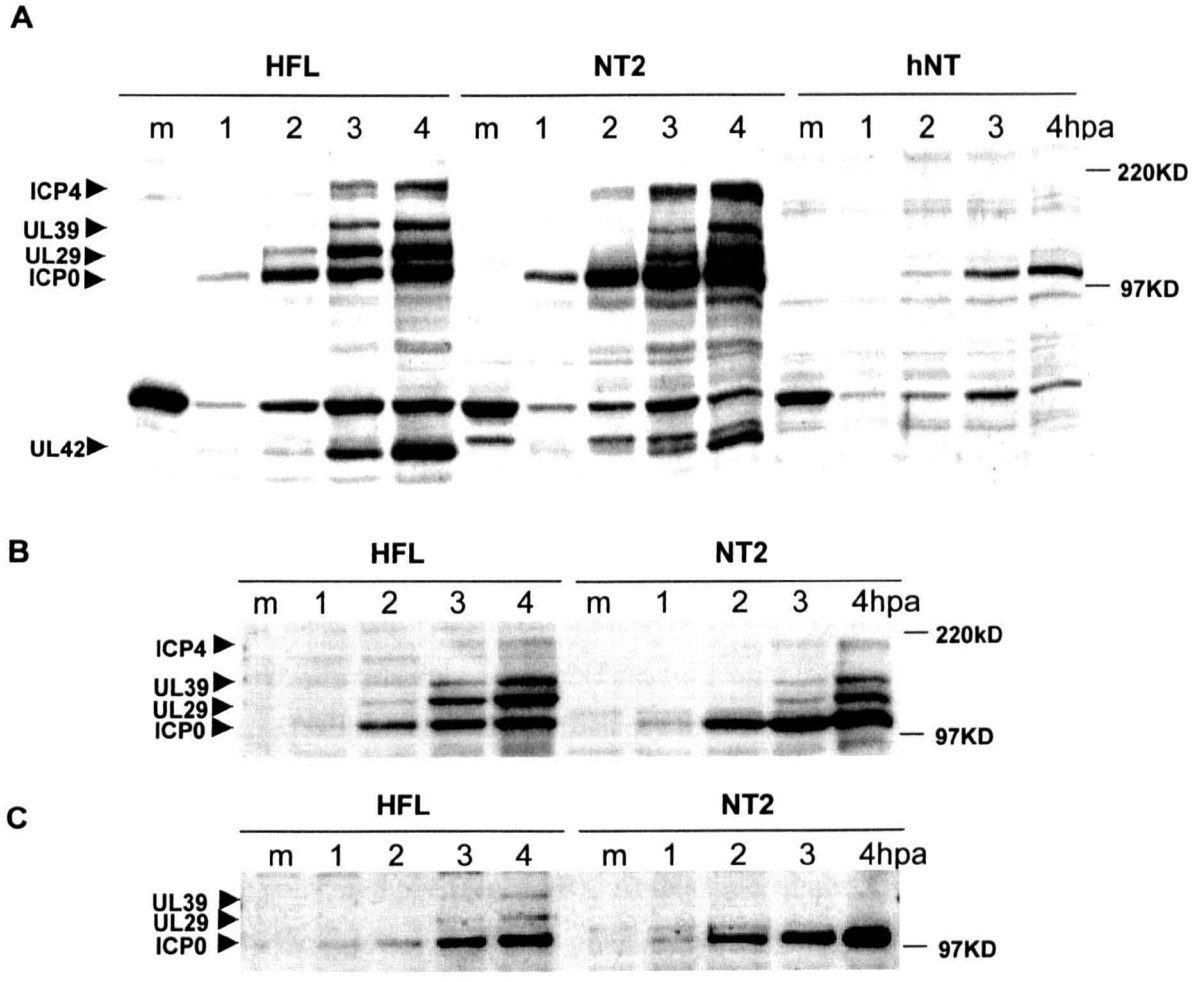

Fig. 4.7 Comparison of the rates of viral gene expression in HFL, NT2 and differentiated hNT cells.

Cells were infected with 5 (A) 1 (B) or 0.2 (C) pfu per cell of wild type HSV-1 strain 17+ and harvested at 0 (labeled as m), 1, 2, 3, and 4h after absorption (hpa), then processed by SDS-PAGE and western blot analysis. A mixture of antibodies recognising several viral proteins was employed to detect IE proteins ICP0 and ICP4, and also E genes UL39, UL29, and UL42 (as indicated on the left). The expression levels of ICP0 and ICP4 genes are relatively higher in NT2 cells compared to HFL cells, and the rate of appearance and relative amounts of the E proteins are reduced in NT2 cells. In hNT cells, little viral gene expression, apart from ICP0, is apparent. (B-C) At the lower MOI infection, expression of viral E genes is again much slower in NT2 than in HFL cells.

Note that the use of the western blot approach means that the absolute levels of the proteins are not being measured, but that the results clearly demonstrate differences between relative expression levels of the proteins in the different experimental conditions.

that the defect in the expression of other viral proteins is not due to failure of the virus to penetrate the cell. Instead, the cells appear to be blocked at a stage when ICP0 is being expressed, but the infection fails to develop to the later stages.

4.4.2 Immunofluorescence detection of viral proteins

The results of the western blot analysis (Fig. 4.7) show the viral gene expression profiles in populations of infected cells in the three cell lines. However, the defect in viral gene expression in NT2 cells could be explained by a low proportion of infected NT2 cells expressing very high levels of ICP0 while the other cells fail to be infected at all. To investigate this possibility, an immunofluorescence assay was employed to detect viral gene expression in infected HFL, NT2, and hNT neurons. At 2 hours after infection, with a multiplicity of 1, most HFL and NT2 cells were detectably infected as judged by the expression of ICP0, whereas only a few hNT neurons were infected (Fig. 4.8A). Although ICP0 was expressed with an equivalent efficiency in NT2 and HFL cells, the expression of UL29 in NT2 cells was much less efficient than in HFL cells and no infected hNT neurons progressed to the early gene expression stage (Fig. 4.8A). Similar results were obtained from a later time point, at 8 hpa (Fig. 4.8B). At this time, almost all the infected HFL cells had progressed to the expression of early proteins, but only 50% of infected NT2 and hNT neurons expressed UL29 (Fig. 4.9A). This effect was more significant at lower virus input multiplicities. On reduction of the multiplicity to 0.1 pfu per cell, at 2 hpa, one fourth of infected HFL cells expressed UL29, but none of the infected NT2 cells expressed UL29 (Fig. 4.9B). The deficiency in the progression of viral infection in NT2 cells and hNT cells was not overcome by elongation of the length of infection to 8 hours (Fig. 4.9B).

4.5 Infection of NT2 and hNT cells with an ICP0-deficient virus

The efficient expression of ICP0, but not other viral proteins, in NT2 and hNT neurons implies that the induction of gene expression by ICP0 is not very effective. Two ICP0-deficient mutant viruses were used to investigate the function of ICP0 in viral infection of NT2 cells and hNT neurons. The mutants selected for this study included the ICP0 null mutant *dl*1403 and the USP7-binding negative mutant M1. It had been reported that *dl*1403 has a severe multiplicity-dependent growth defect in HFL cells and that this defect varied

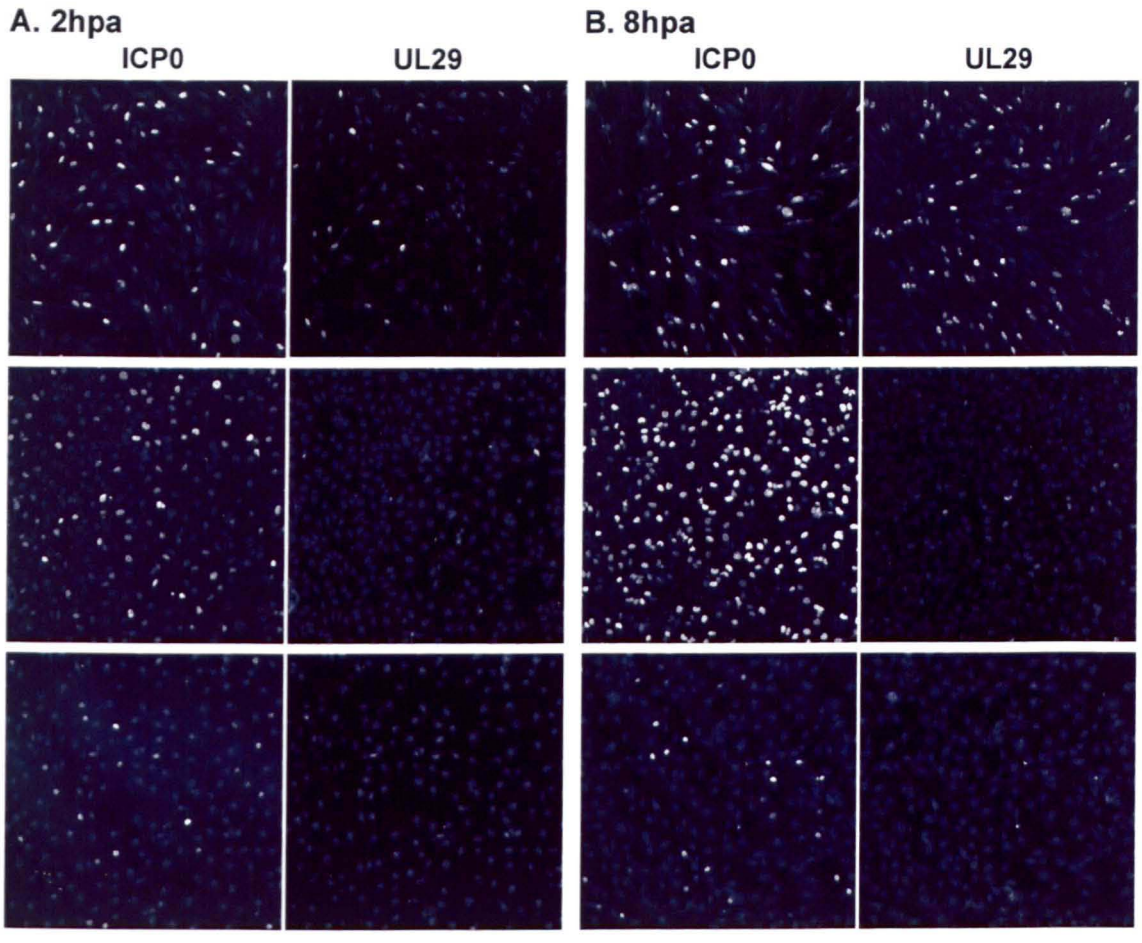

Fig. 4.8 Inefficient progression of viral infection in NT2 and hNT cells.

HFL (top panels), NT2 (middle panels), and hNT (bottom panels) cells were infected with wild-type stain 17+ at 1 pfu per cell. Infected cells were fixed 2 (A) and 8 (B) hr after absorption and prepared for immunofluorescence and simultaneous staining for ICP0 (left-hand panels in each time point of infection) and UL29 (right-hand panels in each time point of infection), using MAb 11060 and serum r515 as markers of viral IE and E gene expression. At a early time of infection (2hpa) in hNT cells, the number of infected cells expressing ICP0 and UL29 is much less than in HFL and NT2 cells. The number of NT2 cells expressing ICP0 is equivalent to the HFL infections, but relatively few NT2 cells are expressing large amount of UL29. The deficiency in the progression of viral infection in NT2 and hNT cells was not overcome at 8hpa.

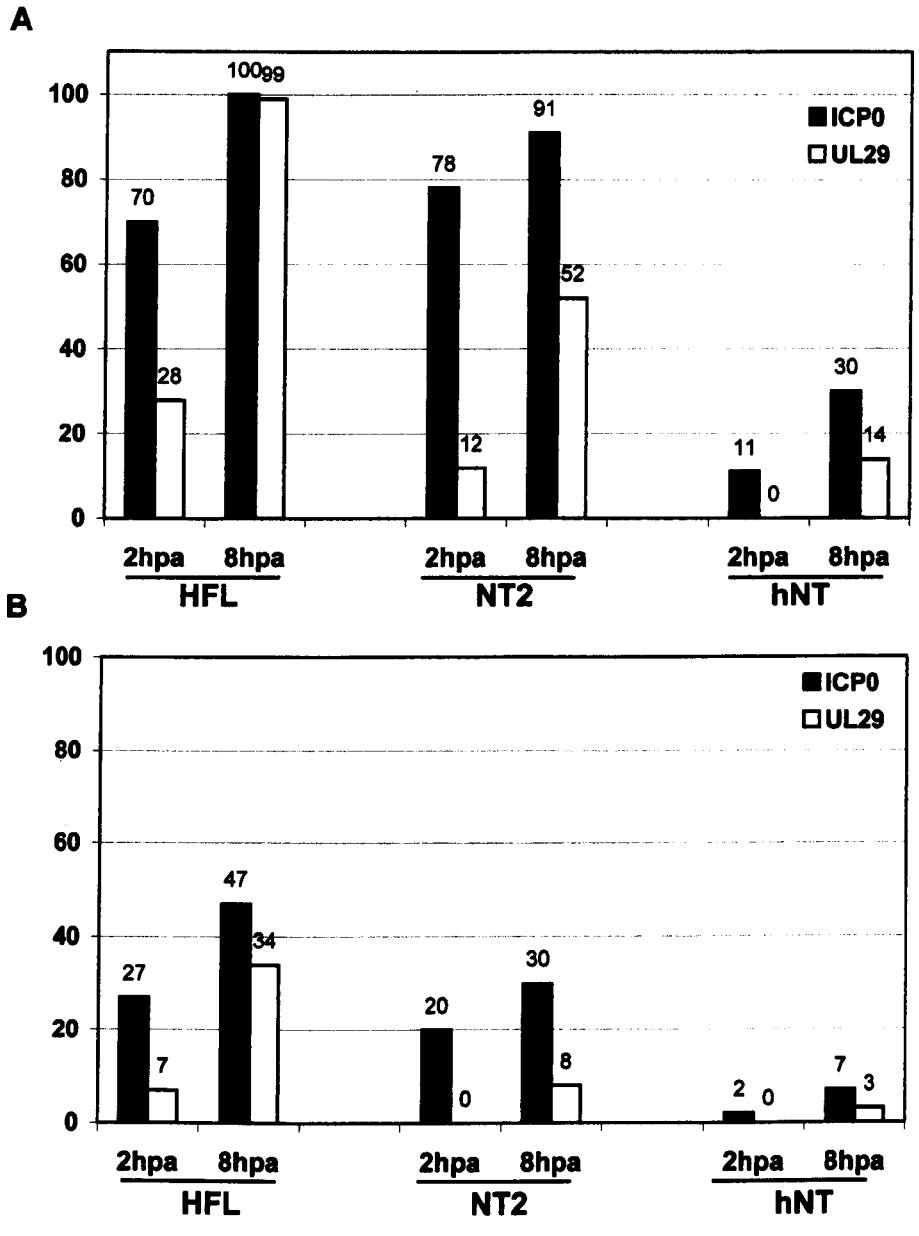

Fig. 4.9 Comparison of the rates of viral gene expression in HFL, NT2 and differentiated hNT cells.

Cells were infected with 1 (A) or 0.1 (B) pfu per cell of wild type HSV-1 strain 17+ and immuno-stained for ICP0 and UL29 2 and 8 hours post infection (hpa) followed by statistical analysis of the efficiency of infection.

defect varied between cell types (Stow & Stow, 1986). To compare the yields of these viruses in the various cell types, the titres of the viral stocks were first titrated in U2OS cells in which ICP0 function is not required, thus allowing efficient replication of wild type and ICP0 mutant viruses (Yao & Schaffer, 1995). HFL and NT2 cells were infected by each virus at various MOIs, and the progeny virus was again titrated in U2OS cells to remove any bias in the results that would result from titration in a cell line that was less permissive for the ICP0 mutant viruses. The yields of *dl*1403 progeny viruses were relatively lower in HFL cells compared to wild type virus, even at an MOI of 500 (Table 4.2). However, the results presented show that replication of *dl*1403 in NT2 cells was extremely poor, particularly at a low multiplicity of infection (Table 4.2). At a multiplicity of 5 this mutant virus replicated a further 69-fold less in NT2 cells than in HFL cells, and extension of the infection to 48 hours did not affect the results (Table 4.2). In NT2 cells, M1 virus replicated less well than 17+, but relatively efficiently compared to *dl*1403 (Table 4.2). Interestingly, the ability of ICP0 to bind to USP7 appeared to be very important in NT2 cells. At 36 hpa with a multiplicity of 0.01, M1 virus had an approximate 2500-fold reduction of progeny viral yield in NT2 compared to HFL cells (Table 4.2). This finding of the poor growth of M1 in NT2 cells was also supported by results using another USP7-binding negative mutant virus, D12, in which ICP0 residues from 494 to 633 had been deleted (Meredith *et al.*, 1995). The results revealed that D12 virus replicated very inefficiently in NT2 cells and the fold reduction was very similar to that seen with M1 (data not shown). In hNT neurons, the fold reduction of progeny virus yields from *dl*1403 and M1 viruses were similar to those in NT2 cells, although M1 virus replicated slightly better in hNT neurons than in NT2 cells (Table 4.2).

4.6 Characterisation of the function of ICP0 in NT2 cells

Results from western blot analysis revealed that ICP0 was relatively highly expressed in NT2 cells but early proteins were not. This defect was particularly evident at low multiplicities of infection (Fig. 4.7B, 4.7C). In addition, at an equivalent efficiency of ICP0 expression during infection, the progression of HSV-1 infection was much slower in NT2 cells compared with HFL cells, since only a small portion of infected NT2 cells could successfully progress to the early stage of infection, even at 8 hpa (Fig. 4.9). Furthermore, the ICP0-null virus, *dl*1403 had severe growth deficiency (Table 4.2) and another ICP0-

Table 4.2 Efficiency of replication of HSV-1 strain 17+ and ICP0 mutants dl1403 and M1 in HFL, NT2, and hNT cells[a]

Virus and input MOI[b]		Titer (pfu/ml) at 36 h		Fold reduction		
		HFL	NT2	HFL vs. NT2 at 36 h	HFL vs. NT2 at 48 h	NT2 vs. hNT at 36 h
17+	0.01	2.0×10^8	4.3×10^5	465	244	3.0
	0.1	8.7×10^7	8.7×10^6	10	12	1.6
	1	7.1×10^7	2.8×10^7	3	3	3.7
*dl*1403	5	3.8×10^6	5.5×10^4	69	77	4.7
	50	8.2×10^6	5.1×10^5	16	10	1.2
	500	7.6×10^6	5.1×10^5	15	10	2.5
M1	0.01	1.5×10^7	5.7×10^3	2667	26000	0.3
	0.1	7.1×10^7	6.1×10^4	1164	562	0.46
	1	7.3×10^7	1.4×10^5	514	17	0.57

[a] Virus 17+, dl1403, and M1 were used to infect the three cell types at the indicated multiplicities (calculated on the basis of titration in U2OS cells). Cells and medium were harvested 36 and 48h later and sonicated, and the progeny was titrated on U2OS cells. Actual titration figures are given for the 36-h sample. The fold reduction of the virus titers in NT2 compared to HFL cells are shown at the two time points. Note that the yields of virus in HFL cells do not decrease with multiplicity because rapid viral replication ensures all the cells become infected during the time course of the experiment. The high figure for the reduction of M1 replication at the lowest multiplicity in NT2 cells was due to further replication of the virus between 36 and 48 h in HFL cells but not in NT2 cells. Comparative yields of the viruses in NT2 and hNT cells from a separate are given in the last column. vs., versus.

[b] MOI, multiplicity of infection.

defect virus, M1, grew very poorly in NT2 cells as compared to HFL cells (Table 4.2). These data suggest that ICP0 is important for infection in NT2 cells, but even the wild type protein might not function normally in these two neuronal cell lines. To address this question, further experiments were performed to investigate the function of ICP0 in NT2 cells and hNT neurons.

4.6.1 The stability of ND10 proteins in NT2 and hNT cells during HSV-1 infection

A significant virus-host interaction during HSV-1 infection is that ICP0 firstly colocalises with and then degrades PML, Sp100, and CENP-C resulting in disruption of both ND10 and centromere structures (reviewed by Everett, 2000). The function of ICP0 was explored initially by investigating the localisation of ND10 and centromere proteins in NT2 and hNT cells during HSV-1 infection. Cells were infected by 17+ at an MOI of 1 for 2 and 4 hours and double-labeled for ICP0 and PML, hDaxx, or CENP-C. The samples were examined by confocal microscopy to determine the efficiency of disruption of ND10 and centromeres by ICP0. Compared to HFL cells, overall, ND10 and centromere proteins were relatively stable in NT2 and hNT cells during HSV-1 infection. In up to 96% of infected HFL cells expressing ICP0, staining of ND10 proteins was not visible, even at early times of infection (Fig. 4.10). In contrast to the rapid loss of discrete staining of ND10 proteins in infected HFL cells, 56% of infected NT2 cells retained intact PML foci at 2 hpa, and in these cells the PML was associated with ICP0 (Fig. 4.10, Table 4.3). Intriguingly, results obtained when NT2 cells were co-stained for ICP0 and CENP-C revealed that at 2 hours after infection, in 55% of infected cells, ICP0 strongly associated with and did not disperse CENP-C (Table 4.3). This association of ICP0 and CENP-C was to a greater degree than that observed in other cell lines (Fig. 4.10). However, this association was dynamic, since at 4 hours after infection most ICP0 was separate from CENP-C, yet the punctate CENP-C foci remained (Fig. 4.10). Similar results were obtained from cells stained for hDaxx and CENP-C (Table 4.3). At 4 hpa, no infected HFL cells contained discrete foci of PML, hDaxx, or CENP-C (Table 4.3). However, at 4 hpa, around one third of infected cells still retained punctate hDaxx staining, and the dispersal or degradation of PML was not affected by an extension of incubation, since more than 50% of infected NT2 cells contained punctate PML foci even at this time after

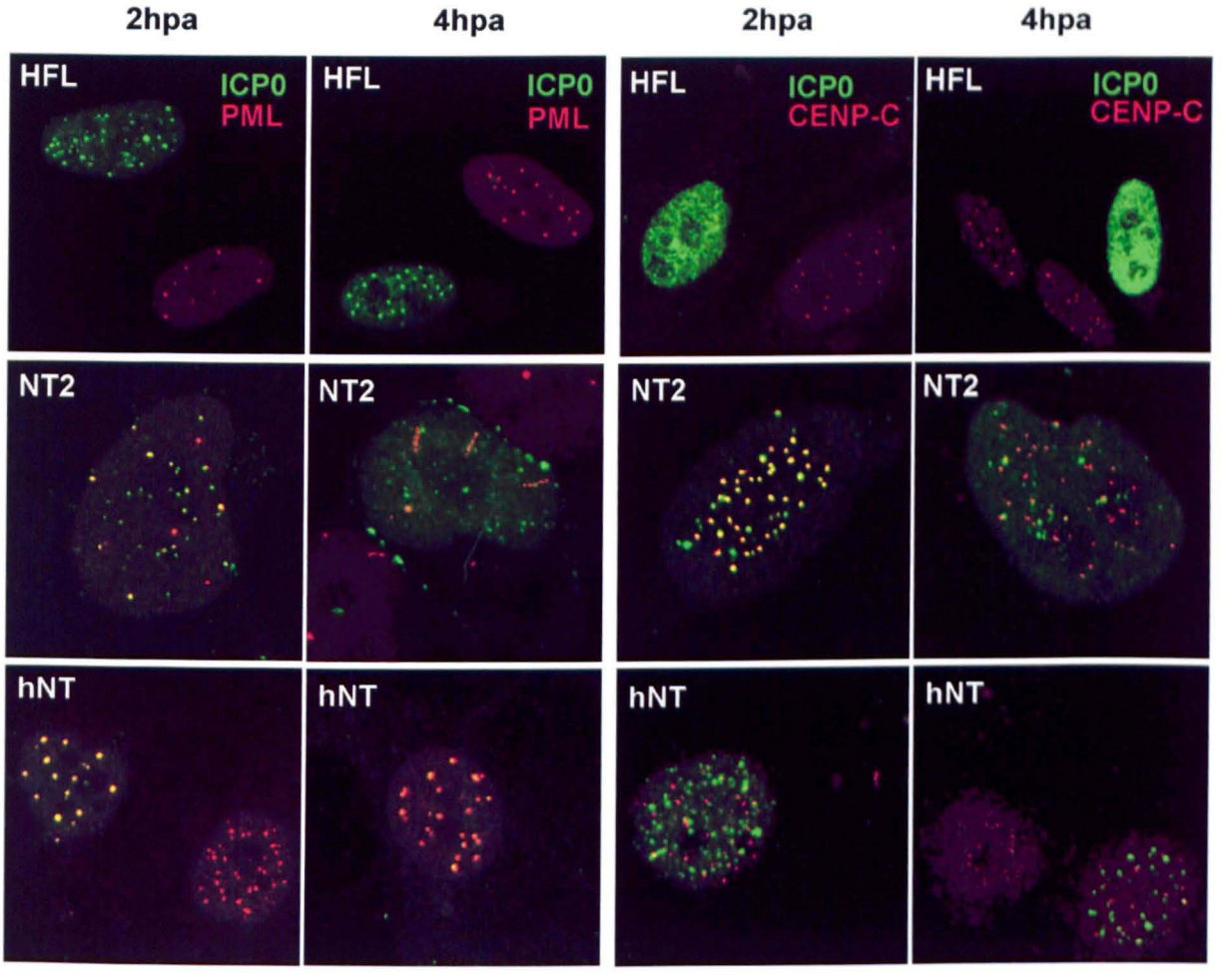

Fig. 4.10 Comparison of the stability of ND10 and centromeres in HFL, NT2 and hNT cells at 2h and 4h after the start of infection. HFL (top panels), NT2 (middle panels), and hNT (bottom panels) cells were infected with wild-type HSV stain 17+ at 1 pfu per cell. After various time of infection, cells were fixed and stained for ICP0 (MAb 11060) and PML (r8) (left-hand pairs of panels) or ICP0 and CENP-C (r554) (right-hand pairs of panels). Both ND10 and centromeres, as judged by PML and CENP-C staining, are more stable in infected NT2 and hNT than in HFL cells.

Table 4.3 Proportion of infected cells retaining ND10 proteins and CENP-C in infected HFL and NT2 cells[a]

Cell type	% of infected cells retaining:					
	PML at:		CENP-C at:		hDaxx at:	
	2h	4h	2h	4h	2h	4h
HFL	4	0	0	0	0	0
NT2	56	54	55	35	49	32

[a] Cells were infected with wild-type HSV-1 stain 17+ at 1 pfu per cell and then fixed and double-stained for ICP0 and PML, CENP-C, or hDaxx separately. The proportion of infected cells retaining punctate staining for PML, CENP-C or hDaxx was calculated after counting 300 infected cells per coverslip at the indicated times after virus adsorption.

infection (Table 4.3). Furthermore, in hNT cells, the loss of punctate ND10 protein staining induced by ICP0 was even less efficient than in NT2 cells (Fig. 4.10). It was noticed that, unlike in NT2 cells, the association of ICP0 and CENP-C was not significantly greater in differentiated hNT neurons than in HFL cells, although the effect of ICP0 on centromere structures was less efficient in hNT neurons compared to HFL cells (Fig. 4.10). These data imply, rather intriguingly, that the localization of ICP0 in NT2 and hNT cells is affected by the alterations in ND10 structure and composition, and to a certain extent mirrors that of hDaxx in uninfected examples of these cell types.

4.6.2 The transactivation ability of ICP0 in NT2 cells

ICP0 has long been known to be a promiscuous transactivator of gene expression in cells transfected with an ICP0 expression plasmid and a gene reporter cassette. A chloramphenicol acetyltransferase (CAT) enzyme reporter system was used to detect the transactivation activity of ICP0 in NT2 cells. Because HFL and hNT cells are refractory to transfection, the ability of ICP0 to activate gene expression in NT2 cells was compared with that in Vero cells (a line frequently used in the past to study the ability of ICP0 to activate gene expression). The reporter cassette used for these experiments was pSS80, which contains the promoter of the ICP6 gene that had been shown in previous studies to be efficiently activated by ICP0 in transfected cells. The amount of pSS80 used in the transfection was first optimized to give a detectable but low level of background expression. Next, cells seeded in Linbro-wells were co-transfected with pSS80 and various amounts of the ICP0 expression plasmid pCI-rtag-cICP0. Each transfection was done in duplicate, one for the CAT assay and the other one for western blot to monitor the expression of the proteins from the transfected plasmids. Transfected cells were harvested on the next day, and one fifth of the crude cell extract was processed for CAT assay, followed by thin layer chromatography (TLC). In Vero cells, the ICP6 promoter was highly transactivated by ICP0, resulting in up to 30-fold increases of CAT activity over the basal level (Fig. 4.11). The highest activation of CAT gene expression in Vero cells was detected from the cells transfected with 5-20 ng of ICP0 plasmid. In contrast, activation of expression from pSS80 by ICP0 was negligible in NT2 cells (Fig. 4.11B). It was noticed that ICP0 was less well expressed in NT2 cells compared to Vero cells transfected with the same amount of the ICP0 plasmid (Fig. 4.11C). However, 200 ng of the ICP0 plasmid in

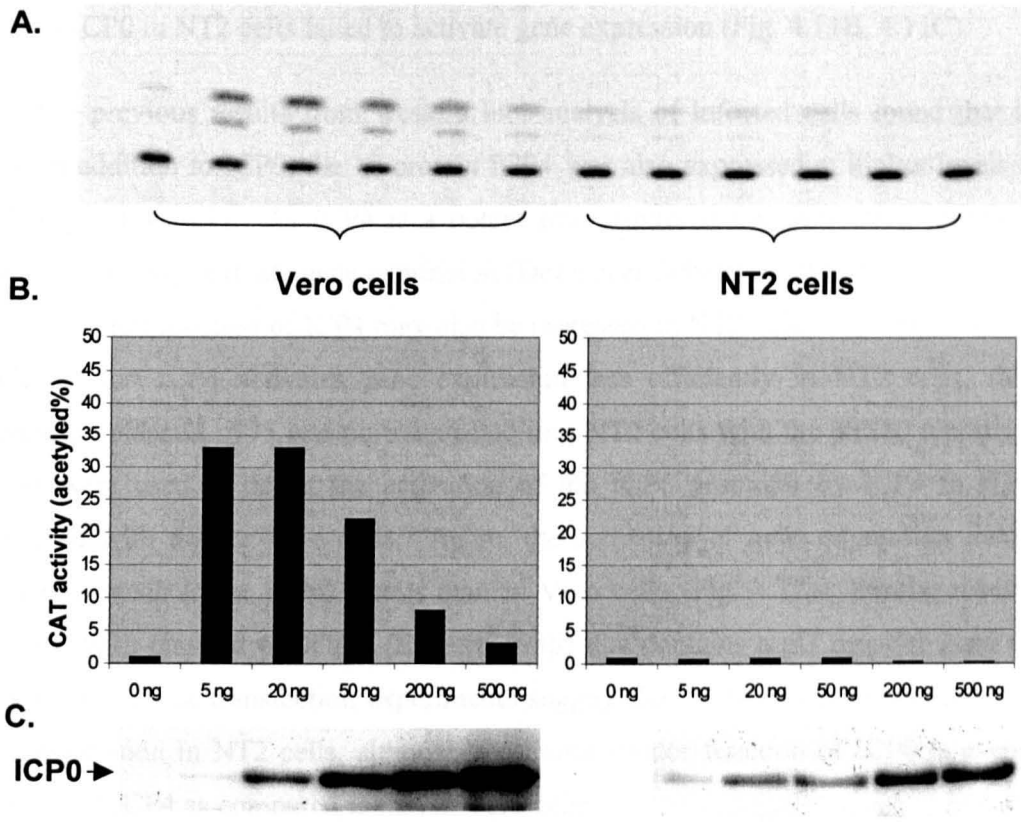

Fig. 4.11 Comparison of the transactivation of an ICP6 expression cassette by ICP0 in NT2 and Vero cells.

Cells were co-transfected with reporter plasmid pSS80 (ICP6 promoter linked to the CAT gene) and the indicated amounts of ICP0 expression plasmid pCI-rtag-cICP0 (see Materials and Methods section). The western blot analysis of total cell proteins of samples transfected in parallel with the same amount of plasmid and probed for ICP0 are shown below. The results of this single experiment were reproduced on several independent occasions.

NT2 cells gave greater expression of ICP0 than 20 ng of the plasmid in Vero cells, yet this level of ICP0 in NT2 cells failed to activate gene expression (Fig. 4.11B, 4.11C).

The previous results from western blot analysis of infected cells found that in NT2 cells, in addition to ICP0, the IE protein ICP4 was also expressed at higher levels than in HFL cells (Fig. 4.7). As ICP4 is a potent transcriptional transactivating protein that is essential for early and late gene expression (DeLuca & Schaffer, 1985), this implies that the transactivation function of ICP4 may also be repressed in NT2 cells. To obtain more direct evidence that ICP4 activates gene expression less efficiently in NT2 cells, the ICP4 expression plasmid p175 was co-transfected into NT2 cells with the pSS80 reporter. CAT assays were used to detect the activation of the ICP6 promoter by ICP4 in NT2 cells compared with that in Vero cells. Again, the activation of gene expression induced by ICP4 was much lower in NT2 cells than in Vero cells (Fig. 4.12). Similar results were obtained with plasmid pgDCAT (Everett, 1986) that contains a gD reporter gene cassette (Fig. 4.13). These transfection experiments suggest that ICP4 is a poor activator of Early gene expression in NT2 cells, although the transactivator function of ICP0 is even worse than that of ICP4 as compared to that in Vero cells.

4.6.3 The establishment of a quiescent infection in NT2 and hNT cells

During latency, the HSV-1 viral genome resides in neuronal cell nuclei in a transcriptionally quiescent form, and ICP0 can influence the balance between lytic infection and latency (Cai *et al.*, 1993, Clements & Stow, 1989, Preston, 2000). Previous studies showed that, at a lower MOI, a virus deficient for ICP0, ICP4 and VP16 could establish and maintain a quiescent infection in human fibroblast cells and the quiescent viral genomes can be reactivated by exogenously expressed ICP0 (Harris *et al.*, 1989, Samaniego *et al.*, 1998). The poor growth of both wild type and ICP0 mutant viruses in NT2 cells and the inefficient activity of ICP0 in NT2 cells imply that a quiescent infection might be established in these cells. To test this possibility, NT2 and hNT cells were infected with *dl*1403/LacZ, a relatively viable virus carrying an ICP0 deletion and a lac Z gene driven by the HCMV promoter. This virus retains fully functional ICP4 and VP16. After infection at an MOI of 0.02 (based on the titre in BHK cells) for 2 days at 37°C, the infected cells were directly stained for β-galactosidase. A long incubation length of two days allows the virus to replicate and to form plaques if efficient infection occurs.

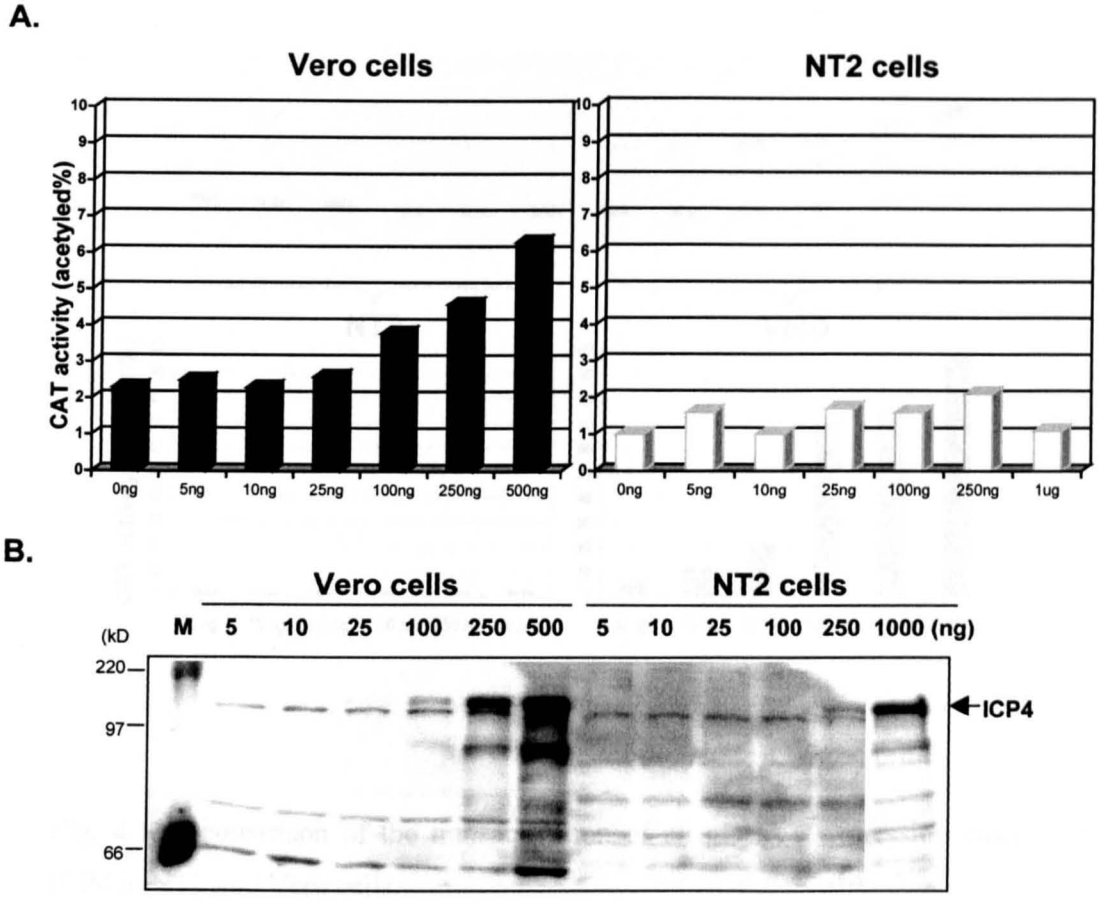

Fig. 4.12 Comparison of the transactivation of an ICP6 expression cassette by ICP4 in NT2 and Vero cells.

Cells were co-transfected with reporter plasmid pSS80 (ICP6 promoter linked to the CAT gene) and the indicated amounts of ICP4 expression plasmid p175 (see Materials and Methods section). The western blot analysis of total cell proteins of samples transfected in parallel with the same amount of plasmid and probed for ICP4 are shown below. The results of this single experiment were reproduced on two independent occasions.

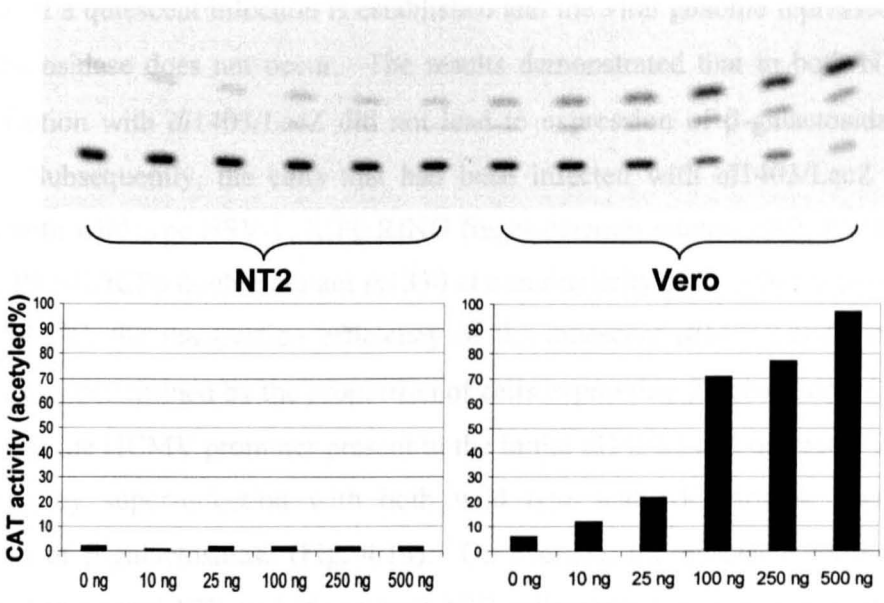

Fig. 4.13 Comparison of the transactivation of an gDCAT expression cassette by ICP4 in NT2 and Vero cells.

Cells were co-transfected with reporter plasmid pgDCAT (glycoprotein D promoter linked to the CAT gene) and the indicated amounts of ICP4 expression plasmid p175 (see Materials and Methods section). The results of this single experiment were reproduced on two independent occasions.

However, if a quiescent infection is established and the viral genome repressed, expression of β-galactosidase does not occur. The results demonstrated that in both NT2 and hNT cells, infection with *dl*1403/LacZ did not lead to expression of β-galactosidase (data not shown). Subsequently, the cells that had been infected with *dl*1403/LacZ were super-infected with wild type HSV-1, ICP0 RING finger deletion mutant FXE, ICP4 mutant *ts*K, or the ICP4 *ts*K/ICP0 double mutant *in*1330 at a multiplicity of 3. After super-infection for 8 hr at 38.5°C, the reactivation efficiency of the quiescent *dl*1403/LacZ virus into lytic infection was determined by the proportion of cells expressing β-galactosidase. The results showed that the HCMV promoter present in the initial dl1403/LacZ quiescent infection was reactivated by super-infection with both wild type and *ts*K viruses, resulting in the expression of β-galactosidase (Fig. 4.14). On average, the quiescent viral genome was reactivated in around 17% and 8% of total NT2 cells super-infected with wild-type HSV-1 and *ts*K virus, respectively (Table 4.4). As the ICP0-deficient viruses FXE and *in*1330 were unable to reactivate the quiescent virus efficiently, these data suggest that as in other cultured cell systems that study HSV-1 quiescence, ICP0 is required for this effect. This experiment was also carried out in hNT cells, the only difference being that the super-infection length was increased to 16 hours due to the relatively poor growth of 17+ in these cells (Fig. 4.14, Table 4.4). As with NT2 cells, ICP0 was found to be an essential factor involved in the reactivation of quiescent infection in hNT cells (Fig. 4.14). Reactivation of the HCMV promoter by wild type 17+ was inhibited by addition of the proteasome inhibitor MG132, demonstrating that, as in a previous study (Everett *et al.*, 1998b), this reactivation activity of ICP0 requires active proteasomes (Fig. 4.14).

Fig. 4.14 Establishment of quiescently infected NT2 and hNT cells using an ICP0-deficient virus and reactivation by superinfecting ICP0-positive virus.

Cells were infected as described in the text (section 4.6.3). NT2 (upper field) and hNT (lower field) cells were initially infected with *dl*1403/lacZ virus and then superinfected with HSV-1 strain 17+ (A), *ts*k (B), FXE (C), *in*1330 (D), 17+ in the presence of MG132 (E), or else were mock infected (F). NT2 and hNT cells were fixed 8 and 16 h post-infection, respectively, and stained for β-galactosidase expression by immunofluorescence.

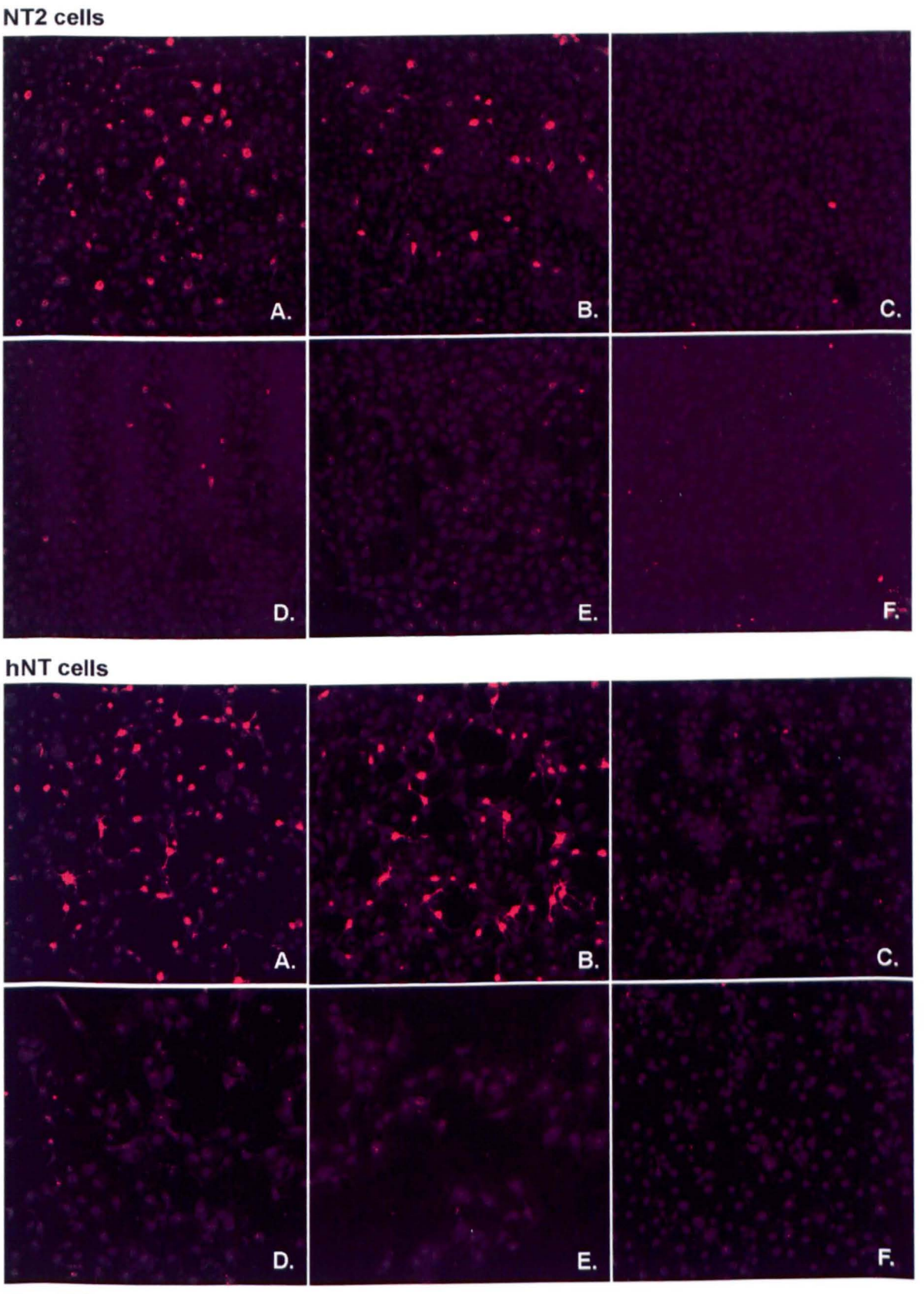

Fig. 4.14

Table 4.4 The reactivation of the HCMV promoter in quiescently infected NT2 and hNT cells

virus[a]	reactivation%	
	NT2	hNT
17+	17	24
tsK	8	21
FXE	0	0
in1330	0	0
mock	0	0

[a] Cells were infected with *dl*1403 virus for 2 days then were super-infected by 17+, *ts*K, FXE, *in*1330 at 3 pfu per cell for 8 hours, or 16 hours for hNT cells. The reactivation efficiency was determined by counting the proportion of cells expressing β-galactosidase. On average, a total number of 200 cells were scored for each data point.

4.7 Discussion

NT2 cells, from a neuronal precursor cell line, were chosen for these studies because of their human origin, *in vitro* inducible neuron differentiation, and suitability for transfection studies. These properties are suitable for studying HSV-1 infection, the functions of specific genes of interest, and the behaviour of ND10 proteins in terms of their interactions with viral proteins in a human neuronal cell context.

The results illustrated that NT2 neuron precursor cells contain atypical ND10 structures with fewer PML and hDaxx foci, and no detectable Sp100. In addition, the distribution of these ND10 constituents was distinct from any other types of cells studied, for instance, the extraordinary track structures of PML foci, and large Daxx accumulations observed in many NT2 cells. During HSV-1 infection in NT2 cells, the ND10 components and centromere protein CENP-C were more resistant to the actions of ICP0, compared to HFL cells. Furthermore, at early times of infection, ICP0 strongly colocalised with ND10 in most cell lines, however it was noticed that in NT2 cells, a greater portion of ICP0 was located in additional specific small foci that did not contain PML (Fig. 4.8). Co-staining with CENP-C revealed that these small foci were likely to be centromeres because ICP0 strongly associated with CENP-C in infected NT2 cells. Therefore centromere structures could be a preferential site for ICP0 localisation in NT2 cells due to the alterations in ND10 composition.

On differentiation of NT2 cells into hNT neurons a typical ND10 structure was developed, despite the retention in some cells of the remarkable track structure of PML foci detected in many hNT cells. In addition, Sp100 was perfectly colocalised with PML in these peculiar structures in hNT cells (Fig. 4.2A). In western blot analysis of viral gene expression, ICP0 was highly expressed in NT2 and hNT cells, but the infection did not progress efficiently to abundant Early gene expression. This directed further study toward the function of ICP0 in these cells.

Results using a CAT assay showed that, even at a high expression level, ICP0 was unable to activate early gene promoters in NT2 cells. Although lower expression of ICP0 and ICP4 was noticed during transfections of plasmids expressing these proteins, these results can not be explained by poor transfection of NT2 cells, since similar HCMV

enhancer-driven plasmids expressing PML and SUMO-1 gave at least 30% positive transfected NT2 cells as estimated by IFA (Fig. 4.15A), and similar amounts of these proteins were expressed in transfected NT2 cells compared to Vero cells, as detected by western blotting (Fig. 4.15B).

In infection of NT2 and hNT cells with *dl*1403/lacZ virus at a low MOI, the HCMV promoter was shut down but it can be reactivated by super-infection with wild type and *ts*K virus. Analysis of reactivation efficiency between 17+ and *ts*K revealed that reactivation by *ts*K virus was slightly less efficient than wild type at 38.5°C (Table 4.4). In other experimental systems of HSV-1 quiescence in cultured cells, *ts*K was as efficient as wild type virus at inducing reactivation (Russell *et al.*, 1987) so it appears that in NT2 cells ICP4 also contributes to (but is insufficient for) the reactivation process. However, results from CAT assays showed that the activation of the ICP6 promoter by ICP4 was less in NT2 cells than in Vero cells. These results suggest that, in addition to very poor function of ICP0, ICP4 also plays a part in the inefficient HSV-1 infection in neuronally-related cells.

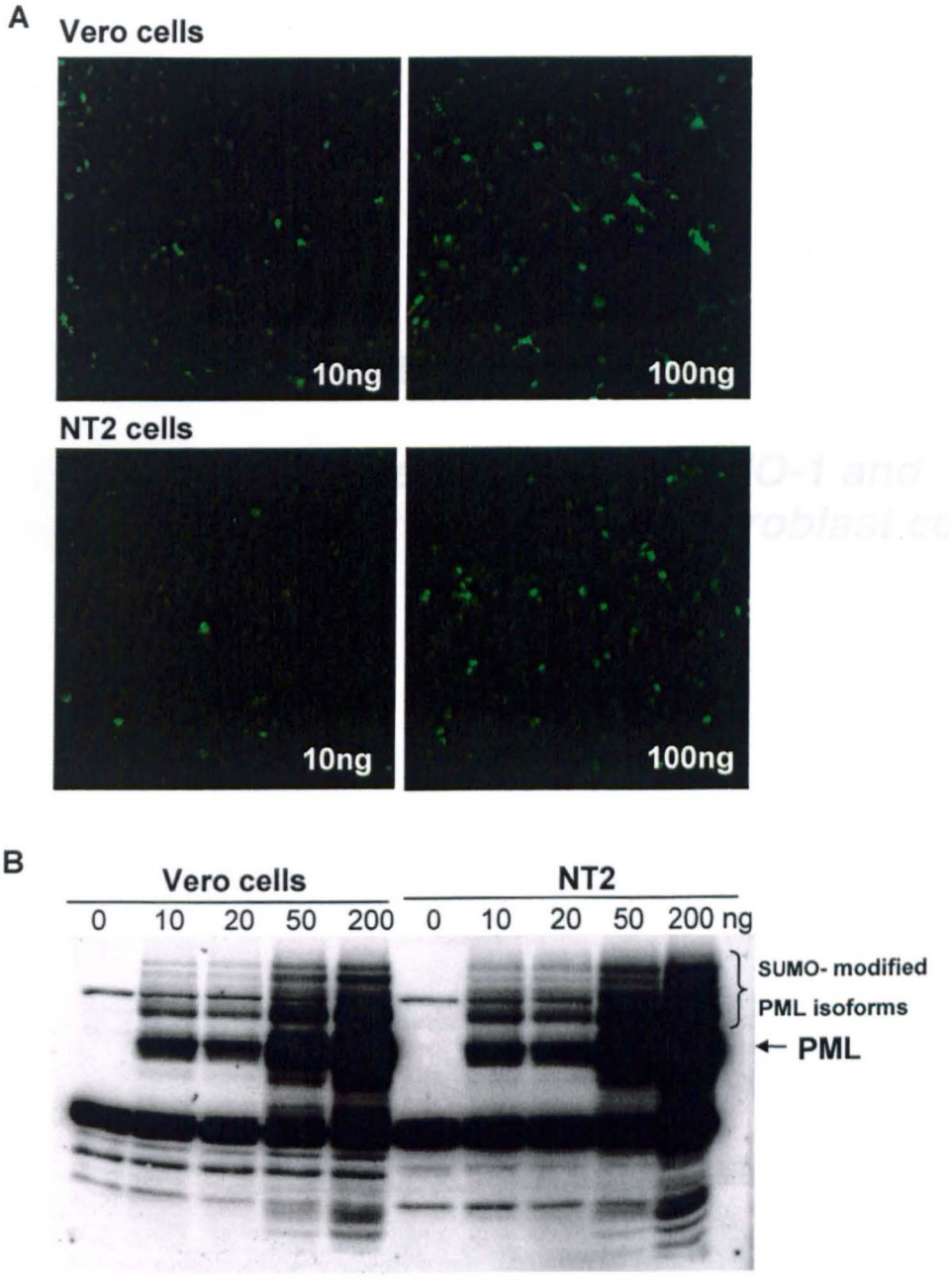

Fig. 4.15 Analysis of the transfection efficiency in NT2 cells compared with Vero cells.

A. Vero (top panel) and NT2 (bottom panel) were transfected with plasmid pCIPIC-1 at a concentration 10ng/Linbro-well or 100ng/Linbro-well followed by immunostaining for SUMO-1.

B. Expression level of PML in Vero and NT2 cells transfected by various amounts, as labeled on the top of the gel, of plasmid PML(F).

RESULTS AND DISCUSSIONS

Chapter 5 Characterisation of SUMO-1 and its conjugation mutants in NT2 and fibroblast cells

Chapter 5 Characterisation of SUMO-1 and its conjugation mutants in NT2 and fibroblast cells

The results from Chapter 3 showed that ND10 proteins have potential effects on viral infection, since initiation of HSV-1 infection was slightly reduced in transfected cells expressing high levels of PML and SUMO-1 compared to those in untransfected cells (section 3.3.2). The immunofluorescence analysis described in Chapter 4 revealed that NT2 cells lack detectable Sp100 and express lower amounts of PML and its SUMO-1 modified isoforms than HFL cells. These observations led me to investigate whether transfection of plasmids expressing ND10 and SUMO-1 proteins into NT2 neuron precursor cells could lead to the development of expression patterns of ND10 proteins closer to those observed in HFL cells, and whether increased expression of ND10 proteins in NT2 cells has any effect on HSV-1 infection.

5.1 High level expression of SUMO-1, but not other ND10 proteins, reduces HSV-1 infection in NT2 cells

5.1.1 The expression pattern of PML in transfected NT2 cells

Firstly, NT2 cells were transfected with a plasmid expressing PML and examined by IFA to investigate whether exogenous PML introduced by transient transfection could lead to the development of ND10 of normal appearance. It was found that the expression patterns and distributions of PML in transfected cells were varied. Compared to endogenous PML (Fig. 5.1A), in some transfected cells, in which PML was moderately expressed, the size of PML foci was enlarged (Fig. 5.1B). Moreover, an increase in the size and number of ND10 structures to the levels similar to those in Hep-2 or BHK cells was observed in some transfected NT2 cells expressing high levels of PML (Fig. 5.1C). This implies that the exogenous PML was recruited into ND10 resulting in ND10 structures that were apparently more typical of those in fibroblast cells. However, it was noticed that in a portion of transfected cells, overexpressed PML was located throughout the nucleus and cytoplasm (Fig. 5.1D).

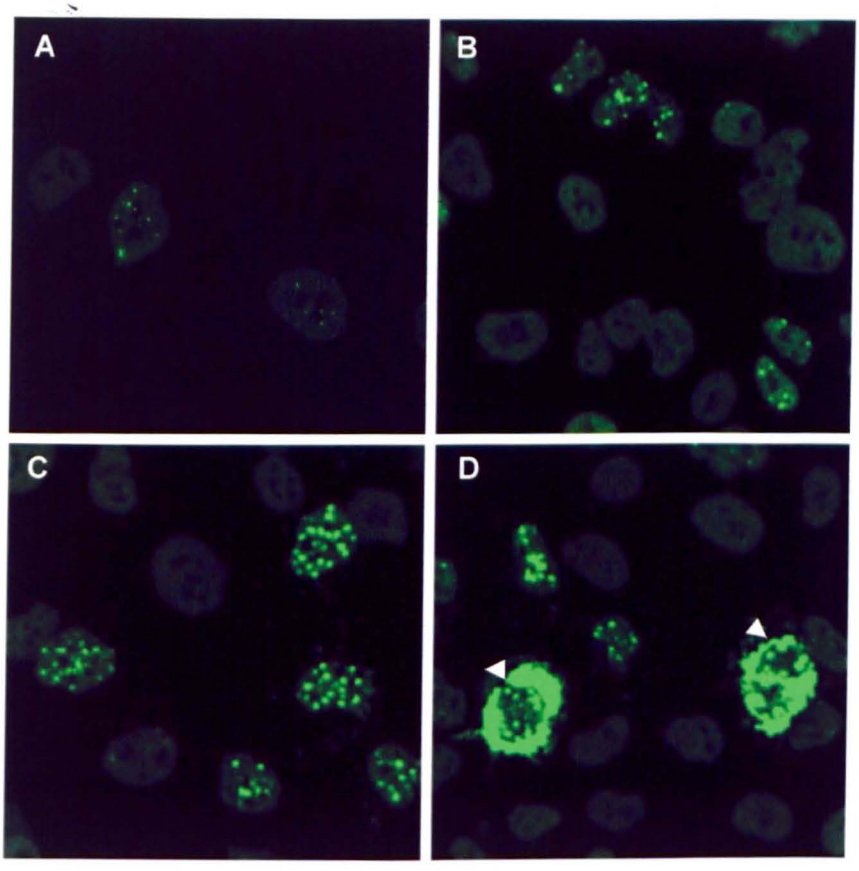

Fig. 5.1 High level expression of PML in transfected NT2 cells.

NT2 cells were transfected and the expression of exogenous PML was detected using a monoclonal antibody F3.

A. The expression pattern of endogenous PML detected by using rabbit serum r8.

B. The sizes of the foci of exogenous PML were bigger than those of endogenous PML.

C. High expression levels of exogenous PML greatly increased the average number of PML foci, and their sizes were much larger than those of endogenous PML.

D. Some transfected cells (indicated by an arrow head) expressed very high levels of PML, and in these cases the protein was located in both nucleus and cytoplasm.

5.1.2 The effect of over-expression of ND10 on HSV-1 infection in NT2 cells

The methods used for this study were the same as described in section 3.3.2; plasmids expressing PML, Sp100, and SUMO-1 were singly transfected into NT2 cells via lipofection followed by infection with HSV-1 at 1 pfu per cell. Since progression of HSV-1 infection in NT2 cells is not efficient, only the IE protein ICP0 was detected to estimate the infection efficiency in transfected NT2 cells compared to untransfected cells. Immunofluorescent results showed that most SUMO-1 transfected cells (detected by green fluorescence) did not express ICP0 (red fluorescence) (Fig. 5.2). At 2 hpa, 16% of untransfected cells were infected, whereas only 7% of the transfected cells were expressing ICP0 (Fig. 5.2B). The reduction of initiation of HSV-1 infection was not overcome by increasing the time of infection, since at 8 hpa more than 50% of untransfected cells were infected, whereas only 13% of SUMO-1 transfected cells expressed ICP0 (Fig. 5.2B). This reduction of infection was not observed in NT2 cells transfected by PML or Sp100 plasmids (data not shown).

5.2 Construction of SUMO-1 conjugation mutants

SUMO-1, like ubiquitin, can be covalently linked to other proteins to alter their behaviour and function (reviewed by Saitoh *et al.*, 1997). However the SUMO-1 translation product has to be cleaved endoproteolytically to expose Gly97, the mature C-terminus, which is critical for SUMO-1 to be conjugated to protein substrates (Kamitani *et al.*, 1997). Since it was found that high levels of SUMO-1 caused modest but reproducible reductions in viral gene expression in BHK and NT2 cells (results from sections 3.3B and 5.1), three SUMO-1 mutants that would be expected to be defective for conjugation were made to investigate the potential role of SUMO-1 in virus infection in more detail. As described previously, SUMO-1 requires processing to remove four amino acid residues (His98-Ser-Thr-Val) from its C-terminus before it can undergo conjugation, and the Gly96-Gly97 residues are essential for the action of the protease that cleaves between Gly97 and His98 (Fig. 5.3A). For construction of the various SUMO-1 mutants, initially, one forward primer and four reverse primers were designed to amplify wild type (GG/HSTV), and three conjugation mutants in which the Gly96-Gly97 were either changed to Gly-Ala (GA-HSTV), or Ala-Gly (AG-HSTV), and with deletion of the most C-terminal four amino acids (AG) (Fig. 5.3B). The forward primer was designed to

A.

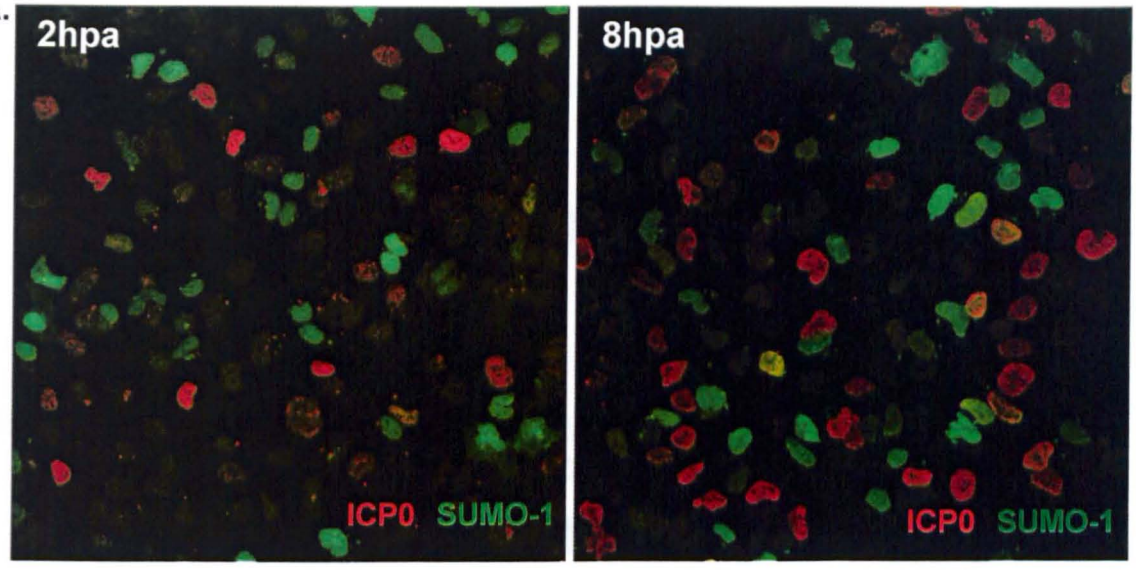

B.

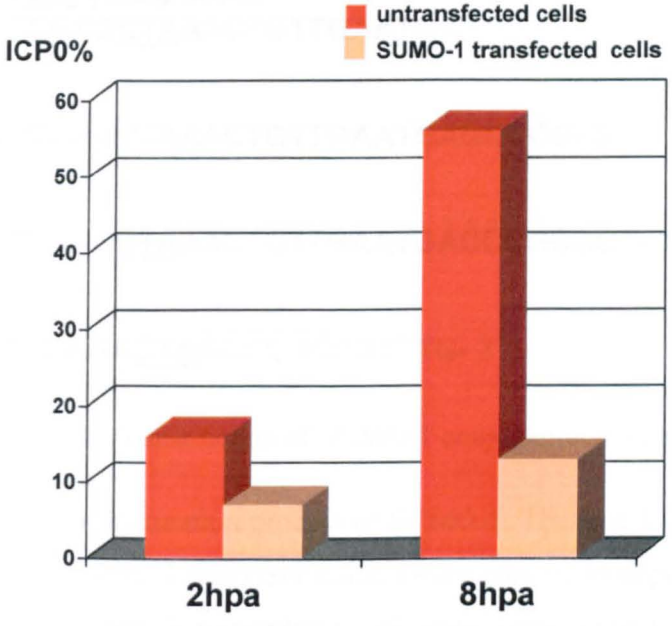

Fig. 5.2 Effect of SUMO-1 on HSV-1 infection in NT2 cells.

NT2 cells were transfected with plasmids expressing SUMO-1 followed by infection by HSV-1 on the next day. The transfected, infected NT2 cells were then fixed and immuno-stained after 2 and 8 hours of infection and examined by confocal microscopy, followed by statistical analysis.

A. Images from IFA showing that most of the transfected cells expressing SUMO-1 were not infected by HSV-1.

B. The proportion of cells expressing ICP0 in untransfected cells are shown as ■, and the proportion of SUMO-1 transfected cells expressing ICP0 are shown as ■.

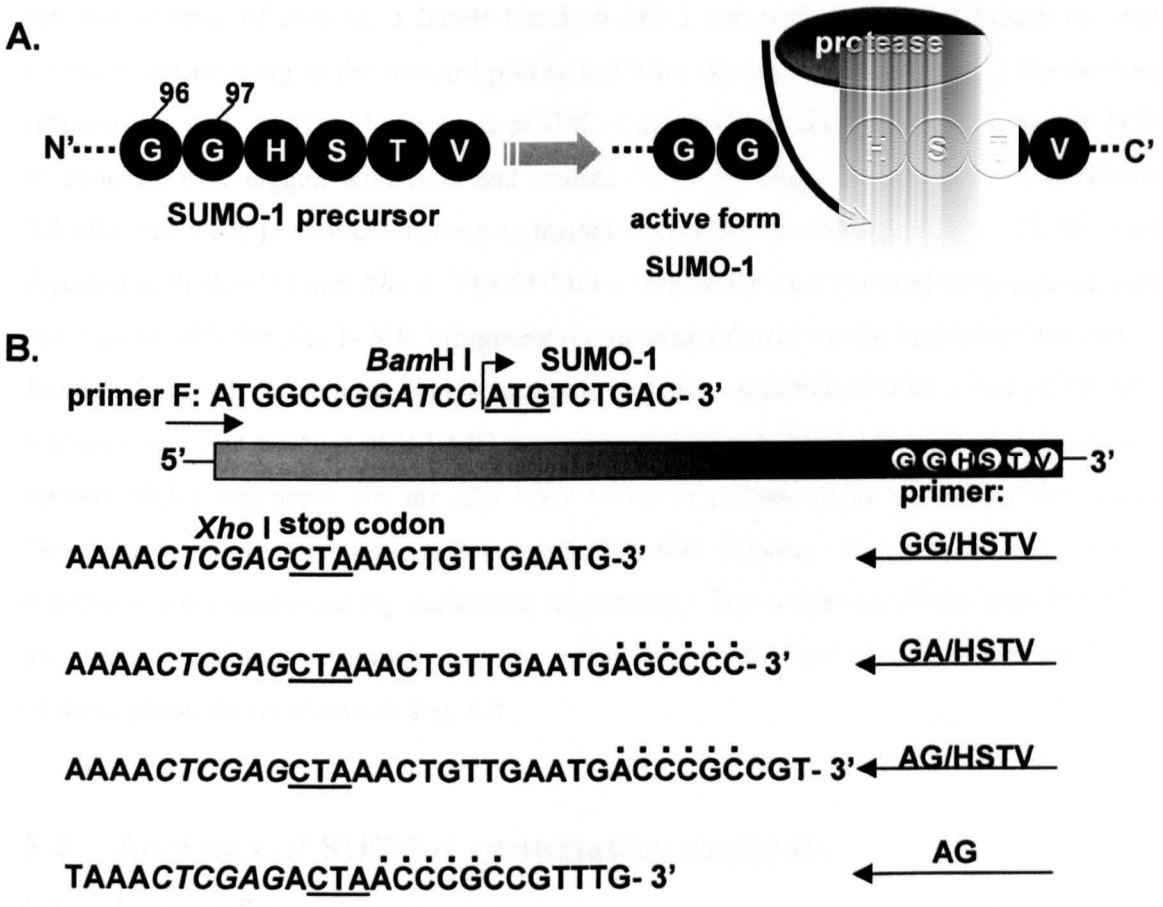

Fig. 5.3 Strategy for construction of SUMO-1 conjugation mutants.

A. The C-terminal maturation process of SUMO-1. The four C-terminal amino acids H-S-T-V in the SUMO-1 precursor molecule are cleaved to expose Gly96-Gly97, the mature C-terminus which is essential for SUMO-1 conjugation to substrates.

B. Five primers were designed for construction of SUMO-1 conjugation mutants. Primer F is a universal forward primer for all mutants and reverse primers GG/HSTV, GA/HSTV and AG/HSTV were designed to generate wild type SUMO-1 and two mutants in which the conserved Gly-Gly has been changed either to Gly-Ala or Ala-Gly respectively. The other primer AG was designed for the construction of the Ala-Gly mutant without the 4 amino acid extension. For the convenience of cloning, two restriction enzyme sites, *Bam*H I and *Xho* I were introduced in the forward and reverse primers respectively.

include the myc epitope tag present in SUMO-1 expressed from plasmid pCIPIC1, and for the convenience of cloning, a *Bam*H I and an *Xho* I site were introduced before the start codon of the myc tag in the forward primer and after the stop codon in the reverse primers respectively (Fig. 5.3B). The original pCIPIC-1 plasmid was used as the template for PCR to generate myc-tagged wild type and mutant SUMO-1 fragments (described in section 2.2.6B) that were phenol/chloroform extracted (described in section 2.2.6B, 2.2.1B) then digested with *Bam*H I and *Xho* I. The SUMO-1 fragments were purified from agarose gels and ligated with the *Xho* I- *Nde* I fragment (containing pCIneo vector backbone) and *Nde* I-*Bam*H I fragment (containing c-myc tag) obtained from plasmid pCIPIC-1 and pCISUMO respectively. The plasmid pCISUMO was generated by subcloning the *Sal* I/*Not* I digested myc-SUMO-1 fragments into the *Xho* I/*Not* I sites of pCIneo vector to destroy the unique *Xho* I site in the vector for the convenience of further cloning. The structures of the four constructs were confirmed by nucleotide sequencing. The sequences of the myc-SUMO-1 loci at the 5' end and the sequences of the substitution or deletion mutated loci in the 3' end of these plasmids are shown in Fig. 5.4.

5.3 Analysis of SUMO-1 conjugation mutants

5.3.1 Immunofluorescence assay

Firstly, an indirect immunofluorescence analysis was used to confirm the expression and investigate the localisation of the SUMO-1 mutant proteins in mammalian cells. Vero cells were transfected with plasmids expressing either wild type or mutant myc-tagged SUMO-1 proteins and were stained with monoclonal antibody 9E10 that recognises the c-myc sequence 24 hours after transfection. As expected, plasmid GG/HSTV expressed wild type SUMO-1, which was concentrated in ND10 and also distributed throughout the nucleus (Fig. 5.5A). When the conserved Gly-Gly residues were changed to Gly-Ala, SUMO-1 lost its ND10 localisation and only relatively diffuse nucleoplasmic staining was observed (Fig. 5.5B). In contrast, the AG/HSTV mutant protein was distributed in a similar pattern to wild type SUMO-1, but in some cells the mutant SUMO-1 was also present in the cytoplasm (Fig. 5.5C). The staining of SUMO-1 expressed by the mutant plasmid AG, from which the C-terminal four amino acids had been deleted and Gly96 substituted with alanine, was similar to AG/HSTV, but large SUMO-1 clumps were observed in the nucleus

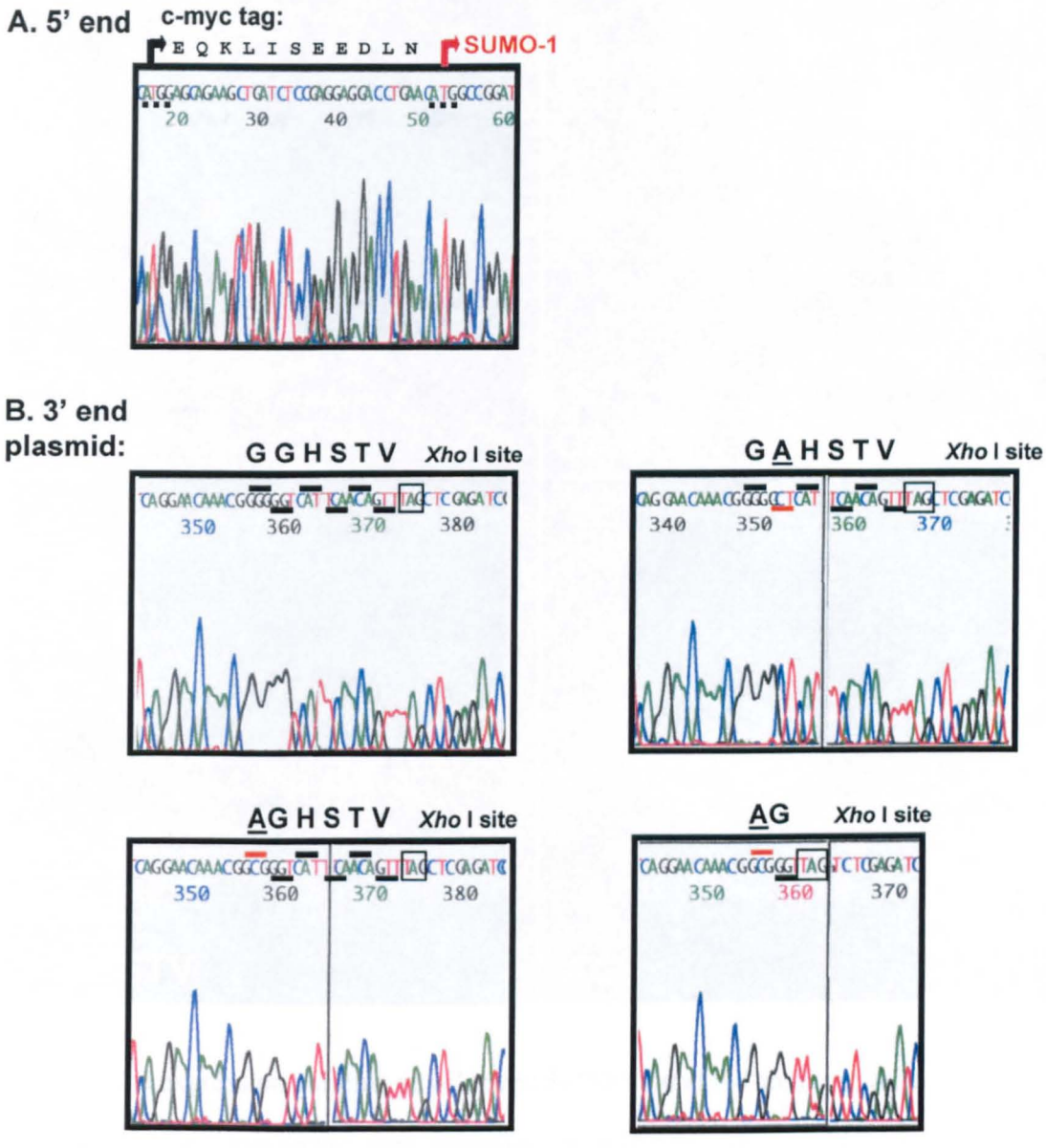

Fig. 5.4 Sequences of wild type SUMO-1 and the conjugation mutant constructs.

A. The forward sequences of the c-myc tag and 5'-end of SUMO-1. The 5'-end sequences were the same for all the SUMO-1 constructs. The start codons of c-myc and SUMO-1 are marked as ▪▪▪.

B. The forward sequences of the 3' end in four SUMO-1 constructs. Nucleotides encoding amino acids GGHSTV, marked as ▬, were present as the sequences in wild type SUMO-1. The nucleotides encoding for Gly-Gly, changed to either Gly-Ala or Ala-Gly in the mutants, are marked as ▬ and the stop codon is shown as ▭.

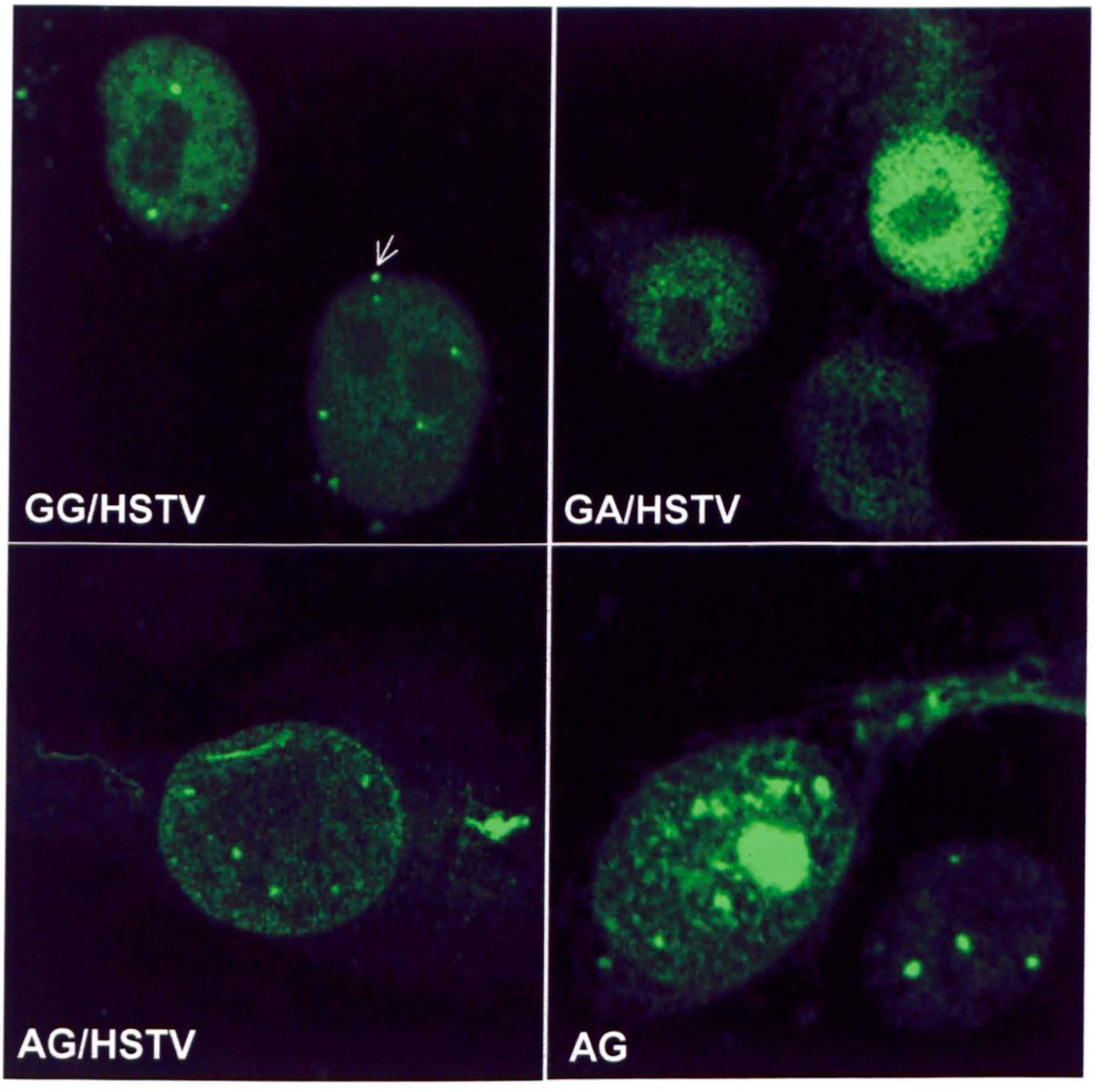

Fig. 5.5 The expression patterns of wild type SUMO-1 and the conjugation mutants.

Vero cells were transfected with plasmids expressing wild type SUMO-1 and with conjugation mutant plasmids as labelled in the lower left corner of each image. Images were obtained by staining transfected cells using a monoclonal antibody 9E10 against c-myc tagged SUMO-1. Most SUMO-1 expressed from the wild type construct GG/HSTV was located in nucleus and also accumulated in ND10 indicated by an arrow sign. SUMO-1 expressed from the GA/HSTV plasmid did not localise at ND10. Some but not all cells expressing the AG/HSTV and AG mutant proteins contained SUMO-1 in ND10-like structures.

of some transfected cells (Fig. 5.5D). Furthermore, in a small portion of AG plasmid transfected cells, the staining of the mutant SUMO-1 included a string-like pattern in the cytoplasm, very similar to cytoskeleton protein staining (Fig. 5.6A). To investigate this further, cells transfected with AG plasmid were co-stained with a rabbit antibody A14 for the myc tag and a mouse antibody for either actin or tubulin, followed by IFA. However the string staining of actin and tubulin was more slender than SUMO-1 and without significant co-localisation with SUMO-1 (Fig. 5.6B and data not shown).

5.3.2 Western blot analysis

Like the ubiquitin system, SUMO-1 can be covalently attached to target proteins by a similar but distinct enzymatic machinery. In an attempt to understand the consequences of the mutations introduced into SUMO-1, cell extracts from cells transfected with these SUMO-1 plasmids were processed for western blotting by using an antibody against the myc tag. Intriguingly, Gly97 is absolutely essential for the action of the C-terminal protease, since when Gly97 was replaced by Ala, only the SUMO-1 precursor form, without any active form, was detected in cells transfected by GA/HSTV plasmids (Fig. 5.7). Similar to the case of wild type SUMO-1, most SUMO-1 precursor proteins expressed from the Gly96 substitution mutant plasmid (AG/HSTV) was cleaved and exhibited a decreased gel mobility (the lower band) from that of the precursor SUMO-1 (the upper band) in 12.5% SDS-PAGE (Fig. 5.7). As expected, only the cleaved form of SUMO-1 was obtained in the deletion mutant SUMO-1 construct (Fig. 5.7). However the high molecular weight SUMO-1 conjugation proteins produced by the three different SUMO-1 mutant constructs were at a lower prevalence than those produced in wild type SUMO-1 expressing cells, although similar amounts of the active form of SUMO-1 was expressed by the AG/HSTV construct (Fig. 5.7).

5.3.3 Interaction of SUMO-1 mutant proteins with ND10

As described previously, two ND10 proteins, PML and Sp100 can be post-translationally modified by SUMO-1 (reviewed by Sternsdorf *et al.*, 1997) and SUMO-1 modification of PML has been suggested to target this protein to ND10 (Muller *et al.*, 1998a). In addition, it has been reported that recruitment of hDaxx, another ND10 constituent, is controlled by SUMO-1 modification of PML (Ishov *et al.*, 1999). The

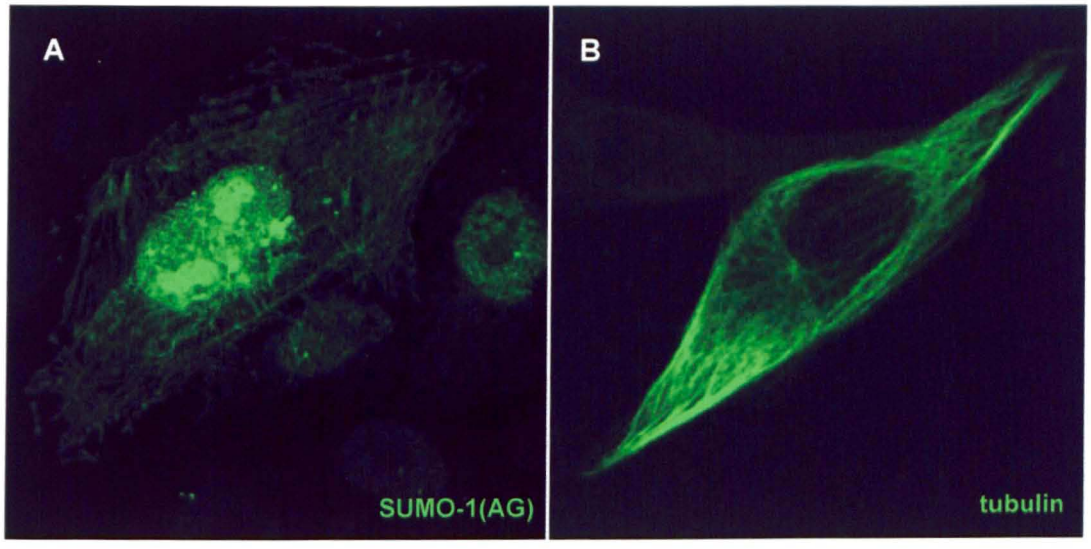

Fig. 5.6 Comparison of the expression pattern of mutant SUMO-l expressed from the AG construct with the staining of tubulin.

A. The string-like distribution of AG mutant SUMO-1.

B. The staining of tubulin. The expression pattern of AG mutant SUMO-1 was different from that of tubulin.

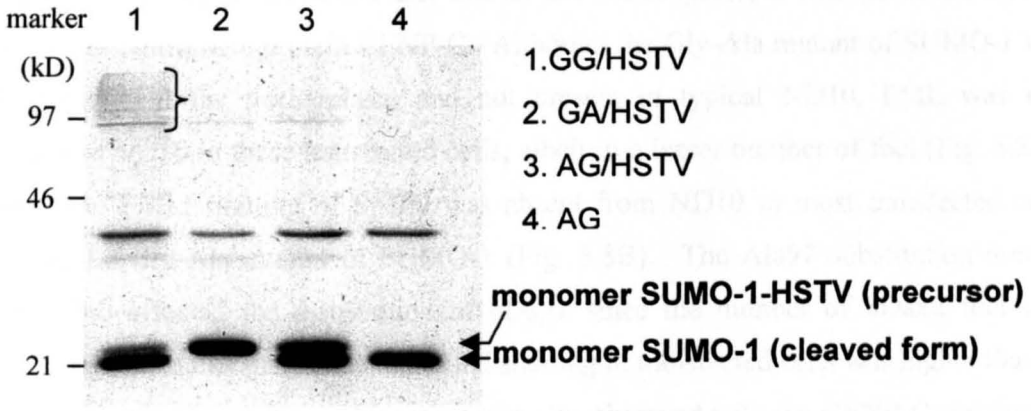

Fig. 5.7 Western blot analysis of SUMO-1 expression.

Vero cells, transfected with different SUMO-1 constructs as labelled at the top of the blot, were directly lysed in 3x boiling mixture then process for SDS-PAGE followed by blotting for c-myc-SUMO-1.

Most wild type SUMO-1 protein molecules expressed from plasmid GG/HSTV were cleaved to generate the active form of SUMO-1, while the percentage of cleaved AG/HSTV molecules was reduced. None of the Gly97 mutant SUMO-1 was processed to the mature cleaved form. The amount of SUMO-1 conjugated to other high molecular weight proteins (as indicated as }) was much greater with wild type SUMO-1 compared to the three mutant forms.

question whether high level expression of the SUMO-1 conjugation mutant proteins affects ND10 assembly and maintenance was tested by co-staining SUMO-1 transfected cells with antibodies for the tagged SUMO-1 and one of the ND10 proteins such as PML, Sp100, hDaxx, or the centromere protein CENP-C. Although the Gly-Ala mutant of SUMO-1 was diffuse throughout the nucleoplasm and not present in typical ND10, PML was still maintained in ND10 in these transfected cells, albeit in a lesser number of foci (Fig. 5.8A). In contrast to PML, staining of Sp100 was absent from ND10 in most transfected cells expressing the Gly-Ala mutant of SUMO-1 (Fig. 5.8B). The Ala97 substitution mutant SUMO-1 also affected the distribution of hDaxx since the number of hDaxx foci was decreased and the nucleoplasmic background staining in transfected cells was higher than in untransfected cells (Fig. 5.8C). This effect was also observed with the CENP-C staining of such transfected cells, a rather surprising result of unknown significance (Fig. 5.8D). SUMO-1, expressed from the AG/HSTV plasmid, had a staining pattern more typical of wild type SUMO-1, however fewer PML and hDaxx foci were detected in transfected cells (Fig. 5.9A, 5.9C). In those cells in which the exogenous SUMO-1 distribution was diffuse, the staining of Sp100 was also dispersed in many cases (Fig. 5.9B). In contrast to its apparent affects on ND10, there was no significant effect of the Ala-Gly mutant SUMO-1 on the centromere protein CENP-C (Fig. 5.9D). Similar results were obtained from the transfected cells expressing mutant SUMO-1 with the Ala96 substitution and the 4 amino acid C-terminal extension deletion (Fig. 5.10).

5.4 The effects of SUMO-1 mutants on HSV-1 infection in NT2 cells

The results from section 5.1 showed that NT2 cells expressing high levels of exogenous SUMO-1 were apparently less susceptible to HSV-1 infection compared to untransfected cells. If high levels of SUMO-1 in some way impedes HSV-1 gene expression, one might predict that the three SUMO-1 mutants, which lost or had less conjugation ability, would not confer this phenotype. To investigate this prediction, the four SUMO-1 plasmid constructs (GG/HSTV, GA/HSTV, AG/HSTV, and AG) were individually transfected into NT2 cells for 24 hours, and then the expression levels of SUMO-1 and ICP0 were determined by IFA after a 8-hour infection (using the same method as described in section 3.3.2 and 5.1). In wild type SUMO-1 transfected cells, up to

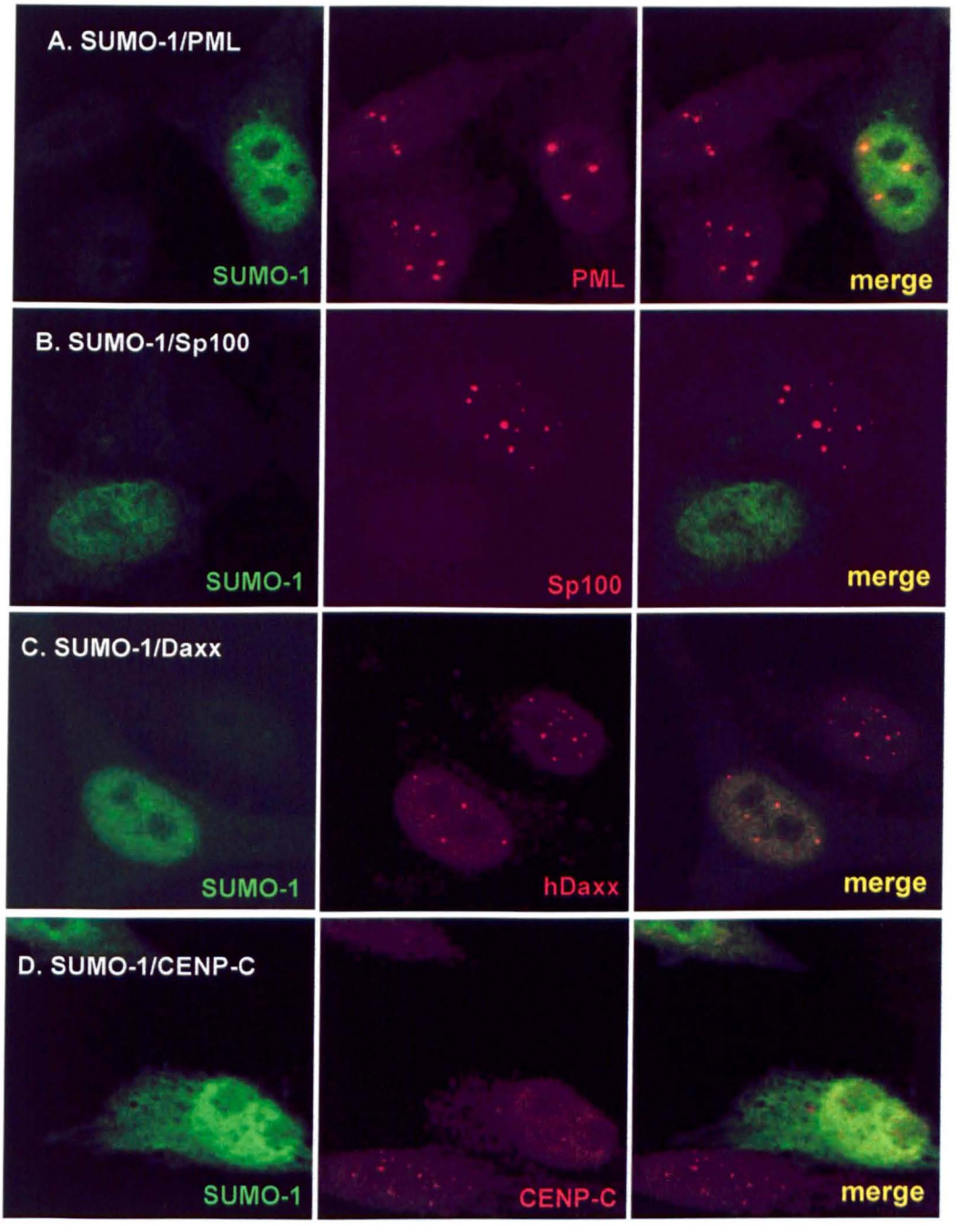

Fig. 5.8 The localisation of GA/HSTV mutant SUMO-1 and other ND10 proteins in transfected cells.

Vero cells transfected with plasmid GA/HSTV were double-stained for SUMO-1 and different ND10 proteins including PML, Sp100, or hDaxx, and also for the centromere protein CENP-C. The combinations of double-staining are indicated in the rightmost row, and are the same in each horizontal row of panels. The labelled proteins are indicated in lower-right corner in each image and the merged view of SUMO-1 with the other ND10 protein indicates the relative localisation of these two proteins.

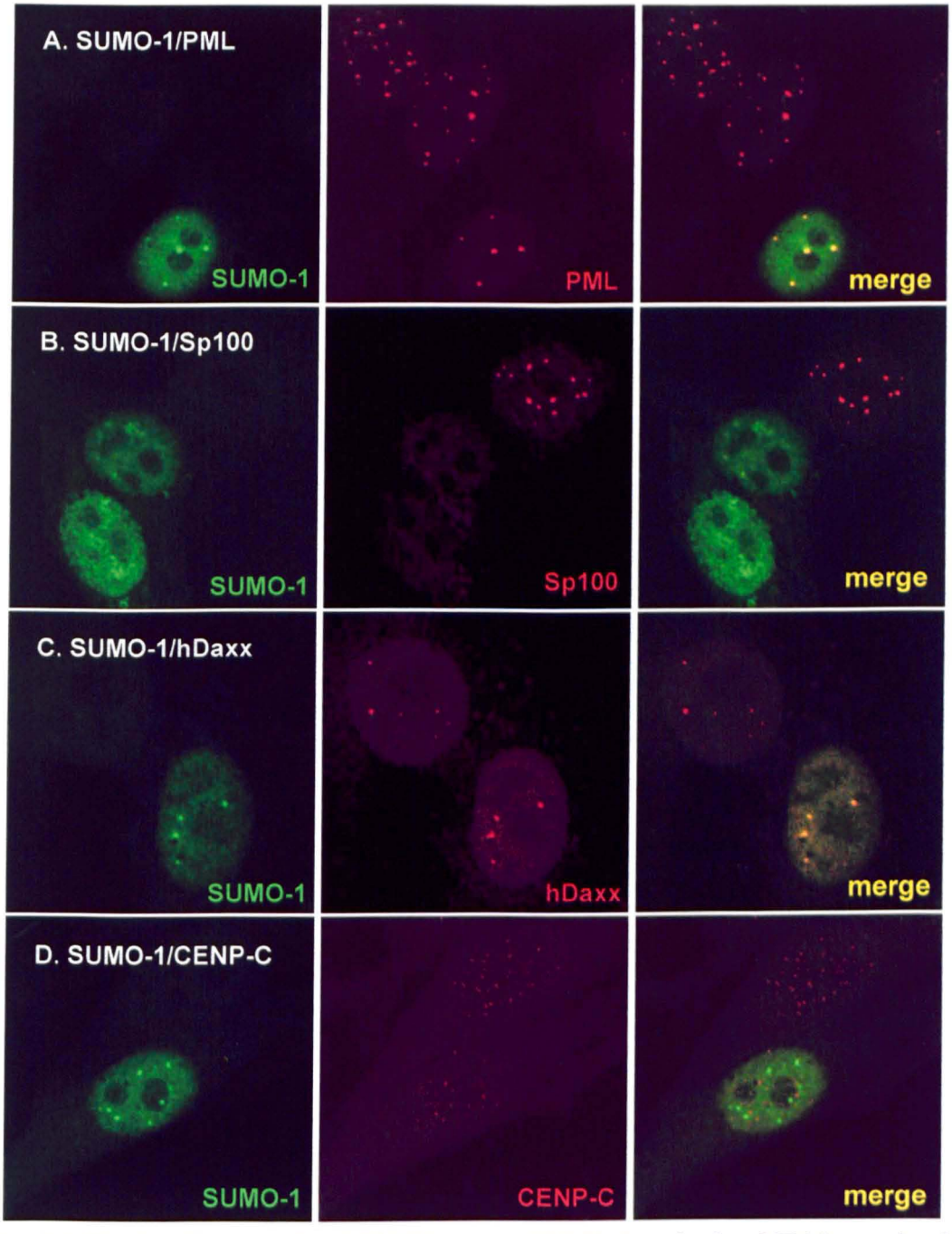

Fig. 5.9 The localisation of AG/HSTV mutant SUMO-1 and other ND10 proteins in transfected cells.

Vero cells transfected with plasmid AG/HSTV were double-stained for SUMO-1 and different ND10 proteins including PML, Sp100, or hDaxx, and also for the centromere protein CENP-C. The combinations of double-staining are indicated in the rightmost row, and are the same in each horizontal row of panels. The labelled proteins are indicated in lower-right corner in each image and the merged view of SUMO-1 with the other ND10 protein indicates the relative localisation of these two proteins.

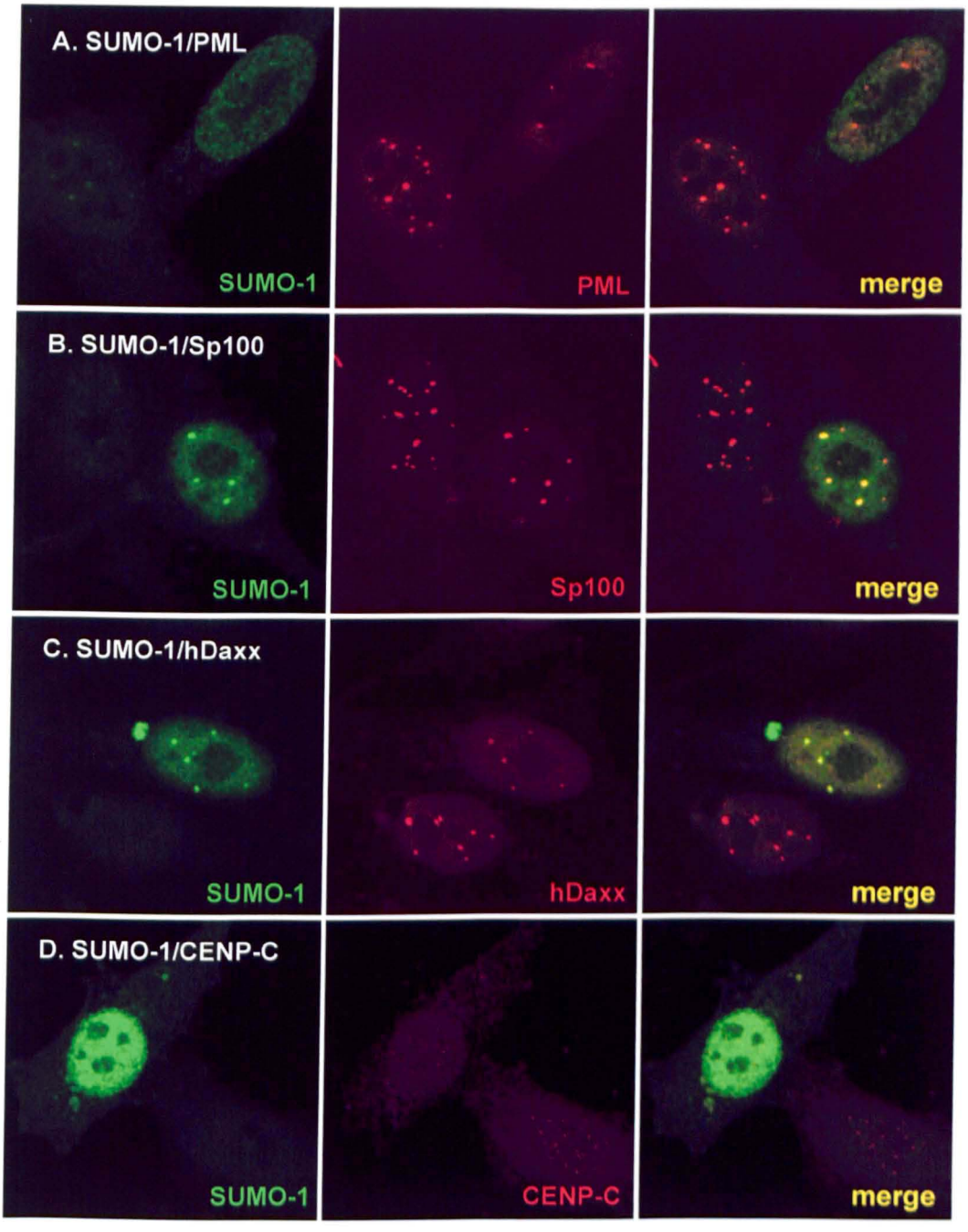

Fig. 5.10 The localisation of the AG mutant of SUMO-1 and other ND10 proteins in transfected cells.

Vero cells transfected with plasmid AG/SUMO-1 were double-stained for SUMO-1 and different ND10 proteins including PML, Sp100, or hDaxx, and also for the centromere protein CENP-C. The combinations of double-staining are indicated in the rightmost row, and are the same in each horizontal row of panels. The labelled proteins are indicated in lower-right corner in each image and the merged view of SUMO-1 with the other ND10 protein indicates the relative localisation of these two proteins.

40% of untransfected cells were infected, but only 20% of SUMO-1 transfected NT2 cells were expressing ICP0 (Fig. 5.11). In contrast, the reduction of infection was not significant in cells expressing the other three mutant forms of SUMO-1 (Fig. 5.11).

5.5 Analysis of the effects of SUMO-1 conjugation mutants on HSV-1 infection by flow cytometry - fluorescence-activated cell sorter (FACS) analysis.

Transient transfection of plasmids expressing proteins of interest and confocal microscopy examination of intracellular effects followed by statistical analysis of the images represents a reproducible and accurate way to explore the effects of proteins on viral infection. Nevertheless it was a time consuming method and the selection of IFA images to be examined could be construed as subjective. Instead of microscopy, FACS analysis could represent a more controllable and large scale method to analyse the effects of any protein expressed from a transfected plasmid on the efficiency of viral infection.

5.5.1 Strategy and methods for FACS analysis

Plasmids were introduced into cells via lipofection. Since FACS is able to process a large scale of sample, cells seeded in a 35mm Petri dish were used for each transfection to enlarge the sample size. To investigate the effect of expression of a particular protein, after infection the proteins of interest were labeled by staining with antibodies as for IFA, and the progression of infection was monitored by detecting fluorescent viral proteins. To avoid cell clumps blocking the cell sorter, a population of single cells is required. To achieve this, the antibody staining reactions was performed after trypsinising and dispersing the transfected and infected cell monolayer to a single cell status (see Material and Methods, section 2.2.15).

This strategy is illustrated by an experiment using virus vEG110wt (see section 3.3.1). Three major groups of cells were sorted by flow cytometry dependent on their fluorescent signals (Fig. 5.12A). In histogram A, group 1 shows the population of transfected cells expressing SUMO-1 protein with a higher PE signal, group 2 shows the population of cells infected by the EGFP virus, and group 3 shows the population of cells that were neither

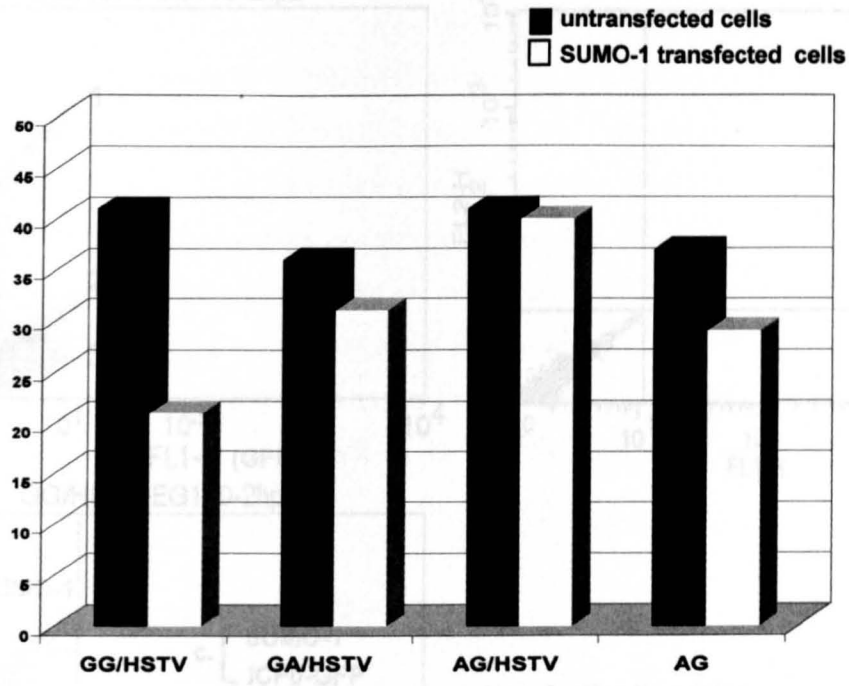

Fig. 5.11 The effects of the mutant SUMO-1 proteins on HSV-1 infection in NT2 cells.

NT2 cells were transfected by plasmids expressing wild type and the mutant forms of SUMO-1 followed by infection by HSV-1 the next day. The transfected and infected NT2 cells were then fixed and immuno-stained after 2 and 8 hours of infection and examined by confocal microscopy followed by statistical analysis.

The proportion of cells expressing ICP0 in untransfected cells is shown as ■ , and the proportion of SUMO-1 in transfected cells expressing ICP0 is shown as □ .

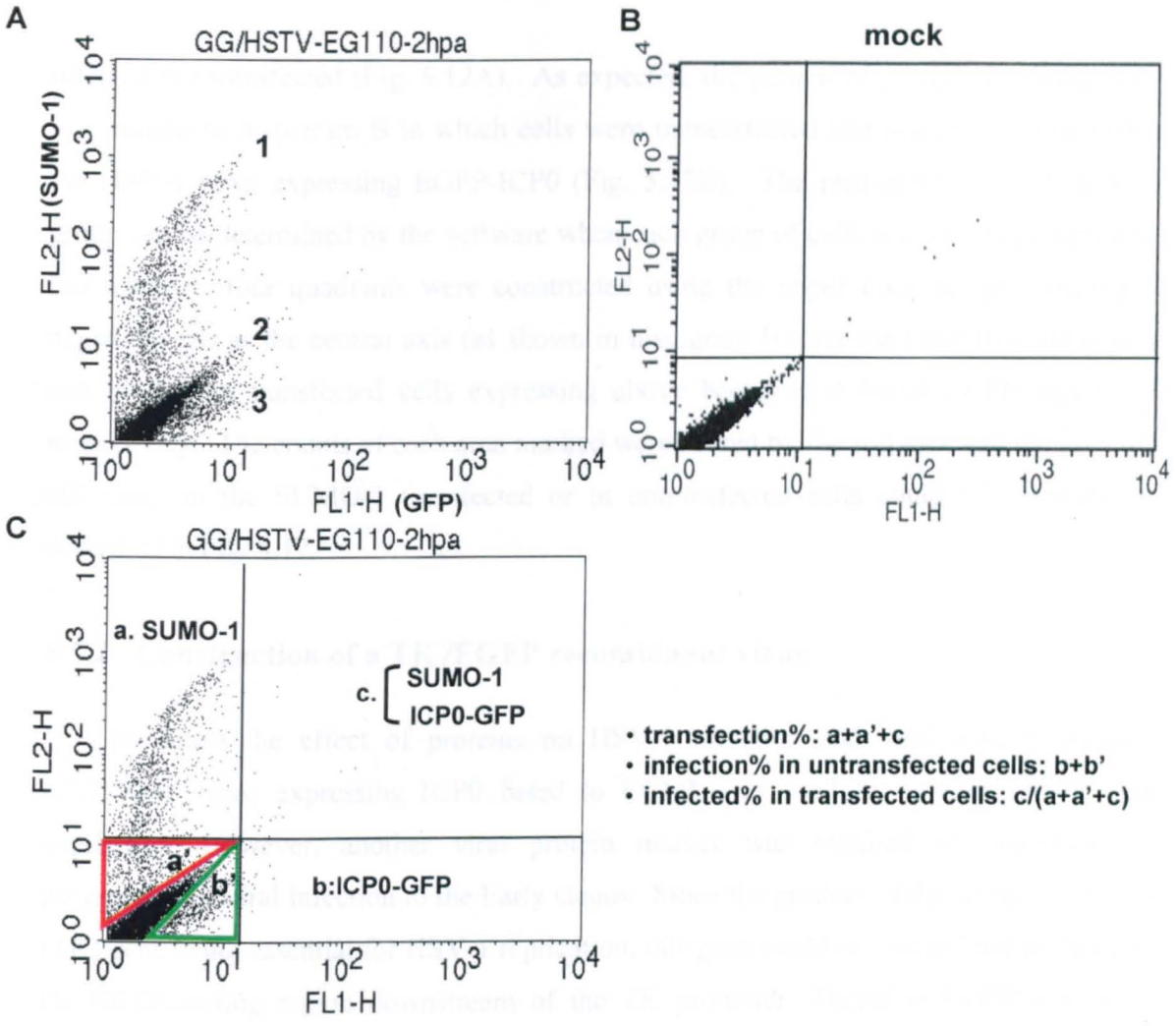

Fig. 5.12 An example of the analysis of the FACS data.

Vero cells transfected by the GG/HSTV plasmid were infected by vEG-110wt the next day followed by fixation and immuno-staining at 2 hpa for FACS analysis.

A. A dot plot diagram presenting three groups of cells from the sample transfected and infected. Group 1 illustrates the transfected cells expressing high levels of SUMO-1 which were labeled with PE detected by FL2-H laser. Group 2 presents the cells neither transfected nor infected. Group 3 includes the infected cells expressing high levels of EGFP-tagged ICP0 which was detected by FL1-H laser.

B. A dot plot diagram of the negative control from which Vero cells were transfected by an empty vector, pCIneo, then infected by HSV-1 17+ the next day. There is only one group of cells without any significant fluorescence in this dot plot diagram.

C. Interpretation and analysis of FACS data. Four quadrants were constructed using the upper limit of the grouping of negative cells as the central axis. Each quadrant demonstrates cells with different fluorescence depending on which proteins are expressed in the cells. The counts in each area marked such as a, b, c, a' and b' were detected by the software and the infection efficiency in the transfected and untransfected cells was calculated by following the simple equation as shown beside panel C.

infected nor transfected (Fig. 5.12A). As expected, the pattern of group 1 in histogram A was similar to histogram B in which cells were untransfected and infected by vEG110wt, the HSV-1 virus expressing EGFP-ICP0 (Fig. 5.12B). The proportions of cells in each group can be determined by the software when each group of cells was gated appropriately. For instance, four quadrants were constructed using the upper limit of the grouping of negative cells as the central axis (as shown in histogram B) and the other two triangles a' and b' contain transfected cells expressing above background levels of PE and EGFP respectively. The counts of each area marked were scored by the software and the infection efficiency in the SUMO-1 transfected or in untransfected cells could be calculated as described in Fig. 5.12.

5.5.2 Construction of a TK⁻/EGFP recombinant virus

To detect the effect of proteins on HSV-1 infection and viral gene expression, vEG110wt virus, expressing ICP0 fused to EGFP, was used to monitor the IE gene expression. However, another viral protein marker was required for assessing the progression of viral infection to the Early stages. Since the product of the thymidine kinase (TK) gene is not essential for HSV-1 replication, this gene could be deleted and replaced by the EGFP coding region downstream of the TK promoter. Therefore EGFP expression would act as a marker for transcription of a typical Early gene during infection.

5.5.2A Construction of the TK⁻/EGFP recombinant plasmid, pTK⁻/EGFP

Plasmid pTK1, provided by Dr. C. M. Preston, contains the *Bam*H I P fragment (from nucleotide 48634 to 45055) of HSV-1 genomic DNA; the open reading frame of the TK gene is located from nucleotide 47802 to 46674. The EGFP fragment was obtained from pEGFP-C1 vector, digested with *Not* I, followed by treatment with Klenow enzyme to blunt the ends and then further digested with *Bam*H I. To replace the TK gene from pTK1 plasmid, the purified 0.8 kb blunt ended/ *Bam*H I EGFP fragment was ligated with the 7 kb vector fragment purified from pTK1 plasmid codigested by *Sac* I (then blunted) and *Bgl* II, resulting in expression of EGFP driven by the TK promoter (Fig. 5.13). One unique restriction enzyme site, *Sca* I, located in the vector backbone, can be used to generate a linear DNA, which is beneficial for homologous recombination. The linear plasmid DNA

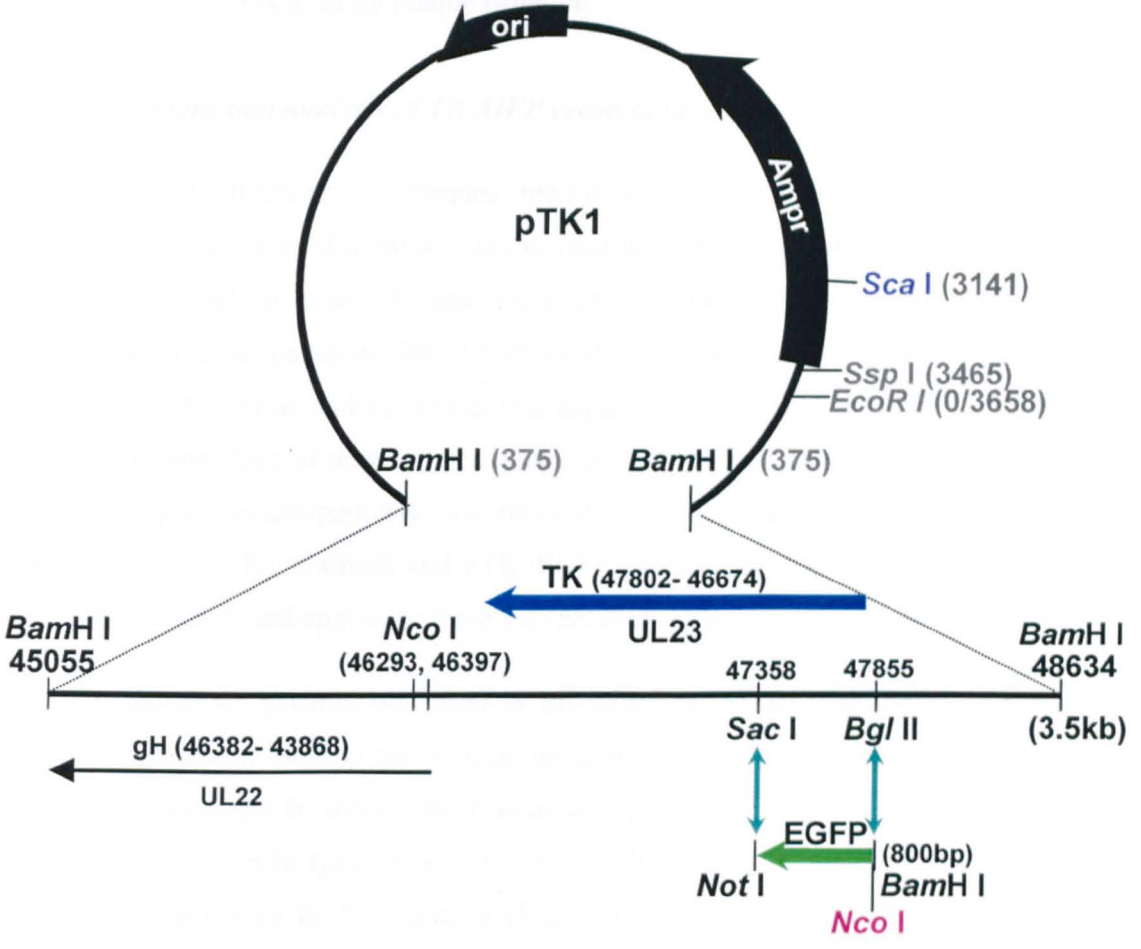

Fig. 5.13 A schematic representation of the pTK⁻/EGFP construct.

The TK gene is located in plasmid pTK1 containing the *Bam*HI P fragment (from nucleotides 45055 to 48634 of the HSV-1 genome). The translated region of the TK protein is between nucleotides 47802 and 46674, indicated by the blue arrow. To construct the TK deleted EGFP recombinant plasmid (pTK⁻/EGFP), plasmid pTK1 was co-digested with *Bgl* II/*Sac* I and the 500bp fragment containing 5' end of the TK gene was replaced by the 800bp fragment containing the EGFP ORF, indicated as a green arrow, resulting in expression of EGFP driven by the TK gene promoter. Insertion of the EGFP fragment introduces an extra *Nco* I site, labelled in pink, in the recombinant DNA.

was then co-transfected into BHK cells with infectious wild type HSV-1 strain 17+ DNA, and the progeny virus used for plaque isolation.

5.5.2B Southern blot analysis of TK⁻/GFP recombinant virus

The green fluorescence plaques identified by phase contrast and fluorescence microscopy were cultured in BHK cells in medium containing ACG to select TK deleted viruses (described in Materials and Methods, section 2.2.16B). The total cell DNA extracted after three rounds of plaque purification was processed for Southern blot analysis. Initially, the DNA of recombinant virus was digested with either *Bam*H I or codigested with different combinations of restriction enzymes, such as with *Bam*H I/ *Bgl* II, or *Bam*H I/ *Nco* I followed by gel electrophoresis. To obtain a clear-cut pattern, various DNAs from wild type 17+ virus, pTK1 plasmid, and pTK⁻/EGFP plasmid were also treated with the same restriction enzymes and applied to the gel as parallel controls.

Parental pTK1 plasmid was used as the template for the preparation of radioactive probes for Southern blotting (method as described in section 2.2.7A). The sizes of the *Bam*H I P fragments in recombinant virus and pTK⁻/GFP plasmid were larger than in plasmid pTK1 and wild type virus, since the 0.5kb fragment containing the TK gene was replaced by the 0.8 kb EGFP fragment (Fig 5.14A). As expected, results from Southern blotting showed that the *Bam*H I fragment from the recombinant virus and pTK⁻/EGFP plasmid had a lower mobility than those of wild type viral DNA and pTK1 plasmid (Fig. 5.14B). Since the *Bgl* II site in the *Bam*H I P fragment was destroyed after the insertion of the EGFP ORF in the UL23 locus, only one fragment (around 3.7kb) was detected in DNA from the recombinant virus and pTK⁻/EGFP plasmid when codigested with *Bam*H I /*Bgl* II (Fig. 5.14B lane 5, 7). Two fragments (2.7kb and 0.78kb) were generated when the *Bam*H I P fragment of wild type viral DNA was codigested with *Bam*H I/*Bgl* II. However only the 2.7kb *Bam*H I-*Bgl* II fragment was observed on the blot and the small fragment was undetectable (Fig. 5.14B, lane 6, 8). One extra *Nco* I site, located at the beginning of the EGFP open reading frame, was introduced into *Bam*H I P fragment when EGFP was inserted in the UL23 locus resulting in three fragments (1.7kb, 1.2kb, 0.8kb) being obtained from recombinant DNA codigested with *Bam*H I /*Nco* I (Fig. 5.14B, lane 9, 11). Without the EGFP insertion, only two fragments (1.2kb and 2.3kb) were detected from wild type viral DNA codigested with *Bam*H I /*Nco* I (Fig. 5.14B, lanes 10, 12). Notably, in lanes 6

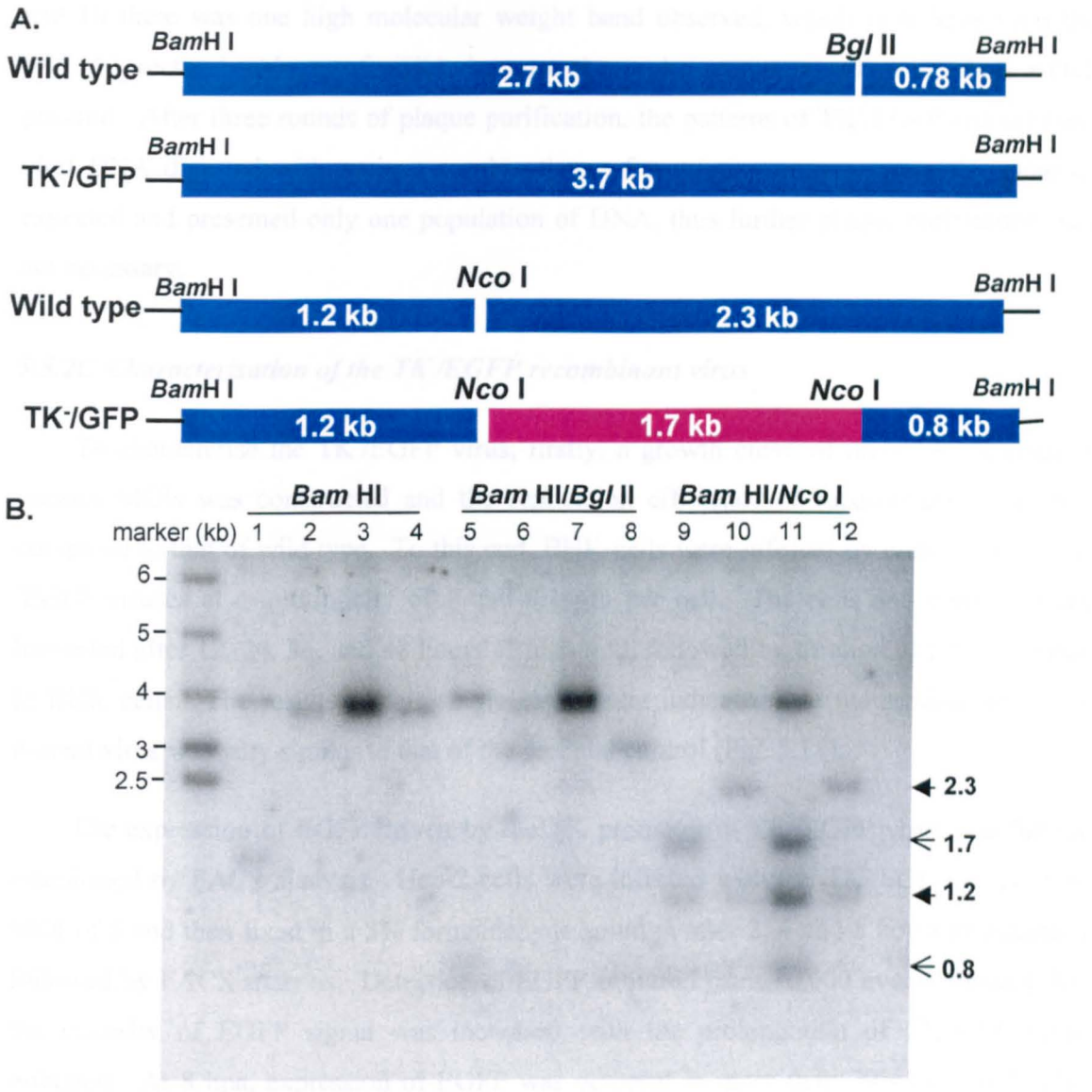

Fig. 5.14 Southern blot analysis of the TK-/EGFP recombinant viral DNA.

A. Illustration of the restriction map of the DNA of wild type and TK-/EGFP recombinant viruses. The sizes of the *Bam*H I P fragment were 3.5 kb in wild type and 3.7 kb in the recombinant viral DNA. A fragment of 0.78 kb in size was generated when wild type viral DNA was codigested with *Bam*H I/ *Bgl* II. One extra *Nco* I site generated from insertion of EGFP fragment results in the 2.5 kb of *Nco* I/*Bam*H I fragment of recombinant DNA divided into two fragments (1.7 and 0.8 kb).

B. The result of Southern blotting. DNA of the recombinant virus (applied in lanes 1, 5, 9) was digested with different restriction enzymes combinations such as *Bam*H I, *Bam*H I/*Bgl* II and *Bam*H I/*Nco* I as labelled at the top of blot followed by hybridisation with a probe prepared using plasmid pTK1 as a template. The results were compared with DNA of the original plasmid pTK1 (applied in lanes 2, 6, 10), parental recombinant plasmid pTK-/EGFP (applied in lanes 3, 7, 11) and wild type virus (applied in lanes 4, 8, 12).

and 10 there was one high molecular weight band observed, which may have been the pAT153 vector backbone of pTK1, because the probe was prepared from whole pTK1 plasmid. After three rounds of plaque purification, the patterns of TK⁻/EGFP recombinant viral DNA digested with various combinations of restriction enzyme were the same as expected and presented only one population of DNA, thus further plaque purification was not necessary.

5.5.2C Characterisation of the TK⁻/EGFP recombinant virus

To characterise the TK⁻/EGFP virus, firstly, a growth curve of recombinant virus at various MOIs was constructed and the replication efficiency of recombinant virus was compared to that of wild type. To this end, BHK cells were infected by either 17+ or TK⁻/EGFP viruses at a multiplicity of 1 and 0.1 pfu per cell. The cells and medium were harvested after 12, 24, 36, and 48 hours of infection, followed by titration of progeny virus in BHK cells. The results of this single experiment indicated that the replication of the mutant virus was very similar to that of the parental control (Fig. 5.15).

The expression of EGFP driven by the TK promoter in TK⁻/EGFP virus was further established by FACS analysis. Hep-2 cells were infected with the TK⁻/EGFP virus at an MOI of 5 and then fixed in a 5% formaldehyde solution after 2, 4 and 8 hours of infection followed by FACS analysis. Detection of EGFP acquired from 10,000 events showed that the intensity of EGFP signal was increased with the prolongation of TK⁻/GFP virus infection. At 8 hpa, expression of EGFP was detected in more than 70% of Hep-2 cells (Fig. 5.16B), whereas no EGFP signal was detected in cells infected with wild type 17+ virus, as a negative control (Fig. 5.16A). This implies that FACS is a reliable system for the detection of fluorescent signals from cells infected by the TK⁻/EGFP virus.

5.5.3 Analysis of the effect of SUMO-1 and SUMO-1 mutants on viral infection by FACS

5.5.3A Vero cells

Vero cells were chosen to establish a FACS method for this study, since preliminary tests showed that Hep-2 cells tended to form big clumps that caused technical problems during the analysis. Furthermore, HSV-1 infection progresses more efficiently in Vero than

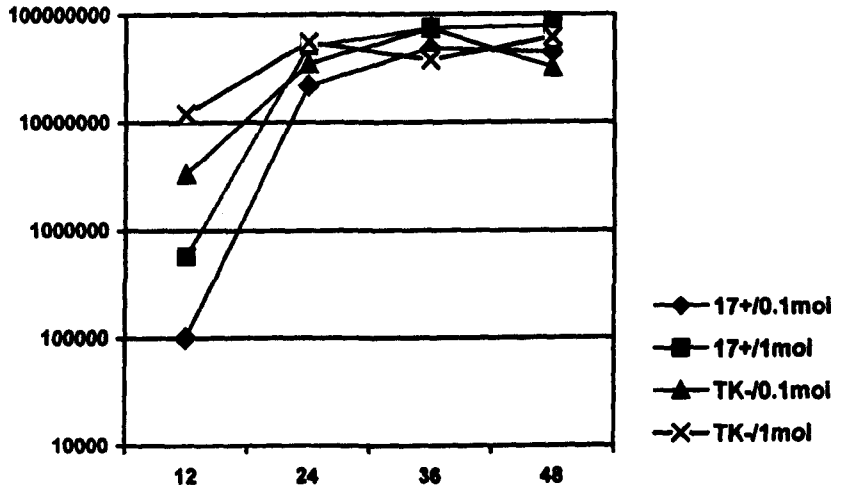

Fig. 5.15 Comparison of the growth curve of the TK-/EGFP recombinant virus with wild type virus.

BHK cells were infected with either 17+ or the TK-/EGFP recombinant virus at MOI of 1 and 0.1. Both the infected cells and medium were harvest after 12, 24, 36 and 48 hours of infection followed by titration of the progeny viruses on BHK cells.

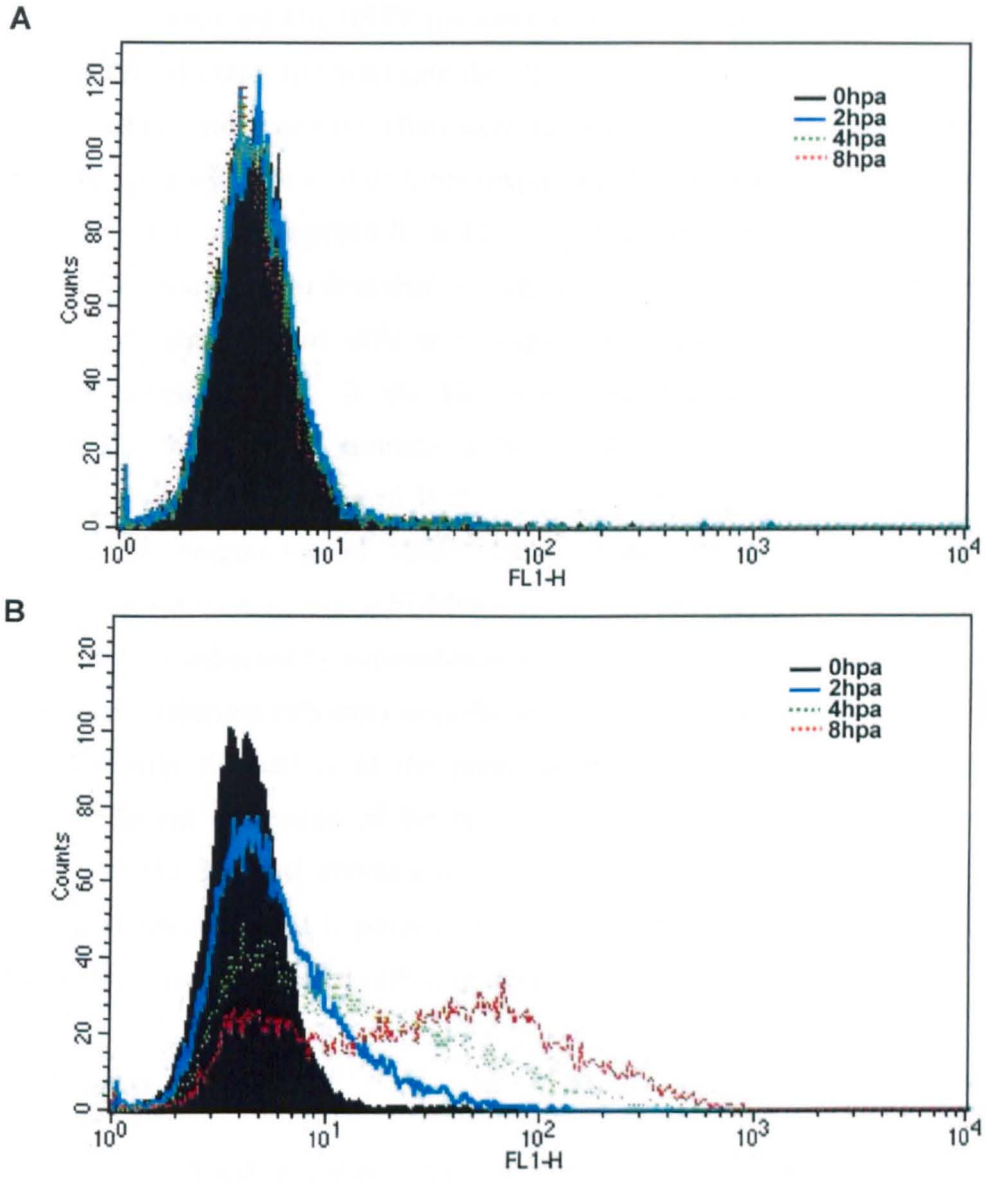

Fig. 5.16 A histogram from the FACS analysis of the TK-/EGFP virus.

A. Hep-2 cells infected by 17+ at an MOI of 5 for various times were analysed by FACS by detection of EGFP fluorescence. There was no significant fluorescence detected.

B. Hep-2 cells infected by the TK-/EGFP recombinant at an MOI of 5 for various times were analysed by FACS by detection of EGFP fluorescence. The EGFP signal increased as infection progressed.

in Hep2 cells. To optimise the conditions for FACS analysis, two SUMO-1 constructs, GG/HSTV (wild type) and GA/HSTV (mutant), were transfected into Vero cells seeded in three 35mm Petri-dishes. To investigate the effects of SUMO-1 on infection progression, different stages of viral gene expression were analysed. One day after transfection, Vero cells were infected with vEG-110wt virus (expressing EGFP linked to ICP0) or with TK-/EGFP virus for 6 hours to monitor IE and Early gene expression respectively. Cells were prepared for FACS analysis as described in section 2.2.15A. In the vEG-110wt infection, at 2 hpa, 3.8% of untransfected cells were expressing detectable levels of EGFP-ICP0, increasing at 6 hpa to 18%. In the TK-/EGFP infection, 17% of untransfected cells expressed EGFP from the TK promoter at 6 hpa. Less than 1% and 6% of wild type SUMO-1 transfected cells expressed ICP0 at 2 hpa and 6 hpa respectively (Fig. 5.17). Furthermore, the progression of viral infection was relatively slower in SUMO-1 transfected cells, since only 3.8% of SUMO-1 transfected cells progressed to the Early gene expression stage as indicated by expression of EGFP from the TK gene (Fig. 5.17). These decreases in viral infection efficiency in cells expressing high levels of exogenous SUMO-1 are consistent with the results of the previous experiments analysed by microscopy. However, inefficient expression of the IE and E genes was also observed from cells transfected with the SUMO-1 conjugation mutant (GA/HSTV) construct (Fig. 5.18). On average, expression of IE and E genes in SUMO-1 mutant transfected cells was 3-5 fold less efficient than in untransfected cells (Fig. 5.18).

5.5.3B NT2 cells

The results from section 5.4 revealed that wild type SUMO-1 had a greater effect on viral infection than the other three SUMO-1 conjugation mutants tested. This result was also confirmed using FACS. As with Vero cells, the proportion of transfected NT2 cells expressing ICP0 was lower than in the untransfected NT2 population, and there was no significant difference in this effect between the wild type and mutant SUMO-1 experiments. At 6 hpa, 10% of untransfected cells expressed ICP0, but only 2.5% of cells transfected by wild type SUMO-1 expressed ICP0 (Fig. 5.19). In other words, the infection efficiency was reduced about 4-fold when NT2 cells expressed high levels of exogenous wild type SUMO-1. However, such a reduction in infection efficiency was also observed in NT2 cells transfected with the other three mutant constructs. The expression of ICP0 was 4.9, 2.6, and 3.4-fold reduced in cells transfected with the GA/HSTV, AG/HSTV, and AG

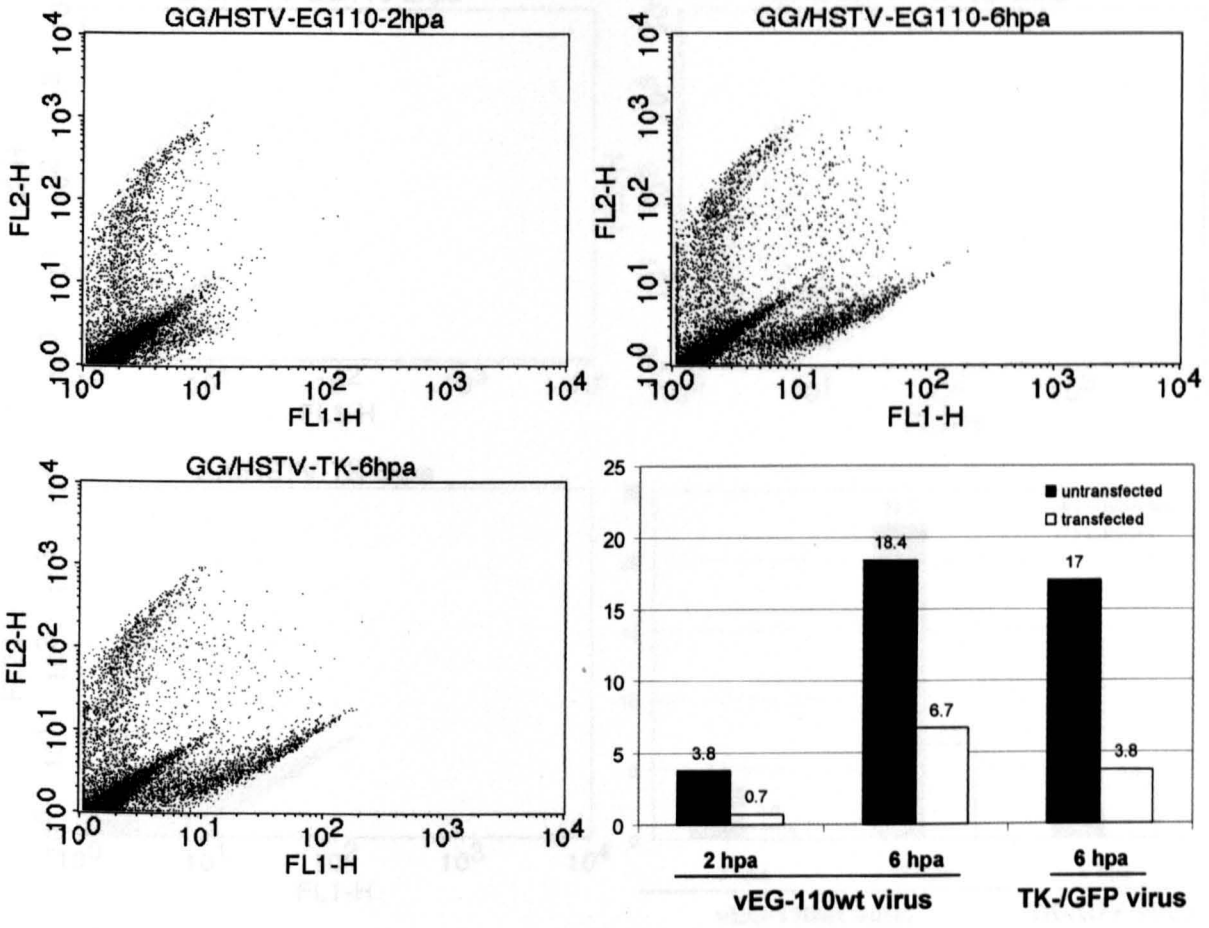

Fig. 5.17 Dot plot diagrams from the FACS analysis of Vero cells transfected with the GG/HSTV plasmid.

Vero cells, transfected with plasmid GG/HSTV, were infected by vEG-110wt at an MOI of 5 for 2 and 6 hours or TK-/EGFP virus for 6 hours (as labelled at the top of each diagram) followed by immunofluorescence staining for FACS analysis. The histograms illustrating the infection efficiency of transfected and untransfected cells were calculated by analysis of the counts from each group of cells obtained from FACS analysis.

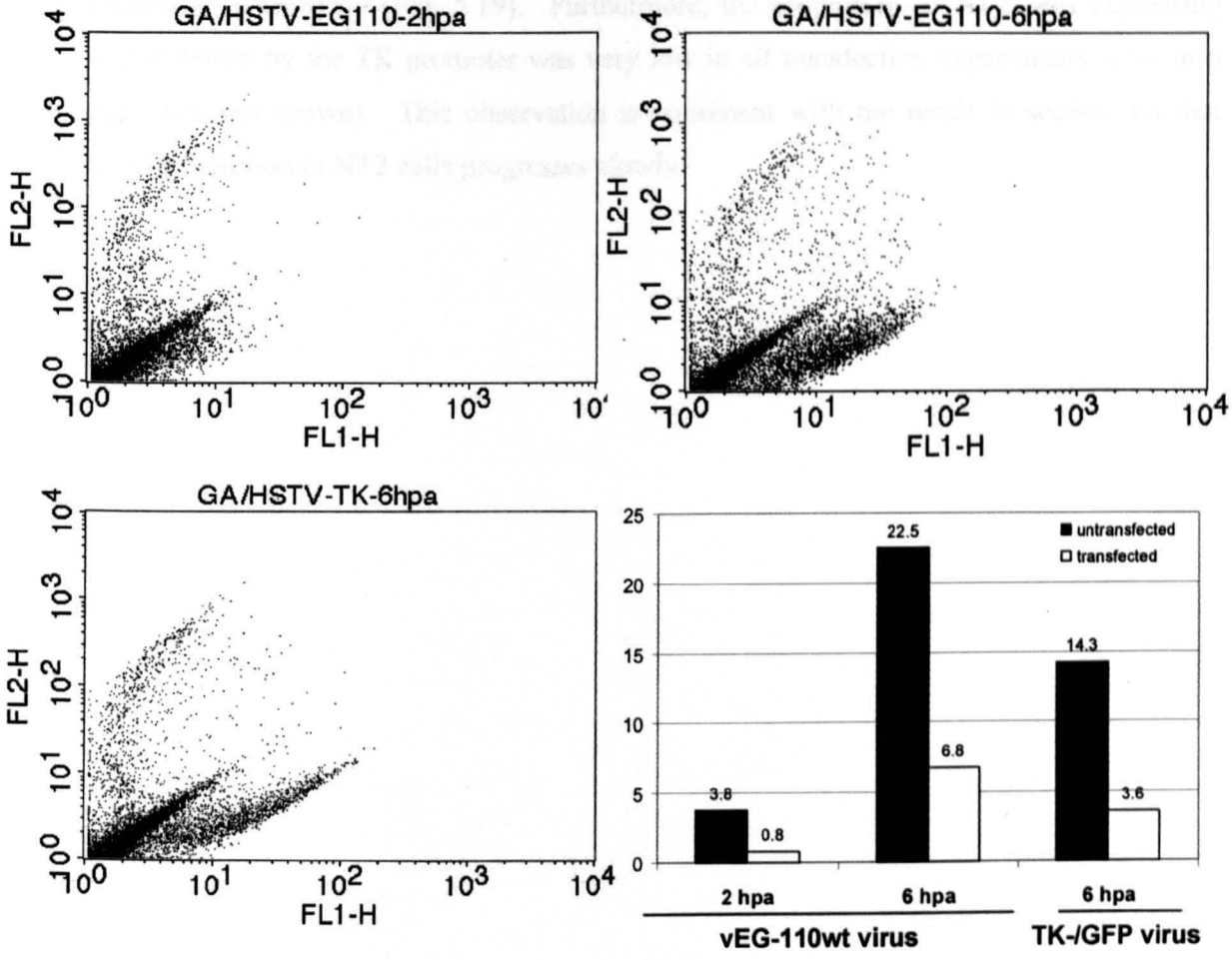

Fig. 5.18 Dot plot diagrams from the FACS analysis of Vero cells transfected with the GA/HSTV plasmid.

Vero cells, transfected with plasmid GA/HSTV, were infected by vEG-110wt at an MOI of 5 for 2 and 6 hours or TK-/EGFP virus for 6 hours (as labelled at the top of each diagram) followed by immunofluorescence staining for FACS analysis. The histograms illustrating the infection efficiency of transfected and untransfected cells were calculated by analysis of the counts from each group of cells obtained from FACS analysis.

plasmids, respectively (Fig. 5.19). Furthermore, the proportion of NT2 cells expressing EGFP driven by the TK promoter was very low in all transfection experiments, even at 6 hpa (data not shown). This observation is consistent with the result in section 4.4 that HSV-1 infection in NT2 cells progresses slowly.

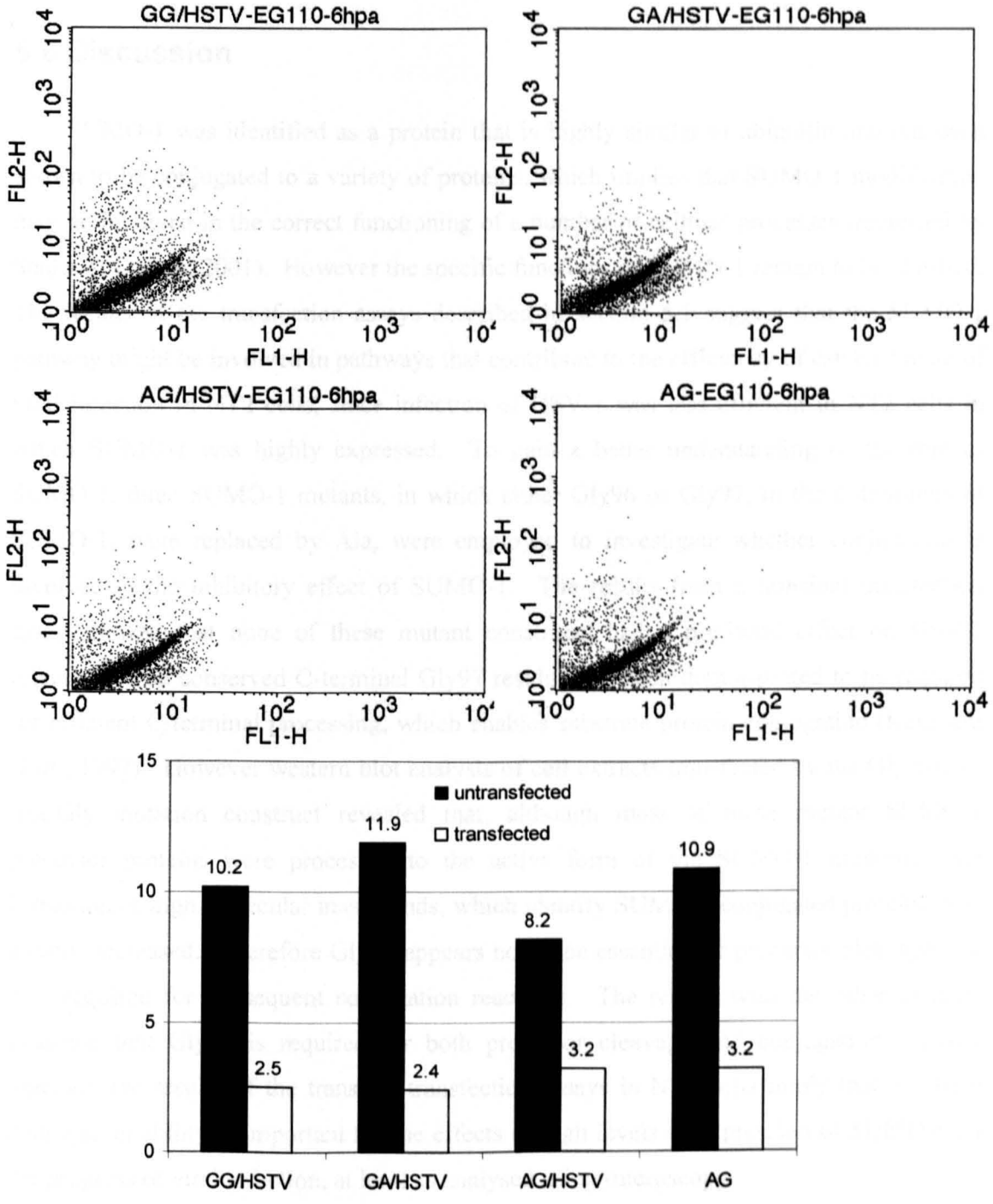

Fig. 5.19 Dot plot diagrams from the FACS analysis of NT2 cells transfected with wild type SUMO-1 or conjugation mutant constructs.

NT2 cells, transfected with plasmid GG/HSTV, GA/HSTV, AG/HSTV, or AG (as labelled at the top of each diagram) were infected by vEG-110wt at an MOI of 5 for 6 hours followed by immunofluorescence staining for FACS analysis. The histograms illustrating the infection efficiency of transfected and untransfected cells were calculated by analysis of the counts from each group of cells obtained from FACS analysis.

5.6 Discussion

SUMO-1 was identified as a protein that is highly similar to ubiquitin and has been shown to be conjugated to a variety of proteins, which implies that SUMO-1 modification may be involved in the correct functioning of a number of cellular processes (reviewed by Seeler & Dejean, 2001). However the specific functions of SUMO-1 remain to be clarified. The results of the transfection assays described in section 5.1 suggest that the SUMO-1 pathway might be involved in pathways that contribute to the efficiency of establishment of viral infection in NT2 cells, since infection of HSV-1 was less efficient in NT2 cells in which SUMO-1 was highly expressed. To gain a better understanding of the role of SUMO-1, three SUMO-1 mutants, in which either Gly96 or Gly97, in the C-terminus of SUMO-1, were replaced by Ala, were employed to investigate whether conjugation is involved in the inhibitory effect of SUMO-1. The results from a transient transfection assay showed that none of these mutant constructs had a profound effect on HSV-1 infection. The conserved C-terminal Gly97 residue has been demonstrated to be required for efficient C-terminal processing, which enables substrate protein conjugation (Kamitani *et al.*, 1997). However western blot analysis of cell extracts transfected by the Gly-Gly to Ala-Gly mutation construct revealed that, although most of these mutant SUMO-1 precursor proteins were processed to the active form of the SUMO-1 monomer, the formation of high molecular mass bands, which identify SUMO-1 conjugated proteins, was greatly decreased. Therefore Gly96 appears not to be essential for precursor cleavage, but it is required for subsequent conjugation reactions. The results with the other mutants illustrate that Gly97 is required for both precursor cleavage and conjugation. Taken together, the results of the transient transfection assays in NT2 cells imply that substrate conjugation ability is important for the effects of high levels of expression of SUMO-1 on the progress of viral infection, at least as analysed using microscopy.

Why high levels of SUMO-1 expression should impede viral infection is unclear. Many cellular processes may have regulatory steps that depend on SUMO-1 modification, and it is possible that increasing the pool of free SUMO-1 could affect the proper functioning of these pathways. SUMO-1 modification is known to be involved in the metabolism of ND10 structures and constituent proteins, and altered equilibria induced by high levels of wild type or mutant SUMO-1 protein expression could induce biochemical

and morphological changes in ND10. Notably, in over 80 % of cells overexpressing SUMO-1 mutant constructs, the staining of hDaxx was dispersed and Sp100 apparently disappeared. Investigation of the staining of SUMO-1 and other ND10 proteins in detail found that loss of hDaxx staining from ND10 is dependent on the localisation of SUMO-1, since if the SUMO-1 was in part present in ND10, hDaxx staining was also present. Unlike hDaxx, staining of PML still remained in ND10-like foci in cells transfected by GA/HSTV, suggesting that the distribution of PML was affected to a lesser degree by the conjugation mutant or dislocated SUMO-1. However, overall the number of PML foci in each transfected cell was lower than in untransfected cells. Loss of hDaxx staining and a decrease the number of PML foci could be due to the mutant SUMO-1 proteins competing with endogenous SUMO-1 and having a dominant negative effect of SUMO-1 conjugation pathways, resulting in diminution of SUMO-1 conjugated PML. This idea is supported by recent studies reporting that SUMO-1 modification of PML is critical to target this protein to ND10 (Muller *et al.*, 1998a), and is also required for recruitment of hDaxx to ND10 (Li *et al.*, 2000). Furthermore, proper SUMO-1 function also seems important for the localisation of Sp100, since Sp100 staining was absent from ND10 in many transfected cells expressing high levels of SUMO-1, although the proportion of transfected cells without Sp100 staining varied between constructs. Loss of Sp100 was detected in up to 75% of cells transfected with the GA/HSTV mutant and only in 22% of cells transfected with AG/HSTV constructs.

However, the situation is yet further complicated by the observation that a proportion of transfected cells expressing high levels of wild type SUMO-1 have a diffuse distribution of SUMO-1, and in these cells ND10 structures are also abnormal. It could be that a proportion of all cells have abnormal ND10, and if such cells are transfected it follows that the SUMO-1 can not be located at ND10. It is also possible that excessive expression of wild type SUMO-1 could in some way have an effect similar to expression of the mutant proteins.

The preliminary experiments described here show that FACS analysis presents an efficient way to distinguish infected and transfected cells. However, the results from two separate series of FACS experiments show that wild type SUMO-1 and also all the conjugation mutants reduced viral infection when expressed at high levels, in contrast with results described in section 5.5 using the original method based on microscopy. Although

the stocks of NT2 cells used for the studies in Chapter 4 remained in good condition, during the later stages of my PhD studies considerable problems were experienced in maintaining robust NT2 cell cultures. It was noticed that after lipofection followed by infection, a significant proportion of NT2 cells were dying and the rest of the cells tended to form big clumps after suspension in solution throughout the procedures used for staining and FACS analysis. The influences of low transfection efficiency, inefficient infection and poor viability of cells generates an unsatisfactory condition for samples to undergo FACS analysis. Despite obtaining fresh stocks of NT2 cells from the original supplier, these problems were not overcome entirely, and therefore this particular result from the FACS analysis remains to be clarified.

It could be argued that the transfection and analysis procedures of the FACS approach might introduce artifacts. However, FACS analysis of Vero cells transfected with a plasmid expressing β-galactosidase was used as a negative control, and no effect on the progress of viral infection was observed (data not shown). Shortage of time prevented further exploration of this potentially general method for studying the effect of expression of proteins from transfected plasmids on the efficiency of viral infection.

Chapter 6 FINAL DISCUSSION

Chapter 6 Final discussion

6.1 Interferon, ICP0, and ND10

In last half century, interferons (IFNs) were discovered as proteins secreted by viral-infected cells to prevent further infection of uninfected neighbouring cells (Isaacs & Lindenmann, 1957, Stark *et al.*, 1998). It has been indicated that the antiviral activity of IFNs is through a set of intracellular signal transductions, which are stimulated by IFN receptors, resulting in induction of gene expression. Among hundreds of genes transcriptionally regulated by IFNs, three families of genes which encode the double-stranded RNA-activated protein kinase (PKR), the 2', 5'-oligoadenylate synthetases (OAS)/RNase L, and the Mx proteins respectively, have been extensively studied with respect to their antiviral activities (reviewed by Shtrichman & Samuel, 2001).

Mossman *et al.* (2001) reported that UV-inactivated wild-type HSV-1, IFN treatment, and HSV-1 mutant KM110 (a double-deletion of ICP0/VP16 which fails to express any viral genes in human embryo lung cells) block plaque formation by superinfecting VSV. In addition, analysis of DNA microarray data revealed that the profile of cellular genes up-regulated by IFN shares high similarity to that induced by mutant KM110, whereas wild type HSV-1 did not induce expression of any of these IFN-inducible proteins, suggesting that an antiviral response induced by HSV-1 infection occurs in the absence of *de novo* viral gene expression (Mossman *et al.*, 2001). Most recently, Mossman and Smiley (2002) further identified that expression of ICP0 and ICP34.5 compromised the IFN-induced antiviral state against viral transcription and translation (Mossman & Smiley, 2002). Together with the observations that ICP0 initially localises to ND10 and subsequently triggers the disruption of ND10 structures by degradation of two IFN inducible ND10 proteins, PML, Sp100 and their SUMO-1 modified forms (Everett *et al.*, 1998a), the results suggest a possible interaction between IFN pathways, ND10 proteins, and ICP0. Briefly, infection by HSV-1 triggers the antiviral state mediated by IFN that induces the expression of cellular proteins (such as PKR, Mx, OAS, and PML) that antagonise viral replication, and on the other hand, the virus has evolved it own defense mechanism by encoding viral proteins such as ICP0 and ICP34.5 to counteract the effect of IFN-inducible proteins (by

degradation of those proteins) and maybe interfere with the expression of cellular proteins stimulated by IFNs.

6.2 Does PML confer resistance to HSV-1 infection?

At the same time while I was approaching the effect of ND10 proteins on HSV-1 infection, PML has been implicated in IFN-mediated antiviral defence. As described in the Introduction chapter (section 1E.5), recent studies performed in various experimental systems have demonstrated that over-expression of PML confers resistance to viral infections e.g. the infection of VSV, influenza A virus, HFV and HCMV. However, the results illustrated in Chapter 3 showed that over-expression of PML (and other ND10 proteins) by a transient transfection method, had no apparent affect on wild-type HSV-1 replication and viral gene expression. Given the differences in terms of the methodology employed, these results should be carefully interpreted. Three aspects involved in this study are discussed in greater depth below.

6.2.1 The localisation of over-expressed ND10 proteins

The immuno-staining with fluorescence revealed a nuclear diffuse pattern of the over-expressed ND10 proteins in a large proportion of cells transfected by both electroporation and lipofection. This result raises the question whether these proteins could function normally in transfected cells when they are not located in ND10. Chelbi-Alix and Hayward's groups performed similar studies in PML- stable-expression cell lines (CHO, U373, or mouse embryo fibroblast cells) in which the exogenous PML is targeted to ND10 in a high proportion of cells (Ahn & Hayward, 2000, Chelbi-Alix *et al.*, 1998, Regad *et al.*, 2001). SUMO-1 modification has been shown to be required for recruitment of PML into ND10 and the SUMO-1 modified PML promotes another ND10 constituent, hDaxx to localise into ND10 (Li *et al.*, 2000, Muller *et al.*, 1998a). As shown in Fig. 3.11, although PML was highly expressed in BHK cells, only a small fraction of the exogenous PML was modified by SUMO-1. These observations indicated the exogenous ND10 proteins expressed by transient transfection methods might not be post-translationally modified properly and therefore not exert their normal functions.

In addition to transient expression systems, a tetracycline-inducible (HeLa) cell line expressing Sp100 was used to address this question in my study. Although Sp100 was induced and localised to ND10, the viral gene expression (ICP0 and UL29) in tetracycline-induced HeLa cells were similar in those in uninduced HeLa cells (data not shown). Coincidentally, Regad *et al.* (2001) reported that stable expression of PML in U373MG cells confers resistance to HFV whereas PML induction in a tetracycline-inducible cell line did not significantly interfere with HFV gene expression, suggesting that only high levels of PML expression affect HFV infection. Taken together, to study the effect of ND10 proteins requires an expression system by which exogenous protein can be expressed in high levels with proper localisation.

Furthermore, as described in Chapter 4 that the expression levels of ND10 proteins are distinct between neuron precursor NT2 and differentiated hNT cells (Fig. 4.2, 4.5). If ND10 mediate the antiviral state against HSV-1 infection, then infection by HSV-1 should be more efficient in NT2 cells, which express only low levels of ND10 proteins. However, in hNT cells, the infection susceptibility of wild type HSV-1 is only slightly lower than that in NT2 (Table. 4.1), although hNT cells express much higher levels of ND10 proteins than NT2 cells. Indeed, hNT cells share a similar profile of PML and Sp100 expression with that in fibroblast (HFL) cells (Fig. 4.2). This seems contrary to the hypothesis previously described. However considering the function of ICP0 is compromised in NT2 and hNT cells, based on the observation that ND10 are relatively stable in these two cell lines during HSV-1 infection (Table 4.3), ND10 proteins may be able to exert their hypothetical repressive functions even when present in relatively low amounts in NT2 cells.

6.2.2 The effect of IFN on HSV-1 infection

If the hypothesis that PML (or possibly other ND10 associated proteins) plays a role in the IFN-induced antiviral state is reasonable, one aspect that should be initially considered is the response of HSV-1 to IFNs' activities during infection in an *in vitro* system. In other words, if HSV-1 infection is resistant to IFNs, induced expression of PML or other ND10 proteins may not affect HSV-1 infection.

Studies of the effect of IFN-α on viral gene expression in individual cells in Chapter 3 (section 3.2.2) demonstrated that in IFN-treated cells, infected with HSV-1 at an MOI of 5,

expression of ICP0 and UL29 was inhibited by 2- to 3-fold at all infection times tested (Table 3.2). These observations are consistent with recent studies in Smiley's group that IFN-α only has a modest effect on wild-type HSV-1 infection (Mossman *et al.*, 2000). Additionally, studies using various MOIs (5, 2, 0.5 pfu per cell) revealed that at an early time of infection (2 hpa), the inhibitory effect of IFN-α on ICP0 expression was slightly stronger when a lower virus input was used (Table 3.3). Taylor *et al.* (2001) reported that IFN repressed gene expression from the ICP4 promoter of HSV-1 and this effect was dependent on IFN type, cell type, and MOI. Given the findings from these studies, pre-treatment with a high dose of IFN (1000U/ml) inhibits viral gene expression when cells were infected with HSV-1 at a low MOI (0.05) (e.g. treatment with IFN-α repressed the ICP4 promoter approximately by 2.5-fold). Once the system for expression of ND10 proteins is optimised, at least a mild inhibition of viral infection in cells over-expressing ND10 should be observed if PML or other ND10 proteins play a part in mediating the IFN-induced antiviral state.

6.2.3 Isoform specific effects

Different splicing variants of PML isoforms (I-VII, to date) have been implicated in mediating particular effects resulting from their specific interactions with certain cellular proteins (reviewed by Jensen *et al.*, 2001). For instance, p53 is recruited into ND10 through the interaction with a specific PML splicing variant, the isoform III (Fogal *et al.*, 2000). Furthermore, the antiviral effects of PML that have been demonstrated so far have been performed using different isoforms, for instance: PML III (641 a.a.) confers resistance to VSV, influenza, and HFV infection (Chelbi-Alix *et al.*, 1998, Regad *et al.*, 2001), and PML VI (560a.a) is capable of inhibiting HCMV replication (Ahn & Hayward, 2000). In addition, Burkham *et al.* demonstrated different PML isoforms have various intracellular localisations and during HSV-1 infection, and some, but not all, PML isoforms were recruited into replication compartments (Burkham *et al.*, 2001). Taken together, these findings imply that various PML isoforms may undergo different fates, for instance, recruitment to ND10, or localisation at sites district from ND10, and interactions with specific cellular proteins, subsequently leading to different effects on viral infections.

Two different forms of PML were used in the studies in this thesis. Plasmid pPML(F) encodes the 633 a.a. isoform IV, while the isoform expressed by PML-RH was not

identified by the authors. Both highly expressed PML (Fig. 3.11, and Fig. 4.15), however only the PML encoded from the PML (F) construct was greatly modified by SUMO-1 (Fig. 4. 15). This phenomenon has been routinely observed in other lines of research in our laboratory. Although all the PML isoforms contain the three SUMO-1 modification sites, the observation described above indicates that the different expression machinery (or different PML isoforms) may affect post-translation modification of PML by SUMO-1, which possibly influences their biological functions. Thus, in the future, it will be important to use several different isoforms to elucidate the effect on viral replication or the fate of PML during viral infection.

6.3 The possible role of SUMO-1 in HSV-1 infection in NT2 cells

Results in Chapter 5 showed that in transfected NT2 cells over-expressing SUMO-1, infection by HSV-1 was decreased by 3- to 5-fold at all infection times tested (Fig. 5.2). Pathways involving SUMO-1 have been implicated in an antiviral effect by Engelhardt *et al.* (2001) using the IFN-induced Mx1 protein, which has been found to inhibit a wide range of viral infections (Engelhardt *et al.*, 2001, reviewed by Haller *et al.*, 1998). Mx1 was found to interact with several proteins associated with SUMO-1 pathways. In particular SUMO-1 and its E1 enzyme (Aos2/Uba2) as well as some ND10 components strongly interacted with the Mx1 protein. In addition, results of immunofluorescence assays revealed that the staining of both endogenous and exogenous Mx1 protein partially overlaps with SUMO-1 and ND10 proteins (hDaxx, PML and Sp100) in HeLa cells treated with IFN. These observations suggest that when the expression of Mx1 was stimulated by IFN, it may accumulate close to ND10, where some viruses initially localise, and facilitate its antiviral effect. This indicates a role for SUMO-1 and ND10 in the antiviral action of Mx1. However, Mx1 is a mouse protein and there is no known equivalent in humans.

As described in the Introduction, SUMO-1 has been found to covalently modify ND10 and a number of cellular proteins (reviewed by Seeler & Dejean, 2001). Recent studies have described that a number of viral early gene products such as IE1 and IE2 (from HCMV), E1 (from BPV), and BZLF1 (from EBV) are substrates of SUMO-1 modification, however, to date, no HSV-1 viral protein has been shown to be conjugated by SUMO-1. Thus over-expression of SUMO-1 does not seem to directly affect HSV-1 proteins, but

there may be an effect through other SUMO-1 substrates. In contrast to ubiquitination, conjugation to SUMO-1 does not lead to degradation, but can alter substrate intracellular localisation, protein-protein interactions, and functional activity. The possible effect of SUMO-1 on HSV-1 infection in NT2 cells with respect to these aspects is discussed in the following sections.

6.3.1 The effect of SUMO-1 modification of PML

Although the precise significance of SUMO-1 modification remains unclear, it has been demonstrated to directly contribute to recruitment of proteins (e.g. PML and p53) into ND10. As illustrated in Fig. 4.5, SUMO-1 modified forms of PML were hardly detected in NT2 cells, which indicates that either less endogenous SUMO-1 exists in NT2 cells or, somehow, SUMO-1 is not able to be conjugated to PML efficiently. However there is a possibility that high levels of SUMO-1 may simultaneously increase the proportion of PML modified by SUMO-1, resulting in more of the diffuse nucleoplasmic form of PML being recruited into ND10 where PML executes its function. Although over-expression of exogenous PML did not affect HSV-1 infection in NT2 cells (data not shown), again the interpretation of this result should consider the fact that PML was largely expressed in the nucleoplasm and cytoplasm (but not in ND10) of transfected cells (discussed in section 6.2.1).

Some lines of evidence have shown that SUMO-1 modification of Sp100 stabilises the interaction of Sp100 with heterochromatin protein HP1 implying a role of SUMO-1 in the dynamic interplay between chromatin and ND10 (Seeler *et al.*, 2001). In addition, SUMO-1 conjugation of PML has been demonstrated to be required for the targeting of proteins (e.g. hDaxx and p53) to ND10 structures, and to modulate their functions in transcription regulation and cell survival control (Li *et al.*, 2000, Fogal *et al.*, 2000). Sp100 was undetectable in NT2 cells, therefore the effect of SUMO-1 modification on viral infection is unlikely to be through the effect of Sp100. As the results in Chapter 3 showed that transient transfection of HP1 or hDaxx strongly repressed the transactivation activity of ICP0 in Vero cells, similar studies using different combinations of constructions expressing hDaxx and HP1 with or without PML or SUMO-1 will allow the elucidation of the effect of SUMO-1 and SUMO-1 modified PML on the regulation of viral gene transcription.

6.3.2 The potential role of SUMO-1 modification of other substrates

SUMO-1 has been shown to conjugate to a number of transcriptional regulators such as p53 (Rodriguez *et al.*, 1999), c-jun (Muller *et al.*, 2000), and TIF-1α (Seeler *et al.*, 2001). It has been demonstrated that the effect of SUMO-1 on transcriptional regulation is in substrate- and promoter- specific manners. For example, SUMO-1 modification enhanced p53 transactivation from the PIG3 promoter, but not the p21 promoter (Rodriguez *et al.*, 1999), whereas SUMO-1 functions as a repressor of the transcriptional activation function of c-jun (Muller *et al.*, 2000). Since the precise function of SUMO-1 modification remains unclear, more specific studies are required to determine its possible effect on transcription regulation during HSV-1 infection in NT2 cells.

6.4 The effect of SUMO-1 modification on the maintenance of ND10

Punctate staining of Sp100 and hDaxx was absent from a large proportion of cells over-expressing SUMO-1 conjugation mutants (Fig. 5.8- 5.10). In particular, substitution of Gly (97) to Ala of SUMO-1 results in loss of punctate Sp100 staining from ND10 in over 75% of transfected cells, implying that SUMO-1 might be involved in Sp100 localisation into ND10 at a certain level. However, this result is contrast to the observations in Sternsdorf *et al.* (1999) that mutation of the SUMO-1 modification site, lysine (297), abolished SUMO-1 conjugation to Sp100, but did not affect its ND10 localisation. As Sp100 has been shown to form a homodimer and a region (residues 33-149) has been identified to be required for this function (Sternsdorf *et al.*, 1999), it is possible that endogenous Sp100 modified by SUMO-1 forms a homodimer with the mutant Sp100 molecule and subsequently directs it to ND10. Thus the Sp100 (K297A) mutant could be detected in ND10, although it was not itself SUMO-1 modified. The loss of punctate Sp100 and hDaxx staining was also observed in cells transfected with other SUMO-1 mutants (AG/HSTV, AG) which express partially active forms of SUMO-1, when these proteins were distributed in a nuclear diffuse pattern. These results indicate that the ND10 localisation of SUMO-1 is important for recruitment of proteins into ND10 and for maintenance of ND10 structure.

In summary, there are intriguing hints that the pathways of SUMO-modification, PML, ND10 and IFNs may be inter-connected and contribute to an intracellular antiviral defense, but precise details at present remain elusive.

BIBLIOGRAPHIES

BIBLIOGRAPHIES

Ablashi, D. V., Salahuddin, S. Z., Josephs, S. F., Balachandran, N., Krueger, G. R. & Gallo, R. C. (1991). Human herpesvirus-6 (HHV-6) (short review). *In Vivo* **5**, 193-9.

Ackermann, H.-W., Berthiaume, L. & Tremblay, M. (1998). Virus life in diagrams, pp. 52. Boca Raton: CRC Press.

Ackermann, M., Braun, D. K., Pereira, L. & Roizman, B. (1984). Characterization of herpes simplex virus 1 alpha proteins 0, 4, and 27 with monoclonal antibodies. *J Virol* **52**, 108-18.

Adachi, A. & Oshima, Y. (1999). Cell-dependent functional roles of HIV-1 Nef for virus replication (review). *Int J Mol Med* **3**, 427-30.

Adamson, A. L. & Kenney, S. (2001). Epstein-barr virus immediate-early protein BZLF1 is SUMO-1 modified and disrupts promyelocytic leukemia bodies. *J Virol* **75**, 2388-99.

Affara, N. A., Chalmers, I. J. & Ferguson-Smith, M. A. (1993). Analysis of the SRY gene in 22 sex-reversed XY females identifies four new point mutations in the conserved DNA binding domain. *Hum Mol Genet* **2**, 785-9.

Ahn, J. H. & Hayward, G. S. (1997). The major immediate-early proteins IE1 and IE2 of human cytomegalovirus colocalize with and disrupt PML-associated nuclear bodies at very early times in infected permissive cells. *J Virol* **71**, 4599-613.

Ahn, J. H. & Hayward, G. S. (2000). Disruption of PML-associated nuclear bodies by IE1 correlates with efficient early stages of viral gene expression and DNA replication in human cytomegalovirus infection. *Virology* **274**, 39-55.

Ahn, J. H., Jang, W. J. & Hayward, G. S. (1999). The human cytomegalovirus IE2 and UL112-113 proteins accumulate in viral DNA replication compartments that initiate from the periphery of promyelocytic leukemia protein-associated nuclear bodies (PODs or ND10). *J Virol* **73**, 10458-71.

Ahn, J. H., Xu, Y., Jang, W. J., Matunis, M. J. & Hayward, G. S. (2001). Evaluation of interactions of human cytomegalovirus immediate-early IE2 regulatory protein with small ubiquitin-like modifiers and their conjugation enzyme Ubc9. *J Virol* **75**, 3859-72.

Alcalay, M., Tomassoni, L., Colombo, E., Stoldt, S., Grignani, F., Fagioli, M., Szekely, L., Helin, K. & Pelicci, P. G. (1998). The promyelocytic leukemia gene product (PML) forms stable complexes with the retinoblastoma protein. *Mol Cell Biol* **18**, 1084-93.

Alford, C. A., Stagno, S., Pass, R. F. & Britt, W. J. (1990). Congenital and perinatal cytomegalovirus infections. *Rev Infect Dis* **12 Suppl 7**, S745-53.

Ali, S., Metzger, D., Bornert, J. M. & Chambon, P. (1993). Modulation of transcriptional activation by ligand-dependent phosphorylation of the human oestrogen receptor A/B region. *Embo J* **12**, 1153-60.

Altabef, M., Garcia, M., Lavau, C., Bae, S. C., Dejean, A. & Samarut, J. (1996). A retrovirus carrying the promyelocyte-retinoic acid receptor PML-RARalpha fusion gene transforms haematopoietic progenitors in vitro and induces acute leukaemias. *Embo J* **15**, 2707-16.

Alvira, M. R., Goins, W. F., Cohen, J. B. & Glorioso, J. C. (1999). Genetic studies exposing the splicing events involved in herpes simplex virus type 1 latency-associated transcript production during lytic and latent infection. *J Virol* **73**, 3866-76.

Arbustini, E., Morbini, P., Grasso, M., Diegoli, M., Fasani, R., Porcu, E., Banchieri, N., Perfetti, V., Pederzolli, C., Grossi, P., Dalla Gasperina, D., Martinelli, L., Paulli, M., Ernst, M., Plachter, B., Vigano, M. & Solcia, E. (1996). Human cytomegalovirus early infection, acute rejection, and major histocompatibility class II expression in transplanted lung. Molecular, immunocytochemical, and histopathologic investigations. *Transplantation* **61**, 418-27.

Arthur, J. L., Scarpini, C. G., Connor, V., Lachmann, R. H., Tolkovsky, A. M. & Efstathiou, S. (2001). Herpes simplex virus type 1 promoter activity during latency establishment, maintenance, and reactivation in primary dorsal root neurons in vitro. *J Virol* **75**, 3885-95.

Arvin, A. M. (1996). Varicella-zoster virus: overview and clinical manifestations. *Semin Dermatol* **15**, 4-7.

Ascoli, C. A. & Maul, G. G. (1991). Identification of a novel nuclear domain. *J Cell Biol* **112**, 785-95.

Baer, R., Bankier, A. T., Biggin, M. D., Deininger, P. L., Farrell, P. J., Gibson, T. J., Hatfull, G., Hudson, G. S., Satchwell, S. C., Seguin, C. & et al. (1984). DNA sequence and expression of the B95-8 Epstein-Barr virus genome. *Nature* **310**, 207-11.

Balfour, H. H., Jr. (1999). Antiviral drugs. *N Engl J Med* **340**, 1255-68.

Barlow, P. N., Luisi, B., Milner, A., Elliott, M. & Everett, R. (1994). Structure of the C3HC4 domain by 1H-nuclear magnetic resonance spectroscopy. A new structural class of zinc-finger. *J Mol Biol* **237**, 201-11.

Bell, P., Brazas, R., Ganem, D. & Maul, G. G. (2000). Hepatitis delta virus replication generates complexes of large hepatitis delta antigen and antigenomic RNA that affiliate with and alter nuclear domain 10. *J Virol* **74**, 5329-36.

Ben-Zeev, A. & Becker, Y. (1977). Requirement of host cell RNA polymerase II in the replication of herpes simplex virus in alpha-amanitin-sensitive and -resistant cell lines. *Virology* **76**, 246-53.

Bernstein, D. I. & Stanberry, L. R. (1999). Herpes simplex virus vaccines. *Vaccine* **17**, 1681-9.

Bernstein, R. M., Neuberger, J. M., Bunn, C. C., Callender, M. E., Hughes, G. R. & Williams, R. (1984). Diversity of autoantibodies in primary biliary cirrhosis and chronic active hepatitis. *Clin Exp Immunol* **55**, 553-60.

Biron, K. K., Stanat, S. C., Sorrell, J. B., Fyfe, J. A., Keller, P. M., Lambe, C. U. & Nelson, D. J. (1985). Metabolic activation of the nucleoside analog 9-[(2-hydroxy-1-(hydroxymethyl)ethoxy]methyl)guanine in human diploid fibroblasts infected with human cytomegalovirus. *Proc Natl Acad Sci U S A* **82**, 2473-7.

Bloch, D. B., de la Monte, S. M., Guigaouri, P., Filippov, A. & Bloch, K. D. (1996). Identification and characterization of a leukocyte-specific component of the nuclear body. *J Biol Chem* **271**, 29198-204.

Block, T., Barney, S., Masonis, J., Maggioncalda, J., Valyi-Nagy, T. & Fraser, N. W. (1994). Long term herpes simplex virus type 1 infection of nerve growth factor-treated PC12 cells. *J Gen Virol* **75**, 2481-7.

Block, T. M., Deshmane, S., Masonis, J., Maggioncalda, J., Valyi-Nagi, T. & Fraser, N. W. (1993). An HSV LAT null mutant reactivates slowly from latent infection and makes small plaques on CV-1 monolayers. *Virology* **192**, 618-30.

Block, T. M., Spivack, J. G., Steiner, I., Deshmane, S., McIntosh, M. T., Lirette, R. P. & Fraser, N. W. (1990). A herpes simplex virus type 1 latency-associated transcript mutant reactivates with normal kinetics from latent infection. *J Virol* **64**, 3417-26.

Bloom, D. C., Hill, J. M., Devi-Rao, G., Wagner, E. K., Feldman, L. T. & Stevens, J. G. (1996). A 348-base-pair region in the latency-associated transcript facilitates herpes simplex virus type 1 reactivation. *J Virol* **70**, 2449-59.

Boddy, M. N., Duprez, E., Borden, K. L. & Freemont, P. S. (1997). Surface residue mutations of the PML RING finger domain alter the formation of nuclear matrix-associated PML bodies. *J Cell Sci* **110**, 2197-205.

Boddy, M. N., Howe, K., Etkin, L. D., Solomon, E. & Freemont, P. S. (1996). PIC 1, a novel ubiquitin-like protein which interacts with the PML component of a multiprotein complex that is disrupted in acute promyelocytic leukaemia. *Oncogene* **13**, 971-82.

Boehmer, P. E., Dodson, M. S. & Lehman, I. R. (1993). The herpes simplex virus type-1 origin binding protein. DNA helicase activity. *J Biol Chem* **268**, 1220-5.

Boehmer, P. E. & Lehman, I. R. (1997). Herpes simplex virus DNA replication. *Annu Rev Biochem* **66**, 347-84.

Booy, F. P., Newcomb, W. W., Trus, B. L., Brown, J. C., Baker, T. S. & Steven, A. C. (1991). Liquid-crystalline, phage-like packing of encapsidated DNA in herpes simplex virus. *Cell* **64**, 1007-15.

Borden, K. L., Campbell Dwyer, E. J. & Salvato, M. S. (1998). An arenavirus RING (zinc-binding) protein binds the oncoprotein promyelocyte leukemia protein (PML) and relocates PML nuclear bodies to the cytoplasm. *J Virol* **72**, 758-66.

Borden, K. L., Lally, J. M., Martin, S. R., O'Reilly, N. J., Solomon, E. & Freemont, P. S. (1996). In vivo and in vitro characterization of the B1 and B2 zinc-binding domains from the acute promyelocytic leukemia protooncoprotein PML. *Proc Natl Acad Sci U S A* **93**, 1601-6.

Boutell, C., Sadis, S. & Everett, R. D. (2002). Herpes simplex virus type 1 immediate-early protein ICP0 and is isolated RING finger domain act as ubiquitin E3 ligases in vitro. *J Virol* **76**, 841-50.

Bratcher, D. F., Harrison, C. J., Bourne, N., Stanberry, L. R. & Bernstein, D. I. (1993). Effect of indomethacin on ultraviolet radiation-induced recurrent herpes simplex virus disease in guinea-pigs. *J Gen Virol* **74**, 1951-4.

Brown, S. M., Ritchie, D. A. & Subak-Sharpe, J. H. (1973). Genetic studies with herpes simplex virus type 1. The isolation of temperature-sensitive mutants, their arrangement into complementation groups and recombination analysis leading to a linkage map. *J Gen Virol* **18**, 329-46.

Browne, H., Bruun, B. & Minson, T. (2001). Plasma membrane requirements for cell fusion induced by herpes simplex virus type 1 glycoproteins gB, gD, gH and gL. *J Gen Virol* **82**, 1419-22.

Brugha, R., Keersmaekers, K., Renton, A. & Meheus, A. (1997). Genital herpes infection: a review. *Int J Epidemiol* **26**, 698-709.

Bryant, H. E., Matthews, D. A., Wadd, S., Scott, J. E., Kean, J., Graham, S., Russell, W. C. & Clements, J. B. (2000). Interaction between herpes simplex virus type 1 IE63 protein and cellular protein p32. *J Virol* **74**, 11322-8.

Bryant, H. E., Wadd, S. E., Lamond, A. I., Silverstein, S. J. & Clements, J. B. (2001). Herpes simplex virus IE63 (ICP27) protein interacts with spliceosome-associated protein 145 and inhibits splicing prior to the first catalytic step. *J Virol* **75**, 4376-85.

Burkham, J., Coen, D. M., Hwang, C. B. & Weller, S. K. (2001). Interactions of herpes simplex virus type 1 with ND10 and recruitment of PML to replication compartments. *J Virol* **75**, 2353-67.

Cai, W., Astor, T. L., Liptak, L. M., Cho, C., Coen, D. M. & Schaffer, P. A. (1993). The herpes simplex virus type 1 regulatory protein ICP0 enhances virus replication during acute infection and reactivation from latency. *J Virol* **67**, 7501-12.

Cai, W. & Schaffer, P. A. (1991). A cellular function can enhance gene expression and plating efficiency of a mutant defective in the gene for ICP0, a transactivating protein of herpes simplex virus type 1. *J Virol* **65**, 4078-90.

Cai, W. H., Gu, B. & Person, S. (1988). Role of glycoprotein B of herpes simplex virus type 1 in viral entry and cell fusion. *J Virol* **62**, 2596-604.

Cai, W. Z. & Schaffer, P. A. (1989). Herpes simplex virus type 1 ICP0 plays a critical role in the de novo synthesis of infectious virus following transfection of viral DNA. *J Virol* **63**, 4579-89.

Cao, T., Duprez, E., Borden, K. L., Freemont, P. S. & Etkin, L. D. (1998). Ret finger protein is a normal component of PML nuclear bodies and interacts directly with PML. *J Cell Sci* **111**, 1319-29.

Carfi, A., Willis, S. H., Whitbeck, J. C., Krummenacher, C., Cohen, G. H., Eisenberg, R. J. & Wiley, D. C. (2001). Herpes simplex virus glycoprotein D bound to the human receptor HveA. *Mol Cell* **8**, 169-79.

Carrozza, M. J. & DeLuca, N. (1998). The high mobility group protein 1 is a coactivator of herpes simplex virus ICP4 in vitro. *J Virol* **72**, 6752-7.

Carter, K. L. & Roizman, B. (1996). The promoter and transcriptional unit of a novel herpes simplex virus 1 alpha gene are contained in, and encode a protein in frame with, the open reading frame of the alpha 22 gene. *J Virol* **70**, 172-8.

Carvalho, T., Seeler, J. S., Ohman, K., Jordan, P., Pettersson, U., Akusjarvi, G., Carmo-Fonseca, M. & Dejean, A. (1995). Targeting of adenovirus E1A and E4-ORF3 proteins to nuclear matrix-associated PML bodies. *J Cell Biol* **131**, 45-56.

Cha, T. A., Tom, E., Kemble, G. W., Duke, G. M., Mocarski, E. S. & Spaete, R. R. (1996). Human cytomegalovirus clinical isolates carry at least 19 genes not found in laboratory strains. *J Virol* **70**, 78-83.

Challberg, M. D. (1986). A method for identifying the viral genes required for herpesvirus DNA replication. *Proc Natl Acad Sci U S A* **83**, 9094-8.

Challberg, M. D. & Kelly, T. J. (1989). Animal virus DNA replication. *Annu Rev Biochem* **58**, 671-717.

Chang, H. Y., Nishitoh, H., Yang, X., Ichijo, H. & Baltimore, D. (1998). Activation of apoptosis signal-regulating kinase 1 (ASK1) by the adapter protein Daxx. *Science* **281**, 1860-3.

Chang, Y., Cesarman, E., Pessin, M. S., Lee, F., Culpepper, J., Knowles, D. M. & Moore, P. S. (1994). Identification of herpesvirus-like DNA sequences in AIDS-associated Kaposi's sarcoma. *Science* **266**, 1865-9.

Chee, M. S., Bankier, A. T., Beck, S., Bohni, R., Brown, C. M., Cerny, R., Horsnell, T., Hutchison, C. A., 3rd, Kouzarides, T., Martignetti, J. A. & et al. (1990). Analysis of the protein-coding content of the sequence of human cytomegalovirus strain AD169. *Curr Top Microbiol Immunol* **154**, 125-69.

Chelbi-Alix, M. K. & de The, H. (1999). Herpes virus induced proteasome-dependent degradation of the nuclear bodies-associated PML and Sp100 proteins. *Oncogene* **18**, 935-41.

Chelbi-Alix, M. K., Pelicano, L., Quignon, F., Koken, M. H., Venturini, L., Stadler, M., Pavlovic, J., Degos, L. & de The, H. (1995). Induction of the PML protein by interferons in normal and APL cells. *Leukemia* **9**, 2027-33.

Chelbi-Alix, M. K., Quignon, F., Pelicano, L., Koken, M. H. & de The, H. (1998). Resistance to virus infection conferred by the interferon-induced promyelocytic leukemia protein. *J Virol* **72**, 1043-51.

Chen, A., Mannen, H. & Li, S. S. (1998). Characterization of mouse ubiquitin-like SMT3A and SMT3B cDNAs and gene/pseudogenes. *Biochem Mol Biol Int* **46**, 1161-74.

Chen, J. X., Zhu, X. X. & Silverstein, S. (1991). Mutational analysis of the sequence encoding ICP0 from herpes simplex virus type 1. *Virology* **180**, 207-20.

Chen, Y. M. & Knipe, D. M. (1996). A dominant mutant form of the herpes simplex virus ICP8 protein decreases viral late gene transcription. *Virology* **221**, 281-90.

Cheung, A. K. (1989). DNA nucleotide sequence analysis of the immediate-early gene of pseudorabies virus. *Nucleic Acids Res* **17**, 4637-46.

Cho, Y., Lee, I., Maul, G. G. & Yu, E. (1998). A novel nuclear substructure, ND10: distribution in normal and neoplastic human tissues. *Int J Mol Med* **1**, 717-24.

Ciufo, D. M., Mullen, M. A. & Hayward, G. S. (1994). Identification of a dimerization domain in the C-terminal segment of the IE110 transactivator protein from herpes simplex virus. *J Virol* **68**, 3267-82.

Claesson-Welsh, L. & Spear, P. G. (1986). Oligomerization of herpes simplex virus glycoprotein B. *J Virol* **60**, 803-6.

Clements, G. B. & Stow, N. D. (1989). A herpes simplex virus type 1 mutant containing a deletion within immediate early gene 1 is latency-competent in mice. *J Gen Virol* **70**, 2501-6.

Clements, J. B., Watson, R. J. & Wilkie, N. M. (1977). Temporal regulation of herpes simplex virus type 1 transcription: location of transcripts on the viral genome. *Cell* **12**, 275-85.

Coen, D. M., Weinheimer, S. P. & McKnight, S. L. (1986). A genetic approach to promoter recognition during trans induction of viral gene expression. *Science* **234**, 53-9.

Conner, J., Murray, J., Cross, A., Clements, J. B. & Marsden, H. S. (1995). Intracellular localisation of herpes simplex virus type 1 ribonucleotide reductase subunits during infection of cultured cells. *Virology* **213**, 615-23.

Cook, W. J., Gu, B., DeLuca, N. A., Moynihan, E. B. & Coen, D. M. (1995). Induction of transcription by a viral regulatory protein depends on the relative strengths of functional TATA boxes. *Mol Cell Biol* **15**, 4998-5006.

Corbellino, M., Poirel, L., Aubin, J. T., Paulli, M., Magrini, U., Bestetti, G., Galli, M. & Parravicini, C. (1996). The role of human herpesvirus 8 and Epstein-Barr virus in the pathogenesis of giant lymph node hyperplasia (Castleman's disease). *Clin Infect Dis* **22**, 1120-1.

Corey, L. (1993). Herpes simplex virus infections during the decade since the licensure of acyclovir. *J Med Virol* **Suppl**, 7-12.

Corey, L., Langenberg, A. G., Ashley, R., Sekulovich, R. E., Izu, A. E., Douglas, J. M., Jr., Handsfield, H. H., Warren, T., Marr, L., Tyring, S., DiCarlo, R., Adimora, A. A., Leone, P., Dekker, C. L., Burke, R. L., Leong, W. P. & Straus, S. E. (1999). Recombinant glycoprotein vaccine for the prevention of genital HSV-2 infection: two randomized controlled trials. Chiron HSV Vaccine Study Group. *Jama* **282**, 331-40.

Costanzo, F., Campadelli-Fiume, G., Foa-Tomasi, L. & Cassai, E. (1977). Evidence that herpes simplex virus DNA is transcribed by cellular RNA polymerase B. *J Virol* **21**, 996-1001.

Crawford, D. H. (2001). Biology and disease associations of Epstein-Barr virus. *Philos Trans R Soc Lond B Biol Sci* **356**, 461-73.

Cullen, B. R. (1987). Use of eukaryotic expression technology in the functional analysis of cloned genes. *Methods Enzymol* **152**, 684-704.

Danaher, R. J., Jacob, R. J., Chorak, M. D., Freeman, C. S. & Miller, C. S. (1999a). Heat stress activates production of herpes simplex virus type 1 from quiescently infected neurally differentiated PC12 cells. *J Neurovirol* **5**, 374-83.

Danaher, R. J., Jacob, R. J. & Miller, C. S. (1999b). Establishment of a quiescent herpes simplex virus type 1 infection in neurally-differentiated PC12 cells. *J Neurovirol* **5**, 258-67.

Daniel, M. T., Koken, M., Romagne, O., Barbey, S., Bazarbachi, A., Stadler, M., Guillemin, M. C., Degos, L., Chomienne, C. & de The, H. (1993). PML protein expression in hematopoietic and acute promyelocytic leukemia cells. *Blood* **82**, 1858-67.

Dargan, D. J., Jamieson, F. E., MacLean, J., Dolan, A., Addison, C. & McGeoch, D. J. (1997). The published DNA sequence of human cytomegalovirus strain AD169 lacks 929 base pairs affecting genes UL42 and UL43. *J Virol* **71**, 9833-6.

Darnell, J. E., Jr., Kerr, I. M. & Stark, G. R. (1994). Jak-STAT pathways and transcriptional activation in response to IFNs and other extracellular signaling proteins. *Science* **264**, 1415-21.

Davison, A. J. & Scott, J. E. (1986). The complete DNA sequence of varicella-zoster virus. *J Gen Virol* **67**, 1759-816.

de The, H., Lavau, C., Marchio, A., Chomienne, C., Degos, L. & Dejean, A. (1991). The PML-RAR alpha fusion mRNA generated by the t(15;17) translocation in acute promyelocytic leukemia encodes a functionally altered RAR. *Cell* **66**, 675-84.

Deatly, A. M., Spivack, J. G., Lavi, E. & Fraser, N. W. (1987). RNA from an immediate early region of the type 1 herpes simplex virus genome is present in the trigeminal ganglia of latently infected mice. *Proc Natl Acad Sci U S A* **84**, 3204-8.

DeLuca, N. A. & Schaffer, P. A. (1985). Activation of immediate-early, early, and late promoters by temperature-sensitive and wild-type forms of herpes simplex virus type 1 protein ICP4. *Mol Cell Biol* **5**, 1997-208.

Desbois, C., Rousset, R., Bantignies, F. & Jalinot, P. (1996). Exclusion of Int-6 from PML nuclear bodies by binding to the HTLV-I Tax oncoprotein. *Science* **273**, 951-3.

Desterro, J. M., Rodriguez, M. S., Kemp, G. D. & Hay, R. T. (1999). Identification of the enzyme required for activation of the small ubiquitin-like protein SUMO-1. *J Biol Chem* **274**, 10618-24.

Desterro, J. M., Thomson, J. & Hay, R. T. (1997). Ubch9 conjugates SUMO but not ubiquitin. *FEBS Lett* **417**, 297-300.

Devi-Rao, G. B., Goodart, S. A., Hecht, L. M., Rochford, R., Rice, M. K. & Wagner, E. K. (1991). Relationship between polyadenylated and nonpolyadenylated herpes simplex virus type 1 latency-associated transcripts. *J Virol* **65**, 2179-90.

Di Luca, D., Mirandola, P., Ravaioli, T., Bigoni, B. & Cassai, E. (1996). Distribution of HHV-6 variants in human tissues. *Infect Agents Dis* **5**, 203-14.

Djavani, M., Rodas, J., Lukashevich, I. S., Horejsh, D., Pandolfi, P. P., Borden, K. L. & Salvato, M. S. (2001). Role of the promyelocytic leukemia protein PML in the interferon sensitivity of lymphocytic choriomeningitis virus. *J Virol* **75**, 6204-8.

Dolan, A., Jamieson, F. E., Cunningham, C., Barnett, B. C. & McGeoch, D. J. (1998). The genome sequence of herpes simplex virus type 2. *J Virol* **72**, 2010-21.

Dueland, A. N. (1996). Latency and reactivation of varicella zoster virus infections. *Scand J Infect Dis Suppl* **100**, 46-50.

Dunn, C., O'Dowd, A. & Randall, R. E. (1999). Fine mapping of the binding sites of monoclonal antibodies raised against the Pk tag. *J Immunol Methods* **224**, 141-50.

Duprez, E., Saurin, A. J., Desterro, J. M., Lallemand-Breitenbach, V., Howe, K., Boddy, M. N., Solomon, E., de The, H., Hay, R. T. & Freemont, P. S. (1999). SUMO-1 modification of the acute promyelocytic leukaemia protein PML: implications for nuclear localisation. *J Cell Sci* **112**, 381-93.

Dyck, J. A., Maul, G. G., Miller, W. H., Jr., Chen, J. D., Kakizuka, A. & Evans, R. M. (1994). A novel macromolecular structure is a target of the promyelocyte-retinoic acid receptor oncoprotein. *Cell* **76**, 333-43.

Earnshaw, W. C. (1988). Mitotic chromosome structure. *Bioessays* **9**, 147-50.

Earnshaw, W. C. & Rothfield, N. (1985). Identification of a family of human centromere proteins using autoimmune sera from patients with scleroderma. *Chromosoma* **91**, 313-21.

Ecob-Prince, M. S., Preston, C. M., Rixon, F. J., Hassan, K. & Kennedy, P. G. (1993). Neurons containing latency-associated transcripts are numerous and widespread in dorsal root ganglia following footpad inoculation of mice with herpes simplex virus type 1 mutant in1814. *J Gen Virol* **74**, 985-94.

Eissenberg, J. C., James, T. C., Foster-Hartnett, D. M., Hartnett, T., Ngan, V. & Elgin, S. C. (1990). Mutation in a heterochromatin-specific chromosomal protein is associated with suppression of position-effect variegation in Drosophila melanogaster. *Proc Natl Acad Sci U S A* **87**, 9923-7.

Elias, P., Gustafsson, C. M., Hammarsten, O. & Stow, N. D. (1992). Structural elements required for the cooperative binding of the herpes simplex virus origin binding protein to oriS reside in the N-terminal part of the protein. *J Biol Chem* **267**, 17424-9.

Elion, G. B., Furman, P. A., Fyfe, J. A., de Miranda, P., Beauchamp, L. & Schaeffer, H. J. (1977). Selectivity of action of an antiherpetic agent, 9-(2- hydroxyethoxymethyl) guanine. *Proc Natl Acad Sci U S A* **74**, 5716-20.

Engelhardt, O. G., Ullrich, E., Kochs, G. & Haller, O. (2001). Interferon-induced antiviral Mx1 GTPase is associated with components of the SUMO-1 system and promyelocytic leukemia protein nuclear bodies. *Exp Cell Res* **271**, 286-95.

Epstein, M. A., Achong, B. G. & Barr, Y. M. (1964). Virus particles in cultured lymphoblasts from Burkitt's lymphoma. *Lancet* 1, 702-3.

Everett, R. D. (1984a). A detailed analysis of an HSV-1 early promoter: sequences involved in trans-activation by viral immediate-early gene products are not early-gene specific. *Nucleic Acids Res* **12**, 3037-56.

Everett, R. D. (1984b). Trans activation of transcription by herpes virus products: requirement for two HSV-1 immediate-early polypeptides for maximum activity. *Embo J* **3**, 3135-41.

Everett (1985). Activation of cellular promoters during herpes virus infection of biochemically transformed cells. *Embo J* **4**, 1973-80.

Everett, R. D. (1986). The products of herpes simplex virus type 1 (HSV-1) immediate early genes 1, 2 and 3 can activate HSV-1 gene expression in trans. *J Gen Virol* **67**, 2507-13.

Everett, R. D. (1987). A detailed mutational analysis of Vmw110, a trans-acting transcriptional activator encoded by herpes simplex virus type 1. *Embo J* **6**, 2069-76.

Everett, R. D. (1988a). Analysis of the functional domains of herpes simplex virus type 1 immediate-early polypeptide Vmw110. *J Mol Biol* **202**, 87-96.

Everett, R. D. (1988b). Promoter sequence and cell type can dramatically affect the efficiency of transcriptional activation induced by herpes simplex virus type 1 and its immediate-early gene products Vmw175 and Vmw110. *J Mol Biol* **203**, 739-51.

Everett, R. D. (1989). Construction and characterization of herpes simplex virus type 1 mutants with defined lesions in immediate early gene 1. *J Gen Virol* **70**, 1185-202.

Everett, R. D., Orr, A. & Elliott, M. (1991). High level expression and purification of herpes simplex virus type 1 immediate early polypeptide Vmw110. *Nucleic Acids Res* **19**, 6155-61.

Everett, R., Cross, A., Tyler, J. & Orr, A. (1993a). An epitope within the DNA-binding domain of the herpes simplex virus immediate early protein Vmw175 is conserved in the varicella-zoster virus gene 62 protein. *J Gen Virol* **74**, 1955-8.

Everett, R. D., Barlow, P., Milner, A., Luisi, B., Orr, A., Hope, G. & Lyon, D. (1993b). A novel arrangement of zinc-binding residues and secondary structure in the C3HC4 motif of an alpha herpes virus protein family. *J Mol Biol* **234**, 1038-47.

Everett, R. D., Cross, A. & Orr, A. (1993c). A truncated form of herpes simplex virus type 1 immediate-early protein Vmw110 is expressed in a cell type dependent manner. *Virology* **197**, 751-6.

Everett, R. D. & Maul, G. G. (1994). HSV-1 IE protein Vmw110 causes redistribution of PML. *Embo J* **13**, 5062-9.

Everett, R., O'Hare, P., O'Rourke, D., Barlow, P. & Orr, A. (1995a). Point mutations in the herpes simplex virus type 1 Vmw110 RING finger helix affect activation of gene expression, viral growth, and interaction with PML-containing nuclear structures. *J Virol* **69**, 7339-44.

Everett, R., Orr, A. & Elliott, M. (1995b). The equine herpesvirus 1 gene 63 RING finger protein partially complements Vmw110, its herpes simplex virus type 1 counterpart. *J Gen Virol* **76**, 2369-74.

Everett, R. D., Meredith, M., Orr, A., Cross, A., Kathoria, M. & Parkinson, J. (1997). A novel ubiquitin-specific protease is dynamically associated with the PML nuclear domain and binds to a herpesvirus regulatory protein. *Embo J* **16**, 1519-30.

Everett, R. D., Freemont, P., Saitoh, H., Dasso, M., Orr, A., Kathoria, M. & Parkinson, J. (1998a). The disruption of ND10 during herpes simplex virus infection correlates with the Vmw110- and proteasome-dependent loss of several PML isoforms. *J Virol* **72**, 6581-91.

Everett, R. D., Orr, A. & Preston, C. M. (1998b). A viral activator of gene expression functions via the ubiquitin-proteasome pathway. *Embo J* **17**, 7161-9.

Everett, R. D., Earnshaw, W. C., Findlay, J. & Lomonte, P. (1999a). Specific destruction of kinetochore protein CENP-C and disruption of cell division by herpes simplex virus immediate-early protein Vmw110. *Embo J* **18**, 1526-38.

Everett, R. D., Earnshaw, W. C., Pluta, A. F., Sternsdorf, T., Ainsztein, A. M., Carmena, M., Ruchaud, S., Hsu, W. L. & Orr, A. (1999b). A dynamic connection between centromeres and ND10 proteins. *J Cell Sci* **112**, 3443-54.

Everett, R. D., Meredith, M. & Orr, A. (1999c). The ability of herpes simplex virus type 1 immediate-early protein Vmw110 to bind to a ubiquitin-specific protease contributes to

its roles in the activation of gene expression and stimulation of virus replication. *J Virol* **73**, 417-26.

Everett, R. D. (2000). ICP0, a regulator of herpes simplex virus during lytic and latent infection. *Bioessays* **22**, 761-70.

Everett, R. D. (2001). DNA viruses and viral proteins that interact with PML nuclear bodies. *Oncogene* **20**, 7266-73.

Fagioli, M., Alcalay, M., Tomassoni, L., Ferrucci, P. F., Mencarelli, A., Riganelli, D., Grignani, F., Pozzan, T., Nicoletti, I. & Pelicci, P. G. (1998). Cooperation between the RING + B1-B2 and coiled-coil domains of PML is necessary for its effects on cell survival. *Oncogene* **16**, 2905-13.

Flint, J. & Shenk, T. (1997). Viral transactivating proteins. *Annu Rev Genet* **31**, 177-212.

Fogal, V., Gostissa, M., Sandy, P., Zacchi, P., Sternsdorf, T., Jensen, K., Pandolfi, P. P., Will, H., Schneider, C. & Del Sal, G. (2000). Regulation of p53 activity in nuclear bodies by a specific PML isoform. *Embo J* **19**, 6185-95.

Forrester, A., Farrell, H., Wilkinson, G., Kaye, J., Davis-Poynter, N. & Minson, T. (1992). Construction and properties of a mutant of herpes simplex virus type 1 with glycoprotein H coding sequences deleted. *J Virol* **66**, 341-8.

Freemont, P. S. (1993). The RING finger. A novel protein sequence motif related to the zinc finger. *Ann N Y Acad Sci* **684**, 174-92.

Freemont, P. S. (2000). RING for destruction? *Curr Biol* **10**, R84-7.

Freemont, P. S., Hanson, I. M. & Trowsdale, J. (1991). A novel cysteine-rich sequence motif. *Cell* **64**, 483-4.

Furlong, D., Swift, H. & Roizman, B. (1972). Arrangement of herpesvirus deoxyribonucleic acid in the core. *J Virol* **10**, 1071-4.

Gao, M. & Knipe, D. M. (1991). Potential role for herpes simplex virus ICP8 DNA replication protein in stimulation of late gene expression. *J Virol* **65**, 2666-75.

Gao, M., Matusick-Kumar, L., Hurlburt, W., DiTusa, S. F., Newcomb, W. W., Brown, J. C., McCann, P. J., 3rd, Deckman, I. & Colonno, R. J. (1994). The protease of herpes simplex virus type 1 is essential for functional capsid formation and viral growth. *J Virol* **68**, 3702-12.

Gelman, I. H. & Silverstein, S. (1985). Identification of immediate early genes from herpes simplex virus that transactivate the virus thymidine kinase gene. *Proc Natl Acad Sci U S A* **82**, 5265-9.

Gelman, I. H. & Silverstein, S. (1986). Co-ordinate regulation of herpes simplex virus gene expression is mediated by the functional interaction of two immediate early gene products. *J Mol Biol* **191**, 395-409.

Geraghty, R. J., Krummenacher, C., Cohen, G. H., Eisenberg, R. J. & Spear, P. G. (1998). Entry of alphaherpesviruses mediated by poliovirus receptor-related protein 1 and poliovirus receptor. *Science* **280**, 1618-20.

Gerdes, J. C. & Smith, D. S. (1983). Recurrence phenotypes and establishment of latency following rabbit keratitis produced by multiple herpes simplex virus strains. *J Gen Virol* **64**, 2441-54.

Glaser, S. L. & Jarrett, R. F. (1996). The epidemiology of Hodgkin's disease. *Baillieres Clin Haematol* **9**, 401-16.

Goddard, A. D., Borrow, J., Freemont, P. S. & Solomon, E. (1991). Characterization of a zinc finger gene disrupted by the t(15;17) in acute promyelocytic leukemia. *Science* **254**, 1371-4.

Gompels, U. A., Nicholas, J., Lawrence, G., Jones, M., Thomson, B. J., Martin, M. E., Efstathiou, S., Craxton, M. & Macaulay, H. A. (1995). The DNA sequence of human herpesvirus-6: structure, coding content, and genome evolution. *Virology* **209**, 29-51.

Gong, L., Kamitani, T., Fujise, K., Caskey, L. S. & Yeh, E. T. (1997). Preferential interaction of sentrin with a ubiquitin-conjugating enzyme, Ubc9. *J Biol Chem* **272**, 28198-201.

Gong, L., Li, B., Millas, S. & Yeh, E. T. (1999). Molecular cloning and characterization of human AOS1 and UBA2, components of the sentrin-activating enzyme complex. *FEBS Lett* **448**, 185-9.

Gong, L., Millas, S., Maul, G. G. & Yeh, E. T. (2000). Differential regulation of sentrinized proteins by a novel sentrin-specific protease. *J Biol Chem* **275**, 3355-9.

Gorman, C. M., Moffat, L. F. & Howard, B. H. (1982). Recombinant genomes which express chloramphenicol acetyltransferase in mammalian cells. *Mol Cell Biol* **2**, 1044-51.

Gostissa, M., Hengstermann, A., Fogal, V., Sandy, P., Schwarz, S. E., Scheffner, M. & Del Sal, G. (1999). Activation of p53 by conjugation to the ubiquitin-like protein SUMO-1. *Embo J* **18**, 6462-71.

Gottlieb, J., Marcy, A. I., Coen, D. M. & Challberg, M. D. (1990). The herpes simplex virus type 1 UL42 gene product: a subunit of DNA polymerase that functions to increase processivity. *J Virol* **64**, 5976-87.

Granzow, H., Klupp, B. G., Fuchs, W., Veits, J., Osterrieder, N. & Mettenleiter, T. C. (2001). Egress of alphaherpesviruses: comparative ultrastructural study. *J Virol* **75**, 3675-84.

Griffiths, P. D. (2001). Herpesvirus: from the cradle to the grave. *Microbiology Today* **28**, 182-4.

Grotzinger, T., Sternsdorf, T., Jensen, K. & Will, H. (1996). Interferon-modulated expression of genes encoding the nuclear-dot- associated proteins Sp100 and promyelocytic leukemia protein (PML). *Eur J Biochem* **238**, 554-60.

Gu, B. & DeLuca, N. (1994). Requirements for activation of the herpes simplex virus glycoprotein C promoter in vitro by the viral regulatory protein ICP4. *J Virol* **68**, 7953-65.

Guldner, H. H., Szostecki, C., Schroder, P., Matschl, U., Jensen, K., Luders, C., Will, H. & Sternsdorf, T. (1999). Splice variants of the nuclear dot-associated Sp100 protein contain homologies to HMG-1 and a human nuclear phosphoprotein-box motif. *J Cell Sci* **112**, 733-47.

Guzowski, J. F., Singh, J. & Wagner, E. K. (1994). Transcriptional activation of the herpes simplex virus type 1 UL38 promoter conferred by the cis-acting downstream activation sequence is mediated by a cellular transcription factor. *J Virol* **68**, 7774-89.

Halford, W. P., Gebhardt, B. M. & Carr, D. J. (1996). Mechanisms of herpes simplex virus type 1 reactivation. *J Virol* **70**, 5051-60.

Halford, W. P. & Schaffer, P. A. (2000). Optimized viral dose and transient immunosuppression enable herpes simplex virus ICP0-null mutants To establish wild-type levels of latency in vivo. *J Virol* **74**, 5957-67.

Halford, W. P. & Schaffer, P. A. (2001). ICP0 is required for efficient reactivation of herpes simplex virus type 1 from neuronal latency. *J Virol* **75**, 3240-9.

Haller, O., Frese, M. & Kochs, G. (1998). Mx proteins: mediators of innate resistance to RNA viruses. *Rev Sci Tech* **17**, 220-30.

Handler, C. G., Eisenberg, R. J. & Cohen, G. H. (1996). Oligomeric structure of glycoproteins in herpes simplex virus type 1. *J Virol* **70**, 6067-70.

Hardy, W. R. & Sandri-Goldin, R. M. (1994). Herpes simplex virus inhibits host cell splicing, and regulatory protein ICP27 is required for this effect. *J Virol* **68**, 7790-9.

Harris, R. A., Everett, R. D., Zhu, X. X., Silverstein, S. & Preston, C. M. (1989). Herpes simplex virus type 1 immediate-early protein Vmw110 reactivates latent herpes simplex virus type 2 in an in vitro latency system. *J Virol* **63**, 3513-5.

Harris, R. A. & Preston, C. M. (1991). Establishment of latency in vitro by the herpes simplex virus type 1 mutant in1814. *J Gen Virol* **72**, 907-13.

Herold, B. C., Visalli, R. J., Susmarski, N., Brandt, C. R. & Spear, P. G. (1994). Glycoprotein C-independent binding of herpes simplex virus to cells requires cell surface heparan sulphate and glycoprotein B. *J Gen Virol* **75**, 1211-22.

Herold, B. C., WuDunn, D., Soltys, N. & Spear, P. G. (1991). Glycoprotein C of herpes simplex virus type 1 plays a principal role in the adsorption of virus to cells and in infectivity. *J Virol* **65**, 1090-8.

Hidaka, Y., Liu, Y., Yamamoto, M., Mori, R., Miyazaki, C., Kusuhara, K., Okada, K. & Ueda, K. (1993). Frequent isolation of human herpesvirus 7 from saliva samples. *J Med Virol* **40**, 343-6.

Hildesheim, A. & Levine, P. H. (1993). Etiology of nasopharyngeal carcinoma: a review. *Epidemiol Rev* **15**, 466-85.

Hobbs, W. E. & DeLuca, N. A. (1999). Perturbation of cell cycle progression and cellular gene expression as a function of herpes simplex virus ICP0. *J Virol* **73**, 8245-55.

Hochstrasser, M. (1996). Ubiquitin-dependent protein degradation. *Annu Rev Genet* **30**, 405-39.

Hochstrasser, M. (2001). SP-RING for SUMO: new functions bloom for a ubiquitin-like protein. *Cell* **107**, 5-8.

Hogenesch, J. B., Chan, W. K., Jackiw, V. H., Brown, R. C., Gu, Y. Z., Pray-Grant, M., Perdew, G. H. & Bradfield, C. A. (1997). Characterization of a subset of the basic-helix-loop-helix-PAS superfamily that interacts with components of the dioxin signaling pathway. *J Biol Chem* **272**, 8581-93.

Hollenbach, A. D., Sublett, J. E., McPherson, C. J. & Grosveld, G. (1999). The Pax3-FKHR oncoprotein is unresponsive to the Pax3-associated repressor hDaxx. *Embo J* **18**, 3702-11.

Holmes, D. S. & Quigley, M. (1981). A rapid boiling method for the preparation of bacterial plasmids. *Anal Biochem* **114**, 193-7.

Homa, F. L. & Brown, J. C. (1997). Capsid assembly and DNA packaging in herpes simplex virus. *Rev Med Virol* **7**, 107-122.

Homer, E. G., Rinaldi, A., Nicholl, M. J. & Preston, C. M. (1999). Activation of herpesvirus gene expression by the human cytomegalovirus protein pp71. *J Virol* **73**, 8512-8.

Honess, R. W. & Roizman, B. (1974). Regulation of herpesvirus macromolecular synthesis. I. Cascade regulation of the synthesis of three groups of viral proteins. *J Virol* **14**, 8-19.

Hsu, W. L. & Everett, R. D. (2001). Human neuron-committed teratocarcinoma NT2 cell line has abnormal ND10 structures and is poorly infected by herpes simplex virus type 1. *J Virol* **75**, 3819-31.

Hughes, T. A., La Boissiere, S. & O'Hare, P. (1999). Analysis of functional domains of the host cell factor involved in VP16 complex formation. *J Biol Chem* **274**, 16437-43.

Imbalzano, A. N., Coen, D. M. & DeLuca, N. A. (1991). Herpes simplex virus transactivator ICP4 operationally substitutes for the cellular transcription factor Sp1 for efficient expression of the viral thymidine kinase gene. *J Virol* **65**, 565-74.

Imbalzano, A. N. & DeLuca, N. A. (1992). Substitution of a TATA box from a herpes simplex virus late gene in the viral thymidine kinase promoter alters ICP4 inducibility but not temporal expression. *J Virol* **66**, 5453-63.

Isaacs, A. & Lindenmann, J. (1957). Virus interference. I. The interferon. *Proc R Soc Lond B* **147**, 258-67.

Ishov, A. M. & Maul, G. G. (1996). The periphery of nuclear domain 10 (ND10) as site of DNA virus deposition. *J Cell Biol* **134**, 815-26.

Ishov, A. M., Sotnikov, A. G., Negorev, D., Vladimirova, O. V., Neff, N., Kamitani, T., Yeh, E. T., Strauss, J. F. & Maul, G. G. (1999). PML is critical for ND10 formation and recruits the PML-interacting protein daxx to this nuclear structure when modified by SUMO-1. *J Cell Biol* **147**, 221-34.

Ishov, A. M., Stenberg, R. M. & Maul, G. G. (1997). Human cytomegalovirus immediate early interaction with host nuclear structures: definition of an immediate transcript environment. *J Cell Biol* **138**, 5-16.

Jackson, P. K. (2001). A new RING for SUMO: wrestling transcriptional responses into nuclear bodies with PIAS family E3 SUMO ligases. *Genes Dev* **15**, 3053-8.

Jamieson, D. R., Robinson, L. H., Daksis, J. I., Nicholl, M. J. & Preston, C. M. (1995). Quiescent viral genomes in human fibroblasts after infection with herpes simplex virus type 1 Vmw65 mutants. *J Gen Virol* **76**, 1417-31.

Javier, R. T., Stevens, J. G., Dissette, V. B. & Wagner, E. K. (1988). A herpes simplex virus transcript abundant in latently infected neurons is dispensable for establishment of the latent state. *Virology* **166**, 254-7.

Jeffries, D. J. (1991). Intra-uterine and neonatal herpes simplex virus infection. *Scand J Infect Dis Suppl* **80**, 21-6.

Jensen, K., Shiels, C. & Freemont, P. S. (2001). PML protein isoforms and the RBCC/TRIM motif. *Oncogene* **20**, 7223-33.

Johnson, D. C. & Feenstra, V. (1987). Identification of a novel herpes simplex virus type 1-induced glycoprotein which complexes with gE and binds immunoglobulin. *J Virol* **61**, 2208-16.

Johnson, P. A. & Everett, R. D. (1986). The control of herpes simplex virus type-1 late gene transcription: a 'TATA-box'/cap site region is sufficient for fully efficient regulated activity. *Nucleic Acids Res* **14**, 8247-64.

Jons, A., Dijkstra, J. M. & Mettenleiter, T. C. (1998). Glycoproteins M and N of pseudorabies virus form a disulfide-linked complex. *J Virol* **72**, 550-7.

Jons, A., Granzow, H., Kuchling, R. & Mettenleiter, T. C. (1996). The UL49.5 gene of pseudorabies virus codes for an O-glycosylated structural protein of the viral envelope. *J Virol* **70**, 1237-41.

Jordan, R. & Schaffer, P. A. (1997). Activation of gene expression by herpes simplex virus type 1 ICP0 occurs at the level of mRNA synthesis. *J Virol* **71**, 6850-62.

Kamitani, T., Kito, K., Nguyen, H. P., Wada, H., Fukuda-Kamitani, T. & Yeh, E. T. (1998). Identification of three major sentrinization sites in PML. *J Biol Chem* **273**, 26675-82.

Kamitani, T., Nguyen, H. P. & Yeh, E. T. (1997). Preferential modification of nuclear proteins by a novel ubiquitin-like molecule. *J Biol Chem* **272**, 14001-4.

Karr, B. M. & Read, G. S. (1999). The virion host shutoff function of herpes simplex virus degrades the 5' end of a target mRNA before the 3' end. *Virology* **264**, 195-204.

Kastner, P., Perez, A., Lutz, Y., Rochette-Egly, C., Gaub, M. P., Durand, B., Lanotte, M., Berger, R. & Chambon, P. (1992). Structure, localization and transcriptional properties of two classes of retinoic acid receptor alpha fusion proteins in acute promyelocytic leukemia (APL): structural similarities with a new family of oncoproteins. *Embo J* **11**, 629-42.

Katano, H., Ogawa-Goto, K., Hasegawa, H., Kurata, T. & Sata, T. (2001). Human-herpesvirus-8-encoded K8 protein colocalizes with the promyelocytic leukemia protein (PML) bodies and recruits p53 to the PML bodies. *Virology* **286**, 446-55.

Kawaguchi, Y., Bruni, R. & Roizman, B. (1997a). Interaction of herpes simplex virus 1 alpha regulatory protein ICP0 with elongation factor 1delta: ICP0 affects translational machinery. *J Virol* **71**, 1019-24.

Kawaguchi, Y., Tanaka, M., Yokoymama, A., Matsuda, G., Kato, K., Kagawa, H., Hirai, K. & Roizman, B. (2001). Herpes simplex virus 1 alpha regulatory protein ICP0 functionally interacts with cellular transcription factor BMAL1. *Proc Natl Acad Sci U S A* **98**, 1877-1882.

Kawaguchi, Y., Van Sant, C. & Roizman, B. (1997b). Herpes simplex virus 1 alpha regulatory protein ICP0 interacts with and stabilizes the cell cycle regulator cyclin D3. *J Virol* **71**, 7328-36.

Kawaguchi, Y., Van Sant, C. & Roizman, B. (1998). Eukaryotic elongation factor 1delta is hyperphosphorylated by the protein kinase encoded by the U(L)13 gene of herpes simplex virus 1. *J Virol* **72**, 1731-6.

Kellum, R., Raff, J. W. & Alberts, B. M. (1995). Heterochromatin protein 1 distribution during development and during the cell cycle in Drosophila embryos. *J Cell Sci* **108**, 1407-18.

Kelly, C., Van Driel, R. & Wilkinson, G. W. (1995). Disruption of PML-associated nuclear bodies during human cytomegalovirus infection. *J Gen Virol* **76**, 2887-93.

Kemp, L. M., Gelman, I. H., Silverstein, S. J. & Latchman, D. S. (1990). Regulation of herpes simplex virus immediate-early gene promoters in mouse neuroblastoma cells. *Neurosci Lett* **118**, 185-8.

Kikuchi, G. E., Glorioso, J. C. & Nairn, R. (1990). Cross-linking studies show that herpes simplex virus type 1 glycoprotein C molecules are clustered in the membrane of infected cells. *J Gen Virol* **71**, 455-8.

Kim, K. I., Baek, S. H., Jeon, Y. J., Nishimori, S., Suzuki, T., Uchida, S., Shimbara, N., Saitoh, H., Tanaka, K. & Chung, C. H. (2000). A new SUMO-1-specific protease, SUSP1, that is highly expressed in reproductive organs. *J Biol Chem* **275**, 14102-6.

Kinghorn, G. R. (1993). Genital herpes: natural history and treatment of acute episodes. *J Med Virol* **Suppl**, 33-8.

Kinghorn, G. R. (1994). Epidemiology of genital herpes. *J Int Med Res* **22**, 14A-23A.

Kiriakidou, M., Driscoll, D. A., Lopez-Guisa, J. M. & Strauss, J. F., 3rd (1997). Cloning and expression of primate Daxx cDNAs and mapping of the human gene to chromosome 6p21.3 in the MHC region. *DNA Cell Biol* **16**, 1289-98.

Koffa, M. D., Clements, J. B., Izaurralde, E., Wadd, S., Wilson, S. A., Mattaj, I. W. & Kuersten, S. (2001). Herpes simplex virus ICP27 protein provides viral mRNAs with access to the cellular mRNA export pathway. *Embo J* **20**, 5769-78.

Korioth, F., Maul, G. G., Plachter, B., Stamminger, T. & Frey, J. (1996). The nuclear domain 10 (ND10) is disrupted by the human cytomegalovirus gene product IE1. *Exp Cell Res* **229**, 155-8.

Kristensson, K., Lycke, E., Roytta, M., Svennerholm, B. & Vahlne, A. (1986). Neuritic transport of herpes simplex virus in rat sensory neurons in vitro. Effects of substances interacting with microtubular function and axonal flow [nocodazole, taxol and erythro-9-3-(2-hydroxynonyl)adenine]. *J Gen Virol* **67**, 2023-8.

Kuo, M. Y., Chao, M. & Taylor, J. (1989). Initiation of replication of the human hepatitis delta virus genome from cloned DNA: role of delta antigen. *J Virol* **63**, 1945-50.

Kwong, A. D. & Frenkel, N. (1987). Herpes simplex virus-infected cells contain a function(s) that destabilizes both host and viral mRNAs. *Proc Natl Acad Sci U S A* **84**, 1926-30.

Kwong, A. D., Kruper, J. A. & Frenkel, N. (1988). Herpes simplex virus virion host shutoff function. *J Virol* **62**, 912-21.

La Boissiere, S., Hughes, T. & O'Hare, P. (1999). HCF-dependent nuclear import of VP16. *Embo J* **18**, 480-9.

Laemmli, U. K. (1970). Cleavage of structural proteins during the assembly of the head of bacteriophage T4. *Nature* **227**, 680-5.

Lafferty, W. E., Coombs, R. W., Benedetti, J., Critchlow, C. & Corey, L. (1987). Recurrences after oral and genital herpes simplex virus infection. Influence of site of infection and viral type. *N Engl J Med* **316**, 1444-9.

Landry, M. L. & Bull, C. (1992). Herpes simplex types 1 and 2: latency in the genital tract of guinea pigs. *Intervirology* **33**, 204-10.

Lapenta, V., Chiurazzi, P., van der Spek, P., Pizzuti, A., Hanaoka, F. & Brahe, C. (1997). SMT3A, a human homologue of the S. cerevisiae SMT3 gene, maps to chromosome 21qter and defines a novel gene family. *Genomics* **40**, 362-6.

Laquerre, S., Argnani, R., Anderson, D. B., Zucchini, S., Manservigi, R. & Glorioso, J. C. (1998). Heparan sulfate proteoglycan binding by herpes simplex virus type 1 glycoproteins B and C, which differ in their contributions to virus attachment, penetration, and cell-to-cell spread. *J Virol* **72**, 6119-30.

Le, X. F., Vallian, S., Mu, Z. M., Hung, M. C. & Chang, K. S. (1998). Recombinant PML adenovirus suppresses growth and tumorigenicity of human breast cancer cells by inducing G1 cell cycle arrest and apoptosis. *Oncogene* **16**, 1839-49.

Lee, C. K. & Knipe, D. M. (1985). An immunoassay for the study of DNA-binding activities of herpes simplex virus protein ICP8. *J Virol* **54**, 731-8.

Lee, S. S., Dong, Q., Wang, T. S. & Lehman, I. R. (1995). Interaction of herpes simplex virus 1 origin-binding protein with DNA polymerase alpha. *Proc Natl Acad Sci U S A* **92**, 7882-6.

Lee, S. S. & Lehman, I. R. (1997). Unwinding of the box I element of a herpes simplex virus type 1 origin by a complex of the viral origin binding protein, single-strand DNA binding protein, and single-stranded DNA. *Proc Natl Acad Sci U S A* **94**, 2838-42.

Lee, S. S. & Lehman, I. R. (1999). The interaction of herpes simplex type 1 virus origin-binding protein (UL9 protein) with Box I, the high affinity element of the viral origin of DNA replication. *J Biol Chem* **274**, 18613-7.

Lees-Miller, S. P., Long, M. C., Kilvert, M. A., Lam, V., Rice, S. A. & Spencer, C. A. (1996). Attenuation of DNA-dependent protein kinase activity and its catalytic subunit by the herpes simplex virus type 1 transactivator ICP0. *J Virol* **70**, 7471-7.

Lehman, I. R. & Boehmer, P. E. (1999). Replication of herpes simplex virus DNA. *J Biol Chem* **274**, 28059-62.

Lehming, N., Le Saux, A., Schuller, J. & Ptashne, M. (1998). Chromatin components as part of a putative transcriptional repressing complex. *Proc Natl Acad Sci U S A* **95**, 7322-6.

Leib, D. A., Coen, D. M., Bogard, C. L., Hicks, K. A., Yager, D. R., Knipe, D. M., Tyler, K. L. & Schaffer, P. A. (1989). Immediate-early regulatory gene mutants define different stages in the establishment and reactivation of herpes simplex virus latency. *J Virol* **63**, 759-68.

Lennette, E. T., Blackbourn, D. J. & Levy, J. A. (1996). Antibodies to human herpesvirus type 8 in the general population and in Kaposi's sarcoma patients. *Lancet* **348**, 858-61.

Leppard, K. N. & Everett, R. D. (1999). The adenovirus type 5 E1b 55K and E4 Orf3 proteins associate in infected cells and affect ND10 components. *J Gen Virol* **80**, 997-1008.

Li, H., Leo, C., Zhu, J., Wu, X., O'Neil, J., Park, E. J. & Chen, J. D. (2000). Sequestration and inhibition of Daxx-mediated transcriptional repression by PML. *Mol Cell Biol* **20**, 1784-96.

Li, S. J. & Hochstrasser, M. (1999). A new protease required for cell-cycle progression in yeast. *Nature* **398**, 246-51.

Ligas, M. W. & Johnson, D. C. (1988). A herpes simplex virus mutant in which glycoprotein D sequences are replaced by beta-galactosidase sequences binds to but is unable to penetrate into cells. *J Virol* **62**, 1486-94.

Liu, Y., Gong, W., Huang, C. C., Herr, W. & Cheng, X. (1999). Crystal structure of the conserved core of the herpes simplex virus transcriptional regulatory protein VP16. *Genes Dev* **13**, 1692-703.

Lomonte, P. & Everett, R. D. (1999). Herpes simplex virus type 1 immediate-early protein Vmw110 inhibits progression of cells through mitosis and from G(1) into S phase of the cell cycle. *J Virol* **73**, 9456-67.

Long, M. C., Leong, V., Schaffer, P. A., Spencer, C. A. & Rice, S. A. (1999). ICP22 and the UL13 protein kinase are both required for herpes simplex virus-induced modification of the large subunit of RNA polymerase II. *J Virol* **73**, 5593-604.

Lu, P., Jones, F. E., Saffran, H. A. & Smiley, J. R. (2001). Herpes simplex virus virion host shutoff protein requires a mammalian factor for efficient in vitro endoribonuclease activity. *J Virol* **75**, 1172-85.

Mador, N., Goldenberg, D., Cohen, O., Panet, A. & Steiner, I. (1998). Herpes simplex virus type 1 latency-associated transcripts suppress viral replication and reduce immediate-early gene mRNA levels in a neuronal cell line. *J Virol* **72**, 5067-75.

Mahajan, R., Delphin, C., Guan, T., Gerace, L. & Melchior, F. (1997). A small ubiquitin-related polypeptide involved in targeting RanGAP1 to nuclear pore complex protein RanBP2. *Cell* **88**, 97-107.

Mahajan, R., Gerace, L. & Melchior, F. (1998). Molecular characterization of the SUMO-1 modification of RanGAP1 and its role in nuclear envelope association. *J Cell Biol* **140**, 259-70.

Marchetti, A., Buttitta, F., Miyazaki, S., Gallahan, D., Smith, G. H. & Callahan, R. (1995). Int-6, a highly conserved, widely expressed gene, is mutated by mouse mammary tumor virus in mammary preneoplasia. *J Virol* **69**, 1932-8.

Marsden, H. S., Cross, A. M., Francis, G. J., Patel, A. H., MacEachran, K., Murphy, M., McVey, G., Haydon, D., Abbotts, A. & Stow, N. D. (1996). The herpes simplex virus type 1 UL8 protein influences the intracellular localization of the UL52 but not the ICP8 or POL replication proteins in virus-infected cells. *J Gen Virol* **77**, 2241-9.

Matunis, M. J., Coutavas, E. & Blobel, G. (1996). A novel ubiquitin-like modification modulates the partitioning of the Ran-GTPase-activating protein RanGAP1 between the cytosol and the nuclear pore complex. *J Cell Biol* **135**, 1457-70.

Matunis, M. J., Wu, J. & Blobel, G. (1998). SUMO-1 modification and its role in targeting the Ran GTPase-activating protein, RanGAP1, to the nuclear pore complex. *J Cell Biol* **140**, 499-509.

Maul, G. G. (1998). Nuclear domain 10, the site of DNA virus transcription and replication. *Bioessays* **20**, 660-7.

Maul, G. G. & Everett, R. D. (1994). The nuclear location of PML, a cellular member of the C3HC4 zinc-binding domain protein family, is rearranged during herpes simplex virus infection by the C3HC4 viral protein ICP0. *J Gen Virol* **75**, 1223-33.

Maul, G. G., Guldner, H. H. & Spivack, J. G. (1993). Modification of discrete nuclear domains induced by herpes simplex virus type 1 immediate early gene 1 product (ICP0). *J Gen Virol* **74**, 2679-90.

Maul, G. G., Ishov, A. M. & Everett, R. D. (1996). Nuclear domain 10 as preexisting potential replication start sites of herpes simplex virus type-1. *Virology* **217**, 67-75.

Maul, G. G., Negorev, D., Bell, P. & Ishov, A. M. (2000). Review: properties and assembly mechanisms of ND10, PML bodies, or PODs. *J Struct Biol* **129**, 278-87.

Maul, G. G., Yu, E., Ishov, A. M. & Epstein, A. L. (1995). Nuclear domain 10 (ND10) associated proteins are also present in nuclear bodies and redistribute to hundreds of nuclear sites after stress. *J Cell Biochem* **59**, 498-513.

Mavromara-Nazos, P., Silver, S., Hubenthal-Voss, J., McKnight, J. L. & Roizman, B. (1986). Regulation of herpes simplex virus 1 genes: alpha gene sequence requirements for transient induction of indicator genes regulated by beta or late (gamma 2) promoters. *Virology* **149**, 152-64.

McCarthy, A. M., McMahan, L. & Schaffer, P. A. (1989). Herpes simplex virus type 1 ICP27 deletion mutants exhibit altered patterns of transcription and are DNA deficient. *J Virol* **63**, 18-27.

McClain, K. L., Leach, C. T., Jenson, H. B., Joshi, V. V., Pollock, B. H., Parmley, R. T., DiCarlo, F. J., Chadwick, E. G. & Murphy, S. B. (1995). Association of Epstein-Barr virus with leiomyosarcomas in children with AIDS. *N Engl J Med* **332**, 12-8.

McGeoch, D. J., Dalrymple, M. A., Davison, A. J., Dolan, A., Frame, M. C., McNab, D., Perry, L. J., Scott, J. E. & Taylor, P. (1988). The complete DNA sequence of the long unique region in the genome of herpes simplex virus type 1. *J Gen Virol* **69**, 1531-74.

McGeoch, D. J., Dolan, A., Donald, S. & Rixon, F. J. (1985). Sequence determination and genetic content of the short unique region in the genome of herpes simplex virus type 1. *J Mol Biol* **181**, 1-13.

McNamee, E. E., Taylor, T. J. & Knipe, D. M. (2000). A dominant-negative herpesvirus protein inhibits intranuclear targeting of viral proteins: effects on DNA replication and late gene expression. *J Virol* **74**, 10122-31.

Meredith, M., Orr, A., Elliott, M. & Everett, R. (1995). Separation of sequence requirements for HSV-1 Vmw110 multimerisation and interaction with a 135-kDa cellular protein. *Virology* **209**, 174-87.

Meredith, M., Orr, A. & Everett, R. (1994). Herpes simplex virus type 1 immediate-early protein Vmw110 binds strongly and specifically to a 135-kDa cellular protein. *Virology* **200**, 457-69.

Merrick, W. C. (1992). Mechanism and regulation of eukaryotic protein synthesis. *Microbiol Rev* **56**, 291-315.

Mindel, A., Adler, M. W., Sutherland, S. & Fiddian, A. P. (1982). Intravenous acyclovir treatment for primary genital herpes. *Lancet* **1**, 697-700.

Montgomery, R. I., Warner, M. S., Lum, B. J. & Spear, P. G. (1996). Herpes simplex virus-1 entry into cells mediated by a novel member of the TNF/NGF receptor family. *Cell* **87**, 427-36.

Moolten, F. L. (1986). Tumor chemosensitivity conferred by inserted herpes thymidine kinase genes: paradigm for a prospective cancer control strategy. *Cancer Res* **46**, 5276-81.

Morgan, C., Rose, H. M. & Mednis, B. (1968). Electron microscopy of herpes simplex virus. I. Entry. *J Virol* **2**, 507-16.

Moriya, A., Yoshiki, A., Kita, M., Fushiki, S. & Imanishi, J. (1994). Heat shock-induced reactivation of herpes simplex virus type 1 in latently infected mouse trigeminal ganglion cells in dissociated culture. *Arch Virol* **135**, 419-25.

Mosca, J. D., Bednarik, D. P., Raj, N. B., Rosen, C. A., Sodroski, J. G., Haseltine, W. A., Hayward, G. S. & Pitha, P. M. (1987). Activation of human immunodeficiency virus by herpesvirus infection: identification of a region within the long terminal repeat that responds to a trans-acting factor encoded by herpes simplex virus 1. *Proc Natl Acad Sci U S A* **84**, 7408-12.

Mossman, K. L., Macgregor, P. F., Rozmus, J. J., Goryachev, A. B., Edwards, A. M. & Smiley, J. R. (2001). Herpes simplex virus triggers and then disarms a host antiviral response. *J Virol* **75**, 750-8.

Mossman, K. L., Saffran, H. A. & Smiley, J. R. (2000). Herpes simplex virus ICP0 mutants are hypersensitive to interferon. *J Virol* **74**, 2052-6.

Mossman, K. L. & Smiley, J. R. (2002). Herpes simplex virus ICP0 and ICP34.5 counteract distinct interferon- induced barriers to virus replication. *J Virol* **76**, 1995-8.

Mu, Z. M., Chin, K. V., Liu, J. H., Lozano, G. & Chang, K. S. (1994). PML, a growth suppressor disrupted in acute promyelocytic leukemia. *Mol Cell Biol* **14**, 6858-67.

Mullen, M. A., Ciufo, D. M. & Hayward, G. S. (1994). Mapping of intracellular localization domains and evidence for colocalization interactions between the IE110 and IE175 nuclear transactivator proteins of herpes simplex virus. *J Virol* **68**, 3250-66.

Muller, S., Berger, M., Lehembre, F., Seeler, J. S., Haupt, Y. & Dejean, A. (2000). c-Jun and p53 activity is modulated by SUMO-1 modification. *J Biol Chem* **275**, 13321-9.

Muller, S. & Dejean, A. (1999). Viral immediate-early proteins abrogate the modification by SUMO-1 of PML and Sp100 proteins, correlating with nuclear body disruption. *J Virol* **73**, 5137-43.

Muller, S., Matunis, M. J. & Dejean, A. (1998a). Conjugation with the ubiquitin-related modifier SUMO-1 regulates the partitioning of PML within the nucleus. *Embo J* **17**, 61-70.

Muller, S., Miller, W. H., Jr. & Dejean, A. (1998b). Trivalent antimonials induce degradation of the PML-RAR oncoprotein and reorganization of the promyelocytic leukemia nuclear bodies in acute promyelocytic leukemia NB4 cells. *Blood* **92**, 4308-16.

Nahmias, A. J., Lee, F. K. & Beckman-Nahmias, S. (1990). Sero-epidemiological and -sociological patterns of herpes simplex virus infection in the world. *Scand J Infect Dis Suppl* **69**, 19-36.

Neff, N. F., Ellis, N. A., Ye, T. Z., Noonan, J., Huang, K., Sanz, M. & Proytcheva, M. (1999). The DNA helicase activity of BLM is necessary for the correction of the genomic instability of bloom syndrome cells. *Mol Biol Cell* **10**, 665-76.

Negorev, D., Ishov, A. M. & Maul, G. G. (2001). Evidence for separate ND10-binding and homo-oligomerization domains of Sp100. *J Cell Sci* **114**, 59-68.

Negorev, D. & Maul, G. G. (2001). Cellular proteins localized at and interacting within ND10/PML nuclear bodies/PODs suggest functions of a nuclear depot. *Oncogene* **20**, 7234-42.

Nesburn, A. B., Cook, M. L. & Stevens, J. G. (1972). Latent herpes simplex virus. Isolation from rabbit trigeminal ganglia between episodes of recurrent ocular infection. *Arch Ophthalmol* **88**, 412-7.

Nesburn, A. B., Elliott, J. H. & Leibowitz, H. M. (1967). Spontaneous reactivation of experimental herpes simplex keratitis in rabbits. *Arch Ophthalmol* **78**, 523-9.

Newcomb, W. W., Homa, F. L., Thomsen, D. R., Booy, F. P., Trus, B. L., Steven, A. C., Spencer, J. V. & Brown, J. C. (1996). Assembly of the herpes simplex virus capsid: characterization of intermediates observed during cell-free capsid formation. *J Mol Biol* **263**, 432-46.

Newcomb, W. W., Homa, F. L., Thomsen, D. R., Trus, B. L., Cheng, N., Steven, A., Booy, F. & Brown, J. C. (1999). Assembly of the herpes simplex virus procapsid from purified components and identification of small complexes containing the major capsid and scaffolding proteins. *J Virol* **73**, 4239-50.

Nicholas, J. (1996). Determination and analysis of the complete nucleotide sequence of human herpesvirus. *J Virol* **70**, 5975-89.

O'Hare, P. (1993). The virion transactivator of herpes simplex virus. *Semin Virol* **4**, 145-55.

O'Hare, P. & Hayward, G. S. (1985). Evidence for a direct role for both the 175,000- and 110,000-molecular-weight immediate-early proteins of herpes simplex virus in the transactivation of delayed-early promoters. *J Virol* **53**, 751-60.

Okuma, T., Honda, R., Ichikawa, G., Tsumagari, N. & Yasuda, H. (1999). In vitro SUMO-1 modification requires two enzymatic steps, E1 and E2. *Biochem Biophys Res Commun* **254**, 693-8.

Okura, T., Gong, L., Kamitani, T., Wada, T., Okura, I., Wei, C. F., Chang, H. M. & Yeh, E. T. (1996). Protection against Fas/APO-1- and tumor necrosis factor-mediated cell death by a novel protein, sentrin. *J Immunol* **157**, 4277-81.

Oroskar, A. A. & Read, G. S. (1987). A mutant of herpes simplex virus type 1 exhibits increased stability of immediate-early (alpha) mRNAs. *J Virol* **61**, 604-6.

Oroskar, A. A. & Read, G. S. (1989). Control of mRNA stability by the virion host shutoff function of herpes simplex virus. *J Virol* **63**, 1897-906.

Parkinson, J. & Everett, R. D. (2000). Alphaherpesvirus proteins related to herpes simplex virus type 1 ICP0 affect cellular structures and proteins. *J Virol* **74**, 10006-17.

Parkinson, J., Lees-Miller, S. P. & Everett, R. D. (1999). Herpes simplex virus type 1 immediate-early protein vmw110 induces the proteasome-dependent degradation of the catalytic subunit of DNA- dependent protein kinase. *J Virol* **73**, 650-7.

Pearson, M. & Pelicci, P. G. (2001). PML interaction with p53 and its role in apoptosis and replicative senescence. *Oncogene* **20**, 7250-6.

Peng, H., Begg, G. E., Schultz, D. C., Friedman, J. R., Jensen, D. E., Speicher, D. W. & Rauscher, F. J., 3rd (2000). Reconstitution of the KRAB-KAP-1 repressor complex: a model system for defining the molecular anatomy of RING-B box-coiled-coil domain-mediated protein-protein interactions. *J Mol Biol* **295**, 1139-62.

Perng, G. C., Slanina, S. M., Yukht, A., Ghiasi, H., Nesburn, A. B. & Wechsler, S. L. (2000). The latency-associated transcript gene enhances establishment of herpes simplex virus type 1 latency in rabbits. *J Virol* **74**, 1885-91.

Perry, L. J., Rixon, F. J., Everett, R. D., Frame, M. C. & McGeoch, D. J. (1986). Characterization of the IE110 gene of herpes simplex virus type 1. *J Gen Virol* **67**, 2365-80.

Petroski, M. D. & Wagner, E. K. (1998). Purification and characterization of a cellular protein that binds to the downstream activation sequence of the strict late UL38 promoter of herpes simplex virus type 1. *J Virol* **72**, 8181-90.

Piazza, F., Gurrieri, C. & Pandolfi, P. P. (2001). The theory of APL. *Oncogene* **20**, 7216-22.

Pleasure, S. J. & Lee, V. M. (1993). NTera 2 cells: a human cell line which displays characteristics expected of a human committed neuronal progenitor cell. *J Neurosci Res* **35**, 585-602.

Pleasure, S. J., Page, C. & Lee, V. M. (1992). Pure, postmitotic, polarized human neurons derived from NTera 2 cells provide a system for expressing exogenous proteins in terminally differentiated neurons. *J Neurosci* **12**, 1802-15.

Pluta, A. F., Earnshaw, W. C. & Goldberg, I. G. (1998). Interphase-specific association of intrinsic centromere protein CENP-C with HDaxx, a death domain-binding protein implicated in Fas-mediated cell death. *J Cell Sci* **111**, 2029-41.

Post, L. E. & Roizman, B. (1981). A generalized technique for deletion of specific genes in large genomes: alpha gene 22 of herpes simplex virus 1 is not essential for growth. *Cell* **25**, 227-32.

Preston, C. M. (1979). Abnormal properties of an immediate early polypeptide in cells infected with the herpes simplex virus type 1 mutant tsK. *J Virol* **32**, 357-69.

Preston, C. M. (2000). Repression of viral transcription during herpes simplex virus latency. *J Gen Virol* **81**, 1-19.

Preston, C. M. & Nicholl, M. J. (1997). Repression of gene expression upon infection of cells with herpes simplex virus type 1 mutants impaired for immediate-early protein synthesis. *J Virol* **71**, 7807-13.

Preston, V. G., Davison, A. J., Marsden, H. S., Timbury, M. C., Subak-Sharpe, J. H. & Wilkie, N. M. (1978). Recombinants between herpes simplex virus types 1 and 2: analyses of genome structures and expression of immediate early polypeptides. *J Virol* **28**, 499-517.

Quignon, F., De Bels, F., Koken, M., Feunteun, J., Ameisen, J. C. & de The, H. (1998). PML induces a novel caspase-independent death process. *Nat Genet* **20**, 259-65.

Quinlan, M. P., Chen, L. B. & Knipe, D. M. (1984). The intranuclear location of a herpes simplex virus DNA-binding protein is determined by the status of viral DNA replication. *Cell* **36**, 857-68.

Quinlan, M. P. & Knipe, D. M. (1985). Stimulation of expression of a herpes simplex virus DNA-binding protein by two viral functions. *Mol Cell Biol* **5**, 957-63.

Ralph, W. M., Cabatingan, M. S. & Schaffer, P. A. (1994). Induction of herpes simplex virus type 1 immediate-early gene expression by a cellular activity expressed in Vero and NB41A3 cells after growth arrest-release. *J Virol* **68**, 6871-82.

Read, G. S. & Frenkel, N. (1983). Herpes simplex virus mutants defective in the virion-associated shutoff of host polypeptide synthesis and exhibiting abnormal synthesis of alpha (immediate early) viral polypeptides. *J Virol* **46**, 498-512.

Read, G. S., Karr, B. M. & Knight, K. (1993). Isolation of a herpes simplex virus type 1 mutant with a deletion in the virion host shutoff gene and identification of multiple forms of the vhs (UL41) polypeptide. *J Virol* **67**, 7149-60.

Reardon, J. E. & Spector, T. (1989). Herpes simplex virus type 1 DNA polymerase. Mechanism of inhibition by acyclovir triphosphate. *J Biol Chem* **264**, 7405-11.

Regad, T. & Chelbi-Alix, M. K. (2001). Role and fate of PML nuclear bodies in response to interferon and viral infections. *Oncogene* **20**, 7274-86.

Regad, T., Saib, A., Lallemand-Breitenbach, V., Pandolfi, P. P., de The, H. & Chelbi-Alix, M. K. (2001). PML mediates the interferon-induced antiviral state against a complex retrovirus via its association with the viral transactivator. *Embo J* **20**, 3495-505.

Renne, R., Lagunoff, M., Zhong, W. & Ganem, D. (1996). The size and conformation of Kaposi's sarcoma-associated herpesvirus (human herpesvirus 8) DNA in infected cells and virions. *J Virol* **70**, 8151-4.

Rice, S. A. & Knipe, D. M. (1988). Gene-specific transactivation by herpes simplex virus type 1 alpha protein ICP27. *J Virol* **62**, 3814-23.

Rice, S. A., Long, M. C., Lam, V., Schaffer, P. A. & Spencer, C. A. (1995). Herpes simplex virus immediate-early protein ICP22 is required for viral modification of host

RNA polymerase II and establishment of the normal viral transcription program. *J Virol* **69**, 5550-9.

Rixon, F. J. (1993). Structure and assembly of herpesviruses. *Seminars in Virology* **4**, 135-44.

Rixon, F. J., Atkinson, M. A. & Hay, J. (1983). Intranuclear distribution of herpes simplex virus type 2 DNA synthesis: examination by light and electron microscopy. *J Gen Virol* **64**, 2087-92.

Rodahl, E. & Haarr, L. (1997). Analysis of the 2-kilobase latency-associated transcript expressed in PC12 cells productively infected with herpes simplex virus type 1: evidence for a stable, nonlinear structure. *J Virol* **71**, 1703-7.

Rodger, G., Boname, J., Bell, S. & Minson, T. (2001). Assembly and organization of glycoproteins B, C, D, and H in herpes simplex virus type 1 particles lacking individual glycoproteins: No evidence for the formation of a complex of these molecules. *J Virol* **75**, 710-6.

Rodriguez, M. S., Desterro, J. M., Lain, S., Midgley, C. A., Lane, D. P. & Hay, R. T. (1999). SUMO-1 modification activates the transcriptional response of p53. *Embo J* **18**, 6455-61.

Roizman, B. & Sears, A. E. (1996). Herpes simplex viruses and their replication. In *Fields: Virology*, pp. 2231-95. Edited by B. N. Fields, D. M. Knipe, P. M. Howley, M. S. Charnock, J. L. Hirsch, J. L. Melnick, T. P. Monath & B. Roizman. Philadelphia: Raven.

Roop, C., Hutchinson, L. & Johnson, D. C. (1993). A mutant herpes simplex virus type 1 unable to express glycoprotein L cannot enter cells, and its particles lack glycoprotein H. *J Virol* **67**, 2285-97.

Russell, J., Stow, N. D., Stow, E. C. & Preston, C. M. (1987). Herpes simplex virus genes involved in latency in vitro. *J Gen Virol* **68**, 3009-18.

Sacks, W. R., Greene, C. C., Aschman, D. P. & Schaffer, P. A. (1985). Herpes simplex virus type 1 ICP27 is an essential regulatory protein. *J Virol* **55**, 796-805.

Sacks, W. R. & Schaffer, P. A. (1987). Deletion mutants in the gene encoding the herpes simplex virus type 1 immediate-early protein ICP0 exhibit impaired growth in cell culture. *J Virol* **61**, 829-39.

Saitoh, H. & Hinchey, J. (2000). Functional heterogeneity of small ubiquitin-related protein modifiers SUMO-1 versus SUMO-2/3. *J Biol Chem* **275**, 6252-8.

Saitoh, H., Pu, R. T. & Dasso, M. (1997). SUMO-1: wrestling with a new ubiquitin-related modifier. *Trends Biochem Sci* **22**, 374-6.

Saitoh, H., Sparrow, D. B., Shiomi, T., Pu, R. T., Nishimoto, T., Mohun, T. J. & Dasso, M. (1998). Ubc9p and the conjugation of SUMO-1 to RanGAP1 and RanBP2. *Curr Biol* **8**, 121-4.

Saitoh, H., Tomkiel, J., Cooke, C. A., Ratrie, H., 3rd, Maurer, M., Rothfield, N. F. & Earnshaw, W. C. (1992). CENP-C, an autoantigen in scleroderma, is a component of the human inner kinetochore plate. *Cell* **70**, 115-25.

Samaniego, L. A., Neiderhiser, L. & DeLuca, N. A. (1998). Persistence and expression of the herpes simplex virus genome in the absence of immediate-early proteins. *J Virol* **72**, 3307-20.

Sandri-Goldin, R. M. (1998). ICP27 mediates HSV RNA export by shuttling through a leucine-rich nuclear export signal and binding viral intronless RNAs through an RGG motif. *Genes Dev* **12**, 868-79.

Sandri-Goldin, R. M. & Mendoza, G. E. (1992). A herpesvirus regulatory protein appears to act post-transcriptionally by affecting mRNA processing. *Genes Dev* **6**, 848-63.

Saurin, A. J., Borden, K. L., Boddy, M. N. & Freemont, P. S. (1996). Does this have a familiar RING? *Trends Biochem Sci* **21**, 208-14.

Sawtell, N. M. (1997). Comprehensive quantification of herpes simplex virus latency at the single-cell level. *J Virol* **71**, 5423-31.

Sawtell, N. M. (1998). The probability of in vivo reactivation of herpes simplex virus type 1 increases with the number of latently infected neurons in the ganglia. *J Virol* **72**, 6888-92.

Sawtell, N. M. & Thompson, R. L. (1992). Rapid in vivo reactivation of herpes simplex virus in latently infected murine ganglionic neurons after transient hyperthermia. *J Virol* **66**, 2150-6.

Scarr, R. B., Smith, M. R., Beddall, M. & Sharp, P. A. (2000). A novel 50-kilodalton fragment of host cell factor 1 (C1) in G(0) cells. *Mol Cell Biol* **20**, 3568-75.

Schaeffer, H. J., Beauchamp, L., de Miranda, P., Elion, G. B., Bauer, D. J. & Collins, P. (1978). 9-(2-hydroxyethoxymethyl) guanine activity against viruses of the herpes group. *Nature* **272**, 583-5.

Schenk, P., Pietschmann, S., Gelderblom, H., Pauli, G., Ludwig, H. & Schenck, P. (1988). Monoclonal antibodies against herpes simplex virus type 1-infected nuclei defining and localizing the ICP8 protein, 65K DNA-binding protein and polypeptides of the ICP35 family. *J Gen Virol* **69**, 99-111.

Schrag, J. D., Prasad, B. V., Rixon, F. J. & Chiu, W. (1989). Three-dimensional structure of the HSV1 nucleocapsid. *Cell* **56**, 651-60.

Sears, A. E., Halliburton, I. W., Meignier, B., Silver, S. & Roizman, B. (1985). Herpes simplex virus 1 mutant deleted in the alpha 22 gene: growth and gene expression in permissive and restrictive cells and establishment of latency in mice. *J Virol* **55**, 338-46.

Seeler, J. S. & Dejean, A. (2001). SUMO: of branched proteins and nuclear bodies. *Oncogene* **20**, 7243-9.

Seeler, J. S., Marchio, A., Losson, R., Desterro, J. M., Hay, R. T., Chambon, P. & Dejean, A. (2001). Common properties of nuclear body protein SP100 and TIF1alpha chromatin factor: role of SUMO modification. *Mol Cell Biol* **21**, 3314-24.

Seeler, J. S., Marchio, A., Sitterlin, D., Transy, C. & Dejean, A. (1998). Interaction of SP100 with HP1 proteins: a link between the promyelocytic leukemia-associated nuclear bodies and the chromatin compartment. *Proc Natl Acad Sci U S A* **95**, 7316-21.

Sekulovich, R. E., Leary, K. & Sandri-Goldin, R. M. (1988). The herpes simplex virus type 1 alpha protein ICP27 can act as a trans-repressor or a trans-activator in combination with ICP4 and ICP0. *J Virol* **62**, 4510-22.

Shen, Z., Pardington-Purtymun, P. E., Comeaux, J. C., Moyzis, R. K. & Chen, D. J. (1996). UBL1, a human ubiquitin-like protein associating with human RAD51/RAD52 proteins. *Genomics* **36**, 271-9.

Shtrichman, R. & Samuel, C. E. (2001). The role of gamma interferon in antimicrobial immunity. *Curr Opin Microbiol* **4**, 251-9.

Shukla, D. & Spear, P. G. (2001). Herpesviruses and heparan sulfate: an intimate relationship in aid of viral entry. *J Clin Invest* **108**, 503-10.

Skepper, J. N., Whiteley, A., Browne, H. & Minson, A. (2001). Herpes simplex virus nucleocapsids mature to progeny virions by an envelopment --> deenvelopment --> reenvelopment pathway. *J Virol* **75**, 5697-702.

Smibert, C. A., Johnson, D. C. & Smiley, J. R. (1992). Identification and characterization of the virion-induced host shutoff product of herpes simplex virus gene UL41. *J Gen Virol* **73**, 467-70.

Soliman, T. M., Sandri-Goldin, R. M. & Silverstein, S. J. (1997). Shuttling of the herpes simplex virus type 1 regulatory protein ICP27 between the nucleus and cytoplasm mediates the expression of late proteins. *J Virol* **71**, 9188-97.

Soliman, T. M. & Silverstein, S. J. (2000). Herpesvirus mRNAs are sorted for export via Crm1-dependent and -independent pathways. *J Virol* **74**, 2814-25.

Southern, E. M. (1975). Detection of specific sequences among DNA fragments separated by gel electrophoresis. *J Mol Biol* **98**, 503-17.

Spector, D. L. (2001). Nuclear domains. *J Cell Sci* **114**, 2891-3.

Spivack, J. G. & Fraser, N. W. (1988). Expression of herpes simplex virus type 1 latency-associated transcripts in the trigeminal ganglia of mice during acute infection and reactivation of latent infection. *J Virol* **62**, 1479-85.

Spruance, S. L., Overall, J. C., Jr., Kern, E. R., Krueger, G. G., Pliam, V. & Miller, W. (1977). The natural history of recurrent herpes simplex labialis: implications for antiviral therapy. *N Engl J Med* **297**, 69-75.

Stadler, M., Chelbi-Alix, M. K., Koken, M. H., Venturini, L., Lee, C., Saib, A., Quignon, F., Pelicano, L., Guillemin, M. C., Schindler, C. & et al. (1995). Transcriptional induction of the PML growth suppressor gene by interferons is mediated through an ISRE and a GAS element. *Oncogene* **11**, 2565-73.

Stanberry, L. R. (1995). Herpes simplex virus vaccines as immunotherapeutic agents. *Trends Microbiol* **3**, 244-7.

Stanberry, L. R., Kern, E. R., Richards, J. T., Abbott, T. M. & Overall, J. C., Jr. (1982). Genital herpes in guinea pigs: pathogenesis of the primary infection and description of recurrent disease. *J Infect Dis* **146**, 397-404.

Stark, J. J., Dillman, R. O., Schulof, R., Wiemann, M. C., Barth, N. M., Honeycutt, P. J. & Soori, G. (1998). Interferon-alpha and chemohormonal therapy for patients with advanced melanoma: final results of a phase I-II study of the Cancer Biotherapy Research Group and the Mid-Atlantic Oncology Program. *Cancer* **82**, 1677-81.

Steffy, K. R. & Weir, J. P. (1991). Mutational analysis of two herpes simplex virus type 1 late promoters. *J Virol* **65**, 6454-60.

Steiner, I., Spivack, J. G., Lirette, R. P., Brown, S. M., MacLean, A. R., Subak-Sharpe, J. H. & Fraser, N. W. (1989). Herpes simplex virus type 1 latency-associated transcripts are evidently not essential for latent infection. *Embo J* **8**, 505-11.

Sternsdorf, T., Grotzinger, T., Jensen, K. & Will, H. (1997). Nuclear dots: actors on many stages. *Immunobiology* **198**, 307-31.

Sternsdorf, T., Guldner, H. H., Szostecki, C., Grotzinger, T. & Will, H. (1995). Two nuclear dot-associated proteins, PML and Sp100, are often co-autoimmunogenic in patients with primary biliary cirrhosis. *Scand J Immunol* **42**, 257-68.

Sternsdorf, T., Jensen, K., Reich, B. & Will, H. (1999). The nuclear dot protein sp100, characterization of domains necessary for dimerization, subcellular localization, and modification by small ubiquitin-like modifiers. *J Biol Chem* **274**, 12555-66.

Stevens, J. G. & Cook, M. L. (1971). Latent herpes simplex virus in spinal ganglia of mice. *Science* **173**, 843-5.

Stevens, J. G., Wagner, E. K., Devi-Rao, G. B., Cook, M. L. & Feldman, L. T. (1987). RNA complementary to a herpesvirus alpha gene mRNA is prominent in latently infected neurons. *Science* **235**, 1056-9.

Stow, E. C. & Stow, N. D. (1989). Complementation of a herpes simplex virus type 1 Vmw110 deletion mutant by human cytomegalovirus. *J Gen Virol* **70**, 695-704.

Stow, N. D. & Stow, E. C. (1986). Isolation and characterization of a herpes simplex virus type 1 mutant containing a deletion within the gene encoding the immediate early polypeptide Vmw110. *J Gen Virol* **67**, 2571-85.

Stuurman, N., de Graaf, A., Floore, A., Josso, A., Humbel, B., de Jong, L. & van Driel, R. (1992). A monoclonal antibody recognizing nuclear matrix-associated nuclear bodies. *J Cell Sci* **101**, 773-84.

Sullivan, K. F., Hechenberger, M. & Masri, K. (1994). Human CENP-A contains a histone H3 related histone fold domain that is required for targeting to the centromere. *J Cell Biol* **127**, 581-92.

Suzuki, T., Ichiyama, A., Saitoh, H., Kawakami, T., Omata, M., Chung, C. H., Kimura, M., Shimbara, N. & Tanaka, K. (1999). A new 30-kDa ubiquitin-related SUMO-1 hydrolase from bovine brain. *J Biol Chem* **274**, 31131-4.

Suzutani, T., Nagamine, M., Shibaki, T., Ogasawara, M., Yoshida, I., Daikoku, T., Nishiyama, Y. & Azuma, M. (2000). The role of the UL41 gene of herpes simplex virus type 1 in evasion of non-specific host defence mechanisms during primary infection. *J Gen Virol* **81**, 1763-71.

Szekely, L., Pokrovskaja, K., Jiang, W. Q., de The, H., Ringertz, N. & Klein, G. (1996). The Epstein-Barr virus-encoded nuclear antigen EBNA-5 accumulates in PML-containing bodies. *J Virol* **70**, 2562-8.

Szostecki, C., Guldner, H. H., Netter, H. J. & Will, H. (1990). Isolation and characterization of cDNA encoding a human nuclear antigen predominantly recognized by autoantibodies from patients with primary biliary cirrhosis. *J Immunol* **145**, 4338-47.

Taylor, J. L., Unverrich, D., O'Brien, W. J. & Wilcox, K. W. (2000). Interferon coordinately inhibits the disruption of PML-positive ND10 and immediate-early gene expression by herpes simplex virus. *J Interferon Cytokine Res* **20**, 805-15.

Thompson, R. L. & Sawtell, N. M. (1997). The herpes simplex virus type 1 latency-associated transcript gene regulates the establishment of latency. *J Virol* **71**, 5432-40.

Thompson, R. L. & Sawtell, N. M. (2000). HSV latency-associated transcript and neuronal apoptosis. *Science* **289**, 1651.

Thompson, R. L. & Sawtell, N. M. (2001). Herpes simplex virus type 1 latency-associated transcript gene promotes neuronal survival. *J Virol* **75**, 6660-75.

Torii, S., Egan, D. A., Evans, R. A. & Reed, J. C. (1999). Human Daxx regulates Fas-induced apoptosis from nuclear PML oncogenic domains (PODs). *Embo J* **18**, 6037-49.

Towbin, H., Staehelin, T. & Gordon, J. (1979). Electrophoretic transfer of proteins from polyacrylamide gels to nitrocellulose sheets: procedure and some applications. *Proc Natl Acad Sci U S A* **76**, 4350-4.

Trus, B. L., Booy, F. P., Newcomb, W. W., Brown, J. C., Homa, F. L., Thomsen, D. R. & Steven, A. C. (1996). The herpes simplex virus procapsid: structure, conformational changes upon maturation, and roles of the triplex proteins VP19c and VP23 in assembly. *J Mol Biol* **263**, 447-62.

Vallian, S., Chin, K. V. & Chang, K. S. (1998). The promyelocytic leukemia protein interacts with Sp1 and inhibits its transactivation of the epidermal growth factor receptor promoter. *Mol Cell Biol* **18**, 7147-56.

Vallian, S., Gaken, J. A., Trayner, I. D., Gingold, E. B., Kouzarides, T., Chang, K. S. & Farzaneh, F. (1997). Transcriptional repression by the promyelocytic leukemia protein, PML. *Exp Cell Res* **237**, 371-82.

Valyi-Nagy, T., Deshmane, S. L., Raengsakulrach, B., Nicosia, M., Gesser, R. M., Wysocka, M., Dillner, A. & Fraser, N. W. (1992). Herpes simplex virus type 1 mutant strain in1814 establishes a unique, slowly progressing infection in SCID mice. *J Virol* **66**, 7336-45.

Van Sant, C., Kawaguchi, Y. & Roizman, B. (1999). A single amino acid substitution in the cyclin D binding domain of the infected cell protein no. 0 abrogates the neuroinvasiveness of herpes simplex virus without affecting its ability to replicate. *Proc Natl Acad Sci U S A* **96**, 8184-9.

Van Sant, C., Lopez, P., Advani, S. J. & Roizman, B. (2001). Role of Cyclin D3 in the Biology of Herpes Simplex Virus 1 ICP0. *J Virol* **75**, 1888-1898.

Vogelstein, B. & Gillespie, D. (1979). Preparative and analytical purification of DNA from agarose. *Proc Natl Acad Sci U S A* **76**, 615-9.

Wadd, S., Bryant, H., Filhol, O., Scott, J. E., Hsieh, T. Y., Everett, R. D. & Clements, J. B. (1999). The multifunctional herpes simplex virus IE63 protein interacts with heterogeneous ribonucleoprotein K and with casein kinase 2. *J Biol Chem* **274**, 28991-8.

Wadsworth, S., Jacob, R. J. & Roizman, B. (1975). Anatomy of herpes simplex virus DNA. II. Size, composition, and arrangement of inverted terminal repetitions. *J Virol* **15**, 1487-97.

Wagner, E. K. & Bloom, D. C. (1997). Experimental investigation of herpes simplex virus latency. *Clin Microbiol Rev* **10**, 419-43.

Wagner, E. K., Flanagan, W. M., Devi-Rao, G., Zhang, Y. F., Hill, J. M., Anderson, K. P. & Stevens, J. G. (1988). The herpes simplex virus latency-associated transcript is spliced during the latent phase of infection. *J Virol* **62**, 4577-85.

Walz, M. A., Price, R. W. & Notkins, A. L. (1974). Latent ganglionic infection with herpes simplex virus types 1 and 2: viral reactivation in vivo after neurectomy. *Science* **184**, 1185-7.

Wang, Z. G., Ruggero, D., Ronchetti, S., Zhong, S., Gaboli, M., Rivi, R. & Pandolfi, P. P. (1998). PML is essential for multiple apoptotic pathways. *Nat Genet* **20**, 266-72.

Warner, M. S., Geraghty, R. J., Martinez, W. M., Montgomery, R. I., Whitbeck, J. C., Xu, R., Eisenberg, R. J., Cohen, G. H. & Spear, P. G. (1998). A cell surface protein with herpesvirus entry activity (HveB) confers susceptibility to infection by mutants of herpes simplex virus type 1, herpes simplex virus type 2, and pseudorabies virus. *Virology* **246**, 179-89.

Wasserman, W. J., Richter, J. D. & Smith, L. D. (1982). Protein synthesis during maturation promoting factor- and progesterone-induced maturation in Xenopus oocytes. *Dev Biol* **89**, 152-8.

Watson, R. J. & Clements, J. B. (1980). A herpes simplex virus type 1 function continuously required for early and late virus RNA synthesis. *Nature* **285**, 329-30.

Weir, J. P. (2001). Regulation of herpes simplex virus gene expression. *Gene* **271**, 117-30.

Whitley, R., Arvin, A., Prober, C., Corey, L., Burchett, S., Plotkin, S., Starr, S., Jacobs, R., Powell, D., Nahmias, A. & et al. (1991). Predictors of morbidity and mortality in neonates with herpes simplex virus infections. The National Institute of Allergy and Infectious Diseases Collaborative Antiviral Study Group. *N Engl J Med* **324**, 450-4.

Whitley, R. J. (1993). Neonatal herpes simplex virus infections. *J Med Virol* **Suppl**, 13-21.

Whitley, R. J., Corey, L., Arvin, A., Lakeman, F. D., Sumaya, C. V., Wright, P. F., Dunkle, L. M., Steele, R. W., Soong, S. J., Nahmias, A. J. & et al. (1988). Changing presentation of herpes simplex virus infection in neonates. *J Infect Dis* **158**, 109-16.

Whitley, R. J., Soong, S. J., Dolin, R., Galasso, G. J., Ch'ien, L. T. & Alford, C. A. (1977). Adenine arabinoside therapy of biopsy-proved herpes simplex encephalitis. National Institute of Allergy and Infectious Diseases collaborative antiviral study. *N Engl J Med* **297**, 289-94.

Wilcox, C. L. & Johnson, E. M., Jr. (1987). Nerve growth factor deprivation results in the reactivation of latent herpes simplex virus in vitro. *J Virol* **61**, 2311-5.

Wilcox, C. L., Smith, R. L., Everett, R. D. & Mysofski, D. (1997). The herpes simplex virus type 1 immediate-early protein ICP0 is necessary for the efficient establishment of latent infection. *J Virol* **71**, 6777-85.

Wilkie, N. M., Clements, J. B., Boll, W., Mantei, N., Lonsdale, D. & Weissmann, C. (1979). Hybrid plasmids containing an active thymidine kinase gene of Herpes simplex virus 1. *Nucleic Acids Res* **7**, 859-77.

Wilson, A. C., LaMarco, K., Peterson, M. G. & Herr, W. (1993). The VP16 accessory protein HCF is a family of polypeptides processed from a large precursor protein. *Cell* **74**, 115-25.

Woerner, A. M. & Weir, J. P. (1998). Characterization of the initiator and downstream promoter elements of herpes simplex virus 1 late genes. *Virology* **249**, 219-30.

Wu, C. A., Nelson, N. J., McGeoch, D. J. & Challberg, M. D. (1988). Identification of herpes simplex virus type 1 genes required for origin-dependent DNA synthesis. *J Virol* **62**, 435-43.

Wu, F. Y., Ahn, J. H., Alcendor, D. J., Jang, W. J., Xiao, J., Hayward, S. D. & Hayward, G. S. (2001a). Origin-independent assembly of Kaposi's sarcoma-associated herpesvirus DNA replication compartments in transient cotransfection assays and association with the ORF-K8 protein and cellular PML. *J Virol* **75**, 1487-506.

Wu, W. S., Vallian, S., Seto, E., Yang, W. M., Edmondson, D., Roth, S. & Chang, K. S. (2001b). The growth suppressor PML represses transcription by functionally and physically interacting with histone deacetylases. *Mol Cell Biol* **21**, 2259-68.

Xu, Y., Ahn, J. H., Cheng, M., apRhys, C. M., Chiou, C. J., Zong, J., Matunis, M. J. & Hayward, G. S. (2001). Proteasome-independent disruption of PML oncogenic domains (PODs), but not covalent modification by SUMO-1, is required for human cytomegalovirus immediate-early protein IE1 to inhibit PML-mediated transcriptional repression. *J Virol* **75**, 10683-95.

Yang, X., Khosravi-Far, R., Chang, H. Y. & Baltimore, D. (1997). Daxx, a novel Fas-binding protein that activates JNK and apoptosis. *Cell* **89**, 1067-76.

Yang-Yen, H. F. & Rothblum, L. I. (1988). Purification and characterization of a high-mobility-group-like DNA-binding protein that stimulates rRNA synthesis in vitro. *Mol Cell Biol* **8**, 3406-14.

Yankiwski, V., Marciniak, R. A., Guarente, L. & Neff, N. F. (2000). Nuclear structure in normal and Bloom syndrome cells. *Proc Natl Acad Sci U S A* **97**, 5214-9.

Yao, F. & Schaffer, P. A. (1995). An activity specified by the osteosarcoma line U2OS can substitute functionally for ICP0, a major regulatory protein of herpes simplex virus type 1. *J Virol* **69**, 6249-58.

Zelus, B. D., Stewart, R. S. & Ross, J. (1996). The virion host shutoff protein of herpes simplex virus type 1: messenger ribonucleolytic activity in vitro. *J Virol* **70**, 2411-9.

Zhang, T. D., Chen, G. Q., Wang, Z. G., Wang, Z. Y., Chen, S. J. & Chen, Z. (2001). Arsenic trioxide, a therapeutic agent for APL. *Oncogene* **20**, 7146-53.

Zhong, S., Salomoni, P., Ronchetti, S., Guo, A., Ruggero, D. & Pandolfi, P. P. (2000). Promyelocytic leukemia protein (PML) and Daxx participate in a novel nuclear pathway for apoptosis. *J Exp Med* **191**, 631-40.

Zhou, Z. H., Dougherty, M., Jakana, J., He, J., Rixon, F. J. & Chiu, W. (2000). Seeing the herpesvirus capsid at 8.5 A. *Science* **288**, 877-80.